Session 3(a):
Pumps II

Session Chair

Robert G. Kershaw

Arizona Public Service Company (APS)

RCP Vibration Studies: An Examination of Lower Motor Bearing Failures and Their Effects on Shaft Integrity

H.L. Hassenpflug, Ph.D.

AREVA NP

Abstract

Many cases of high vibration and changing vibration in reactor coolant pumps (RCPs) can be traced to one of several types of degradation in the lower motor guide bearing.

This paper presents a comparison of the vibrational characteristics for several failure modes. Included in this list are loss of lubricant, bearing overloading, and time-varying shoe clearance.

Each of the examples studied is from an actual pump which underwent a lower guide bearing failure. In each case the pump was operated for an extended period following the onset of the failure mechanism. This type of operation raises the question of its effect on the fatigue life of the pump shaft and other components. This paper provides a simple assessment of the extent to which fatigue life is impacted.

I. Background

I.1 Design Considerations

Experience has shown that one of the most common failures in nuclear main coolant pumps involves the lower motor bearing. Typically, the lower guide bearing is an oil-immersed, segmented shoe bearing. Figure 1 shows the arrangement for a typical Westinghouse, or similarly designed, reactor coolant pump.

There are several reasons for the frequency of these failures compared to failures in the other bearings. Collectively, the reasons may be summarized in that main coolant pumps are three-bearing machines, wherein the lower guide bearing has the weakest design of the three. Therefore, under conditions such as misalignment where all the bearings have higher-than-normal loads, it is the lower motor bearing that is most likely to fail.

By comparison, the upper motor bearing is typically far-removed from the sources of radial (static) or synchronous (1X) loading, with normal loading applied at the pump impeller.

Further, the upper bearing is typically immersed in the upper oil reservoir. Since the upper oil reservoir provides lubricant for thrust bearings as well as the guide bearing, it is typically an order of magnitude larger than the lower reservoir. Therefore, the time to failure due to oil leakage is an order of magnitude higher for the upper bearing than the lower, and loss-of-lubricant is one of the most common causes of bearing failure in these machines.

The pump bearing is typically a water-lubricated hydrodynamic bearing. It is typically highly overdesigned to accommodate start-up and off-design operation, but spends little time in these operating conditions. With primary coolant as the lubricant, there is minimal potential for a loss-of-lubricant failure in the pump bearing. Both the journal and the bearing are typically coated with a highly wear-resistant surface as well.

I.2 Cases Considered

(1) Normal Operation

This is a reference case against which all the other cases are compared, where alignment and balance and bearing conditions are known to be within the normal range.

(2) Fully-failed Lower guide bearing (loss-of-lubricant)

This case considers the operation of the pump/motor after the lower motor bearing has been completely ‘wiped’ and provides NO support to the shaft.

(3) Severely Misaligned Lower guide bearing (overloading).

In this case, a loss of coolant accident (LOCA) restraint seized and failed to accommodate the thermal expansion of the primary piping to the pump. As a result, the bottom of the motor became misaligned by at least 0.060 inches relative to the position. The characteristics were sufficiently subtle and unique that it was operated for an extended period.

(4) Unidirectional Lower guide bearing failure (loose guide shoe)

In this case, the lower motor bearing was initially assembled to the proper clearance using jackbolts, but the torque on the locking nuts was inadequate to prevent subsequent loosening of the jackbolts. In this case, the failure was unidirectional in that the jackbolts loosened only in the most-heavily loaded direction. The characteristics were also time-dependent in that the jackscrews continued to loosen with ongoing operation.

II. Vibration and Operating Characteristics

II.1 General Comments

Because of the limitations on available monitoring sites on main coolant pumps and motors and limits on the number of data channels available, the anomalies at the lower motor bearing are most commonly observed in data taken at the pump coupling. Therefore, they are often erroneously attributed to the pump. Correct and timely diagnosis of an impending lower motor bearing failure is facilitated by the use of other data such as bearing temperature, DC gap voltage measurement, seal performance, etc.

II.2 Characteristics

(1) Normal Operation

In a pump operating normally, the vibration signature is dominated by residual unbalance. The shaft orbit is nearly circular, with the two directions typically within two mils of one another. A shaft orbit for an RCP operating normally is shown in Figure 2.

(2) Fully-failed Bearing

In main coolant pumps, full failure of a lower motor bearing is an all-too-common failure mode for lower guide bearings. These are usually the result of ‘wiping’, which is, in turn, usually the result of oil starvation. Oil starvation is typically due to the prevalence of oil leaks in the lower oil reservoir and reliability issues in oil level measuring equipment.

Such a failure is normally easily identified using a combination of dynamic data and bearing temperature data. These characteristics are sufficiently predictable that a well-trained, attentive operator may prevent this from coming to fruition.

A slow temperature rise is usually the first indicator of an oil-starved lower guide bearing. This typically occurs over a period of several hours. There is usually little or no change in vibration level during this event. This is, however, the time in the failure sequence where a well-trained operator may choose to do visual verification of oil levels.

The rate at which the bearing temperature rises will increase within the last few minutes prior to failure. In the same time frame, the vibration levels will start to increase. Soon thereafter, the temperature will spike as will the vibration levels. The spike in vibration levels will often go undetected without continuous monitoring.

In failures caused by oil starvation, it is generally not possible to replenish the oil supply in a manner to mitigate complete failure once wiping has begun. Therefore, the failure will continue until the entire bearing surface is ‘wiped’ sufficiently that it bears no load in any direction and hence a full failure.

Following the spike, the vibration levels and temperatures will stabilize with temperatures returning to normal, and vibration levels settling at a level higher than previously observed with a normal-looking orbit, and minimal harmonic

content. In main coolant pumps, the vibration levels may remain acceptable by operating guidelines.

When this occurs, it brings into question the long-term effect of ongoing operation which is discussed in Section III of this paper.

(3) Unidirectional Failure (failure of individual shoes)

When individual shoes fail, the bearing develops stiffness and damping characteristics, normal in one plane of movement, and reduced in the other. In a segmented shoe bearing, there is very little interaction between shoes so the response in the two planes of movement differs strongly.

For the case studied, the failure was first observed by changes in the overall and 1X vibration levels during heatup of the plant. Subsequently, it showed balance sensitivity which varied from one attempt to the next. Once an 'acceptable' balance level was achieved, it then had stable operation until a change in plant conditions precipitated a step change in vibrations.

It again had stable operation until the end of the cycle. At that time, another attempt was made at balancing. By this point, the asymmetry was very prominent, and the historical balance coefficient was successful at reducing vibration in one plane, but did little in the other direction. It also developed a strong sensitivity to component coolant temperature (which cools the bearing lubricant). After approximately two years of operation, it underwent yet another step change in 1X vibrations. At that time, the excessive clearances were identified. The motor was removed from service because of concerns that the same condition could be present in the upper bearing, for which disassembly and inspection require a much greater effort. A series of shaft orbits during the period of operation are shown in Figures 3(a)-3(d).

Because of the progressive nature of the failure and virtually all of the vibration was seen on the pump coupling, the concern of pump shaft cracking was raised and reviewed repeatedly.

There was a point at which the 2X vibration amplitude increased noticeably, giving additional credence to the concern. However, the 2X amplitude stabilized quickly. In retrospect, it is believed that the increase was the result of the bearing behaving non-linearly, stiffening only at high eccentricities.

(4) Severe Misalignment

a. 'Normal' Misalignment

Typically, the lower guide bearings of a main coolant pump are sufficiently rugged to tolerate misalignment due to maintenance errors. Also, they can usually tolerate errors that can, in some pump and/or motor designs, occur in the internal buildup of the motor or pump so that proper motor-to-pump alignment cannot be performed.

In these conditions, one may observe a vibration signature higher in one plane than another. In extreme cases, dry rubs may cause thermal bowing of the shaft, causing vibration amplitudes to increase exponentially; thereby forcing a shutdown.

However, these mechanisms will normally NOT cause immediate damage to the lower motor bearing if it remains well-lubricated, and are unlikely to damage either the pump or motor shaft.

b. Severe Misalignment

The case considered in the current study is of a motor/pump which was, in fact, properly aligned during installation. The misalignment which occurred was the result of binding in a thermal expansion joint at a LOCA restraint. Figure 4 includes a sketch showing the misalignment mechanism. The resulting level of misalignment is higher than would normally result from routine maintenance activities and was at least 0.060 inches. Further, the condition developed when the pump was already running, so an oil film was present. Hence, the evidence collected suggested that hard contact between metal surfaces never occurred. In this case, the motor bearing simply operated in a highly eccentric position.

The vibration characteristics were, in this case, somewhat deceptive. The distortion of the motor stand and other hardware caused the probes to move out of range and saturate. A waveform from the shaft probe in the direction of misalignment is given in Figure 5.

At the time, only the AC component of the vibration signature was being acquired. Therefore, the very large shift in the DC gap voltage went undetected. Those monitoring the vibration signatures believed the apparent probe saturation to be an electrical failure. The first indication that there was a serious problem was when the RCP seal failed from O-ring damage.

Subsequently, the bearing was found to have much of its babbitt surface worn off, and the bearing journal surface was worn heavily, though neither appeared to have made hard contact.

III. Fatigue Considerations

III.1 General Comments

(1) The bending stresses in RCPs and RCP motor shafts are, under normal conditions, quite low, and are only a small fraction of the endurance limit for the materials from which they are fabricated. Nonetheless, shaft fractures and failures do occur and are usually shown to be the result of high-cycle fatigue. Historically, they have occurred in areas where there has been a high stress concentration factor, either as a product of the shaft design or as a result of thermal cycling.

So, with regard to bearing failures and their effects on fatigue life, two questions arise into which this paper attempts to provide insight:

a. Does the failure mechanism cause an increase in the cyclic stress at a location previously identified as a failure site? That is, does the bearing failure mechanism increase the likelihood of a known fatigue failure mode?

b. Does the failure mechanism cause an increase in the cyclic stress at a location NOT previously identified as a failure location to such a level that it may become a failure site? One criterion for 'too-high' is whether the cyclic stress exceeds that seen at a known failure site. If a previously unidentified site is shown to have higher stresses than an identified failure site, then it must also be examined to determine if it has the potential for a high stress concentration.

III.2 Modeling Methodology

(1) Assumptions for Individual Cases

a. Normal Operation

For this case, all bearings are considered to have design values for stiffness and damping. There is no misalignment. For this and all the comparison cases, an impeller discharge load of 2000 lbs was considered.

b. Fully-failed Lower guide bearing

This case considers the operation of the pump/motor with NO lower guide bearing stiffness or damping. The pump-motor combination runs with support only at the upper motor bearing and the pump bearing.

c. Severe Misalignment

There is no loss or increase of stiffness considered for this case. The shaft center is considered displaced, for the purposes of this study, 0.060 inches.

d. Unidirectional Lower guide bearing failure

In this case, which represents a bearing with one or two shoes having excessive clearances, the bearing stiffness is considered normal in one plane, and zero in the other.

(2) In each case, it is assumed that rubbing between the rotating and stationary parts at clearance fits does NOT develop. Rubbing sharply changes the dynamic characteristics as well as the shaft stress distribution because the rub location acts as an additional non-linear support.

Rubbing can usually be identified using the vibration spectrum by the presence of a series of harmonics of running speed (1X, 2X, 3X, etc.) or by harmonics of an integer fraction (1/3X 2/3X, 1X, 4/3X, etc.) of running speed.

(3) Normally a shaft is subjected to cyclic stresses by stationary forces such as misalignment or pump discharge loading, and is subjected only to constant stresses by dynamic synchronous forces (e.g., unbalance). The stationary nature of stresses due to synchronous forces assumes, however, that the amplitudes of vibration in the two planes of movement are the same (i.e., circular synchronous whirl).

To illustrate this point, a comparison of the shaft bending stresses for two cycles of shaft revolution is presented in Figure 6. It presents the stress due to (1) a stationary load such as misalignment, (2) synchronous loading (such as unbalance) on a shaft where the response is 'normal', (3) a synchronous load on a shaft where the bearing is fully-failed, and (4) a synchronous load on a shaft where the bearing is failed in one direction only. The figure is provided for comparison and does not represent the actual calculated stresses for the unidirectional failure considered here.

The figure illustrates that the bending stress due to a unidirectional failure oscillates between that for a normal bearing and that of a fully-failed bearing, and thus creates an additional cyclic stress on the shaft. The oscillation occurs at twice the shaft rotational frequency.

Generally, both types of cyclic stress need to be considered to accurately determine the shaft fatigue. However, for cases where the dynamic responses have been shown to remain similar in both planes of movement during 'failed' operation, it has been assumed that the dominant effect on bending stress, and therefore fatigue, is due to the stationary loads. That is, if the measured vibration bears the appearance of circular synchronous whirl, the cyclic loading due to unbalance is ignored.

Of the cases examined in this presentation, the synchronous loading is considered only for the case of the unidirectional bearing failure.

III.3 Results

(1) All Cases

The first question raised with regard to fatigue life is whether the cyclic stresses at known failure sites would be worsened by any of the failure mechanisms considered.

Based on the assumption that rubbing does not develop at points below the lower bearing (such as the labyrinth seals), then NONE of the mechanisms considered will cause an increase in the cyclic stresses at the location for which Westinghouse and pumps of similar design are known to fail.

Because the most common failure site is below the lower-most bearing point, it is affected only by the impeller loading.

Table 1 compares the shaft bending stresses due to static loading in the fully-failed and severely misaligned bearings to those in a normal bearing. The location of the highest bending stress is shown in bold print for each case. The fatigue loading for the unidirectional failure is not easily compared because of the effects of dynamic loading.

Table 2 provides a comparison of the bearing reaction forces for the same cases as in Table 1.

(2) Normal Operation Only

For normal operation of a main coolant pump, the dynamic responses in the two planes of shaft vibration are similar, and are the result of residual unbalance and runout. Under these conditions, the dynamic response contributes very little to the fatigue loading of the rotating assembly. There will be minimal high cycle fatigue loading to the rotating components due to normal radial loading (static) such as pump discharge loading.

(3) Fully-Failed Bearing

In this case, the stiffness of the support assembly is drastically changed. There may be an increase in the unbalance response and/or runout conditions due to the failed support. However, the dynamic response remains approximately axisymmetric. The major change in the cyclic stresses is the result of static loading. While the full failure of the lower guide bearing does not affect the stress below the pump bearing, the cyclic stresses in the shaft seal region increase to a point that they are of approximately the same magnitude as those seen at the maximum stress location in a normal pump shaft. This is not expected to pose a major problem for shaft integrity because there are no sharp thermal transition areas in the seal region. It does, however, suggest a sharp reduction in the life of seal components such as o-rings and rubbing faces, since these do not have the same extensive design margins of safety as the shaft.

(4) Severe Misalignment

Under conditions of severe misalignment, the static response is increased, and depending on the extent of misalignment can cause increased fatigue loading in the rotating components. For the case studied, the shaft fatigue loads are increased most sharply in the upper seal and lower motor shaft areas. This is consistent with findings in the field. During the refurbishment of this motor, the bearing journal was found to be worn to such an extent that the wear was easily visible with the naked eye.

(5) Unidirectional Failure

When individual shoes come loose, the bearing has stiffness and damping characteristics which are quite different in one plane from those in the other. The model assumes that, although the responses in the two planes of movement are different, they are largely independent.

The value of the cyclic stress due to static loading is, therefore, approximated by the average of the cyclic stress with a normal bearing and that seen with a fully-failed bearing. In this case, there is an additional cyclic stress component due to the dynamic loading. The amplitude of this component is equal to the difference between the amplitudes of the fully-failed and the normal bearing cases. Because the two components of cyclic loading occur at different frequencies, the combination of their effects may be combined using methods such as Miner's rule. However, since neither component approaches the endurance limit of any coolant pump shaft material, it is safe to say that the expected life of the shaft will still be infinite following such a bearing failure.

As with the other cases, the increased cyclic loading may be expected to reduce the durability of other components such as the seal. The maximum stress seen in this case is the same as that seen with the fully-failed bearing, so the location of the greatest concern is the same also. Because of the added cyclic stresses attributable to the dynamic loading, the unidirectional bearing failure may be expected to have a more detrimental effect on adjacent components than the fully-failed bearing.

IV. Summary

IV.1 Vibration History

(1) In all cases, vibration data should be augmented with any other data available to support a timely and correct diagnosis and correction.

(2) Vigilance regarding oil level monitoring and bearing temperature are vital tools to assist in preventing the 'wiping' of a lower guide bearing. Vibration changes typically develop a matter of hours before the bearing becomes a 'fully-failed' bearing.

(3) For severe misalignment, caused as in the test case by restraint binding, monitoring of shaft centerline position (DC gap voltage) should be used as corroborating information whenever vibration data appears saturated.

(4) For a unidirectional failure (loosening shoes), the vibration undergoes a series of discrete shifts, increasing 1X running speed component each time. The symptoms are distinct from those due to a shaft crack in that only minimal 2X running speed vibration appears, and that the rate of progression does not increase.

(5) Also for a unidirectional bearing failure, as the failure progresses, the two responses in the two planes of movement become increasingly different from one another.

IV.2 Fatigue

(1) Because the most common failure site is below the lower-most bearing point, it is affected only by the impeller loading. **Based on the assumption that no rubbing occurs, lower guide bearing failures do NOT increase the likelihood of the typical shaft failure mode in Westinghouse pumps where failure occurs at the thermal sleeve anti-rotation pin.**

(2) A fully-failed bearing and a severely misaligned bearing have similar effects with regard to the stresses in the shaft, and cause an increase in fatigue stresses near the upper end of the shaft seal.

(3) With a fully-failed bearing, the cyclic stresses in the seal region may be greater than those seen at the thermal sleeve anti-rotation pin location.

(4) With a severely misaligned bearing, the cyclic stresses in the seal region are likely to be considerably higher than those seen at the anti-rotation pin location.

(5) The stresses in the seal region are still very low, and would only be expected to pose a problem in the presence of a high stress concentration.

(6) In the case of severe misalignment, the stresses at the lower end of the motor are also increased substantially. For the fully-failed bearing, the stresses in the lower motor shaft increase only by approximately 30% for the case studied herein.

(7) Other components such as rubbing face seals or shaft sleeve o-rings, which may not have as large design margins as the shaft itself, may be damaged either by a lower guide bearing failure or by misalignment.

(8) The unidirectional failure, while causing additional cyclic shaft stress compared to a fully-failed bearing, still does not challenge the integrity of the shaft.

Table 1

Comparison Max Shaft Stress for Static Conditions

	Normal	**Failed**	**Misaligned (0.060 inches)**
Below Pump Brg.	**1.0 KSI**	1.0 KSI	1.0 KSI
Upper Seal	0.1 KSI	**1.06 KSI**	**2.2 KSI**
Mtr. Shaft Extension	0.2 KSI	0.4 KSI	1.9 KSI

[KSI = kip per square inch, where kip = 1000 pounds force]

Table 2

Comparison of Reaction Forces for Bearing Conditions

(as a fraction of impeller discharge load)

Bearing	**Normal**	**Failed**	**Misaligned (0.060 inches)**
Pump	- 1.4	- 1.13	- 2.1
Lower Motor	+0.5	0.0	+1.85
Upper Motor	- 0.1	+ 0.13	- 0.75

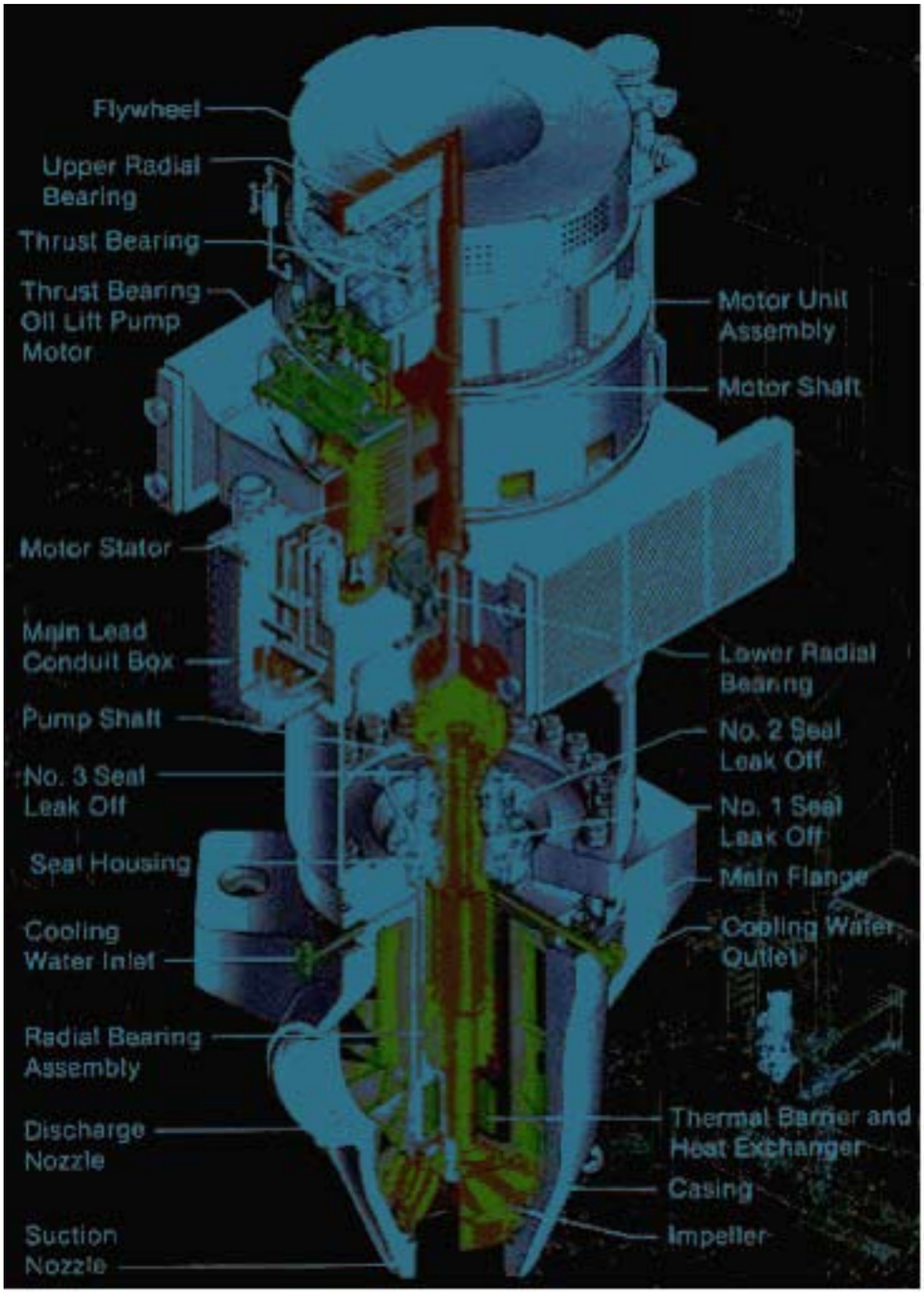

Figure 1 – Typical Westinghouse-Style Reactor Coolant Pump and Motor

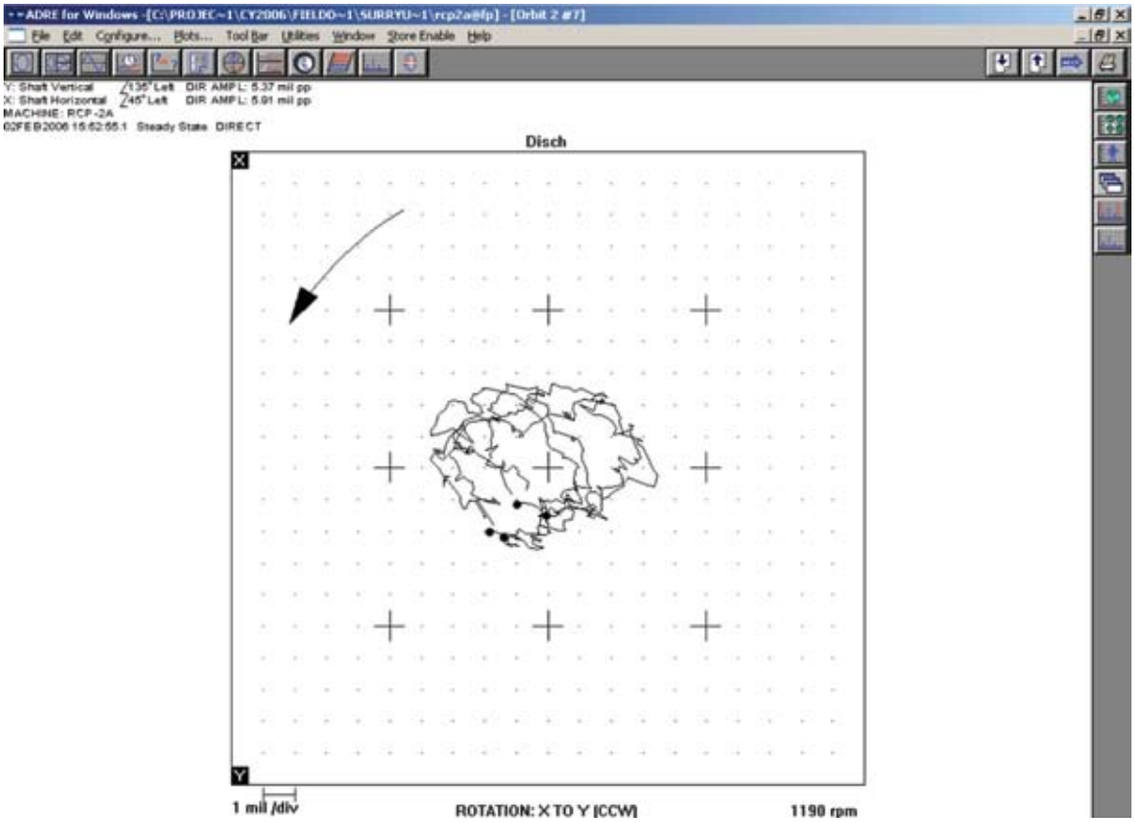

Figure 2 – Shaft Orbit for an RCP during Normal Operation

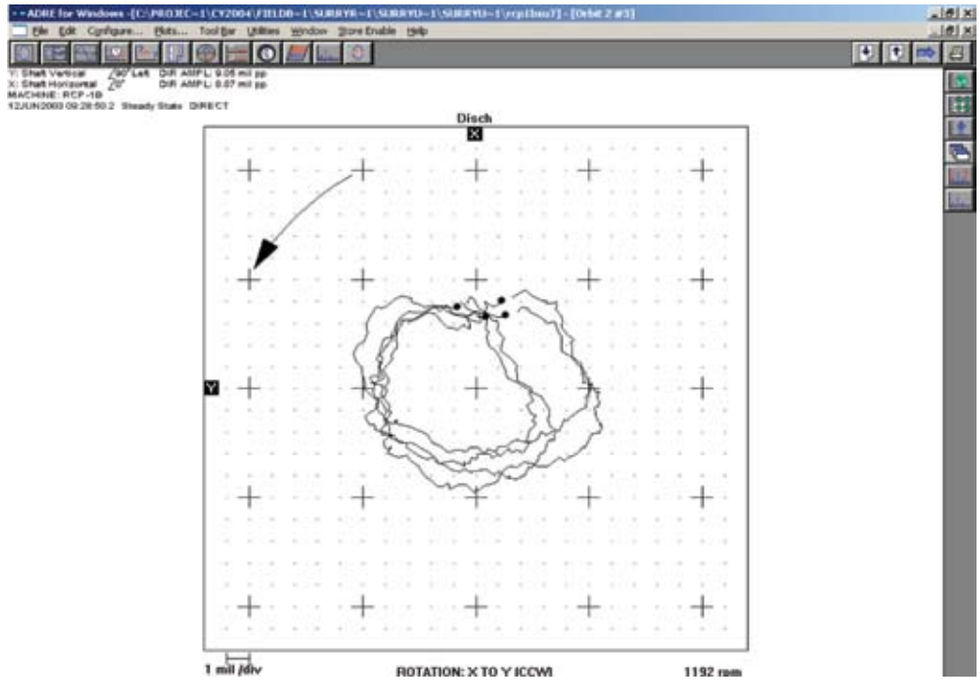

Figure 3(a) – Shaft Orbit for a pump with Unidirectional Bearing Failure (initial operation)

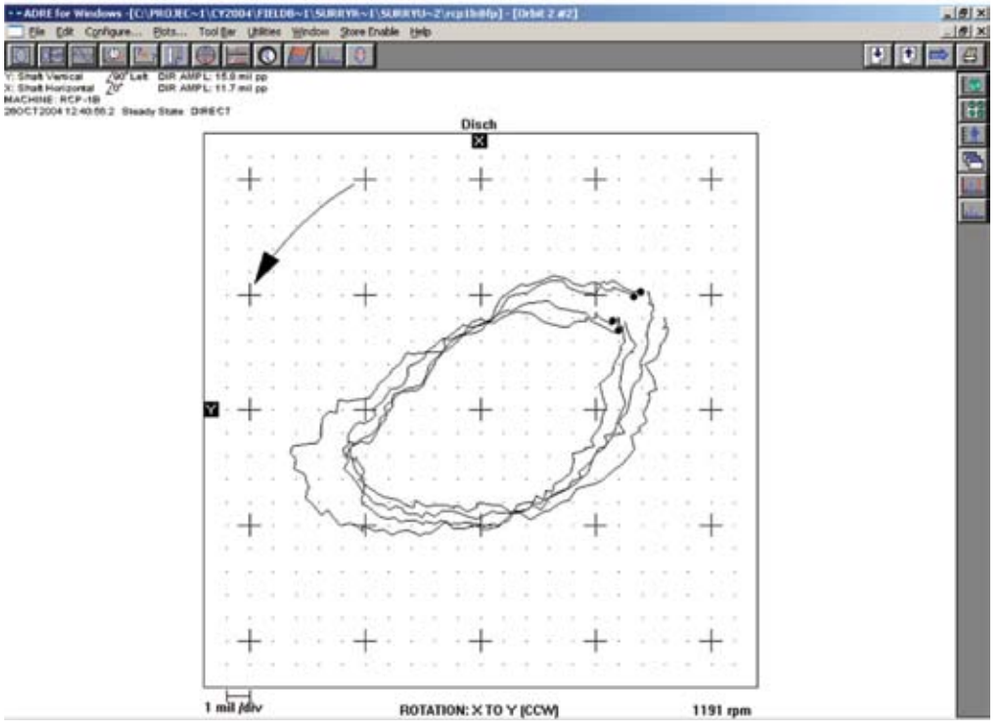

Figure 3(b) – Shaft Orbit for a pump with Unidirectional Bearing Failure (after 14 months of operation)

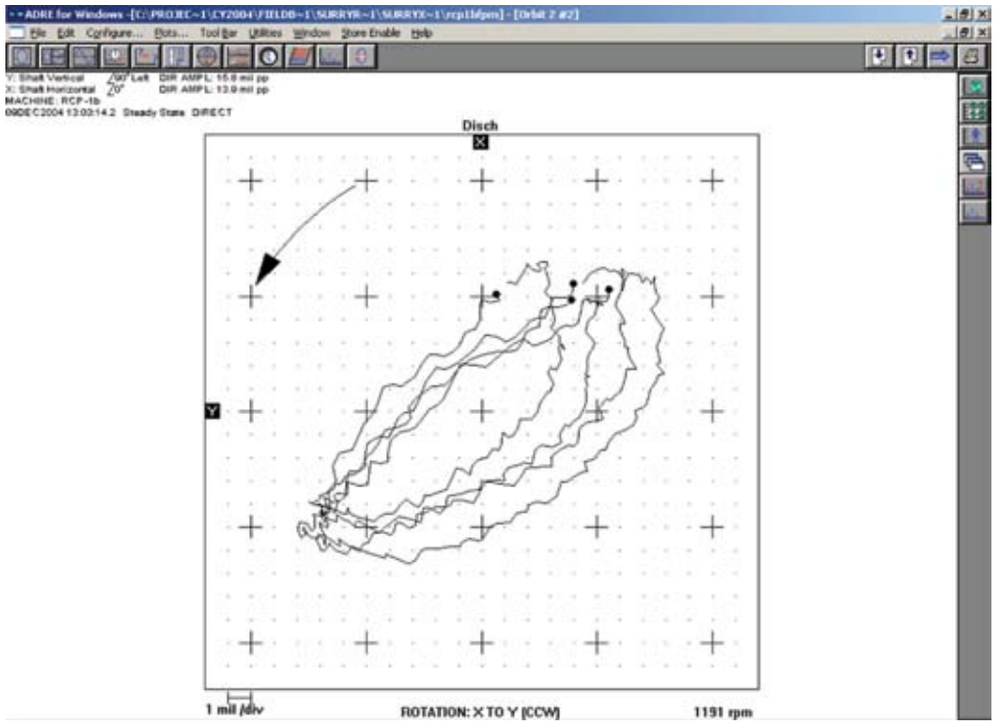

Figure 3(c) – Shaft Orbit for a pump with Unidirectional Bearing Failure (following 15 months of operation and balancing)

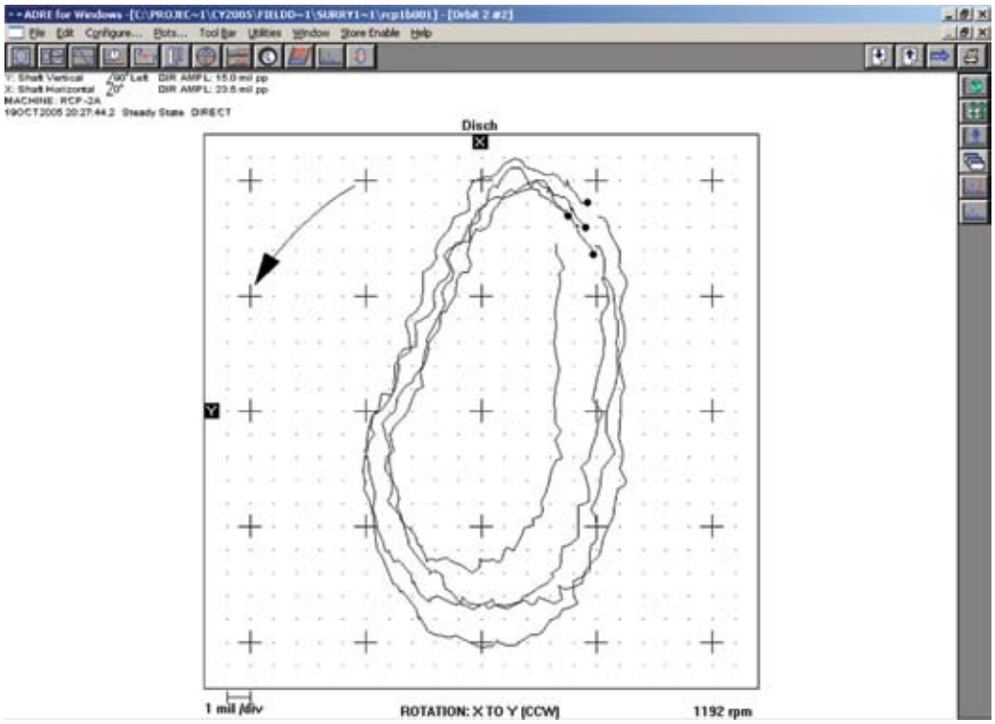

Figure 3(d) – Shaft Orbit for a pump with Unidirectional Bearing Failure (just prior to forced repair)

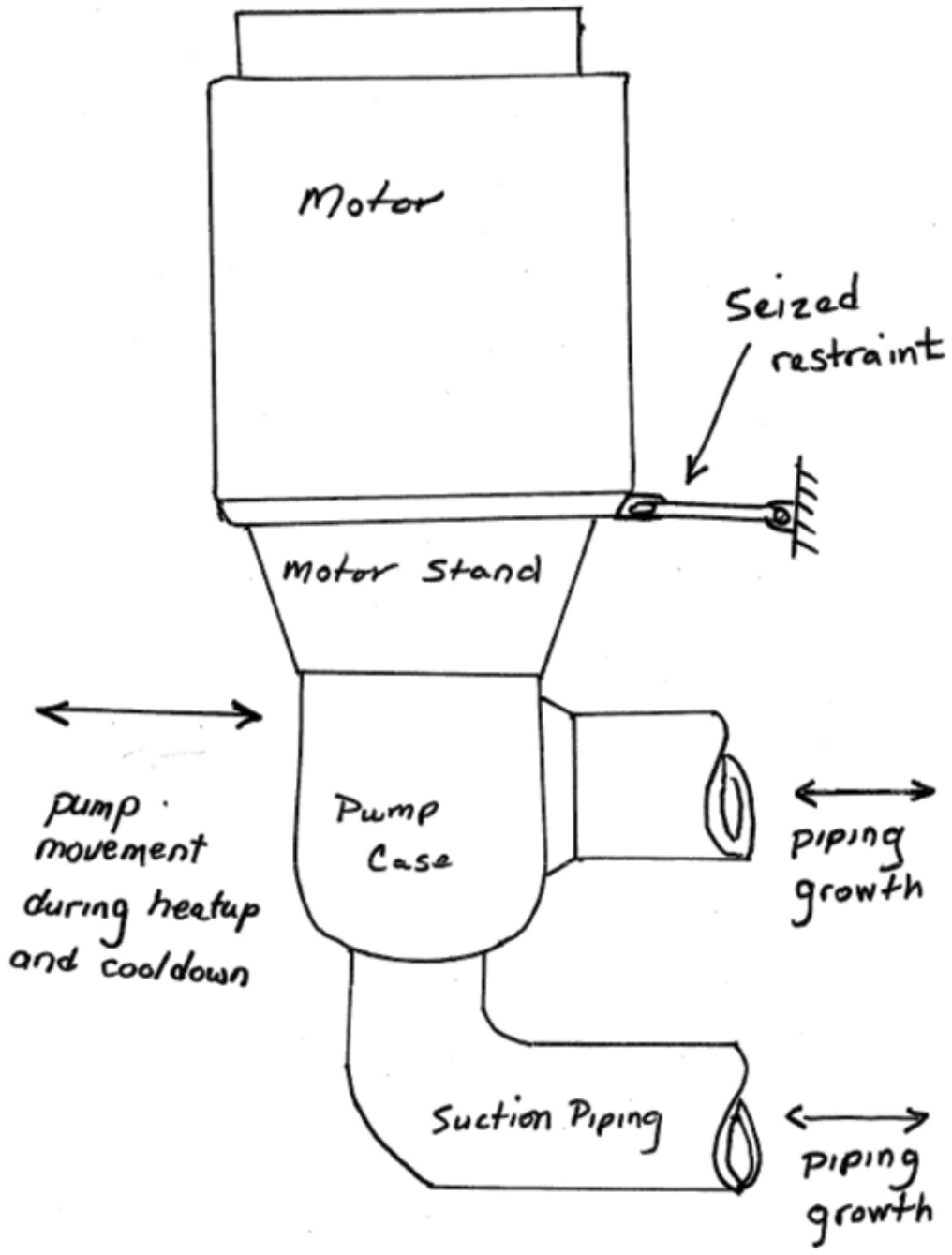

Figure 4 – Simplified Sketch showing Misalignment Mechanism

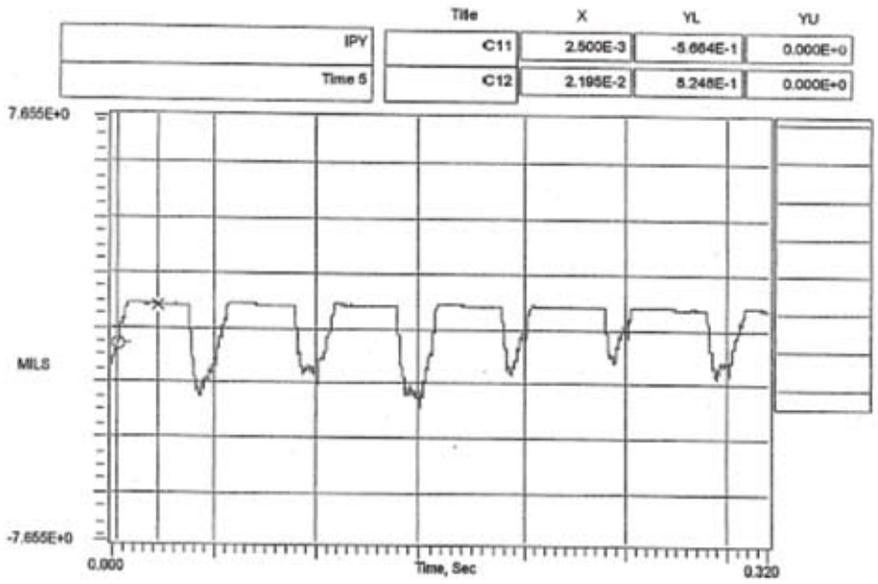

Figure 5 – RCP Shaft Vibration Time History for Severe Misalignment (clipping due to proximity probe out of range)

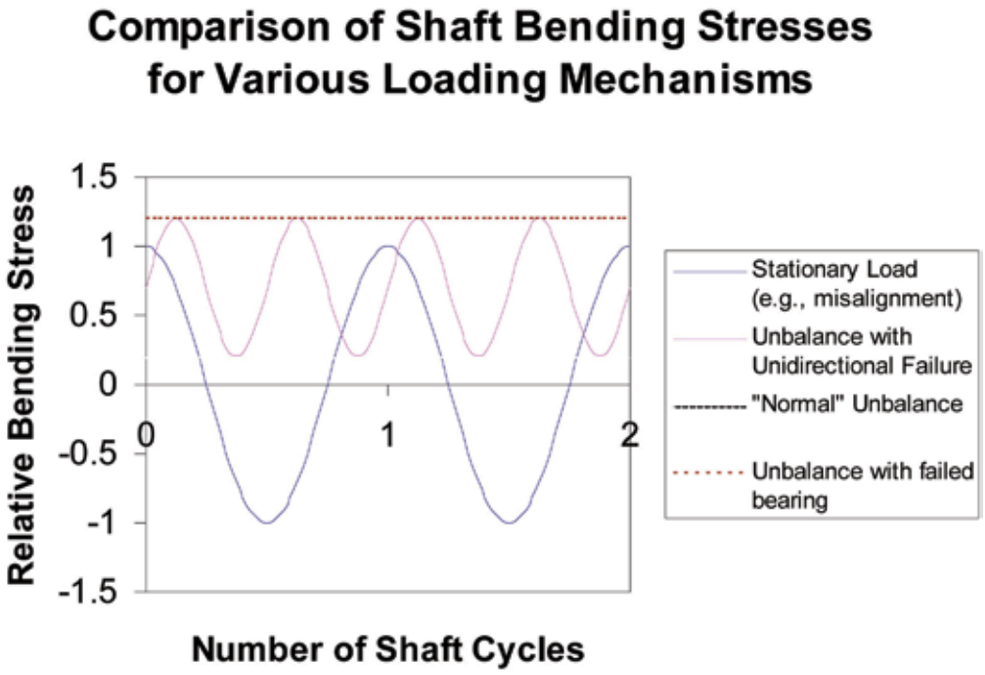

Figure 6 – Comparison of Shaft Bending Stresses for Various Loading Mechanisms

Scale Model Testing of Air Transport through Pump Suction Piping

Robert Hammersley and Robert Henry, *Fauske & Associates, LLC*

Mark Radspinner, *Arizona Public Service*

Frank Ferraraccio and Steve Swantner, *Westinghouse Electric Co.*

Abstract

This paper summarizes a scale model test program conducted for the Palo Verde Nuclear Generating Stations. The test program investigated the potential to transport an air volume initially trapped in a horizontal segment of the containment sump outlet line through a vertical downcomer and subsequently into the Emergency Core Cooling System (ECCS) and Containment Spray (CS) pump suction lines. The testing was conducted in three phases. The first two phases modeled the pump suction transfer from the Refueling Water Tank (RWT) to the containment sump. The first phase investigated the manner in which the liquid outflow from the sump interacted with the air volume, the ability of the liquid outflow to transport air through the vertical downcomer, and the flow pattern of the two-phase mixture in the downcomer. The second phase investigated the nature of the two-phase flow pattern produced in the pump suction piping for the High Pressure Safety Injection (HPSI), Low Pressure Safety Injection (LPSI), and CS systems. The third phase investigated the sensitivity of model scaling factors on the transport process.

A range of containment overpressure and system flow rates were investigated in the tests. The set of conditions that would be expected for a large beak loss-of-coolant accident (LOCA) event were found to result in the air being transported from the horizontal segment into the vertical segment and subsequently to the pump suctions. The two-phase flow pattern in the vertical segment was observed to be liquid continuous with dispersed air bubbles. The two-phase flow pattern in the pump suction lines was observed to approach a stratified state in the lower pump suction header. The ultimate dispersion of the stratified air was found to be specific to the orientation of the HPSI pump and CS pump suction connections off the lower header. The majority of the initial air mass displaced from the pump suction line accumulated in the pump suction header was subsequently discharged through the HPSI pump. Limited air was observed to be discharged through the CS pump for those cases where the HPSI pump was not running with or without the LPSI pump running. Very little air was only intermittently discharged to the LPSI pump.

This paper provides a description of the test facility, test processes, along with an overview of the sensitivity of boundary conditions, system operating parameters, and model scale on the observed transport process and associated flow regimes.

1.0 Introduction

These Phase 2 integral system tests were preceded by a Phase 1 test program (4 inch transparent piping with a single pump) and phenomenological tests (transient tests in transparent 8 inch piping). Both of these showed that (a) air would be transported into and downward through the downcomer and (b) Froude number scaling was not appropriate for the downcomer.

In this Phase 2 one-sixth scaled integral system study, a range of containment overpressures and system flow rates were studied for the containment sump recirculation phase of ECCS operation. A set of conditions that would be expected for a range of LOCA break sizes were investigated to assess the potential for air, initially trapped between the containment sump suction valves, to be pulled into the suction piping for the HPSI, the CS and LPSI pumps. These were examined through three similar, but different, experimental configurations that included operating pumps as follows:

Configuration 2A - HPSI and CS,

Configuration 2B - LPSI and CS,

Configuration 2C - HPSI, LPSI and CS.

The experimental results from the scaled Configuration 2A were used to formulate the test conditions for full scale tests with HPSI and CS pumps performed at a different laboratory. All three of the scaled configurations were used to characterize the response of the plant systems.

2.0 Experimental Apparatus

Figure 1 is a schematic illustration of Configuration 2C which encompasses the other two configurations. This apparatus was constructed with transparent plastic pipe and is a one-sixth scale model of a single train of HPSI, LPSI and CS for the plant system and includes the two isolation valves with one atmosphere of air initially trapped between the valves. The only deviation from the one-sixth scale is the downcomer pipe length. In two-phase vertical downflow, the water velocity determines the potential for downward air transport. Hence, to represent the plant conditions the scaling deviates from the Froude number as given by

$$N_{Fr} = \frac{U}{\sqrt{gD}} \qquad (1)$$

to one in which the downward water velocity is the same as in the plant. To accomplish this, the downcomer pipe is 3 inches in diameter instead of the 4 inches dictated by Froude number scaling. (In the above equation, U is the water velocity, D is the pipe internal diameter, and g is the gravitational acceleration.)

Scaling of the plant geometry was followed in terms of the location and geometry of the suction locations for the three pumps. Of particular note is that the suction piping for the HPSI pump is a horizontal pipe at the equator of the pump suction header whereas the CS and LPSI suctions are at a 45° downward angle. As is discussed later, this HPSI suction location is influential in determining the extent of air transported into the HPSI suction piping.

Before initiating these tests with multiple pumps, which permitted flow control to the individual suction connections, other tests were performed with a single pump at one-sixth scale and transient tests at one-third scale with the HPSI and CS pumps simulated. It was these tests that clearly illustrated the importance of the downward water velocity in the downcomer. Moreover, the one-third scale tests revealed a vortex formation at the HPSI suction location with a hydraulic jump immediately downstream of this suction. Whether this occurred in the scale model of the plant was one of the principal objectives of the integral system tests.

To measure the air transported to the HPSI pump, an air separator was installed on the HPSI suction line as illustrated in Figure 1. This separator captures the air, which is measured by a differential pressure sensor (see Figure 2). In addition, this enables the HPSI pump to continue at full flow which is conservative with respect to maximizing the air transport to the HPSI pump. The air accumulation rate in this separator was measured for different HPSI flow rates and used to determine the spectrum of air intrusion rates to be used in the full scale tests with a horizontal shaft, multi-stage HPSI pump.

Due to the location of the CS suction port (downstream of the HPSI takeoff) and the 45° downward orientation, very little air was pulled into this pump suction flow. A small separator at the top of the pipe was used to measure the rate of air ingestion from the pipe suction header. This was used to formulate the test conditions to be examined for the full scale tests with a vertical shaft, single stage pump like that used for the CS.

In addition to the rate of air transport to the pumps, the two-phase flow pattern was also an important parameter for the full scale tests. Consequently, digital video cameras were positioned to observe the transient flow structure in the following locations:

- between the two butterfly valves used for sump isolation,
- at the top of the downcomer,
- at the HPSI suction takeoff from the lower pump suction header,
- along the HPSI suction piping just upstream of the air separator,
- at the CS suction takeoff from the lower pump suction header, and
- at the LPSI suction takeoff at the end of the lower pump suction header.

These direct observations proved to be invaluable in assessing the transient air-water flow patterns as well as in demonstrating the appropriateness of the scaling analyses (Froude number for the horizontal lines and water velocity for the downcomer).

3.0 Test Performance

All of the tests were conducted by initiating flow from the simulated Refueling Water Tank (RWT) to the pump suction header and then to the operating pumps. Since this only establishes the initial condition in the pump suction header, the discharge flows of the operating pumps are returned to the RWT.

The test is initiated when the recirculation actuation signal (RAS) begins to simultaneously open the two butterfly isolation valves of the simulated containment sump. Depending on the pressure in the containment sump at this time, the air is somewhat compressed and transported to the downcomer pipe.

As the isolation valves open, the pipe suction header is exposed to the containment pressure plus the static head of the water in the containment sump and the downcomer piping. This pressure exceeded the pressure in the RWT and caused the check valve on the RWT suction to close. With this action, the pump suction header water supply is transferred from the RWT to the containment sump. Once this occurs, the transport of air through the suction piping is determined by the Froude number in the horizontal piping and the water velocity in the downcomer.

Since the experiment did not include a representation of the Reactor Coolant System (RCS), the pump discharge flow rates were switched from a return to the simulated RWT to the containment sump. This manual (by a test engineer) switchover occurred as the water flow from the sump was observed to fill the region between the butterfly valves and was nearly simultaneous with the audible closing of the check valve on the RWT suction line. After this switchover, each test could be run until the air transport to the pumps was completed. This included those conditions in which the water flow rate from the sump was insufficient to sweep the air from between the butterfly valves and the air rose against the flow backward into the containment gas space.

4.0 Important Test Results

In both the plant system and the experimental facility, the operation of the CS pump provides sufficient flow to sweep the trapped air from between the isolation valves into, and down through, the downcomer piping and then into the lower pump suction header. Therefore, the tests of greatest interest are those with the CS pump operating during the switchover to containment sump recirculation, which is the expected behavior for the plant. Furthermore at the time of RAS, the LPSI pump is automatically shut down while the HPSI pump continues to run with a discharge flow rate determined by the RCS pressure, which would be determined by the LOCA size causing the accident state. Therefore, the major focus for the tests was the air ingestion for those conditions with the CS running at full flow and HPSI flow rates consistent with small, medium and large break conditions within the RCS.

As discussed above, with the RAS signal, the inboard and outboard butterfly valves open simultaneously over a 20 second interval. These valves are oriented stem vertically such that the openings begin at the equator of a horizontal pipe connecting them. As a result of the accident condition, the pressure in the containment plus static sump water level head is greater than the 1 atmosphere (atm) air volume between the valves, hence, the inrush of water from the sump compresses the air. Water can be seen to enter around the sides of the inboard valve and preferentially accumulate in the bottom of the horizontal pipe.

Before the air-water mixture can be transported into the downcomer pipe, the containment pressure needs to exceed the back pressure on the check valve downstream of the outboard valve. This back pressure is caused by the water head in the RWT and, for those accident conditions where this does not occur within about 10 seconds, the air will flow backwards into the containment. Therefore, the accident sequence conditions of interest in these tests are those with a sufficient containment pressure to open the downstream check valve within a few seconds. It is further noted that a higher containment pressure causes more compression of the air volume. Since the primary quantity of interest is the void fraction transported to the pumps, the lowest pressure sufficient to open the downstream check valve as the butterfly valve is opened, would give the maximum potential for the largest void fraction entering the suction location. In the spectrum of LOCA sizes, the small break LOCAs would give the limiting condition. However, the smallest

break LOCAs would not be sufficient to quickly open the downstream check valve and the compressed air would be forced back into the containment by buoyancy.

Figure 3 shows the developing two-phase mixture 5 seconds after the motor-operated valves (MOVs) begin to open for a limiting sequence which opens the check valve. A frothy mixture is observed to be generated with an air bubble formed between frothy regions near the outboard valve. Two seconds later the air bubble has been reduced to a small region near the top of the pipe, i.e. most of the air has already been transported into the downcomer. Therefore, these scaled tests with the same Froude number as would occur in the plant system illustrate that the pump suction flow rate, which is principally due to the CS pump, would transport the trapped air into the downcomer pipe.

Digital video observations near the top of the downcomer show that a kinematic shock can be formed with some initial holdup of air. However, as the transient progresses, the air is eventually pulled into the downcomer flow. Similar observations at the bottom of the downcomer reveal a bubbly mixture as the flow exits this pipe and is transported into the horizontal pump suction header. The same flow patterns were observed in the transient one-third scaled tests that were conducted in preparation for these integral system tests. Maintaining the same velocity in the downcomer as the plant would experience caused this flow pattern. If Froude number scaling had been used, the water velocity in the downcomer for the one-sixth scaled test would have been comparable to the bubble rise velocity. Under these conditions, the air would tend to form large bubbles and rise against the flow (Wallis, 1969). In the plant system, the downward water velocity is approximately twice the bubble rise velocity (when the CS is operating) and the air would be swept along with the flow.

Observations from both the one-sixth and one-third scaled tests show that the flow pattern quickly transitions from bubbly to stratified flow as the mixture enters the horizontal pump suction header. This was seen within one to two pipe diameters. This further emphasizes the need for Froude number scaling in the horizontal parts of the system model. Consequently, the flow pattern at the HPSI suction port is stratified as the air begins to collect along the top of the header. As the void fraction in the header increases and the air-water surface approaches the top of the HPSI suction port, a vortex is formed that pulls air into the HPSI pump suction piping. Figures 4 and 5 show that this vortex as observed in the one-third and one-sixth scaled tests respectively. Note the similarity in the conditions at the entrance to the HPSI takeoff and the annular flow pattern developed as the air and water enter the pipe. Similar behavior at these different scales further supports Froude number scaling. The curvature of the opposite wall of the port is normal, and not reversed, and is indicative of a high void fraction, annular flow pattern.

As the air-water mixture enters the HPSI piping, a stratified flow pattern re-develops. This was an important observation for designing the full scale HPSI test facility; particularly for the small break conditions with a reduced HPSI flow due to the elevated RCS pressure. With the 90° downturn at the pump entrance, a reduced flow resulted in very little air entering the HPSI pump when the air separator was replaced with a straight pipe.

Figure 6 illustrates the rate at which the air mass was captured in the separator for different transients. Note that the air accumulates very quickly at the beginning of the transient and tapers off to a relatively slow accumulation rate (some air was observed to exit from solution). To aid in designing the full scale HPSI test, this air accumulation information was interpreted in terms of the rate of accumulation and these are illustrated in Figure 7 which shows the maximum rate develops in the one-sixth scale model within a few seconds of air arriving at the separator. This information was then translated into the most limiting case and interpreted in terms of the full scale test for the design and performance of the full scale experiments. Figure 8 illustrates this limiting air mass flow rate that was used for the full scale test. Recall that this information represents a conservative transfer of air to the pump suction since there was no degradation in the HPSI pump flow rate for the scaled test in which the separator was installed.

5.0 Conclusions

The following conclusions were derived from the three Phase 2 configurations for the one-sixth scaled integral system experiments representing the Palo Verde sump suction line behavior.

Configuration 2A

1. All of the important physical phenomena observed in the one-third scale tests were also observed in the one-sixth scale tests. This demonstrates that the scaling evaluations appropriately considered the governing physical processes.

2. The air-water mixing which occurred between the two butterfly valves in general created a well mixed two-phase bubbly flow pattern which transported the majority of the air out of the horizontal section and into the vertical downcomer.

3. An important aspect of a scaled experiment is to have a vertical downcomer designed such that, like the plant, the downward water velocity is considerably greater than the bubble rise velocity. For these integral tests, this was accomplished by reducing the downcomer diameter from 4 inches to 3 inches. As a result, there was no significant air holdup in the vertical downcomer and the air is transported to the lower horizontal header at the appropriate rate. Furthermore, those tests with HPSI and CS operating showed no bubble coalescence in the reduced diameter downcomer.

4. As the air is delivered to the lower horizontal header, a stratified flow pattern is developed. This flow regime is sustained by continuing downward flow and the experiments demonstrated that the CS pump flow alone will keep the air in the header. With the substantial water head provided by the vertical downcomer in the plant, this adds essentially 1 atm additional overpressure to the static pressure and adds to the compression of the air thereby reducing the air volume.

5. For those conditions with relatively low or no HPSI flow rate, the air occupies the upper regions of the horizontal pump suction header with an essentially uniform void profile along the length of the horizontal header (except at the entrance to the HPSI).

6. For the higher HPSI flow rates, a vortex is developed at the HPSI suction port that, in essence, limits the stratified layer in the suction header to that region from the beginning of the horizontal length to the tee for the HPSI branch. With a vortex at the HPSI take-off, there is a hydraulic jump formed which has a height that approaches the pipe radius. As a result, the hydraulic jump nearly closes off the entire cross section of the suction header downstream of the take-off. Under these conditions, virtually all of the air that is transported from the horizontal header is drawn through the HPSI suction line and this is approximately 60% to 80% of the gas initially resident between the upstream butterfly valve and the check valve in the sump suction line.

7. For all conditions there is little (< 5% void fraction) or no gas transported down the containment spray suction line. Therefore, there is no significant challenge to operation of the containment spray pump as a result of this set of conditions with 1 atm of air initially in the sump suction line.

8. For the flow through the HPSI suction line, the dominant flow pattern is one of stratified flow. This was observed in both the one-third scale tests and in the one-sixth scale integral system tests.

9. Using the numerous experimental tests performed in the integral system, the greatest delivery air mass and mass flow rate to the HPSI pump was developed for each nominal HPSI flow rate. Using the information from these scaled experiments, the effective air delivery rate histories to the HPSI pump were translated to be tested at full scale. Because these data were developed from measurements where there was no feedback on the pump a conservative interpretation is developed. Therefore, this data was applied to the full scale pump in a piecemeal approach that began with the appropriate air delivery rate early in the two-phase transient and then uses the feedback from the measured pump behavior to deduce the longer term air transport conditions. In this manner, the integral behavior for the pump was tested along with the approximate feedback as a result of the pump performance while undergoing air ingestion.

Configuration 2B

While not a design basis configuration, the opportunity to restart a LPSI pump after RAS is permitted within the emergency and abnormal operating procedures (EOP and AOP) for the plant.

1. These scoping experiments which related to the LPSI pump start assuming no HPSI flow demonstrated that the manner in which the LPSI pump was re-started was important.

2. If the LPSI pump were to re-start near runout conditions, considerable air could be drawn into the LPSI suction line.

3. If the LPSI pump re-started near the shutoff head conditions, essentially no air was pulled into the LPSI suction line.

4. It was concluded from these scoping tests that the evaluation for LPSI pump re-start should include a simulation with all three pumps, i.e. HPSI, CS and LPSI. This led to the tests with Configuration 2C.

Configuration 2C

1. These tests were performed with consistent HPSI and LPSI flow rates as if they were pumping to the same RCS pressure. For most of the tests, the HPSI pump was operated until the flow degraded to 50% of the preset initial flow rate, at which time the HPSI pump was isolated. This showed that there was considerable air pulled through the HPSI suction line prior to this isolation which substantially decreased the air in the pump suction header.

2. Experiments were performed to examine the integral response for conditions in which, following loss of HPSI, the control room operators would maintain one train of CS and shut down the other train to start the LPSI pump. These tests demonstrated that a complete shutdown of flow in a single train for a few minutes would enable the air to escape backward up the downcomer, leak through the check valve and flow into the containment sump and hence, to the containment atmosphere. Consequently, there was no air in the horizontal header when the LPSI pump was started.

3. For those experiments with a consistent HPSI and LPSI flow, the LPSI flow was activated at a pressure near that of its shutoff head and the flow rate was incrementally increased at a rate consistent with the RCS depressurization. With the long interval required for the LPSI flow to increase, the air void fractions pulled into the CS and LPSI line during this time were in the range of 2 to 5%. Hence, the air intrusion rates are well within those that have been demonstrated in the open literature (NRC, 1982) to be consistent with successful pump operation.

4. In one test configuration the HPSI continued operation during the entire test. This showed a degraded HPSI flow due to air intrusion; however, air and water flow continued. During this time the flow through the HPSI suction line remained in a stratified flow pattern and continued to pull air into the HPSI suction flow. Furthermore, the flow through the HPSI pump continued in a quasi-steady manner without any significant flow rate or pressure oscillations. A key to developing this operating state is that the air intrusion rate is directly related to the degraded pumping rate.

6.0 References

NRC, 1982, “An Assessment of Residual Heat Removal and Containment Spray Pump Performance Under Air and Debris Ingesting Conditions,” NUREG/CR-2792, September.

Wallis, G. B., 1969, One-Dimensional Two-Phase Flow, McGraw-Hill, New York.

Figure 1 – Phase 2 test configuration 2C for post-RAS air intrusion.

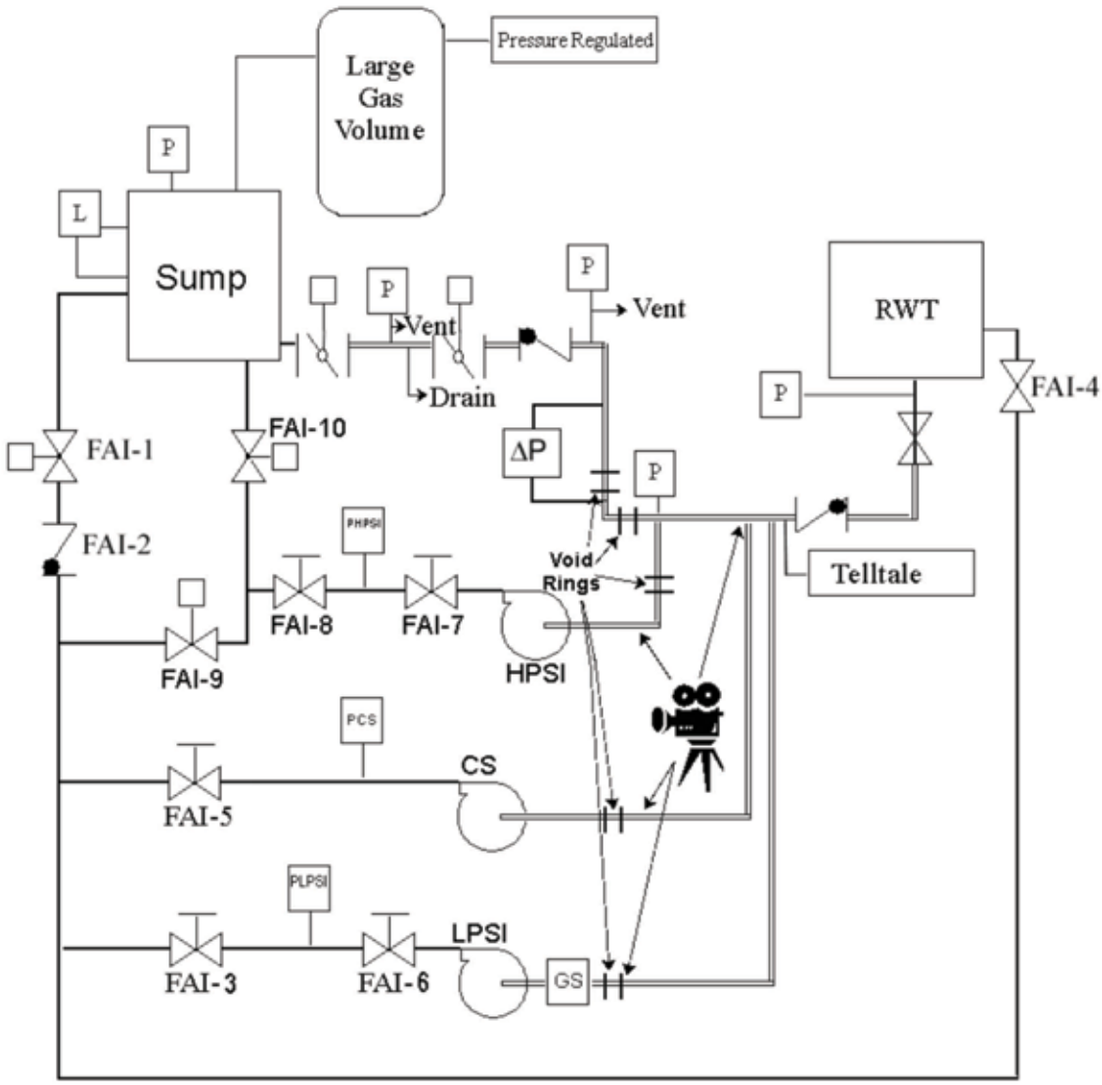

PCS / PLPSI / PHPSI	=	Turbine Flow Meter
P	=	Pressure Measurement
ΔP	=	Differential Pressure Measurement
GS	=	Gas Separator
L	=	Water Level

Notes

- Double line pipe to be transparent.
- Digital movie cameras to record flow patterns at key locations, i.e., vertical downcomer, horizontal header for the three pumps, and branch lines.
- Telltale to confirm check valve position.

Figure 2 – Cutaway view of air-water separator.

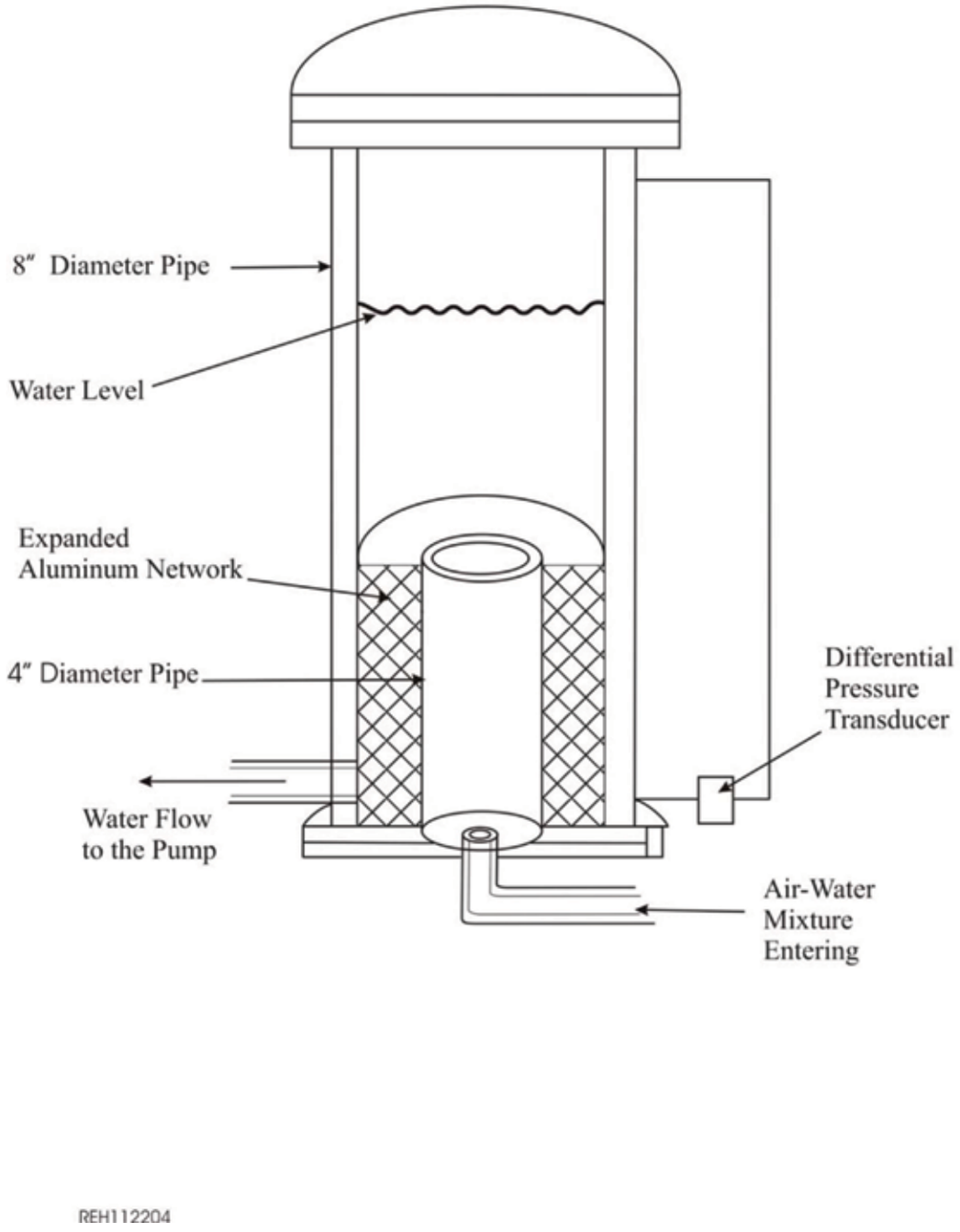

Figure 3 – Test PVA21 5 seconds after MOVs began to open.

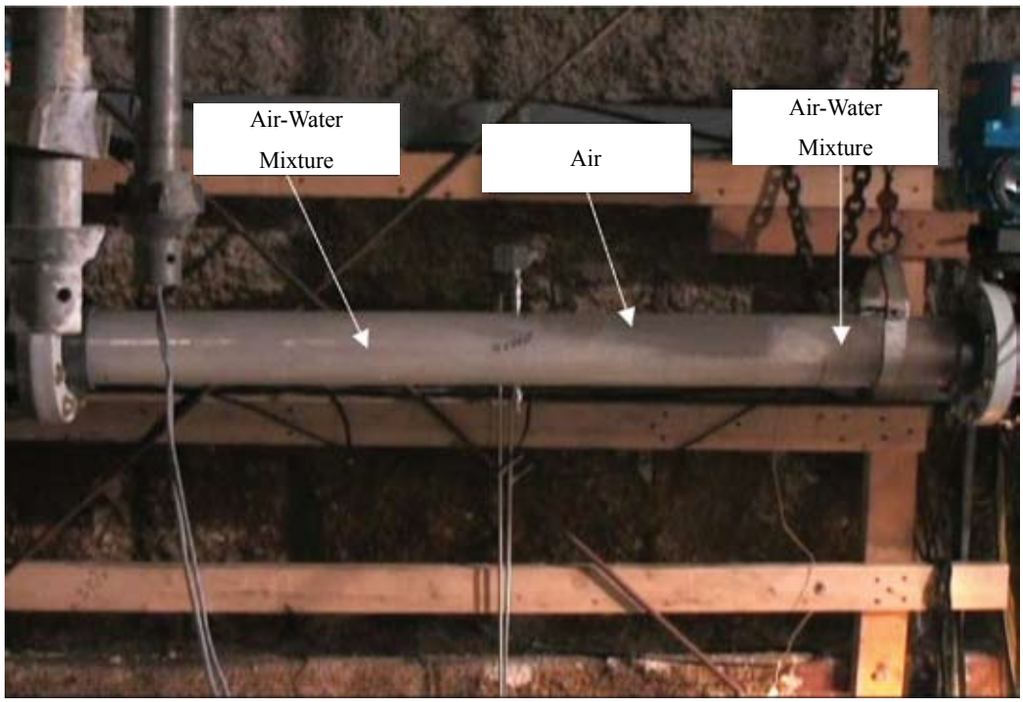

**Figure 4 – Air vortex penetrating into sweepolet tee.
Note (a) angle of water swirl in HPSI suction line, (b) water level
upstream of HPSI takeoff, and (c) water level downstream of this takeoff.**

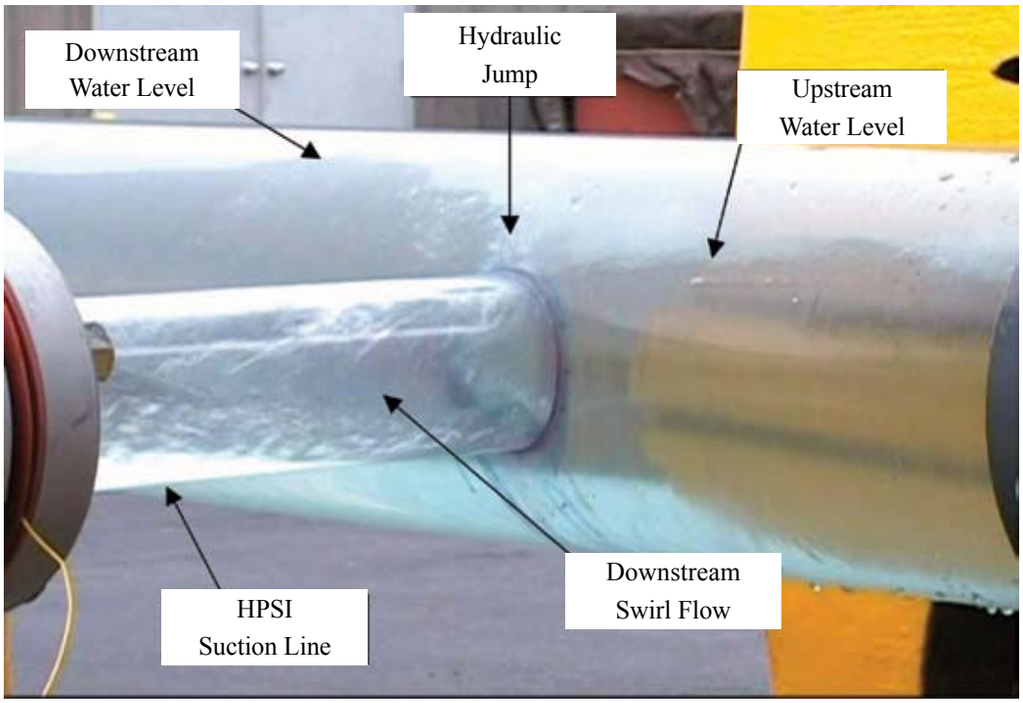

Figure 5 – Vortex in HPSI sweepolet tee for Test PVA21. Note stratified flow pattern in horizontal header and also curvature of opposite pipe wall.

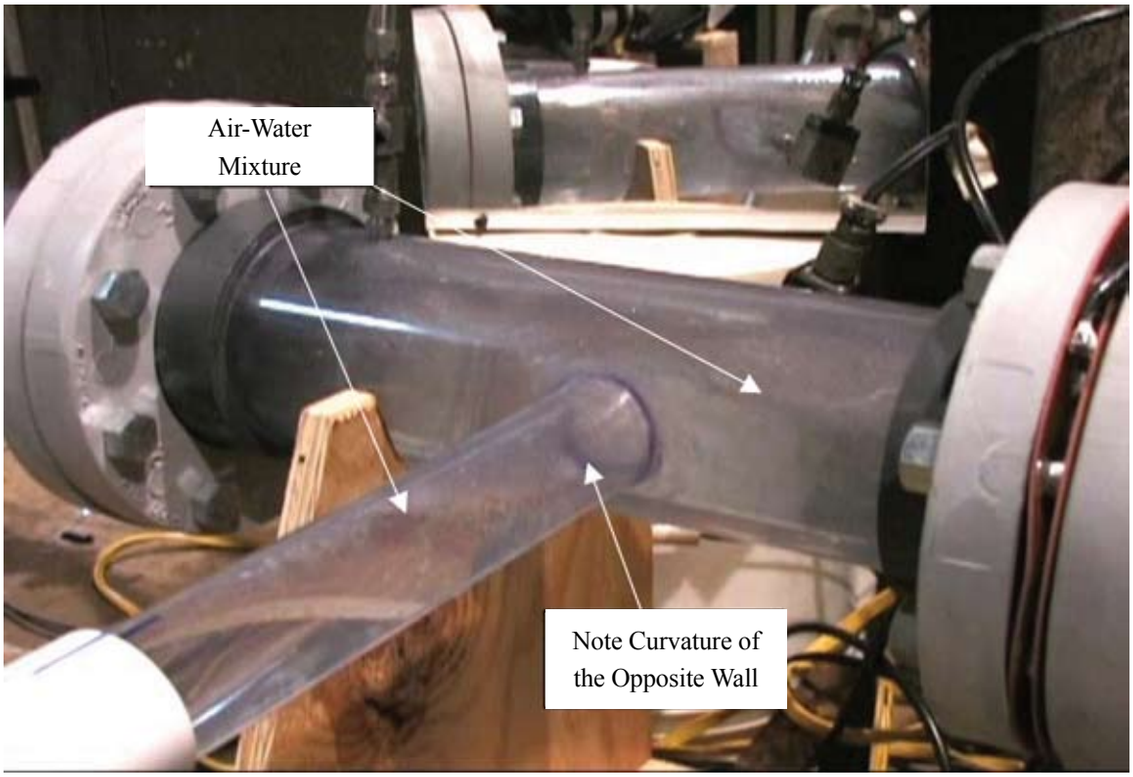

Figure 6 – Mass accumulation histories in air separator for scaled HPSI flow of 1310 gpm. (Nearly system runout conditions)

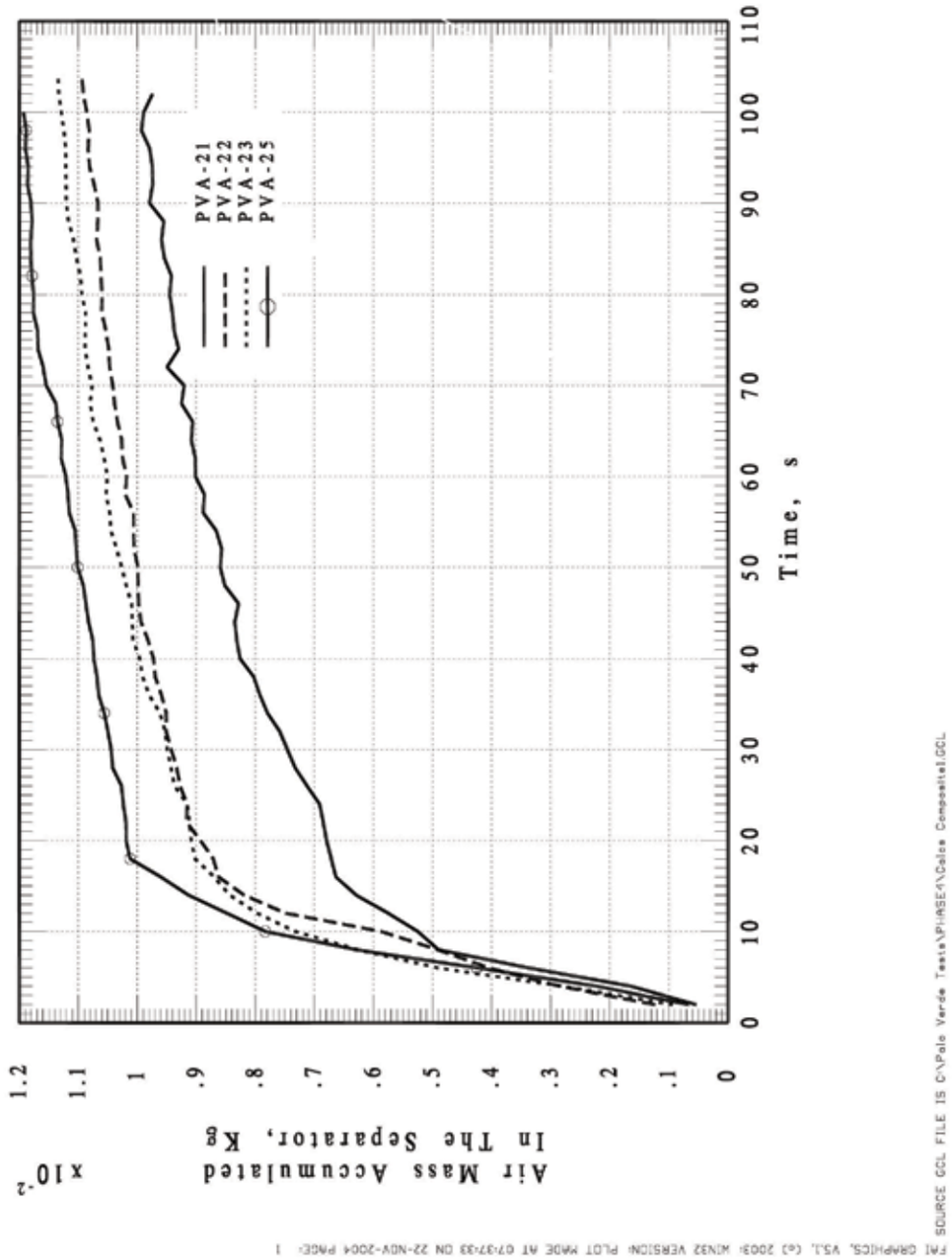

Figure 7 – Air mass flow rates to HPSI pump for scaled flow rate of 1310 gpm.

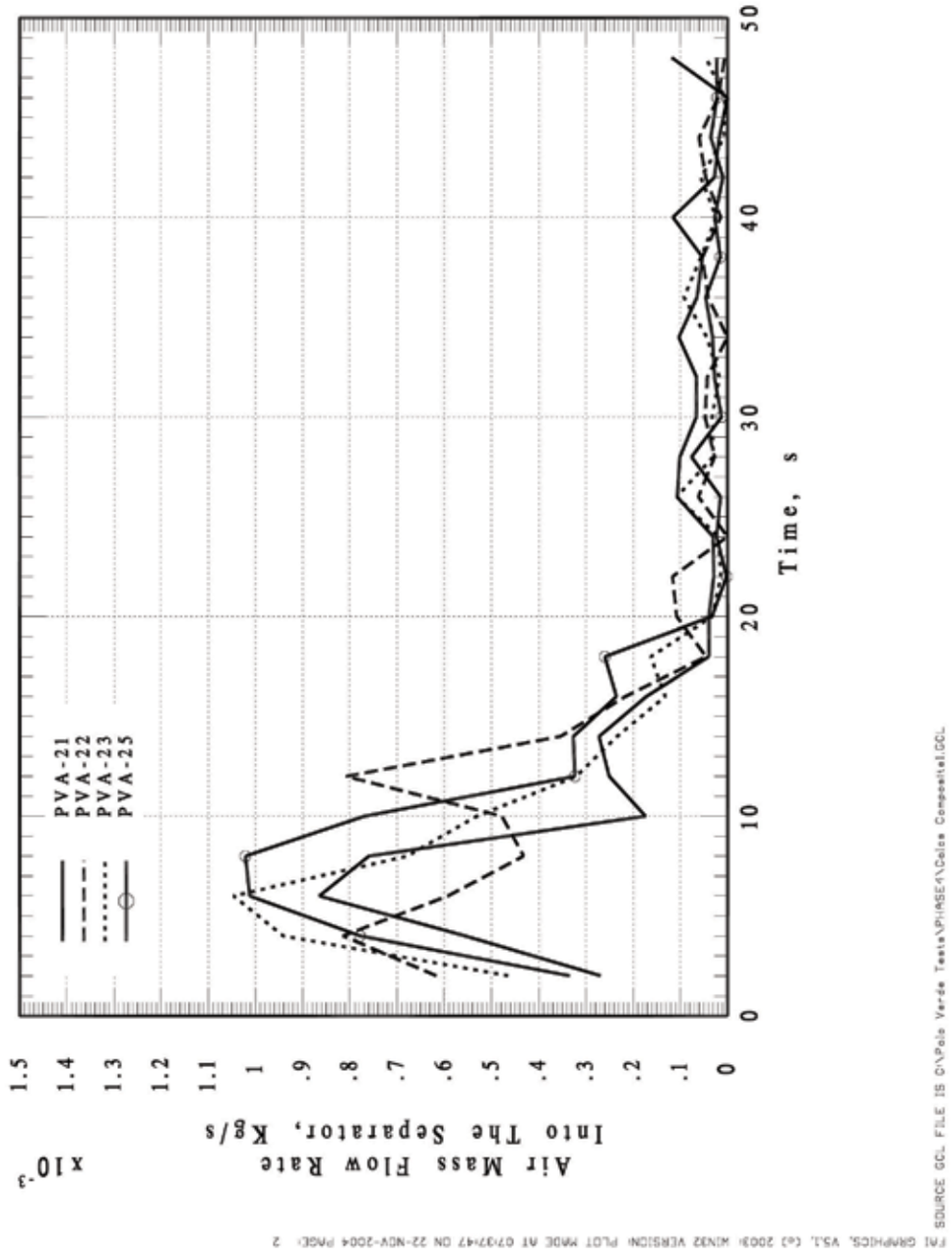

Figure 8 – Scaleup of 1/6th scaled tests to plant condition for full HPSI (1310 gpm) and CS pump flow rates.

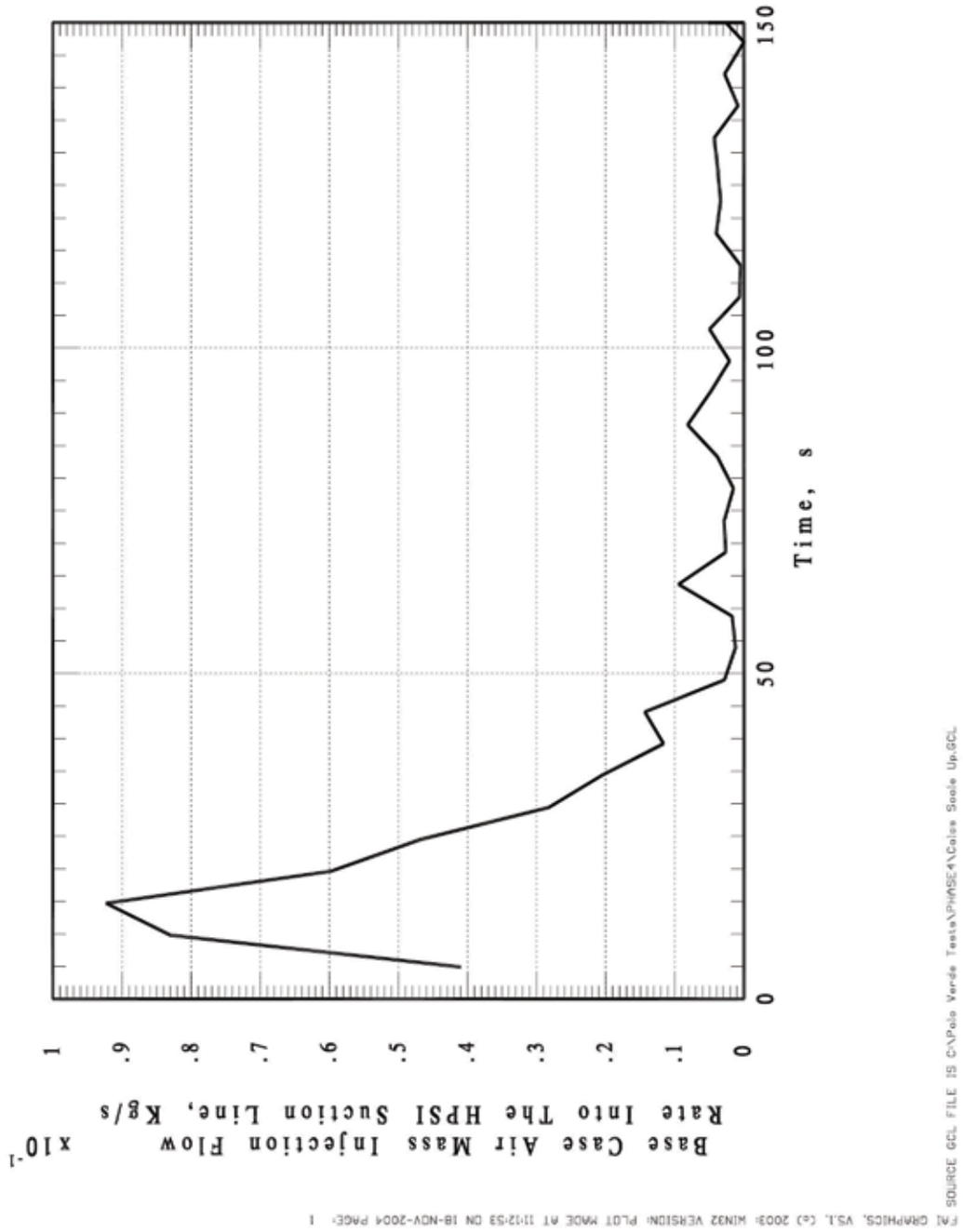

AN APPROACH TO ESTIMATING PWR ECCS THROTTLE VALVE POSITIONS IN SUPPORT OF GSI-191 EVALUATIONS

L. I. Ezekoye, *Westinghouse Electric Company*

W. E. Densmore, *Westinghouse Electric Company*

Frank Ferraraccio and Steve Swantner, *Westinghouse Electric Co.*

Abstract

In September 2004, the Nuclear Regulatory Commission (NRC) issued Generic Letter (GL) 2004-02, "Potential Impact of Debris Blockage on Emergency Recirculation During Design Basis Accidents at Pressurized-Water Reactors," to address Generic Safety Issue 191 (GSI-191) "Assessment of debris accumulation on PWR sump performance." GL 2004-02 requested pressurized water reactor (PWR) licensees to perform a "downstream effects" evaluation of their emergency core cooling system (ECCS) and containment spray system (CSS). GL 2004-02 also gave guidance on what analysis had to be completed in order to resolve GSI-191. These evaluations included a wear and plugging assessment of all ECCS and CSS components, including valves. One of the challenges in performing these evaluations is obtaining the positions of throttle valves in the ECCS. Without knowing the position of the valves, it would be impossible to assess the functionality of the ECCS during the postulated event.

The purpose of this paper is to present an approach which can be used to determine the valve position, given certain flow conditions. Working examples covering globe and butterfly valves are provided.

Introduction

In response to the NRC Generic Letter 2004-02, several nuclear power plants requested Westinghouse to complete a downstream effects evaluation of their ECCS and CSS. The ECCS and CSS in a typical Westinghouse PWR provide the ability to cool the reactor core and containment, respectively, by injecting water first from the Refueling Water Storage Tank (RWST) and then later from the containment sump. Figure 1 shows a pictorial representation of a typical Westinghouse PWR ECCS. In the case of a Loss Of Coolant Accident (LOCA), water in the containment sump may become laden with debris generated by the LOCA. This debris laden water creates the potential for blockage of valves, as well as could wear away valve internals at a more rapid rate than with debris free water.

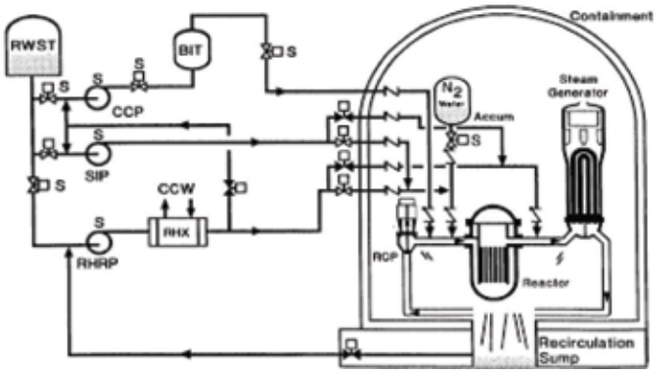

FIGURE 1 – TYPICAL WESTINGHOUSE PWR ECCS

In the process of performing the downstream effects evaluations, it was discovered that in some cases the positions of several throttled valves in High Head Safety Injection (HHSI) systems were unknown. The valves employed in these systems are varied both in size and design depending on the Architect Engineer's preference. Further, the valves can be set at any position for flow balancing. Thus, assessing the effects on the valves relative to the plugging and wear is impossible without either a) perturbing the existing flow balance by manipulating the valve to determine the position relative to full open, or b) performing calculations that should provide a reasonable guidance of valve position provided there is sufficient equipment and system data to support the analysis.

This paper describes an approach to determine the valve flow coefficient, C_V, of two valves and consequentially determine the position, using the C_V. With the valve positions defined, a downstream effects evaluation can proceed. For example, it is possible to assess if plugging can occur if the plug is close to the seat or if the valve is going to wear.

Method Discussion

The approach used to establish the position of the two throttled valves is as follows. First, determine the C_V of the throttled valve by accounting for all pressure drops in the flow path except the throttled valve in question. Second, use the resultant C_V to estimate valve position for both choked and non-choked flow. These steps are as described in further detail below.

Determination of C_v

To determine the C_V of each valve, first determine the characteristics of the flow path in which the particular valve is installed. Flow paths should begin upstream of the valve, at a point of known gage pressure relative to a point of known pressure downstream of the valve. The flow path should be constructed such that all pipe lengths, fittings, meters, valves (other than the throttled valve), and any other structure which could cause a resistance in flow is represented. See Figure 2 for a visual depiction of what a flow path should resemble. The flow path in Figure 2 consists of an orifice (upstream gage pressure point), two valves (including the throttled valve), seven sections of 1" pipe of various lengths, four pipe bends, and one sudden expansion from 1" to 2".

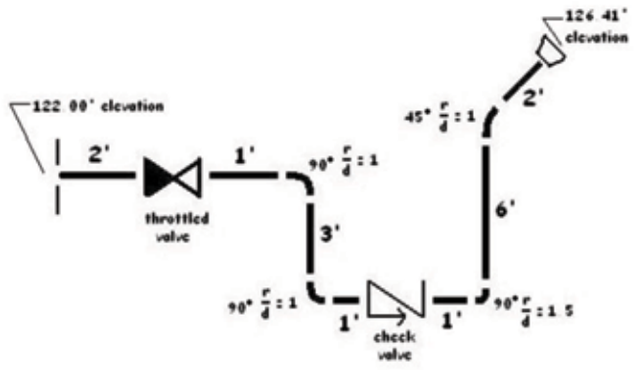

FIGURE 2: EXAMPLE OF FLOW PATH

Once a flow path is constructed, resistance coefficients should be estimated for every component of the flow path, with exception of the throttled valve. Crane Technical paper 410 (Reference 1) provides equations for calculating resistance coefficients for most components.

An overall headloss term, h_L, is then calculated for the entire flow path, using the classical Bernoulli's equation.

$$h_L = (Z_{start} - Z_{end}) + \frac{144(P_{start} - P_{end})}{\rho(g)} \quad (1)$$

where,

h_L = overall headloss in ft

Z_{start} = elevation at start of flow path in ft

Z_{end} = elevation at end of flow path in ft

$P_{start} - P_{end}$ = gage pressure relative to end of flow path in psi

p= density of water in lb/ft3

g = gravitational constant in ft/s2

Using the overall headloss term, an overall resistance coefficient, $K_{start->end}$, is then defined using equation 2.

$$K_{start->end} = \frac{2g}{v^2} h_L \quad (2)$$

where,

$K_{start->end}$ = overall resistance coefficient

v = velocity of working fluid in ft/s

h_L = overall headloss in feet

The resistance coefficients from each component, with exception of the throttled valve, are calculated and summed as:

$$K_\alpha = \sum_{i=1}^{n} K_i \quad (3)$$

where,

K_a = total resistance of other system components

K_i = individual component resistance

The individual component resistances for pipes, elbows, fittings, orifices, valves (full open), and other similar components can be estimated from engineering references (1). The resultant difference between $K_{start->end}$ and K_a represents the valve resistance, i.e. $K_{result} = K_{start->end} - K_a$.

The resultant, K_{result}, is a conservative estimation of the resistance coefficient corresponding to the throttled valve. Equation 4 is then used to convert the resultant resistance coefficient into a C_V.

$$C_v = 29.9 \frac{d_1^2}{\sqrt{K_{result}}} \qquad (4)$$

where,

d_1 = diameter of valve in inches

K_{result} = conservative resistance coefficient of throttled valve.

Determination of Position

Most throttle valves have well defined flow characteristic curves. Hence, given a C_V an estimated position can then be calculated by using the C_V. A C_V vs Turns Open curve or a C_V vs Degrees Open curve is utilized for the particular valve type in question. Both curves are easily supplied by valve manufacturers. A hypothetical globe valve C_V vs Turns Open curve is shown in Figure 3. A hypothetical butterfly valve C_V vs Degrees Open curve is shown in Figure 4.

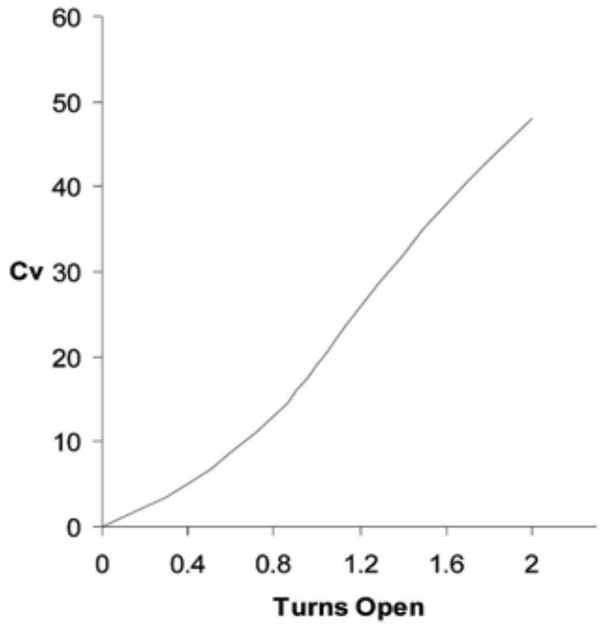

FIGURE 3 – HYPOTHETICAL GLOBE VALVE CV VERSUS TURNS OPEN CURVE

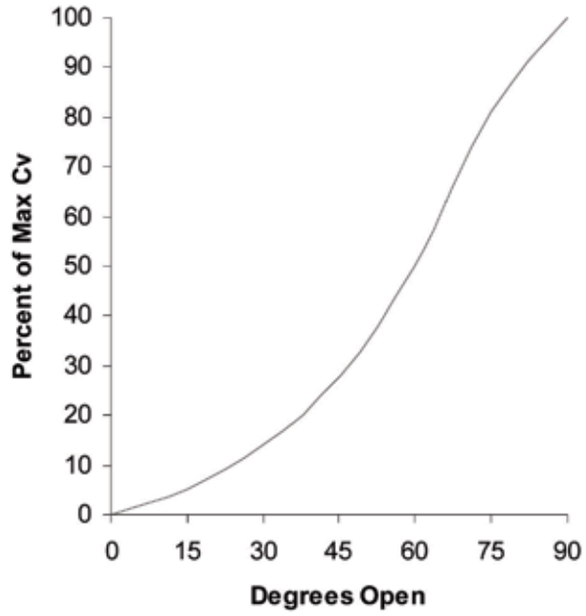

FIGURE 4 – HYPOTHETICAL BUTTERFLY VALVE CV VERSUS DEGREES OPEN CURVE

Incipient Cavitation Index

Given a C_V, a determination should be made as to whether the valve is operating under choked conditions or not. The incipient cavitation index is an appropriate gage as to the existence of choked flow. Manufacturers will routinely publish the incipient cavitation index at which their valves will cavitate. Equation 5 provides a means of calculating the incipient cavitation index of a throttled valve.

$$K_m = \frac{\Delta P}{(P_i - P_v)} \qquad (5)$$

where,

K_m = incipient cavitation index
ΔP = pressure differential across valve
P_i = inlet pressure of the valve
P_v = vapor pressure at fluid temperature

If the calculated incipient cavitation index is greater than the index the manufacturer furnishes for the valve position, the valve must be evaluated for choked conditions. If not, the current lift estimation is valid.

Adjusting for Choke Flow

In choked flow conditions, the choked flow area will be less than the frictional area of the valve for a given inlet condition. Valve manufacturers will typically have information regarding choked flow area and frictional area for their valves. And usually, manufacturers will list the choked flow area and the frictional area as functions of nozzle area.

A simple correlation can be made between the choked flow area, the frictional area and their corresponding lift positions. Equation 6 shows this simple correlation.

$$\frac{A_n}{A_f} = \frac{Lift_{choked}}{Lift_{Cv}} \qquad (6)$$

where,

A_n = choked flow area
A_f = frictional area
$Lift_{choked}$ = Lift position under choked flow
$Lift_{Cv}$ = position calculated without choked flow

Working Examples

Four (4) worked examples are provided to illustrate the methodology.

Problem Statement

For a plant at full power after many years of operation and repeated flow balancing of the ECCS throttle valves, it is not unusual that the record on where the throttle valves are set may not be readily available. However, the flow data exists. Figure 1 is assumed to represent the layout of the ECCS. The following four (4) worked examples are included to illustrate the application of the methodology developed in this paper, using information provided by readily available inputs. In example 1, the valve C_V is calculated based on the system conditions. In example 2, the C_V estimated in example 1 is used to determine the lift for a hypothetical globe valve. In example 3 the valve position in example 2 is evaluated for choked flow. Finally, in example 4 a butterfly valve is evaluated using the same methodology as was applied for the globe valve.

Worked Example #1

This worked example calculates the C_V of a valve using system data and flow balance data. The following inputs are used in conjunction with the flow path shown in Figure 1:

Flow velocity = 5 ft/s

Pipe friction factor = 0.023

P_{start} = 500 psi

P_{end} = 0 psi

Z_{start} = 122.00 ft

Z_{end} = 126.41 ft

p = 62.4 lb/ft^3

g = 32.2 ft/s^2

Utilizing Reference 1, the following resistance coefficients are calculated for the components of the flow path.

$K_{length\ of\ line}$ = 4.42

$K_{bend\ 1}$ = 0.46

$K_{bend\ 2}$ = 0.46

$K_{bend\ 3}$ = 0.32

$K_{bend\ 4}$ = 0.34

K check valve = 1.15

K sudden expansion = 0.56

K α = 7.71

Equations 1, 2, and 3 are then run to produce the following results.

$$h_L = (122.00 - 126.41) + \frac{144(500 - 0)}{62.4(32.2)} = 31.42 \text{ ft}$$

$$K_{start->end} = \frac{2(32.2)}{5^2} 31.42 = 80.94$$

$$K_{start->end} - K_{\alpha} = 80.94 - 7.71 = 73.23$$

$$C_v = 29.9\frac{1^2}{\sqrt{73.23}} = 3.49$$

Therefore, a value of 3.49 is determined to be the C_V of the throttled valve.

Worked Example #2

This worked example translates the C_V calculated in worked example # 1 in a lift position for a hypothetical globe valve. The following inputs are used in this working example:

$C_V = 3.49$

Valve Type = Typical Globe Valve

Full Open Turns Position = 2.0 turns

Full Open Lift Position = 0.23 inches

Using the previously determined C_V of 3.49 and Figure 2, the current turns open position of the valve is 0.301 turns open. Then, by use of equation 4, the turns open position is correlated to the lift position.

$$(\frac{0.23\text{in}}{2.0\text{turns}})(0.301\text{turns}) = 0.03\text{in}$$

Worked Example #3

This worked example adjusts the lift position of the globe valve calculated in worked example #2 for choked conditions. The inputs for this working example are as follows. These values are hypothetical values for hermetically sealed 2 inch valves.

$A_n = 0.68\ A_m$

$A_f = 0.84\ A_m$

A_m = nozzle area

Lift_{Cv} = 0.03 inches

Equation 6 is then carried out to determine the choked lift position.

$$\frac{A_n}{A_f} = \frac{0.68\,A_m}{0.84\,A_m} = \frac{\text{Lift}_{\text{choked}}}{0.03\text{in}}$$

$$(\frac{0.68}{0.84})(0.03) = \text{Lift}_{\text{choked}} = 0.024\text{inches}$$

After adjusting for the choked conditions, the actual lift position of the valve is determined to be 0.024 inches.

Worked Example #4

This worked example translates the C_V calculated in worked example # 1 in a lift position for a hypothetical butterfly valve. The following inputs are used in this working example:

$C_V = 3.49$

Maximum $C_V = 70$

Valve Type = Typical Butterfly Valve

Using the previously determined C_V of 3.49 and Figure 3, the current degrees open of the valve is approximately 15° Open.

ACKNOWLEDGMENTS

The authors acknowledge with thanks the constructive insights provided by Mr. Stephen Swantner and Mr. Joseph Adams, both of Westinghouse, during the development of this paper.

REFERENCES

1. Crane Technical Paper No. 410, “Flow of Fluids through Valves, Fittings, and Pipe,” 1988.

Design and construction of Two-phase coil pump

A. Nourbaksh* , M. Saleki**

Hydraulic Research Machinery Institute

University of Tehran

Abstract

In this study, the design method and construction of a two – phase coil pump have been investigated. The main characteristics, advantages, various applications of such a pump and parameters influencing its performance have been determined. Experimental results for a small and a large coil pump have been obtained. A theoretical relation has been proposed which can accurately estimate the flow rate for such pumps.

Regarding to the ability of pumping gas-liquid two phase slug flow with void fraction between 0 and 1 ($0< \alpha <1$) the domain of its application is very large comparing to the centrifugal pumps.

Keywords: Helical coil Pumps, two phase flow coil pumps

NOMENCLATURE

d = diameter of the tube

D = base diameter of the drum, 2R

L = length of the drum

n = number of turns

P = pitch of the coil (L/n)

ω = angular speed

θ = inclination of the shaft

ϕ_a = air intake angle

ϕ_w = water intake angle

$\beta = \phi_w / \phi_a$ water to air angle ratio

Q= water flow rate

H= pump head

N= rotational speed

N_R = Critical speed

Introduction:

Rotating Helical coil pumps are very attractive machines for pumping gas – liquid two-phase slug flow. This is not in the case of centrifugal pumps which are limited for passing slug flow. The coil pump has very simple construction and easy to use for operation.

The concept of helical as coil type devices for generating mechanical effort dates back to the days of Archimedes (287-212 B.C.) and Leonardo da Vinci (1452-1519 A.D.). The design of a rotating coil pump was reported in the encyclopedia of arts and science in 1745 and was credited to a Swiss scientist in Zurich named Andrew Wintz.

* Professor, anour@ut.ac.ir

** Graduate student, msaleki@me.ut.ac.ir

The idea seems to have been neglected, until 1975 when the Civil Engineering Department of the Loughborough University investigated development of a coil pump that was reported later in the Journal of the Chartered Mechanical Engineer of the U.K., ref [2].

The design and performance evaluation of a helical coil pump for operating with wind turbines for irrigation purposes and use in rural areas has been studied for more than a decade [≈1980≈1990] at the University of British Columbia and was reported in ref[1].

The same study has been investigated in Hydraulic Research Machinery Institute of University of Tehran. In this study, the focus was made to use a coil pump as a two- phase flow machine. Several prototypes have been designed and tested systematically by changing different geometrical parameters to arrive at an optimum design. The concept of a helical pump appeared to be quite attractive and promising for pumping two-phase slug flow. The main problem of this machine is low efficiency which is the subject of the next step study.

Coil pump construction & test arrangement

The main parts of a coil pump and test rig arrangement are shown schematically in

Figure(1):

1- Drum which has normally a cylindrical shape.

2- Suction and discharge reservoir.

3- Coil which is a flexible tube of desired size and turns several times around the drum. The coil inlet is in the suction reservoir and the coil outlet is connected to discharge tank by using a rotary joint.

4- Shaft and accessories.

5- Variable speed motor which provides the possibility of rotating the pump by a pulley.

Testing arrangement provides a possibility of changing systemically the parameters governing the performance of the pump including inclination of the drum Ø, tube coil diameter d, pitch of the coil P, rotational speed *w* and the ratio of water-air inlet φ_w/φ_a, Figure (2).

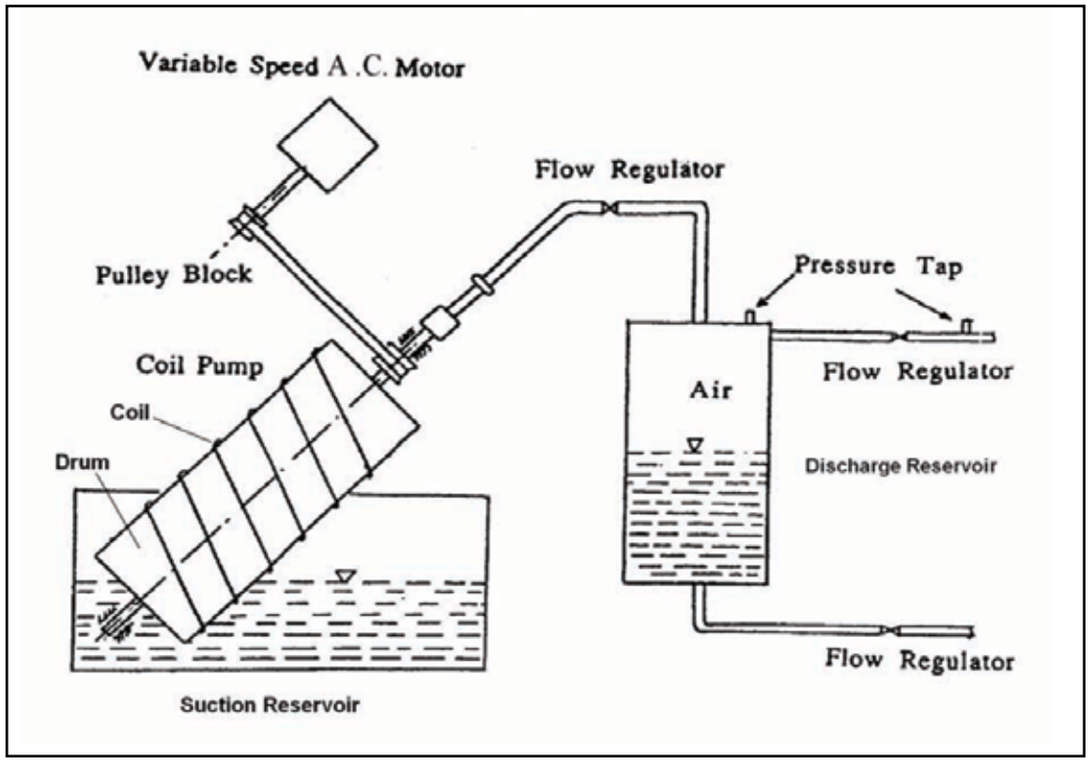

Figure 1 – coil pump and test rig arrangement

The density and temperature of liquid (water) and gas (air) are constant in these experiment tests performed by placing the pump in suction tank reservoir. The water and air intake angle φ_w and φ_a can be varied by changing the water level in the reservoir. By each turn of the drum the alternating slugs of water and air are entering in the coil inlet and transmitted though the discharge pipe. A special tank could be placed at the discharge of the pump for separating water and air.

Experimental results

The influences of many geometrical parameters on pump performance have been studied:

1- Water to air angle ratio, $ß = \varphi_w/\varphi_a$

The water level in the reservoir was observed to have a significant influence on the head and flow rate delivered by the coil pump. For low-water level, the pump delivers more air and its performance is governed by the compressibility effects of the air. But for high-water level, more water passes and the pump has relatively more stable characteristics. The head and flow rate developed by pump versus $ß = \varphi_w/\varphi_a$ are illustrated in figure (3). The water flow rate (Q) increases with a larger value of the ß (the water to air angle ratio (ß) represents the volume fraction of water to air transmitted by the pump). But the head (H) has a maximum around ß=1 to ß=1.2 depending on the different models.

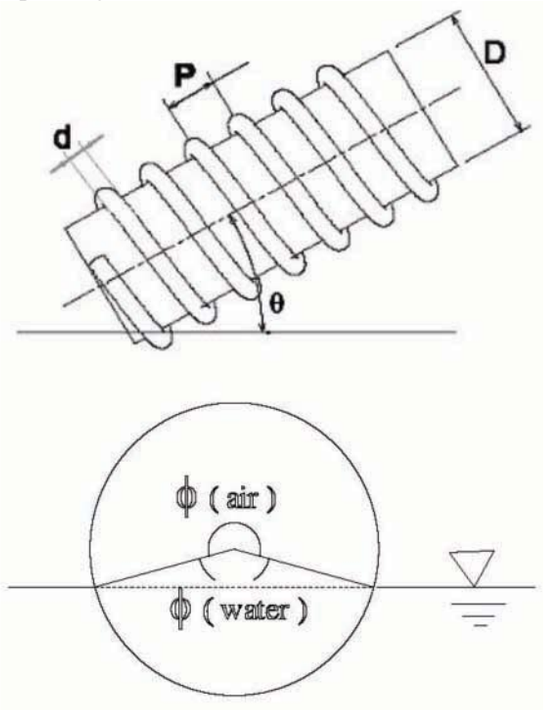

Figure 2 – Geometrical parameters of a coil pump.

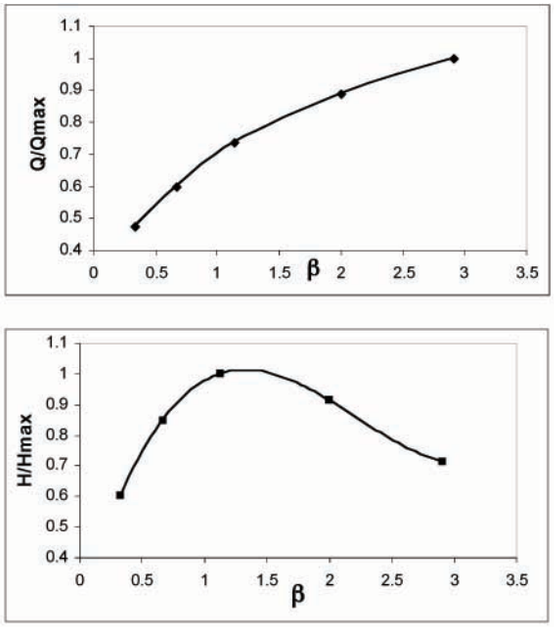

Figure 3 – Flow rate and Head versus $\beta = \phi/\phi$

2. Rotational speed (N)

The effect of rotational speed (N) on the water flow rate has been shown in Figure (4).

Each coil pump has a critical speed (N_R). By increasing rotational speed, the Head (H) and water flow rate (Q) increased until N_R when the function of pump came to be instable and both Q and H decreased rapidly.

Therefore, it is very important to determine the critical speed of a coil pump for different head and to operate the pump under this speed, Figure (5).

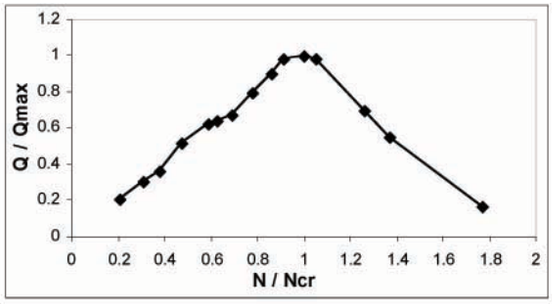

Figure 4 – variation of flow rate with rotational speed

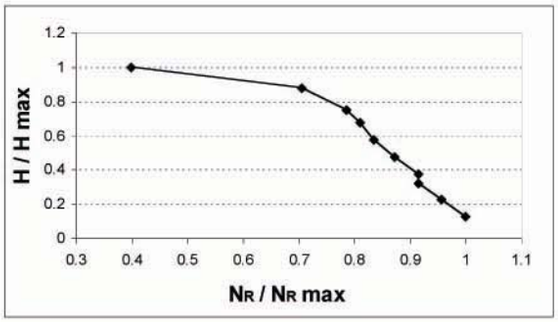

Figure 5 – limit of head delivery with critical speed

3. Coil diameter d

The flow rate increases linearly with square of coil diameter (d^2), but the head is independent of this parameter.

4. Number of turn (n)

The head increases almost linearly by increasing the number of turns of the coil where the pump flow rate (Q) is independent of this parameter, Figure (6), Figure (7).

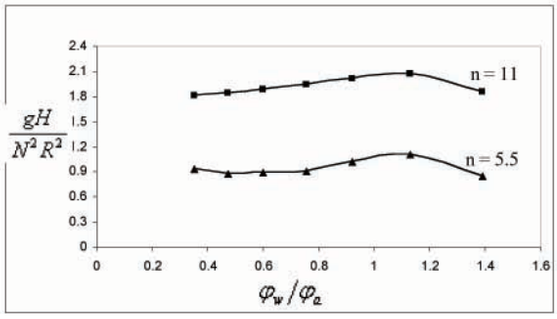

Figure 6 – variation of head with coil turn number

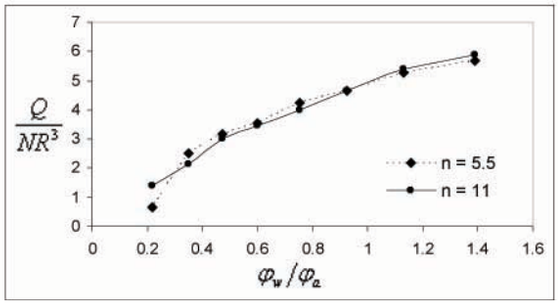

Figure 7 – variation of flow rate with coil turn number

5. Pump performance curve H= f (Q)

The performance curve of coil pump H= f (Q) is almost a vertical line parallel to H axes. See Figure (8)

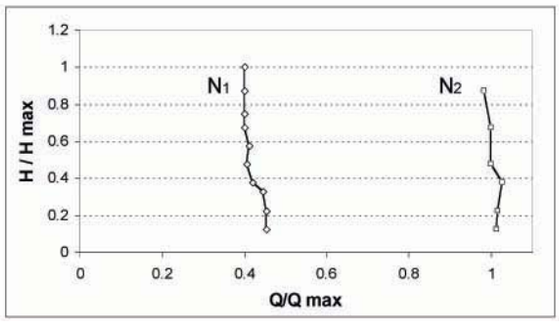

Figure 8 – pump performance curve

Theoretical investigation

Flow through a rotating helical pipe or simply helical pipe flow have been already studied [3, 4 and 5]. An analytical approach of a two-phase flow rotating coil pump is under investigation. However, the water flow rate of a coil pump could be calculated by simple equations:

$$Q_{Th} = 2\pi \frac{\beta}{\beta + 1} \cdot \frac{D}{2} \cdot \frac{\pi d^2}{4} N \qquad (1)$$

$$Q_{Th} = \varnothing_w \frac{D}{2} \cdot \frac{\pi d^2}{n} \cdot N \qquad (2)$$

The values obtained from experimental results and calculated by the equation (1) are compared in Figure (9).

Figure 9 – comparison of flow rate obtained by

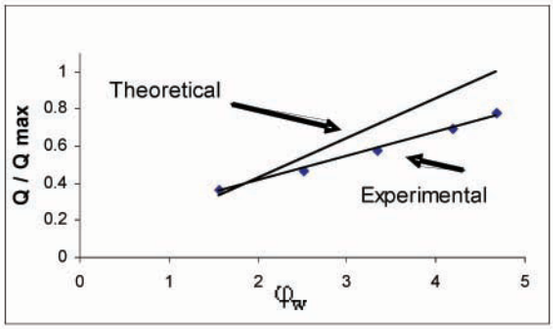

theoretical method and experimental results.

The value of flow rate calculated by the theoretical method (Q_{Th}) is always larger than obtained by experiment (Q_{EX}). However, the ratio of $K = \frac{Q_{EX}}{Q_{Th}}$ is almost constant for different values of $\frac{\varphi_w}{\varphi_a}$ for a coil pump. But this value could be changed for different coil pump depending on the size and other geometrical parameters. For the pump tested, K stays between 0.5 and 0.8.

Therefore the liquid flow rate:

$$Q = 2\pi K \frac{\beta}{\beta + 1} . \frac{D}{2} . \frac{\pi d^2}{4} N \qquad (3)$$

$$Q_{Th} = \varnothing_w . K \frac{D}{2} . \frac{\pi d^2}{n} . N \qquad (4)$$

Conclusion

From the above experimental study, one can conclude that head and water flow rate developed by a coil pump are a function of the following parameters:

$H = f(ß, N, n)$

$Q = f(ß, N, d, D)$

It is very important to notice that each pump has a critical speed N_R whose function became instable. The performance curve $H = f(Q)$ is almost a vertical line parallel to H axes.

The flow rate of a coil pump can be calculated from equations (3) and (4).

References

1. V. J. Modi and A. Nourbaksh, "Design and parametric performance of rotating helical coil pump," Fluid power: Proceedings of the Second THPS International Symposium on Fluid Power, Tokyo, 6-9 September 1993.

2. G. H. Mortimer, "Rotating Coil Pump," Chartered Mechanical Engineer, U.K. Vol. 28, No. 1 (January 1981).

3. Kyoji Yamamoto, "Flow through a rotating helical pipe with circular cross-section," I. J. Heat and Fluid Flow 21, 213-220 (2000).

4. T. J. Huttl, "Naveir – Stokes solutions of laminar flows based on orthogonal helical coordinates," I. J. Numerical Methods in Fluids 29, 749-763(1999).

5. M. Germano, "On the effect of torsion on a helical pipe flow," J. Fluid Mech, Vol.125, pp.1-8 (1982).

Accumulator Flow Rate Using Accumulator Gas Pressure for Non-Intrusive Discharge Check Valve Full Open Exercise Stroke Testing

Ernie Kee, Nathan Corrick, and Dennis Klockentager
South Texas Project Nuclear Operating Company
P.O. Box 289, Wadsworth, Texas 77483 USA
361.972.8907, KeeEJ@stpegs.com

Elmira Popova and Jack Howell
The University of Texas at Austin
Austin, Texas, 78712
512.471.7803, Elmira@mail.utexas.edu

Abstract

A new method to obtain a lower bound estimate of flow rate from the South Texas Project Electric Generating Station Safety Injection Accumulators (tanks partially filled with subcooled water and pressurized with nitrogen gas) is proposed as an alternative way to test the Accumulators' discharge check valves' full open stroke. With the new method, Containment building entry can be avoided by use of permanently installed plant process level and pressure instrumentation (recorded remotely on the plant computer, the Integrated Computer System). Avoiding Containment activities reduces total dose for the tests by about 670 millirem (mrem) and several person-hours of labor compared to other methods that require special test instrumentation installation and work in radiation areas. The effect of instrumentation uncertainty is included in the flow estimate. The lower bound flow estimate is generally useful where a minimum flow rate must be demonstrated and a sufficient margin to actual flow rate is available.

Introduction

We derived a simple method for measuring outflow from the Safety Injection (SI) Accumulators using the nitrogen gas pressure recorded on the plant computer for use in full open exercise testing of accumulator discharge check valves. Meeting the design flow rate is an acceptable non-intrusive test method for verifying that the check valve disk opens to the position necessary to perform its safety function. The outflow calculated by the simple method is based on isentropic expansion of the nitrogen in the accumulator so we can be sure the outflow we calculate will be lower than actual. Because the method produces the lowest possible flow measurement, it is appropriate to use it to compare against the minimum acceptance criteria (that is, the measured flow must exceed the minimum required value for an acceptable test).

The method is most useful when the installed plant level measurement isn't available over a sufficient range to measure the outflow rate. However, the method can also be used in conjunction with other methods as a confirmation of check valve test results from them.

Background

The South Texas Project (STP) is a two unit, pressurized water electric generating station. Each of the units has three individual SI accumulators installed to inject water into the reactor following a postulated pipe failure large enough to temporarily exhaust the normal water inventory in the reactor. The water is chemically treated with neutron-absorbing boric acid to help prevent return to criticality following a postulated accident. The SI accumulators are filled to a specified level with water such that there is enough air space above the water to allow them to be pressurized with nitrogen. The pressure in the accumulator is kept lower than the pressure in the reactor under normal operating conditions.

In the unlikely event of a postulated large pipe failure, the pressurized nitrogen in the accumulators would force the chemically treated water into the reactor as pressure drops below the SI Accumulators' pressure. By using trapped pressurized nitrogen, the SI accumulators do not require any external motive force to restore the reactor water inventory. During normal operation, higher pressure reactor water is kept out of the accumulators by check valves. If the reactor pressure drops below the accumulator pressure, water gets forced past the check valves due to the pressure difference. A motor operated valve is installed in the accumulator outlet to keep the water in the accumulators against nitrogen gas pressure during refueling or other plant operations that cause the outlet pressure (reactor pressure) to be lower than the accumulator nitrogen pressure. The check valves require testing under the American Society of Mechanical Engineers (ASME) Code for Operation and Maintenance of Nuclear Power Plants (OM Code) during refueling outages.

STP has been testing the SI Accumulator check valves using locally installed, temporary acoustic monitoring instrumentation. To install the equipment, scaffolding is required and several personnel must be in radiation areas for significant periods of time during the testing. We have found that, as the plants age, the dose rates in the areas the test instruments are installed result in significant worker exposures (a little under 700 mrem to test the three accumulators). Significant labor and test equipment expense is also a consideration. The testing method we describe in this article effectively eliminates worker radiation exposure for SI Accumulator discharge check valve stroke testing and significantly reduces time spent in testing activities by taking advantage of existing process instrumentation measuring SI Accumulator pressure and water volume.

Approach

Since the SI Accumulators contain a trapped volume of nitrogen, any change in the contained water volume will result in a pressure change which can be read on the gas pressure measurement instruments. We are interested in cases where the water is exhausting from the tank. As long as sufficient water remains in the tank, the nitrogen will expand in reaction to a piston-like action.

Small amounts of heat addition will occur during an expansion process due to gas cooling below the wall and liquid surface temperature during expansion. The different thermodynamic processes governing gas expansion in normal pressure and temperature ranges (such as in the accumulator) are well known and have been established for many years. The extreme thermodynamic processes for this piston-like action are isothermal (where the heat addition brings the temperature back to the pre-expansion value) and isentropic (reversible and adiabatic). Clearly, as long as highly subcooled liquid remains in the tank, any increase in gas volume corresponds to an equal reduction in liquid volume. If the time duration of the expansion is known, the volumetric outflow rate is the same as the volumetric gas expansion rate. Finally if the expansion is observed over small time increments, the volumetric flow can be calculated. Note that since the check valve test starts with no flow, builds to a maximum, and decays off, averaging the flow over discrete time intervals produces lower than actual flow measurement.

Referring to Figure 1, if the pressure in the tank is measured at regular intervals, Ti, and the gas volume is V, then when the outlet valve is opened, the gas will expand and water will exhaust (assuming the nitrogen pressure in the tank is above the pressure on the liquid free surface at the outlet) as illustrated in Figure 2. The pressure history from a typical test will look similar to Figure 3 while the discharge valve is opened and closed.

Although in fact the nitrogen expansion process is polytropic, we assume isentropic for the purpose of flow measurement. By making this assumption, when we use the pressure history to find the rate of gas expansion we will underestimate the gas expansion (since the process actually will be closer to an irreversible, isothermal process). Clearly, heat transfer from the walls and the water surface will contribute to isothermal expansion. Since no external work is present and no other heat sinks are present, the isentropic process is limiting. The general form of the isentropic expansion process during a time increment from T_0 to T_1 (taking the nitrogen volume to be V_1 at T_1) is defined by the equation:

$$\frac{p_0}{p_1} = \left(\frac{V_1}{V_0}\right)^{\gamma} \qquad \text{(Eq. 1)}$$

The value of g for nitrogen can be taken to be 1.4. Also note that the gas pressure must be in absolute pressure (not gauge pressure). Typically, the plant process computer will record the pressure as gauge pressure. We use measurement of level, pressure, and time difference for flow rate. Both the pressure measurement and level measurement have a degree of uncertainty. The level measurement is used only for the

initial level in order to obtain the initial nitrogen volume, V0, and so we don't need to worry about additional uncertainty in the level measurement beyond what exists at the start of the flow measurement. At STP, the level in the accumulators is measured as the total contained water volume, but we are interested in the air volume. Generally, the total contained volume of the accumulator is known from the design documents, so it is easy to find the air volume by simply subtracting the water level (volume) from the total. If there are multiple measurements of level, they can be combined to obtain a more accurate estimate of initial level. However, (in general) one must be careful to properly characterize and combine the uncertainties in each of the measurements to obtain the best estimate of the combination.

For the purposes of the flow measurement, the most conservative direction of the level error is in the direction of lower initial nitrogen volume (inspect Equation 1 with the thought in mind that smaller V_0 calculated from the pressure measurements will produce smaller volumetric increase in the nitrogen space).

Similar to the level measurement, the pressure measurements are subject to uncertainty. In the case of pressure measurement, the uncertainty during the test is important. That is, random fluctuations in pressure could cause the flow rate measurement (increase in air volume) to be larger than without the uncertainty. This could lead to falsely concluding the flow rate was sufficiently high to pass the test (simply due to random noise in the measurement).

As in the level measurement, redundant pressure measurements, where available and properly characterized and combined, can produce much more accurate estimates than a single measurement. When relatively large, random fluctuations are in the pressure measurement, it is possible that using the fractional change in pressure (the pressure ratios at adjacent measurement times) will produce more stable flow rates.

Referring to Equation 1, enumerating successive plant computer measurements of pressure with the subscript i and enumerating successive measurement intervals (i to i+1) with the subscript j then the change in volume for measurement interval j = 0 would be:

$$\left(\frac{p_0}{p_1}\right)^{1/\gamma} = \frac{V_1}{\hat{V}_0} \qquad \text{(Eq. 2a)}$$

taking the error in initial level measurement as ε and $\hat{V}_0 = V_0 - \varepsilon$. Or, keeping in mind we want to use fractional values at each measurement interval, add and subtract 1.0 on the RHS [right hand side] of Equation 2a:

$$\left(\frac{p_0}{p_1}\right)^{1/\gamma} = \frac{V_1 - \hat{V}_0 + \hat{V}_0}{\hat{V}_0} \qquad \text{(Eq. 2b)}$$

let $\Delta V_j = V_{i+1} - V_i$ and rewrite Equation 2b:

$$\Delta V_0 = \hat{V}_0 \left[\left(\frac{p_0}{p_1}\right)^{1/\gamma} - 1\right] \qquad \text{(Eq. 2c)}$$

The flow at this interval is then simply the volume change divided by the measurement time interval, Δt :

$$Q_0 = \frac{\Delta V_0}{\Delta t_0} \qquad \text{(Eq. 2d)}$$

After incrementing *i* and *j*, the volume at the beginning of the next time step (V_i with $\hat{V}_o$ as the first) is found by deducting the change in air volume during the previous time increment from the air volume at the start of the previous tme increment:

$$V_i = V_{i-1} - \Delta V_{j-1}$$

Flow rates at successive time intervals are then found from deducting the last change in air volume from the starting air volume and solving for the next change in volume using the pressure ratio for the interval:

$$Q_j = V_i \left[\left(\frac{p_i}{p_{i+1}}\right)^{1/\gamma} - 1\right] \qquad \text{(Eq. 2e)}$$

The error due to random noise in the pressure measurement can be quantified using the pressure instrument outputs at steady state conditions using Equations 2 to obtain, for example, the variance in the output and then applying a confidence interval to obtain a good bound. This error can be simply added to the minimum flow requirement (that is, raise the minimum acceptance criteria by the amount of the random error).

Equations 2 were applied to actual test measurements in STP Units 1 and 2 for the last set of tests performed (three accumulators in each unit having 2 check valves each). In each of the tests, the results using the current method (acoustic measurement) the check valves stroked open satisfactorily. Figure 4 compares the solutions to Equations 2 against the flow limit for the STP SI Accumulator check valves (about 200 Liters per second [L/s]). As can be seen, the limiting flow was met and exceeded for each of the SI Accumulators' tests.

Cost savings

Currently, the approximate total baseline cost for the complete SI Accumulator check valve testing is approximately $38,100 each performance (once every nine months based on an 18 month outage cycle on two units) with radiation exposure included as a dollar cost. The cost breakdown is shown in Table 1. The costs listed in the table are not exact in general, but instead are based on actual costs for a recent check valve test performance in which all three SI Accumulators' check valves were tested in one unit.

The major costs associated with implementing the simplified method come down to development costs associated with creating the plant process computer application and engineering time to develop and verify the method. Table 2 gives a rough estimate of the development costs, inflation, and the rate of return on capital employed as inputs to the analysis. While the inputs to this type of analysis are subject to relatively large uncertainties, in the present case, the extremely short payback (shown below) and low cost of development compared to the ongoing costs don't justify a detailed sensitivity study on the inputs.

We assume ongoing costs associated with the pressure measurement method are negligible compared to the current method, based on automation of the process allowing the Operator to set up and perform the test using the plant process computer Control Room display of installed instrumentation measurements and then simply print out a test report upon completion. Also, plant process computer processing burden (CPU, data storage, and memory requirements) costs are negligible due to the small computational load and the addition of a small number of data points.

The cost of the current method using discounted cash flow is evaluated for a 5 year and 10 year project assuming 3% inflation, 8% return on capital employed, and 18 month cycle duration. The results of this analysis are shown in Table 3 showing that the project pays back in the first year (first outage) and is worth slightly less than $240,000 in five years and about $400,00 in ten years of useful life.

Conclusions

Development of a simple pressure based accumulator exit flow estimation method has been presented. The theoretical basis of the method has been described. Using the isentropic flow assumption and time averaging produces a theoretical minimum flow rate estimate for the conditions of the test.

The cost savings (including radiation dose as a dollar cost) for using the simplified method over the current method at STP has been shown using a discounted cash flow calculation for up to 10 years of useful life. The simplified method is estimated to pay back in the first year of use and is worth slightly less than $240,000 over 5 years of useful life.

Table 1. Approximate costs incurred using the current method per performance each outage (three SI Accumulators), including radiation.		
Item	Effort	Cost
Measurement equipment setup and testing		
Instrument	4 shifts X 2 techs/shift X 12 hours @ $40/hour	$3,840
Engineering coordinator	4 shifts X 1 Section XI coordinator/shift X 12 hours @ $40.00/hour	$1,920
Operations coordinator	4 shifts X 1 Ops coordinator/shift X 12 hours @ $40.00/hour	$1,920
Test measurements	10 participants X 4 hours @ $40.00/hour	$1,600
Other equipment setup		
Scaffolding (primarily labor)	32 hours per 4'X8' footprint @ $35/hour; 2 footprints X 3 trains (SI-38/ 46A,B,C)	$6,720
Test equipment maintenance	Miscellaneous installation costs due to scheduling and parts (mounts, studs, etc.)	$2.000
Radiation exposure	30,000 $/rem X .670 rem	$20,100
	Total	***$38,100***
Cost per year, with 18 month schedule in each unit (multiply Total by 1.33)		***$50,800***

Table 2. Approximate development costs for the simplified testing method (incurred in the first year of use)		
Procedure revisions	1 person-week	$4,000
Method development and qualification	1 person-week	$4,000
Process computer application development	2 person-weeks	$8,000
Software Quality Assurance	2 person-weeks	$8.000
Training (development and training time)	2 person-weeks	$8,000
Total		***$32,000***

Table 3. Discounted cash flow calculations of the net present value using the current method of testing.			
Year after implementation	Cash flow escalation due to inflation (at 3%)	Discounted cash flow (8% discount rate)	Net present value of the discounted cash flow for the corresponding year(s) after implementation
0	$18,800 ($50,800-$32,000)	$18,800	$18,800
1	$52,324	$48,448	$67,248
2	$53,894	$46,205	$113,453
3	$55,511	$44,066	$157,519
4	$57,176	$42,026	$199,545
5	$58,891	$40,080	$239,626
6	$60,658	$38,225	$277,850
7	$62,478	$36,455	$314,305
8	$64,352	$34,767	$349,073
9	$66,282	$33,158	$382,231
10	$68,271	$31,623	$413,853

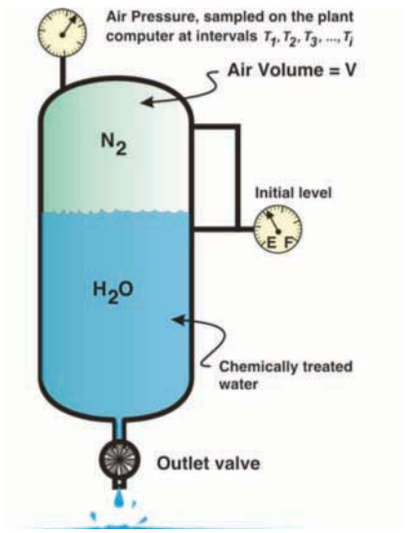

Figure 1 – Accumulator prior to opening the outlet valve.

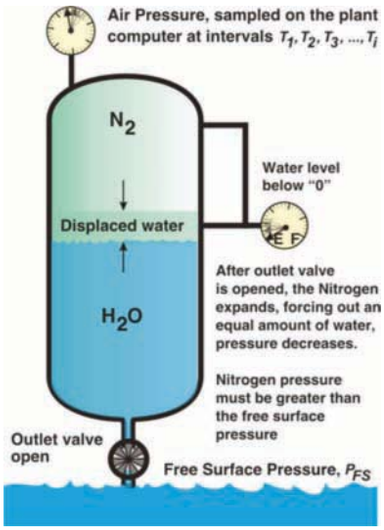

Figure 2 – Accumulator schematic showing displacement of the water during a test.

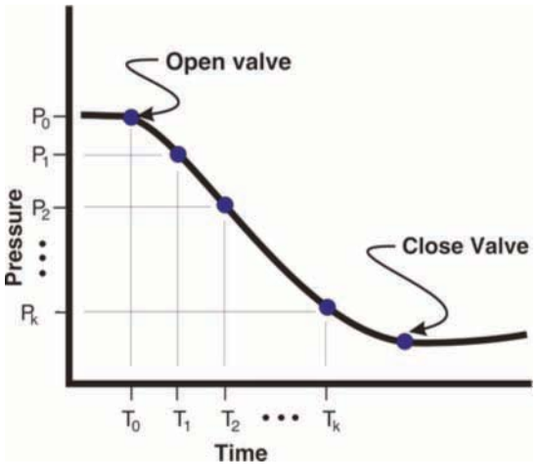

Figure 3 – Typical pressure history of a check valve test showing sample intervals, T1, T2, T3, ..., Tk.

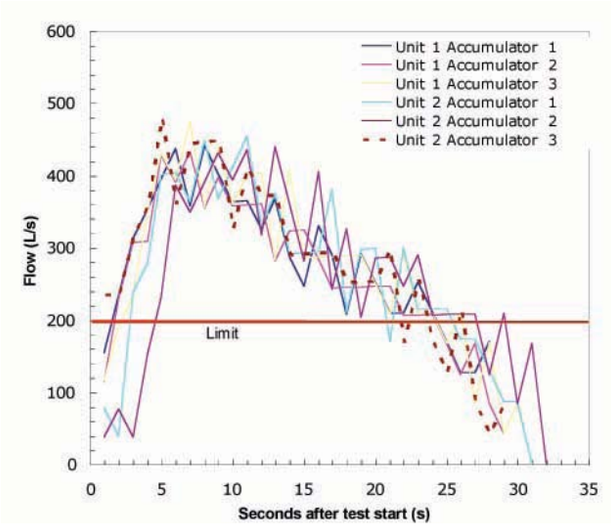

Figure 4 – Flow rates measured in last set of tests in STP Units 1 and 2 in all three SI Accumulatorscompared with the required limit. [3200 gallons per minute (gpm) plus 200 gpm uncertainty = 214.5 L/s]

Session 3(b):
Valves II

Session Chair

Dr. Claude L. Thibault

Consultant

Characteristics of New Valve Seats, Including Surface Roughness After Long Time Exposure to Reactor Water Condition

Yoshihisa Kiyotoki
Hitachi, Ltd., Power Systems, Nuclear System Division

Mitsuo Chigasaki, Junya Kaneda, and Yusaku Maruno
Hitachi, Ltd., Hitachi Research Laboratory,
Department of Materials Research for Power Plants

Abstract

Valve seat aging after long time exposure to reactor water condition has been discussed recently [1]. As the countermeasure for the valve seat aging problem, we have developed the valve "HHV*" with a new valve seat. The evaluation result report of HHV shows that the new valve seat is superior to the conventional valve seat, in terms of corrosion-resistance, coefficient of friction, mechanical-sturdiness, low residual stress, erosion-resistance, low cobalt (Co) release and nondestructive inspection possibility. [2]

To confirm the characteristics of the new valve, an appraisal test at operating plant condition was carried out. We reported that the new valve seat was superior to the conventional valve seat.[2]

Now, we are reporting the new valve seat's characteristics, including the surface roughness and the coefficient of friction due to aging, under the circumstance of the BWR (boiling water reactor) reactor water condition. For the evaluation of the seat surface roughness and the coefficient of friction due to aging, the valve seat specimens (Stellite 6 and new valve seat) were aged in a corrosion autoclave. The result shows that the surface roughness change of the new valve seat due to aging is smaller and the coefficient of friction of the new valve seat due to aging is lower than that of the conventional valve seat. The evaluation result report of the new valve seat shows that the new valve seat is superior to the conventional valve seat in terms of all characteristics including secular change. As described above, it can be said that the use of the valves incorporating the new valve seat in actual nuclear power plants will not only increase the reliability and maintainability of the valves, but also contribute to the increased reliability and maintainability of the plants, in comparison with the use of the valves incorporating the conventional valve seats hardfaced with a Co-based alloy.

*: HHV is the valve with new cobalt base alloy valve seat, whose metal microstructure is different from that of the conventional cobalt base welded overlays.

Introduction

The valves used in nuclear power plants have the seat portions of their valve bodies and the valve casings (hereinafter referred to as valve seats) hardfaced with a Co-based alloy (mainly RCoCr-A, AWS standard) in order to minimize the degradation in the sealing capability and the operational performance of the valves. However, the hardfaced portions are degraded and/or damaged due to surface roughness, cracking, and/or erosion, requiring the repair and/or replacement of the valve seats. In addition, the set pressure drift of safety relief valves, which is called "corrosion bonding," are caused by the adhesion force generated by the corrosion products. Therefore, in terms of the reliability and maintainability of the valves, it is required to minimize the occurrence of the corrosion, cracking and/or erosion of the valve seats. Furthermore, in nuclear power plants, it has been required for a long time to minimize Co release from the valve seats in order to reduce the radiation exposure of the nuclear power plants workers.

In addition to the problems described above, recently it has been pointed out that the friction force on the valve seat made by a Co-based alloy welded overlay increases under the environment of nuclear power plant coolants [1]. The improvement of the valve seat material made by Co-based alloy has been required also for maintaining the operation performance of the valves.

On the other hand, focusing attention on the degradation mechanism of the Co-based hardfacing material(s) used on the valve seats in nuclear power plants, we have

demonstrated that the degradation mechanism can be minimized by changing the metallic structure without altering the chemical composition of the metal, and that the valves can be manufactured having the valve seat material with its various Co-based alloy characteristics improved with this method.[2)]

However, the report described above which evaluated the friction force on the valve seats only made evaluations on the friction characteristics of the valve seats associated with frequent operation. The report did not refer to the evaluation of the friction characteristics of the valve seats associated with aged deterioration under the environment of nuclear power plant coolants. Therefore, we re-evaluated the new valve seat hardfaced with a Co-based alloy containing dispersed eutectic carbide (hereinafter referred to as new valve seat, or developed valve seat) in all aspects. We thought that the new valve seat material developed exhibited less surface roughness under a corrosive environment, compared with conventional valve seat welded overlay with a Co-based alloy containing mesh-like eutectic carbide (hereinafter referred to as conventional valve seat), and added the comparisons of the changes in the surface conditions and the friction force between the conventional valve seat and the new valve seat under the corrosive environment. Shown below are the comparisons of the characteristics including aged deterioration and friction force changes between the conventional valve seat and the new valve seat.

2. Valves having new valve seat

2.1 Basic concept of new valve seat material

For valve seats made by corrosion- and wear-resistant, carbide-dispersed alloy, the metallic structure of the conventional valve seat material is composed of mesh-like eutectic carbide and dendrite. The damaging mechanism is as follows: “First, the mesh-like eutectic carbide is corroded and dropped off due to the dissolved oxygen in fluid. Then, the dendrite is damaged and dropped off due to the mechanical force of the flow. The chemical corrosion and mechanical erosion are repeated to expand the damage to the valve seats, which may produce cracks, depending on the condition of the residual stress.” In addition, Co release from the valve seats, which is said to be a cause for the radiation exposure of workers in nuclear power plants, is thought to occur in the process of this degradation and damaging mechanism.

The observation of the corrosion, cracks, erosion, and Co release that occurred on the Co-based alloy welded overlay material of the valve seats of the valves in actual operating plants confirmed that each of these phenomena was produced by the damaging mechanism above described (see Fig. 1). As a countermeasure against this degradation and damaging mechanism, we thought that a new valve seat material in which the eutectic carbide particles are dispersed in the metal matrix can control the repetition of the chemical corrosion and the mechanical erosion; thereby, minimizing the possible damage to the valve seats as well as Co release. Shown in Fig. 2 are the comparisons, as described above, of the degradation and damaging models between the conventional valve seats and the new valve.

Valve seats were manufactured according to the development concept for the new valve seats above described. Shown in Fig. 3 is the comparison of the metallic structure of the conventional valve seats with that of the new valves. Both types of the valve seats have the chemical composition falling within the range of RCoCr-A (AWS standard).

2.2 Characteristic evaluation

2.2.1 Required characteristics

The following seven characteristics are required for seats of valves used in nuclear power plants:

① Corrosion resistance: The surface roughness caused by aged deterioration should be less. Such roughness may cause leakage or poor operation.

② Sliding property and antigalling property:

(a) The surface roughness associated with frequent operation should not cause sliding resistance large enough to lead to galling.

(b) The surface roughness associated with aged deterioration (secular change) should be small and not cause sliding resistance large enough to lead to galling.

③ Mechanical Sturdiness: The mechanical sturdiness is necessary to prevent the occurrence of valve seat cracks and thus should be maximized.

④ Lower residual stress: Higher tensile residual stress is one of the factors causing valve seat cracks. Residual stress should be minimized as much as possible and, where applicable, compressive residual stress is preferable alternative.

⑤ Erosion resistance: The resistance to erosion should be high under the service conditions. Especially in nuclear power plants, higher resistance to erosion is required in the circumstance of higher dissolved oxygen at higher temperatures.

⑥ Low Co release property: In nuclear power plants, it is required to reduce the amount of Co release from the Co-based alloy in order to lower the radiation exposure of nuclear power plant workers.

⑦ Ease of work and inspection: The alloy should facilitate the detection of the surface and internal defects by non-destructive inspection as well as the fitting work.

2.2.2 Performance evaluation

We conducted performance evaluation tests on the valves incorporating the new valve seats that were designed to meet the seven requirements described above. Summarized in Table 1 are the results of the tests. In comparison with the valves incorporating conventional valve seats, the valves incorporating the new valve seats exhibit the following characteristics: ① Superior corrosion resistance; ② lower coefficient of friction and less aged deterioration (secular change); ③ higher impact strength and toughness; ④ having residual compressive stress instead of residual tensile stress; ⑤ Much higher corrosion resistance; ⑥ approximately one tenth or less of Co release under the condition which needs to minimize Co release; and ⑦ detection of minor internal defects enabled by ultrasonic test (UT).

Detailed below are the results of the evaluation of the characteristics outlined above. (see Table 1)

(1) Corrosion resistance

Strauss test(s) (JIS G0575) were conducted in order to compare the conventional valve seats with new valve seats. Shown in Fig. 4 is the comparison of the results of the Strauss tests run on conventional valve seats and new valve seats. Specifically, the figure shows the cross sections of the specimens cut after undergoing the Strauss tests. As is evident from the figure, the conventional valve seats were selectively corroded and damaged down to quite a deep level; on the other hand, the new valve seats were hardly damaged. Hence, the new valve seats provide better corrosion resistance than the conventional valve seats.

(2) Sliding property and antigalling property

i) Changes in coefficient of friction caused by frequent operation

In order to evaluate the sliding property and antigalling property of the new valves, the sliding property and antigalling property of new valve seats were compared with those of conventional valve seats by reciprocally sliding a movable piece simulating a valve body against a fixed piece simulating the valve seat on the valve casing side in ordinary-temperature water.

Shown in Fig. 5 is the result of the sliding test performed in ordinary-temperature water. The new valve seats exhibit a smaller coefficient of friction than the conventional valve seats by approximately 30%. As evident from this result, the valves incorporating the new valve seats require less driving force and provide better operational reliability of valves than the valves incorporating the conventional valve seats hardfaced with a Co-based alloy.between conventional valve seats and new valve seats

ii) Changes in valve seat surface conditions caused by aged deterioration (secular change)

In order to compare aged deterioration (secular change) of the conventional valve seats with that of new valve seats under an actual operating environment, a corrosion resistance test was conducted in high-temperature water containing a high percentage of dissolved oxygen (288°C; DO:8 ppm [parts per million]) to investigate the changes in the valve seat conditions. Before the corrosion resistance test, the entire valve seat faces were buffed, and the valve seat surfaces of both conventional valve seats and new valve seats had an average surface roughness (Ra) of 0.03 μm [micrometer].

Shown in Fig. 6 are the measurements of the surface roughness of the valve seat surfaces after a specified test time elapsed. The conventional valve seats exhibited greater surface roughness as the test time went by: The surface roughness Ra of the valve seat faces was 0.11 μm after 2078

hours elapsed. On the other hand, the surface roughness (Ra) of the valve seat faces of the new valves slightly increased to 0.05 μm until 500 hours elapsed from the start of the test, and then remained constant until 2078 hours elapsed. As described in paragraph (1) on Corrosion resistance, the mesh-like eutectic carbide precipitated on the conventional valve seats is distributed continuously in the dendrite gaps. Therefore, corrosion will advance continuously along the carbide into the inside of the valve seats if the carbide in contact with the surfaces of the valve seat faces is selectively corroded and damaged. On the other hand, on the new valves carbide is dispersed in granular conditions. Therefore, corrosion will not advance continuously even if the carbide in contact with the surfaces of the valve seat faces is selectively corroded and damaged. For the reasons described above, it is thought that the surface roughness of the new valve seats did not increase after a lapse of 500 hours in the corrosion resistance test.

From these results, the new valve seats are determined to exhibit less surface roughness across ages and expected to show smaller sliding resistance associated with aged deterioration.

After evaluation of the surface condition of valve seats, abrasion resistance tests for evaluation of coefficient of friction were conducted under room temperature water condition. Shown in Figure 7(1) is the example of the coefficient of friction plots of the valve seat after 1000 hours elapsed in high-temperature water containing high percentage of dissolved oxygen (288°C; DO: 8ppm). The results show that the coefficient of friction of new valve seat exhibited lower than that of conventional valve seat. The results of the abrasion resistance tests of 250 hours and 500 hours show the tendency which is similar to that of 1000 hours. Shown in Figure 7(2) are plots of CF* vs. Initial coefficient of friction of conventional valve seat and new valve seat, aged after 250 hours, 500 hours, and 1000 hours in high-temperature water containing a high percentage of dissolved oxygen (288°C; DO: 8ppm). The results of the test (the plots of CF* vs. Initial coefficient of friction of conventional valve seats) show more widespread distribution, compared to that of new valve seats.

*: CF means the difference of highest coefficient of friction and the initial coefficient of friction at individual abrasion resistance test.

The coefficient of friction threshold values, which are estimated from the CF vs. Initial coefficient of friction plots, are shown below.

Conventional valve seat: 0.48

New valve seat: 0.42

From these results, the new valve seats are determined to exhibit lower and more stable coefficient of friction associated with aged deterioration, compared to the conventional valve seat.

(1) The coefficient of friction plot of the valve seats,

The result of abrasion resistance test(s)

(2) △CF* vs. Initial coefficient of friction plots

*△CF : The difference of largest coefficient of friction and the initial coefficient of friction at abrasion resistance test.

(3) Mechanical Sturdiness

Charpy impact test(s) were conducted at ordinary temperatures in order to compare the mechanical sturdiness of the conventional valve seats with that of the new valve seats. As the specimens for the impact tests, flat specimens and U-notched specimens were used. The test results are shown in Table 2.

As indicated in Table 2, the new valve seats were found to have higher Charpy impact values by two to five times and are tougher than the conventional valve seats. Detailed observation of the occurrence of cracking on conventional valve seats welded overlay on actual valve revealed that cracking mainly started at mesh-like eutectic carbide. From this phenomenon, cracking is thought to occur on the conventional valve seats under a corrosive environment in the following mechanism: The valve seats are composed of mesh-like eutectic carbide and dendrite. The former has less corrosion resistance than the latter. Therefore, the eutectic carbide is first selectively corroded and damaged. Then, the area corroded and damaged is acted upon by the residual stress of the valve seats, becoming a starting point of cracking.

The new valve seat material is at least twice tougher and more corrosion resistant as shown in (1) than the conventional valve seats. Consequently, it can be said that cracking is less likely to occur on the new valve seats than on the conventional valve seats.

(4) Residual stress

Residual stress on valve seats was evaluated by manufacturing a carbon steel disc to simulate the gate valve having a 200A bore, and then hardfacing the disc with the Co-based alloy welded overlay used as conventional valve seat material, and with carbide-dispersed alloy, which is used as new valve seat material. The result was as follows: The conventional valve seats were subjected to high residual tensile stress in the lap-direction; the new valve material was subjected to residual compression stress in both lap- and diameter- directions.

Combined with the results of Charpy impact test described above, it can be said that the new valve seats have significantly less potential to induce cracking and provide higher reliability as valve seats than the conventional valve seats.

(5) Erosion resistance

Erosion resistance evaluation test(s) were conducted in a high-temperature atmosphere (containing approximately 8 ppm of dissolved oxygen) in order to perform comparative evaluation of erosion resistance between the conventional valve seats and the new valve seats. Shown in Fig. 9 is the comparison between the erosion occurrence conditions on the conventional valve seats and those on the new valve seats after the tests that lasted for 48 hours. In comparison with the conventional valve seats, the erosion-damaged conditions of the new valve seats were extremely minor, and the damaged volume of the new valve seats was less than one tenth of that of the conventional ones. As for the jet impact areas and the erosion occurrence conditions, the conventional valve seats were erosion damaged on the jet impact areas and their vicinities. Especially the vicinities of the jet impact areas were severely erosion damaged. On the other hand, new valve seats were subjected to minor damage only on the jet impact areas. It is thought that the superior corrosion resistance of the new valve seats greatly contributes to their better erosion resistance.

(6) Co release property

Co release tests were conducted under the water quality conditions listed below in order to compare the Co release between the conventional valve seats and the new valve seats.

Test conditions

- Temperature: 220 °C
- Dissolved oxygen (DO): 200 ppb [parts per billion]
- Test time: 2000 hours

The test result is shown in Fig. 9.

The result shows the following: The new valve seats exhibited one tenth of the amount of Co release from the conventional valve seats, and thus can significantly reduce the amount of Co release.

The radiation to which nuclear power plant workers may be exposed during the periodic inspection of nuclear power plants mainly derives from radiation crud. The radiation crud is formed in the following mechanism: Co is eluted from the equipment containing Co in the system facilities where primary coolant circulates, is subjected to neutron irradiation while circulating through the reactor core, and then forms a radioactive element named Co60, which is a long-lived nuclide. This substance is deposited on the internal surfaces of the equipment.

Based on this result, it can be said that the new valve seats have the radiation exposure reduction effect almost equivalent to that obtained by using the valve seats made of Co-free material. As shown in Fig. 9, the new valve seats can significantly reduce the amount of Co release. Therefore, in nuclear power plants, the adoption of the valves incorporating the new valve seats will substantially decrease the amount of Co release from Co-based alloy to achieve a drastic reduction of the radiation exposure of the nuclear power plant workers.

(7) Ease of work and inspection

We have requested multiple valve manufacturers to evaluate the ease of work. The result shows that there is no difference in the ease of work between the conventional valve seats and the new valve seats. Furthermore, the valves incorporating the new valve seat allows the evaluation of internal defects of valve seats by ultrasonic testing (UT), though the evaluation of internal defects of conventional valve seats by UT is practically impossible. This ensures that the valves incorporating the new valve seats can be shipped from the factory without any internal defect.

2.2.3 Applicability evaluation

As described above, the valves incorporating the new valve seats have the following characteristics: The va

lves have lower friction, and superior corrosion resistance, erosion resistance, and mechanical sturdiness, as well as lower residual stress. In addition, the valves allow the assurance of the shipment without any internal defect by using the ultrasonic test (UT). Furthermore, the valve seats incorporated in the valves cause less amount of Co release, one tenth of the amount of Co release from the conventional valve seats. Therefore, in nuclear power plants, the valves incorporating the new valve seats will control the roughness of the valve seats caused by corrosion and/or erosion which may occur on the conventional valve seats. This effect will contribute to the reduction of the work for fitting the valve seats during the overhaul of the valves as well as to the prevention of lowered sealing capability and operating performance of the valves and of the cracking on the valve seats during plant operation. Especially, the use of the new valve seats in safety valves will minimize the occurrence of corrosion bonding since the new valve seats can reduce the occurrence of corrosion products. In addition, it was found that, in nuclear power plants, the use of the valves incorporating the new valve seats would provide the effect of lowering the radiation exposure of nuclear power plant workers.

As described above, the valves incorporating the new valve seats are thought to contribute to higher maintainability and reliability of nuclear power plants.

2.2.4 Verification in actual operating plant

In order to verify that the excellent characteristics of the valves incorporating the new valve seats, as described above, can be attained in actual plants, both the valve incorporating the conventional valve seat and the valve incorporating the new valve seat were installed under the same service environment (refer to Table 3 for the environmental conditions) in an actual operating nuclear power plant for approximately one year. Then, the respective valves were removed to perform the comparative evaluation of the conditions of the respective valve seats. Shown in Fig. 10 are the major inspection conditions of the conventional valve seats and the new valve seats.

The result of the major inspection of the conventional valve seats and the new valve seats is as follows: The visual inspection revealed the corrosion and black discoloration of the conventional valve seat. On the other hand, there was little damage found on the new valve seats.

The cross sections of valve seats were investigated for detailed examination of the damaged conditions of the valve seats. The result shows the following: In the conventional valve seats, corrosion advanced along the eutectic carbide into the inside of the valve seats, the surface layer was dropped off, the fitting faces of the valve seats before the test were lost, and the sealing capability of the valves were lowered. On the other hand, on the new valve seats, the marks made during the fitting of the valve seats before the test were observed, and there was little damage found but the partial fall-off of the granular carbide in the surface layer.

The result of verification in actual operating plant shows that the valve incorporating the new valve seat is superior to the valve incorporating conventional valve seat, in terms of

Corrosion resistance, erosion resistance, low aged deterioration (secular change) property and low Co release property.

3. Conclusion

As a result, it was verified that the valves incorporating the new valve seats can also attain superior characteristics in actual operating nuclear power plants to the valves incorporating the conventional valve seats. Based on the findings described above, the use of the valves incorporating new valve seats in actual plants will resolve the pending problems associated with the valves incorporating the conventional valve seats. In conclusion, the following effects can be attained:

a) The reduction of the sealing capability of valves can be minimized by controlling the roughness of valve seats associated with corrosion and/or erosion.

b) The reduction of the operating performance of valves can be minimized by controlling the roughness of valve seats associated with corrosion and/or erosion.

c) The amount of work for fitting valve seats during the disassembly of valves can be reduced by controlling the roughness of valve seats associated with corrosion and/or erosion.

d) The cracking on valve seats starting on surface layer(s) can be minimized by increasing corrosion resistance, by reducing residual stress, and by increasing tenacity.

e) The cracking on valve seats starting at internal defect(s) can be inhibited by ensuring no internal defect.

f) The drift phenomena of the set pressure of safety valves caused by corrosion bonding can be minimized by controlling the occurrence of corrosion products.

g) The radiation exposure of nuclear workers during periodic inspection of nuclear power plants can be reduced by minimization of the Co release quantity.

As described above, it can be said that the use of the valves incorporating the new valve seat in actual nuclear power plants will not only increase the reliability and maintainability of the valves, but also contribute to the increased reliability and maintainability of the plants, in comparison with the use of the valves incorporating the conventional valve seats hardfaced with a Co-based alloy.

Now, 20 or more valves incorporating the new valve seat as mentioned above were delivered as HHVs (Hitachi Hyper Valves) for pressurized water reactors (PWRs) and BWRs, and have been used in the actual operating plants in Japan since 2004.

4. Acknowledgments

We would like to express deep appreciation to all the persons concerned at the Chugoku Electric Power Co., Inc., who cooperated closely in the performance evaluation of “valves incorporating the valve seats made by corrosion- and wear-resistant, carbide-dispersed alloy” which are the valves incorporating the valve seats based on a new concept.

5. References

1) J.C. Watkins and K.G. Dewall, NUREG/CR-6807, “Results of NRC-Sponsored Stellite 6 aging and Friction Testing.”

2) Yoshihisa Kiyotoki and Mitsuo Chigasaki, “HHV corrosion resistant, withstand erosion and low Co release,” Proceedings of ASME/JSME Pressure vessel and piping conference 2004.

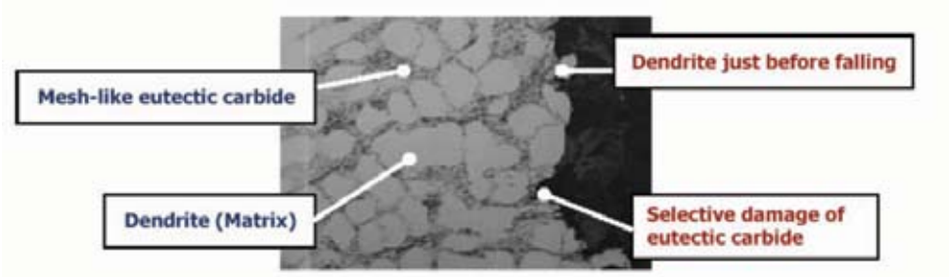

Figure 1 – Case of damage to Co-based alloy overlay welded in an actual operating plant

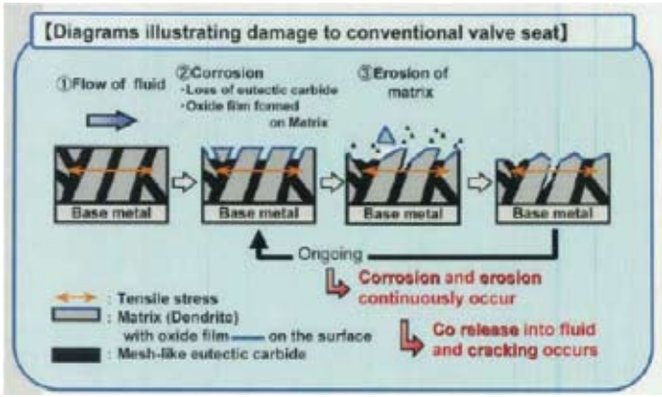

(1) Conventional valve seats

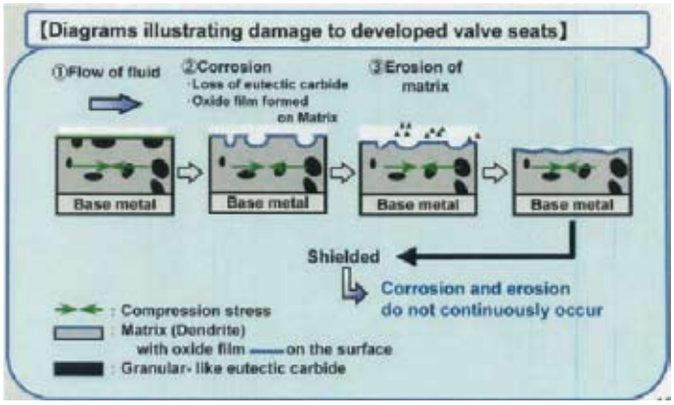

(2) New valve seats

Figure 2 – Comparison of damaging mechanism between conventional valve seat and new valve seat

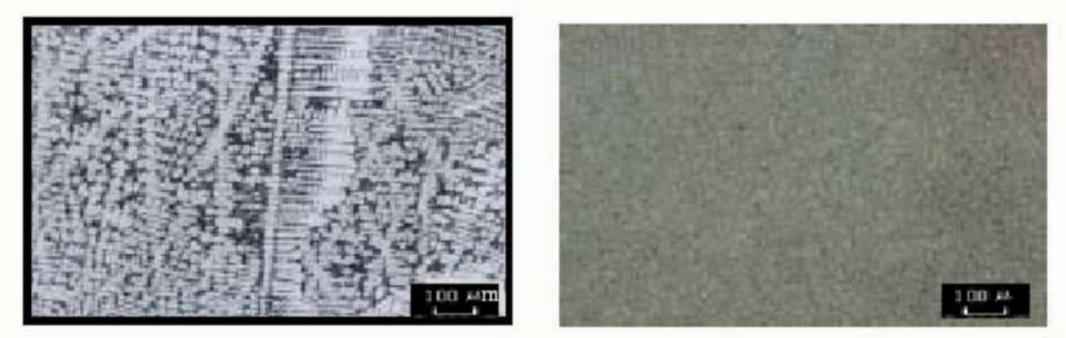

(1) Conventional valve seat **(2) New valve seat**

Figure 3 – Comparison of metallic structure between conventional valve seat and new valve seat

Table 1 Comparison of characteristics between conventional valve seat and new valve seat

Characteristics required for valve seat			Evaluation ○:Requirement satisfied ▲: Requiring improvement	
			Conventional valve seat	New valve seat
①	Corrosion resistance		▲	○[Higher corrosion resistance (Refer to Fig. 4.)]
②	Sliding property, antigalling property	②-1 During frequent operation	○	○[Lower friction (Refer to Fig. 5.)]
		②-2 Secular change of valve seat faces	▲	○[Smaller surface roughness change and lower coefficient of friction (Refer to Fig. 6 and Fig. 7)]
③	Mechanical sturdiness		▲	○[High Charpy Impact values (Refer to Table 2.)]
④	Low residual stress		▲	○[Compressive stress]
⑤	Erosion resistance		▲	○[Refer to Fig. 8.]
⑥	Low Co release		▲	○[Refer to Fig. 9.]
⑦	Ease of work and inspection		▲	○[Ultrasonic test applicable]

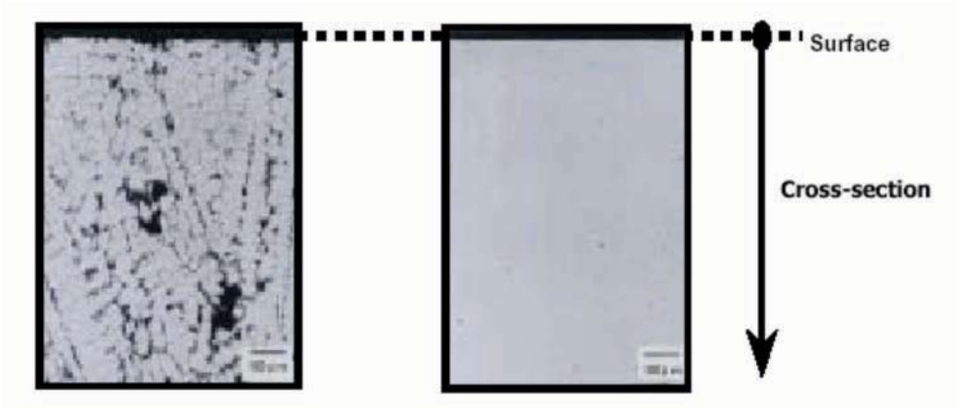

(a) Conventional valve seats **(b) New valve seats**

Figure 4 – Comparison of Strauss test results between conventional valve seat and new valve seat

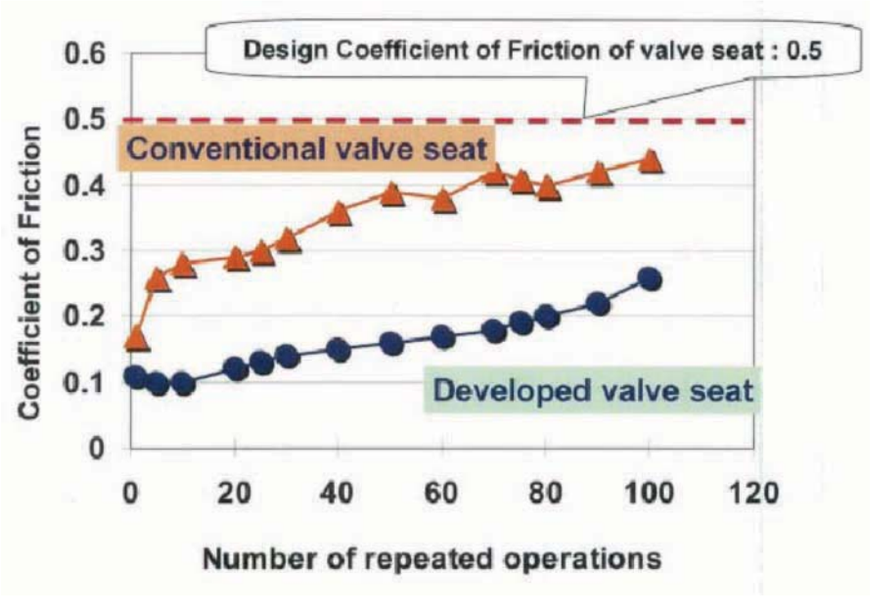

Figure 5 – Comparison of coefficient of friction between conventional valve seats and new valve seats

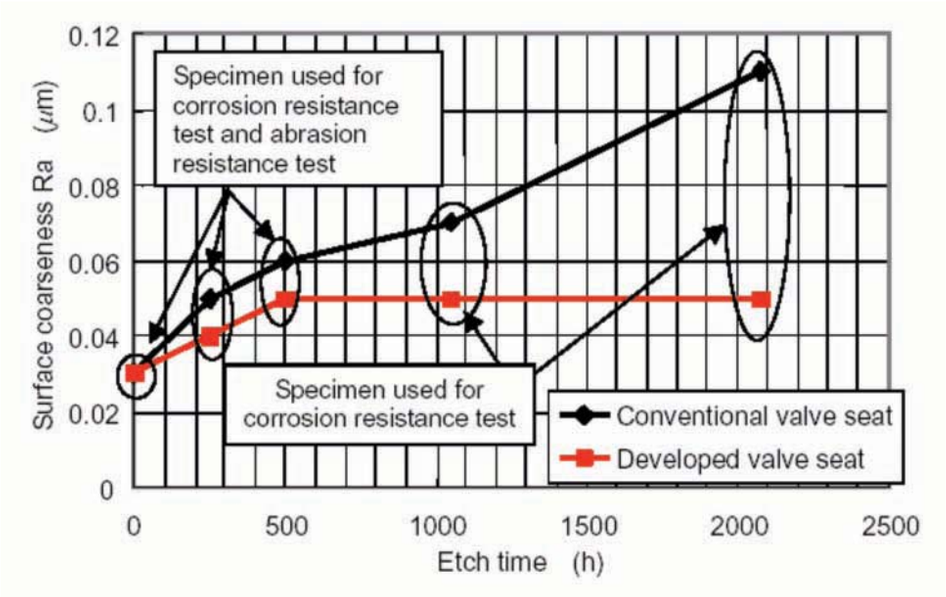

Figure 6 – Surface roughness of valve seat material made by Co-based alloy before and after complete immersion test in high-temperature water

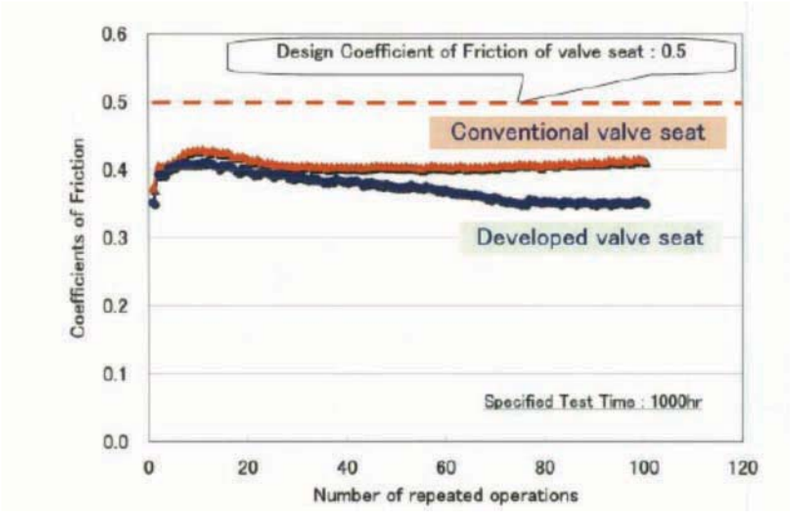

(1) The coefficient of friction plot of the valve seats,

The results of abrasion resistance test(s)

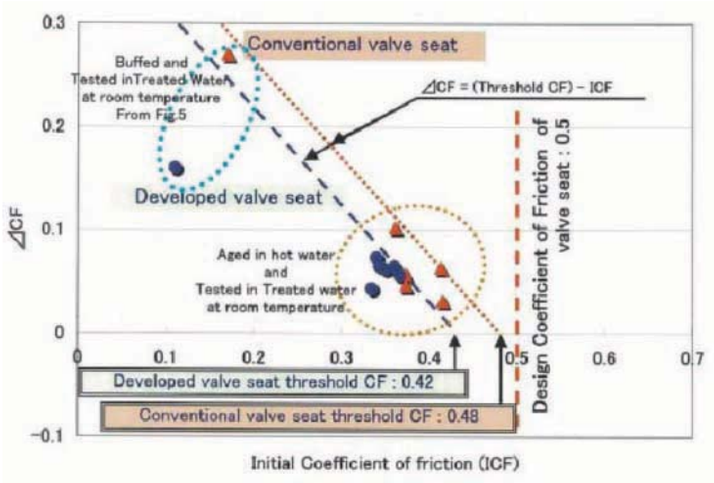

(2) ΔCF* vs. Initial coefficient of friction plots

*ΔCF : The difference of largest coefficient of friction and the initial coefficient of friction at abrasion resistance test.

Figure 7 – Changes of coefficient of friction of valve seat caused by aged deterioration (secular change)

Table 2 Charpy impact test result of conventional valve seat and new valve seat

	Charpy impact test values at ordinary temperatures Joules/centimeter squared (J/cm2)	
	Conventional valve seat	New valve seat
Flat specimen	11.8	59.8
U-notched specimen	3.7	8.2

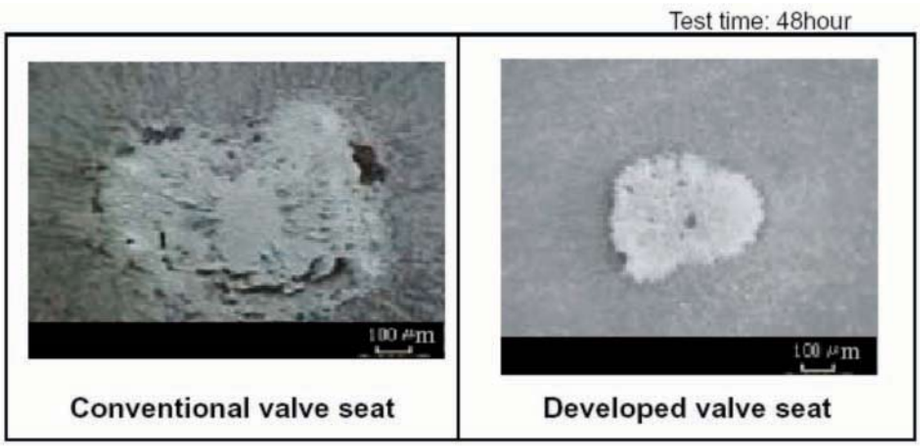

Figure 8 – Comparison of erosion resistance between conventional valve seats and new valve seats

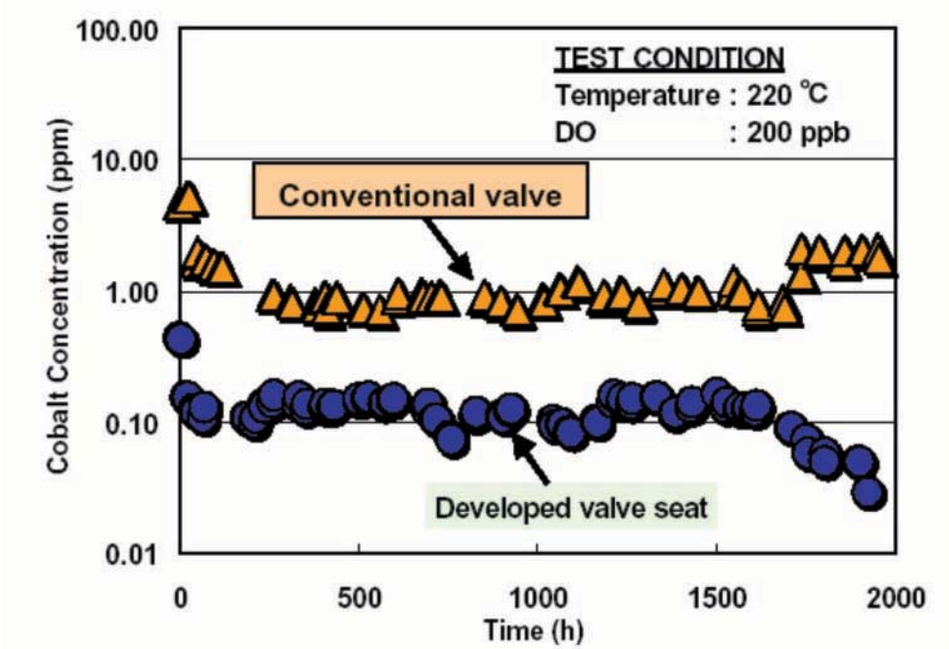

Figure 9 – Comparison of amount of Co release between conventional valve seat and new valve seat

Table 3 Performance verification in actual plant

- Pressure: 7 MPa [Megapascals]
- Temperature: Approx. 285°C
- Fluid: Main steam and its condensed water
- Dissolved oxygen (DO): Approx. 8 ppm

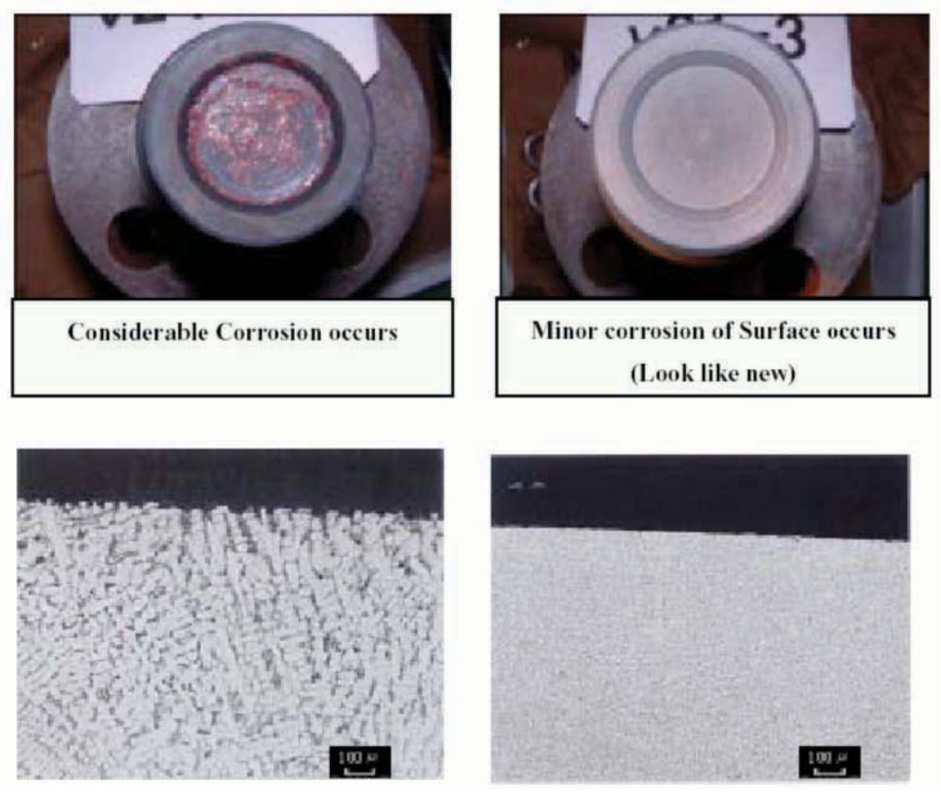

(a) Conventional valve seats (b) New valve seats

Figure 10 – Comparative test in actual plant between conventional valve seat and new valve seat [2)]

(note) Conventional valve seat: hardfaced with RCoCr - A

Friction Factors In Equiwedge Gate Valves Under Flow Interruption Conditions

Ronald S. Farrell
Sr. Engineer
Flowserve, Flow Control Division, Raleigh, NC

Gregory Smyth
Senior Staff Engineer
Wyle Laboratories, Huntsville Facility

Abstract

This paper analyzes flow interruption test data measured on four gate valves ranging from Size 4 to Size 26 regarding friction factors in the body guides, which is a critical input for determining required valve stem thrust for assuring flow isolation. The data was obtained during a QME-1 qualification test program for the Flowserve/Edward Equiwedge Gate Valves with Type A Gas/Hydraulic Actuators. Wyle Laboratories, Huntsville Facility conducted the testing. All the valves are rated as Special Class 900 in accordance with ANSI B16.34 and are Class 2 N-Stamped per the American Society of Mechanical Engineers (ASME) Boiler & Pressure Vessel Code (B&PVC). The actuators are linear piston type and are U-Stamped per Section VIII of the ASME B&PVC.

The conditions for the flow interruption tests and the measured performance data for both the valve and actuator are presented. Comparisons between the required closing force and the available actuator force are made. These comparisons demonstrate that the equipment is capable of reliably performing its intended function of isolating flow. Test results demonstrate a friction factor less than 0.3 during valve closing.

1.0 Introduction

Flowserve and Wyle Laboratories conducted a Qualification in accordance with ASME QME-1-1994 "Qualification of Active Mechanical Equipment used in Nuclear Power Plants" on four Equiwedge Gate Valves each equipped with the Type A Gas/Hydraulic Actuator. The valves were qualified for Main Steam and Main Feedwater Isolation Service in a Pressurized Water Reactor (PWR) Nuclear Power Plant. The test program consisted of the following valve and actuator combinations:

All the valves are rated as Special Class 900 in accordance with ANSI B16.34 1988 Edition, and are Class 2 N-Stamped per the ASME Boiler & Pressure Vessel Code (Division 1, Section III, 1992 Edition including the 1994 Addenda). The actuators were U-Stamped in accordance with Section VIII, Division 1 of the ASME B&PVC (1998 Edition including the 1998 Addenda). Previous to the QME-1 qualification, these valve designs were qualified in accordance with ANSI B16.41-1983, "Functional Qualification Requirements for Power Operated Active Valve Assemblies for Nuclear Power Plants." Numerous qualification tests also were performed during the equipment development and for specific customer applications. In addition, since its introduction in 1978, a large amount of inservice operating history has been obtained.

Valve Size	Actuator Size	Service
26 x 24 x 26	A-100	Main Steam Isolation Valve(MSIV)
4	A-100	Main Steam Isolation Bypass Valve (MSIBV)
20 x 16 x 20	A-260	Economizer Main Feedwater Isolation Valve(EMFIV)
8 x 6 x 8	A-100	Downcomer Main Feedwater Isolation Valve (DMFIV)

The general requirements of the ASME QME-1 Standard for valves and how these requirements were applied to the above listed valves were presented at the NRC/ASME Symposium for Valve and Pump Testing in July 15-18, 2002. The data obtained during the qualification included force measurements from stem mounted strain gages and actuator performance data. Data was obtained throughout the test program including the Flow Interruption and Capability Demonstration. Using the force and performance data, the interaction between the valve and actuator is observed. Since the safety function of this equipment is to isolate the nuclear containment, particularly during a plant accident condition, this paper focuses on the valve closure under flow interruption conditions. The measured data demonstrates the ability of the actuator to isolate flow reliably.

2.0 Service Conditions

These valves are for Main Steam and Main Feedwater Isolation Service in a PWR Nuclear Power Plant. Except for the Main Steam Isolation Bypass Valve, they are maintained in the fully open position during normal plant operation. The Main Steam Isolation Bypass Valve is opened during the startup and shutdown of the plant but is maintained in the fully closed position during plant operation (refer to Figure 1).

The valves were designed for the following conditions:

Their safety related function is to close and provide automatic and positive isolation of the safety related piping and the containment system from the non-safety related piping; therefore, valve opening is not a safety concern. They are required to perform this safety function with sufficient force and within a maximum closure time to achieve isolation before, during and after normal and accident plant conditions.

3.0 Equipment Description

The test valves used in this program were Equiwedge Gate Valves with Type A Actuators (refer to Figures 2 thru 6). These are bi-directional valves that consist of two independent gates separated by a spacer ring. Although a significant differential pressure is sufficient to seal the valve, gate wedging due to the taper in the gates that match the angle of the seat rings aids sealing. The spacer ring maintains flexibility between the gates and prevents binding. The gates are guided throughout the stroke by guides on their sides that fit into grooves in the body (refer to Figure 7). This guiding arrangement prevents contact between the seating surfaces on the gates and seat rings until the valve is approximately 95% from the fully open position such that flow isolation occurs before seating surface contact.

The guide and seating wear surfaces in the valve are hardfaced with a cobalt base alloy (Stellite 21). Flexible graphite is used for the stem packing and the pressure seal bonnet gasket. The valves also have provisions to prevent center cavity over pressurization. This is accomplished by a bypass arrangement on one side of the valve that equalizes

Valve	Normal Operating Pressure (pounds per square inch gage [psig])	Normal Operating Temperature (Fahrenheit [F])	Design Pressure (psig)	Design Temperature (F)
Main Steam Isolation Valve	1055	553	1382	590
Main Steam Isolation Bypass Valve	1155	564	1382	590
Economizer Main Feedwater Isolation Valve	1425	455	2050	500
Downcomer Main Feedwater Isolation Valve	1425	455	2050	500

the center cavity pressure to the high pressure side of the valve. The Type A Valve Actuator is a linear piston actuator composed of hydraulic, pneumatic and electrical systems (refer to Figure 8). Its circuitry is designed to perform either a fast or slow valve closure, an open stroke or exercise cycle. The exercise cycle consists of partially stroking the valve closed (generally 10%) in a slow closure mode and then reopening the valve. The piston rod attaches directly to the valve stem and, by controlling the direction and speed of the piston, the direction and speed of the valve gates are also controlled.

The source of the valve closing force is compressed nitrogen gas contained in a volume on one end of the actuator cylinder. The pressure of the nitrogen is adjusted to suit specific applications. During fast closure, the hydraulic system acts as a classical dashpot so stem closure speed is constant.

The hydraulic system moves the piston in the non-critical direction (i.e., open the valve); this also compresses a fixed mass of nitrogen gas. The hydraulic system also controls the piston speed in the critical direction (i.e., valve closure) while the gas expands to close the valve. The pneumatic system is used to develop the hydraulic force needed for opening the valve and compressing the gas. The electrical system is used to monitor, control and verify the essential parameters and functions of the actuator.

The actuator design was previously qualified to the following Standards:

- IEEE-382, 1985 Edition

Standard for Qualification of Actuators for Power Operated Valve Assemblies with Safety-Related Functions for Nuclear Power Plants

- IEEE-344, 1987 Edition

Recommended Practice for Seismic Qualification of Class 1E Equipment for Nuclear Power Generating Stations

- IEEE-323, 1983 Edition

Qualifying Class 1E Equipment for Nuclear Power Generating Stations

4.0 Flow Interruption and Functional Capability Demonstration

The Flow Interruption and Functional Capability Test was performed to demonstrate the test valve assembly's capability to close against simulated line rupture flow conditions. The testing was performed at the following minimum pressure/temperature conditions:

The general test sequence was as follows:

- With minimum motive power to the actuator and the required pressure/temperature test conditions established, the first flow interruption and functional capability test was performed.
  - Immediately after the closure, a seat leakage test was conducted. The test was performed at a differential pressure equal to the test pressure for a minimum duration of 30 minutes.
  - The valve was unseated against differential pressure and opened.
  - The maximum motive power was applied to the actuator and the required pressure/temperature test conditions established.
  - A second flow interruption and functional capability test was then performed followed by a seat leakage test.

Valve Size	Pressure (psig)	Temperature (F)
26 x 24 x 26	Saturated	564
4	1390	564
20 x 16 x 20	2100	564
8 x 6 x 8	2100	564

All the test valve assemblies successfully closed and seated against the line rupture flow and did not incur any damage.

5.0 Valve/Actuator Performance

Typical performance data for a flow interruption test is shown in Figures 9 and 10. Figure 9 shows the actuator performance data. A review of this figure shows the following:

- The gas force behaves as a non-linear spring. The non-linear behavior is the result of the adiabatic expansion that the gas experiences during a fast valve closure. It is a predictable quantity.
- The hydraulic force varies in a smooth but unpredictable manner. The hydraulic system acts like a classical dashpot and closes the valve at constant stem travel speed while responding to flow resistance. During the closure, there are four distinct transients and, towards the end of the stroke, flow isolation and seating cause two of these transients. Since the hydraulic force is less than the magnitude of the gas force, there is a net downward force acting on the piston.
- The net actuator force is the algebraic sum of the gas force and hydraulic force. As in the case with the hydraulic force, there are 4 distinct transients.

Figure 10 shows the measured valve force during the fast closure. This force represents the algebraic sum of the packing friction force, stem rejection force and the resistive force that results from line rupture flow. During approximately the first 2 seconds of the closure, the valve only experiences the forces due to packing friction and stem rejection; it is fairly constant. However, as the gates progress into the flow stream, the resistive forces due to the flow become significant. Flow resistance reaches a peak during flow isolation and subsequent transition of the gates from the guide rails to the body seats. During and after seat wedging, the stem force results mostly from the net actuator force.

As discussed above, there are 4 distinct transients during the fast closure, and the two towards the end are due to flow isolation and seating. The hydraulic force, the net actuator force, and the valve closing force experience the same transients at the same time. Figure 11 is a comparison between the valve force and actuator force. This comparison demonstrates that, during the fast closure, the net actuator force and the valve force are equal. The hydraulic dashpot causes valve closure at constant stem velocity, and the actuator responds to the force requirements of the valve.

When stem travel stops the hydraulic pressure goes to zero and the final seating force depends totally on the actuator gas pressure. Schematically, the Type A Actuator can be represented as a spring (gas) and dashpot (hydraulic fluid) acting in parallel (refer to Figure 12).

6.0 Friction Factors

The friction factor (μ) is obtained from the following equation, which is consistent with actuator sizing methodology:

$$\mu = \frac{F_S - F_P - P_{UP} A_{STEM}}{\Delta P A_{SEAT}}$$

In the above equation:

F_S - The gross measured stem force

F_P - Measured packing drag force during valve closing from stroke test under no pressure

P_{UP} - Measured upstream pressure

ΔP - Measured differential pressure across the gate

A_{STEM} - Stem cross-section area at packing

A_{SEAT} - Seat area at mean seat diameter

Figures 13 thru 16 show the gross stem forces measured during the flow interruption tests at minimum motive power. Also given are graphs of friction factor, per the above equation, as a function of stroke time at times between flow isolation and hard seating. Although the friction factor should be constant, the figures show a variation. This variation is because the equation is only applicable close to

flow isolation conditions. Before isolation, the assumed seat area is not entirely effective, and shortly after isolation, gate wedging occurs for which the equation is not valid. Then, the point of interest is at flow isolation, and results show that the calculated friction factor is generally constant there as presumed.

Table 6-1 summarizes the flow interruption test results.

The information presented for each valve size is:

1. The initial test pressure

2. The final test differential pressure after seating

3. The measured stem force at flow isolation

3. The measured stem force at seating

This force represents the largest force required to achieve valve seating.

4. The measured actuator force after seating

This is the force produced by the actuator on the valve after the valve is seated. The difference between this force and the valve force at flow isolation represents the margin between the available actuator force and the required stem force.

5. Calculated minimum available actuator force

This force is based on the actuator precharge pressure. It is determined during the initial actuator sizing and considered a minimum force because the actuator is driven under minimum motive power conditions.

6. Calculated maximum available actuator force

This force is the same as item 5 except it is considered a maximum force because the actuator is driven under maximum motive power conditions.

Table 6-1 Flow Interruption Test Results

Parameter	Valve Size			
	26 x 24 26	4	20 x 16 x 20	8 x 6 x 8
Initial Pressure prior to Test (psi)	1375	1538	2175	2100
Test Differential Pressure after Seating (psi)	1168	1528	1492	1740
Measured Stem Force at Flow Isolation (lbs)	112000	4280	46900	9300
Measured Stem Force at Seating (lbs)	151263	7277	69675	16816
Measured Actuator Force after Seating (lbs)	160800	8764	109316	18296
Calculated Minimum Available Actuator Force (lbs)	158362	7680	108639	18301
Calculated Maximum Available Actuator Force (lbs)	180703	8766	123990	20887
Calculated Friction Factor at Flow Isolation	.276	.10	.25	.22

7. Calculated friction factor at flow isolation

As noted in Section 3.0 (Equipment Description), the source of the valve seating force is compressed nitrogen gas contained in a volume on one end of the actuator cylinder. The force produced by the actuator at valve seating is dependent on the initial gas pressure when the valve is backseated. When the valve is backseated, the nitrogen gas is contained in a fixed volume so its initial pressure is dependent on its temperature. The minimum motive power condition for the actuator is the gas pressure at the minimum specified ambient temperature which for this program was 50 oF. The maximum motive power condition for the actuator is the gas pressure at the maximum specified ambient temperature which for this program was 122 F.

It should be noted that the final actuator thrust shown in Figure 13 thru 16 are conservatively low compared to what would occur in service. The net actuator force shown is when the equipment is at the minimum ambient temperature. In actual service, a line rupture condition would only occur when the plant is operating. Under operating conditions, the ambient temperature of the equipment and the actuator gas pressure would both be higher; thus producing a higher seating force.

Figures 13 thru 16 and Table 6-1 show the following:

1. The actuator force adjusts to the valve force to maintain equilibrium.

2. During and after gate wedging, the valve stem force is totally driven by the actuator; thus producing a force margin that is dependent on the actuator gas pressure.

3. The stem force at flow isolation and seating is less than the available actuator force.

The calculated minimum required actuator force forms the basis for determining the required nitrogen gas pressure. As discussed above, the initial gas pressure determines the available actuator force for seating the valve. There are several reasons why the calculated actuator force, based on a 0.3 friction factor, results in significant margin. The main reasons are the thermal expansion coefficient of nitrogen, the valve stroke and the packing friction.

When the actuator performs a fast valve closure, the nitrogen gas experiences an isentropic expansion. The gas pressure at the end of the valve stroke is:

$$Pf = Pi \times (Volf / Voli)^{k}$$

where: Pf = Final Gas Pressure

Pi = Initial Gas Pressure

Voli = Initial Gas Volume

Volf = Final Gas Volume = Voli + Piston Area x Valve Stroke

K = Thermal Expansion Coefficient for Nitrogen

The change in gas pressure depends on its volume change and the thermal expansion coefficient of nitrogen. The assumed expansion coefficient is 1.6. However, this is a limiting value for the pressure range used in this equipment. The actual values are lower which result in higher terminal gas pressures.

The valve stroke determines the change in gas volume during a closure. A shorter stroke causes a smaller change in gas volume. This results in a higher terminal pressure. When the actuator is sized, the stroke used in sizing is the actuator stroke. Since the valve stroke is shorter than the actuator stroke, there is a higher terminal pressure.

As noted above, the initial gas pressure determines the available actuator force for closing the valve. If it is desired to provide greater margin over calculated thrust or to size for a greater differential pressure, it is only necessary to increase the initial gas pressure. Comparing the minimum and maximum calculated actuator forces (refer to Table 6-1), there is approximately a 14% increase in the actuator force at valve seating. However, consideration must be given to the resulting stresses in the valve components and to the maximum pressure capacity of the actuator.

7.0 Conclusions

This paper presents the test conditions and performance results for the flow interruption tests, performed during the QME-1 qualification of the Equiwedge Gate Valve. The test data demonstrate that the actuator is capable of reliably performing its intended function of isolating flow. The results indicate a friction factor that is less than 0.3 during closing.

The actuator hydraulic system acts as a classical dashpot such that the valve closes at constant velocity and hydraulic fluid pressure automatically adjusts to compensate for valve resistance forces. Although not presented in this paper, other cycling performed under no pressure or static pressure conditions show similar results.

In all cases, the actuator force exceeded the required force for flow isolation with significant margin. During and after gate wedging, the actuator drives the stem force exerted on the valve. The available actuator force was sufficient to isolate flow and to hard seat the wedge adequately.

The results presented in this paper are based on minimum motive power conditions. In actual service, because of the higher ambient temperature, the motive power to the actuator would be higher; thus increasing the margin over required thrust. The margin can be increased further by increasing the gas precharge pressure in the actuator.

Note that the QME-1 standard and hence test program did not fully address valve preconditioning or for steam aging effects on Stellite surfaces. The observations of valve preconditioning are documented separately in the paper "Observations of Preconditioning during the ASME QME-1 Qualification of the Edward Equiwedge Gate Valve with the Type A Gas/Hydraulic Actuator" presented at the Ninth EPRI Valve Symposium.

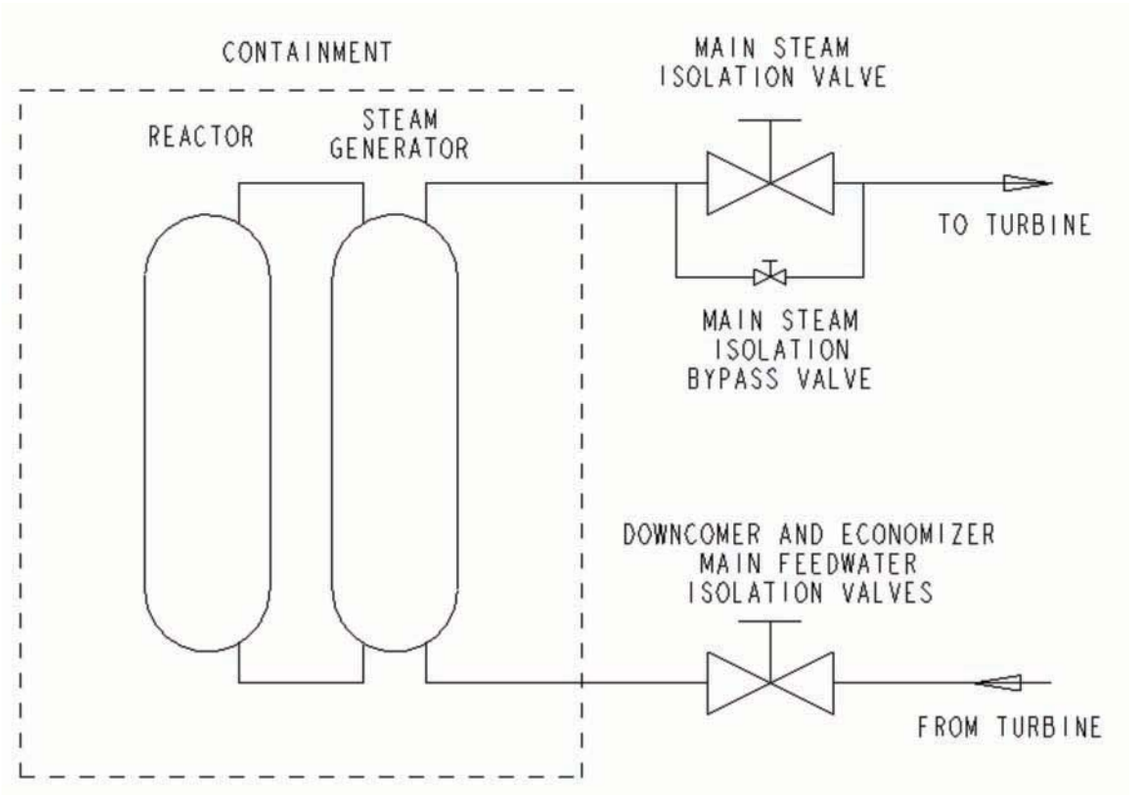

Figure 1 – Schematic for the Main Steam and Main Feedwater Isolation Valves in a PWR Nuclear Power Plant

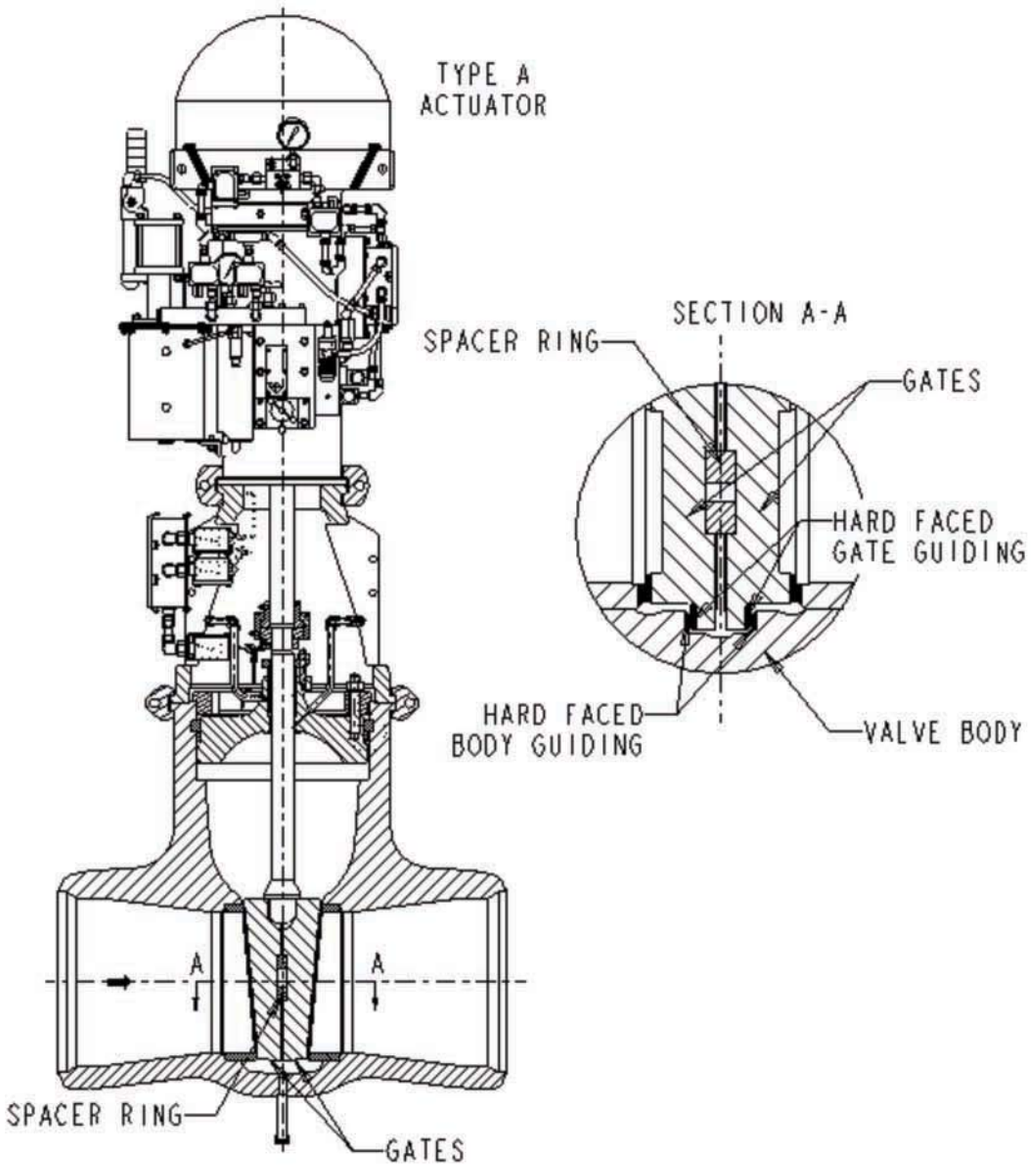

Figure 2 – Cross-section of the Flowserve/Edward Equiwedge Gate Valve with a Type A Actuator

Figure 3

Size 26 x 24 x 26

Main Steam Isolation Valve

Figure 4

Size 4

Main Steam Isolation Bypass Valve

Figure 5

Size 20 x 16 x 20

Economizer Main Feedwater Isolation Valve

Figure 6

Size 8 x 6 x 8

Downcomer Main Feedwater Isolation Valve

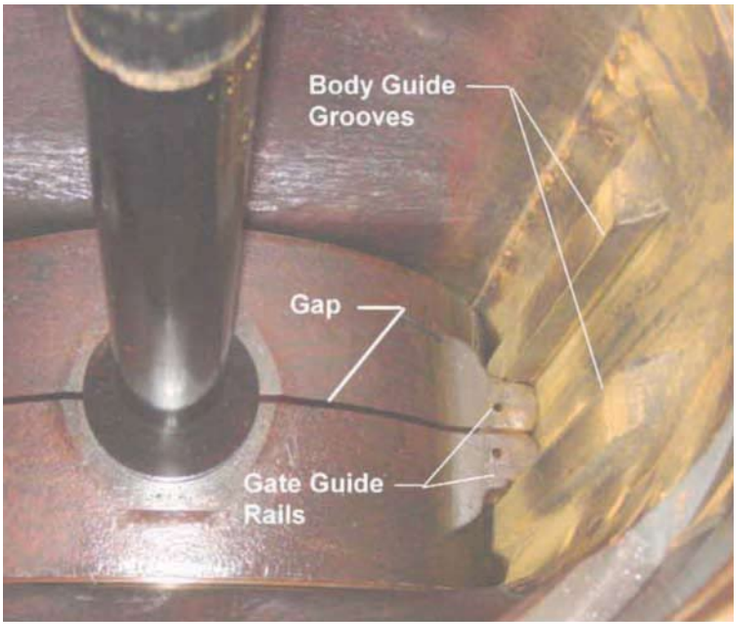

Figure 7

Gate Guiding System

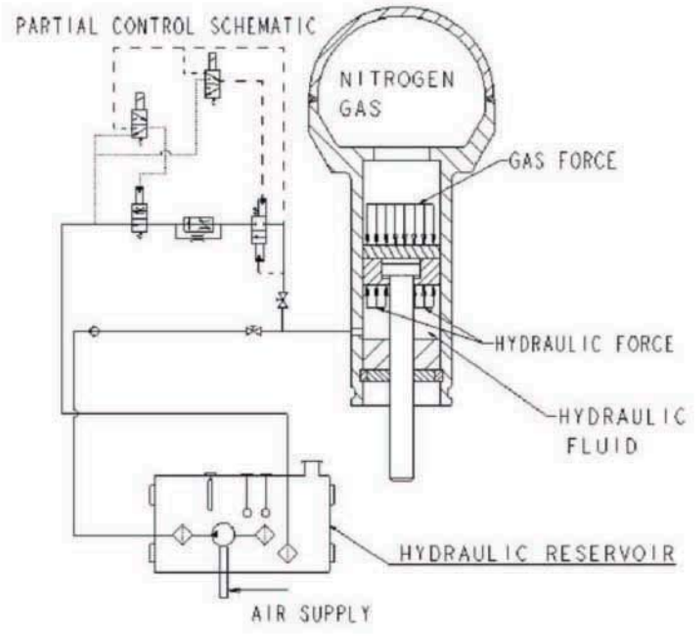

Figure 8

Actuator Cross Section and Partial Control Schematic

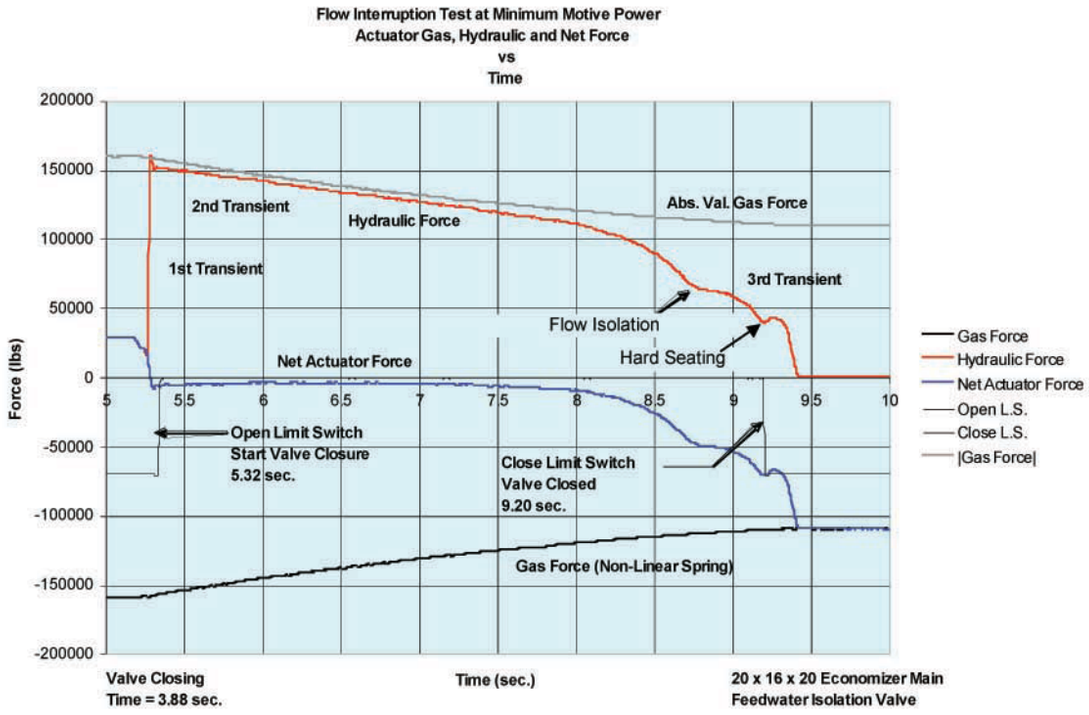

Figure 9

Actuator Performance Data

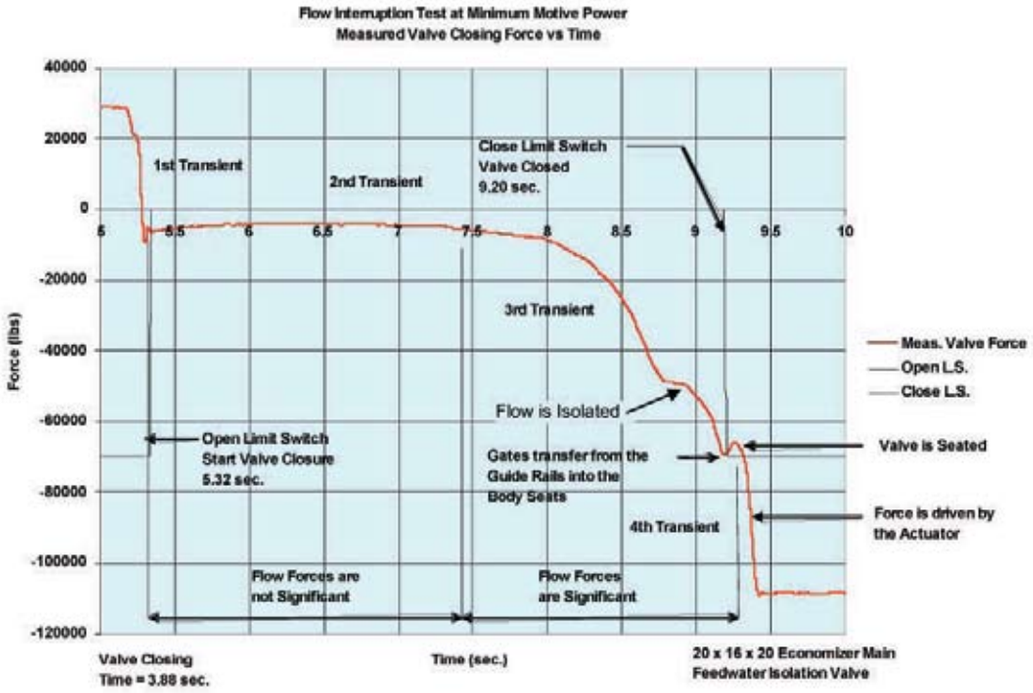

Figure 10

Valve Closing Force

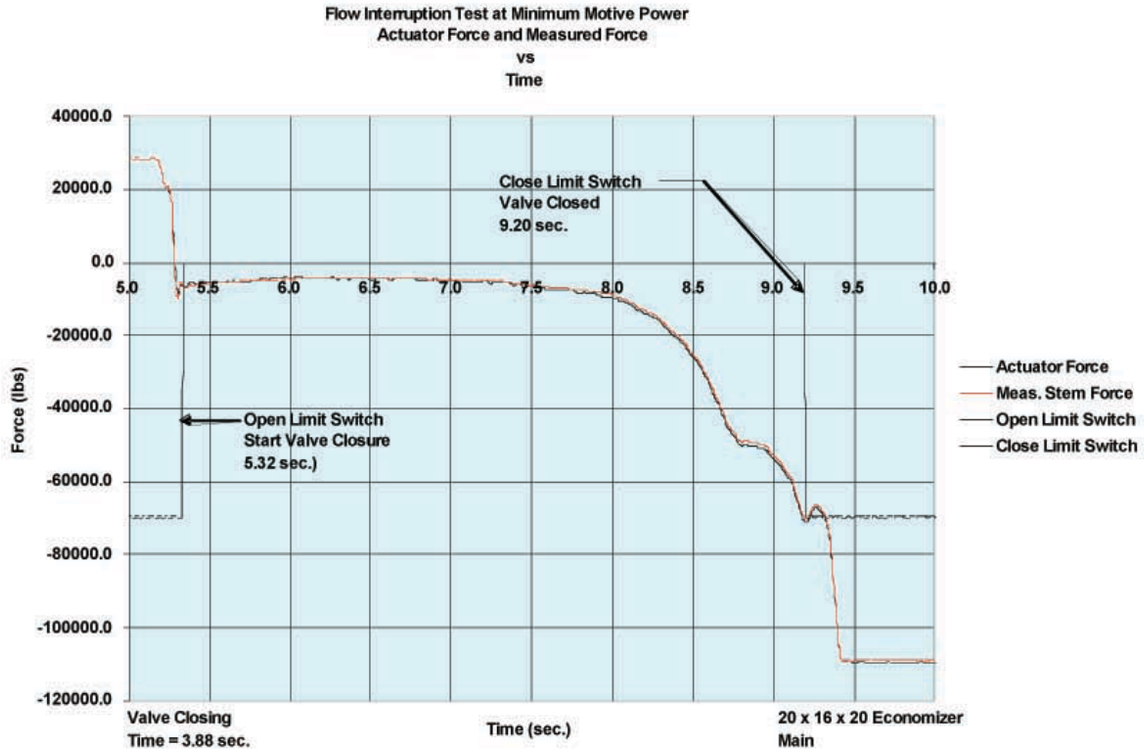

Figure 11

Net Actuator Force and Measured Valve Closing Force

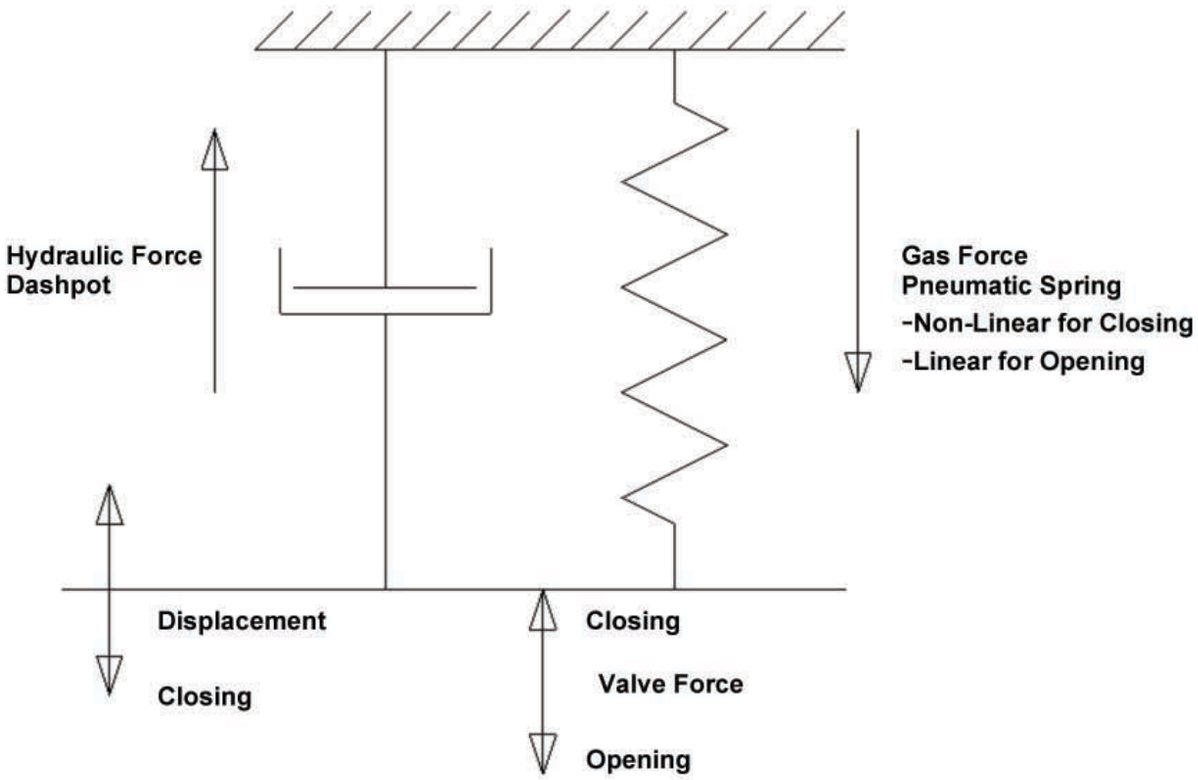

Figure 12

Operating Schematic

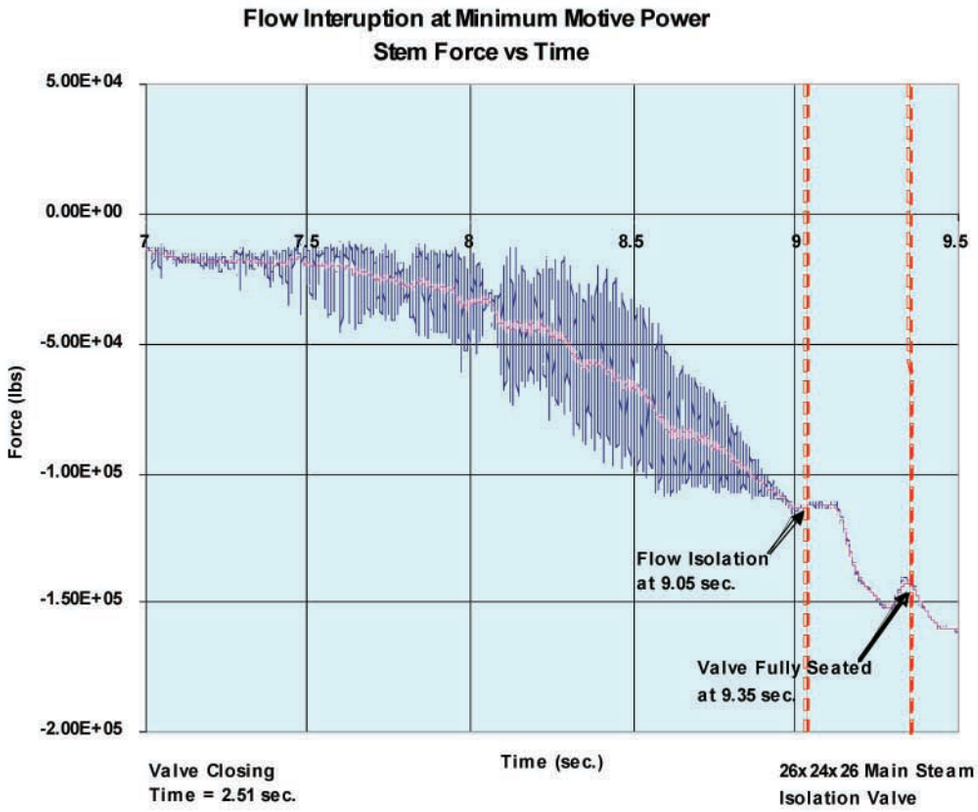

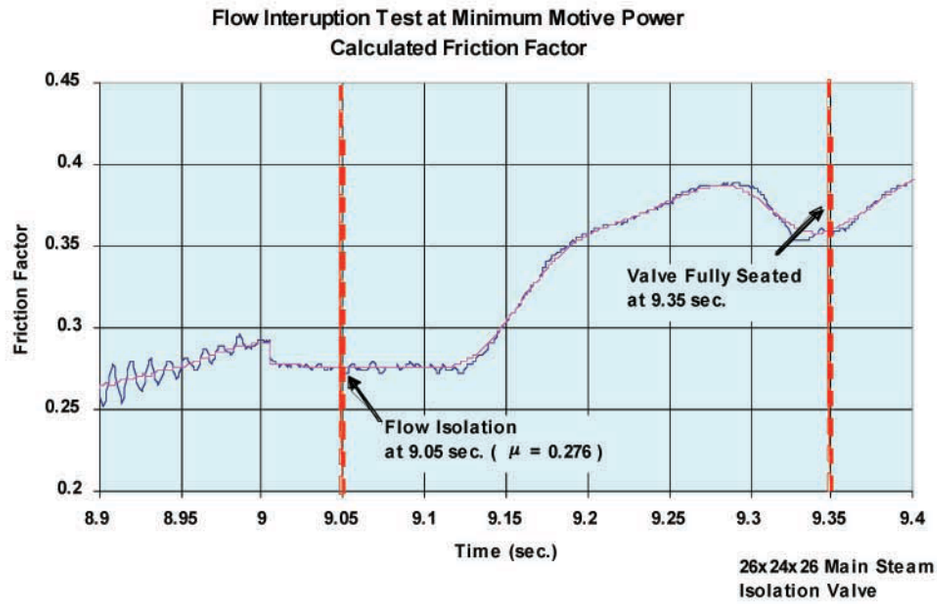

Figure 13

Size 26 x 24 x 26

Valve and Actuator Forces

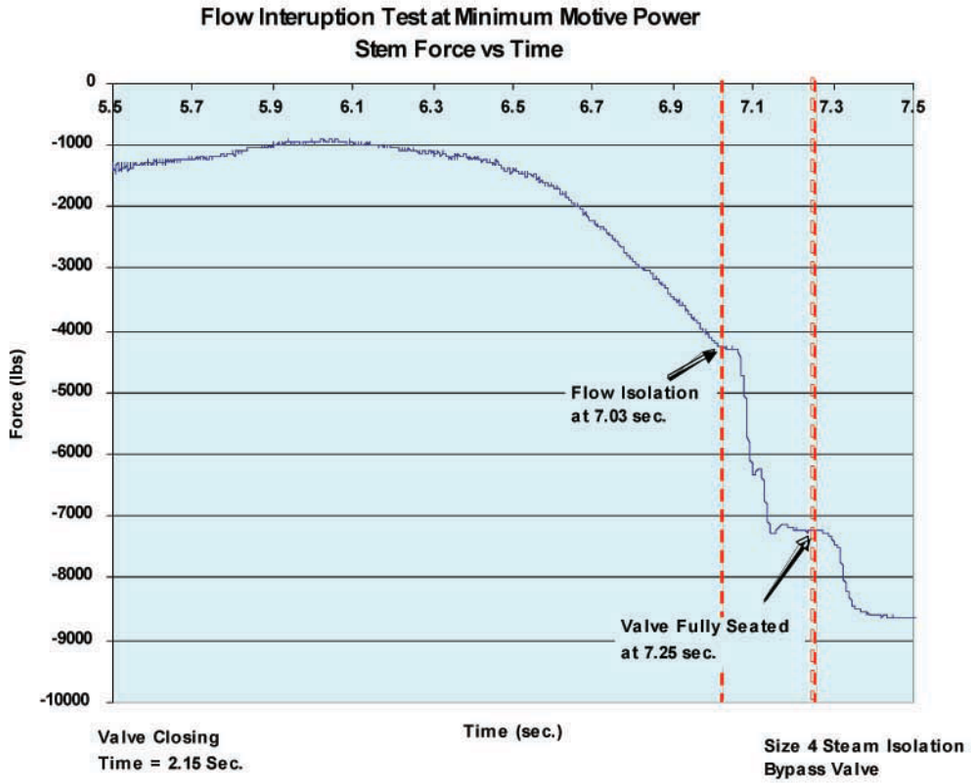

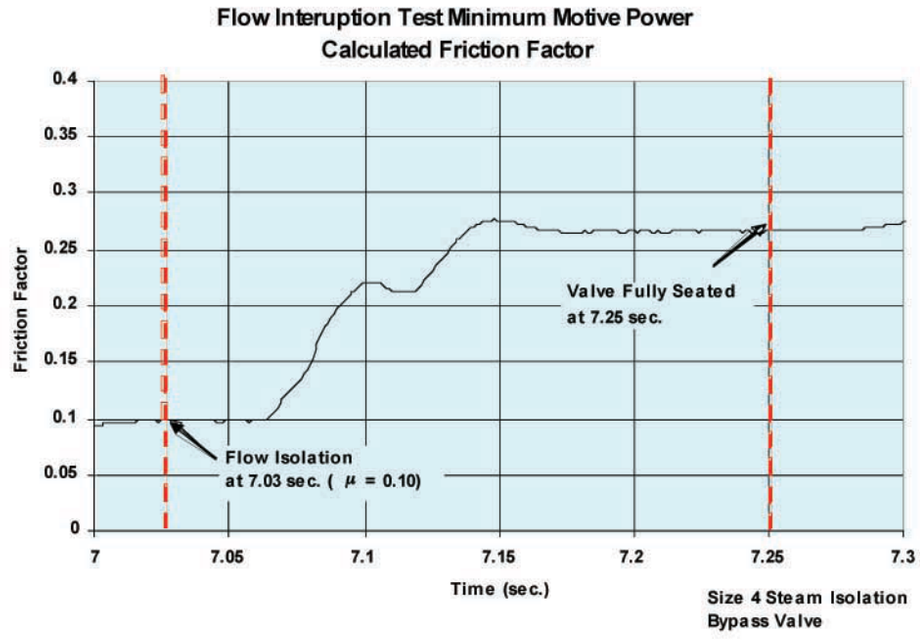

Figure 14

Size 4

Valve and Actuator Forces

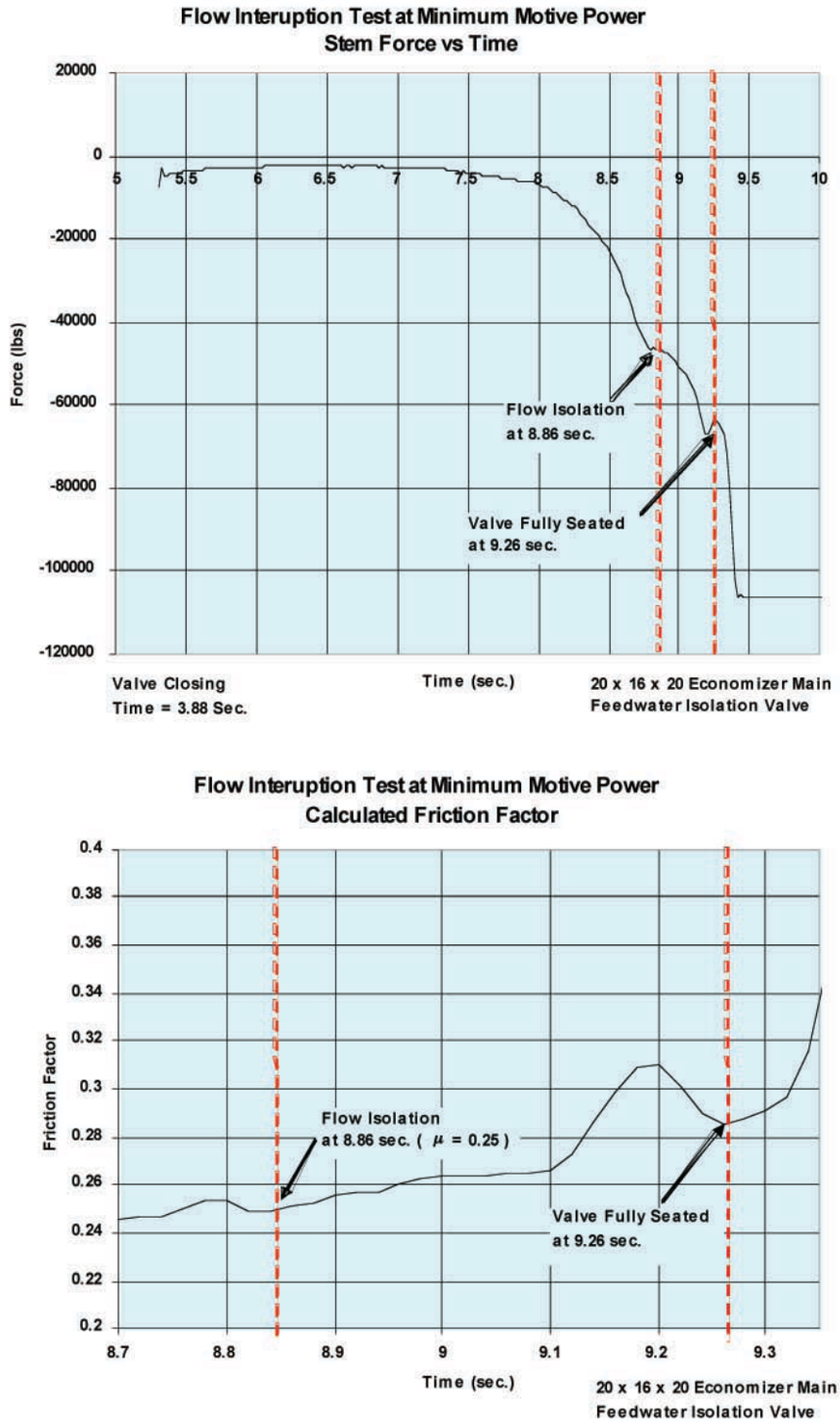

Figure 15

20 x 16 x 20

Valve and Actuator Forces

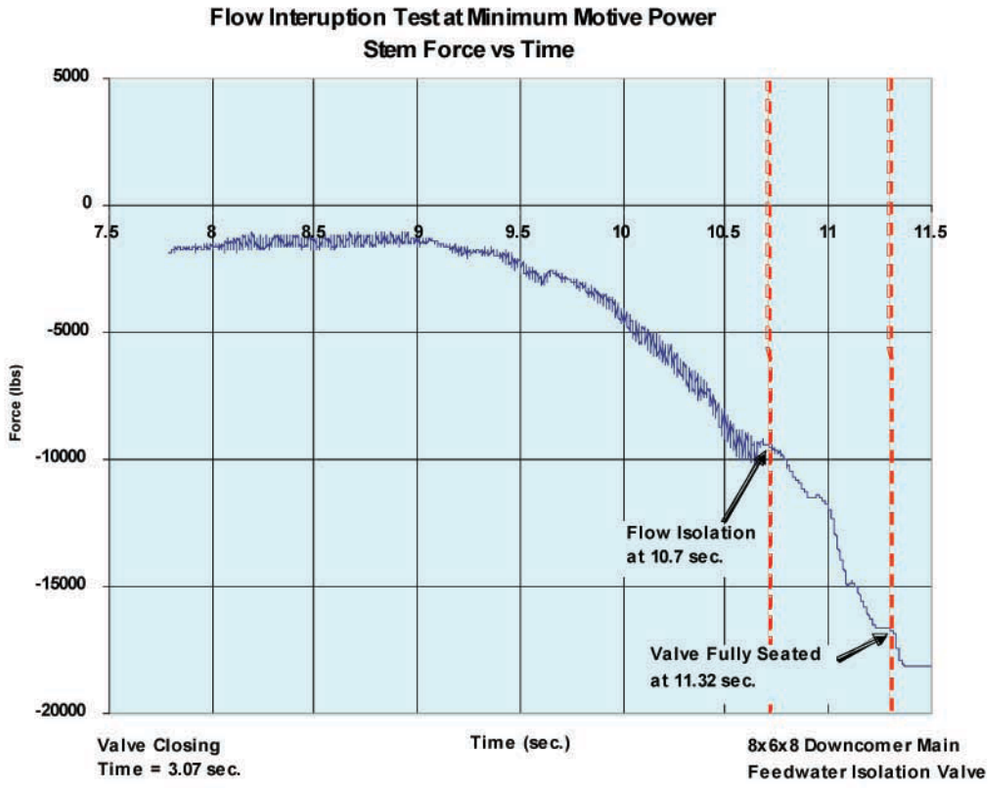

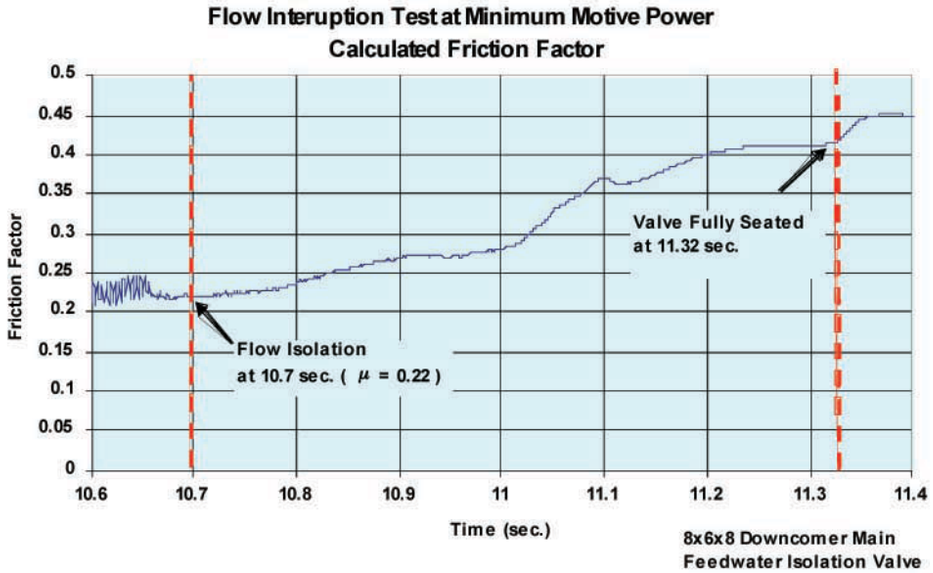

Figure 16

8 x 6 x 8

Valve and Actuator Forces

Avoid letting your Check Valves go to Failure by Trending

Greg Hunter
American Electric Power
D.C. Cook Nuclear Plant

Roger Sagmoe
Nuclear Management Company
Prairie Island Nuclear Plant

Tony Maanavi
Exelon Corporation
Byron Station

Michael Robinson
K&M Consulting, Inc

and

The Nuclear Industry Check Valve Group

Introduction

Trending - what are the attributes that can be trended for determining Check Valve degradation? There are many publications available such as The Maintenance Engineer Fundamentals Handbook, TR-106853 Palo Alto, CA: EPRI, November 1996, Predictive Maintenance Primer Revision Guide, Palo Alto, CA: NMAC, April 1991 1007350, NIC Check Valve Nonintrusive Analysis Guide NIC, Final Report - Revision 0, May 9, 1999, etc. that discuss testing methods and program activities but none provide information activities and attributes that can be trended. The Nuclear Industry Check Valve Group (NIC) has filled that gap. In the summer of 2005, NIC published the "Tracking and Trending Guide for Check Valves." Based on several NIC and Industry test programs along with actual plant experience, NIC along with vendors developed a guide that helps utility personnel apply the proper test for determining the condition of check valves. This paper will discuss performance, condition, and operational/functional readiness activities and attributes. These activities and attributes include, full / partial open, closure, backflow, mechanical exerciser, and seat leakage. Testing techniques/technologies/methods including acoustics, magnetics, eddy current, external inspection, internal inspection, Radiography, etc will be discussed. Yes, trending the proper attribute can keep your check valve from failing.

History

Both the NRC and INPO recommend, as a good practice, trending check valve condition, so incipient failures are identified and maintenance is performed prior to failure. Additionally, based on regulatory activity (NRC issued Information Notice [IN] 2000-21, "Detached Check Valve Disc Not Detected by Use of Acoustic and Magnetic Non-intrusive Test Techniques," and INPO re-emphasized SOER 86-03, "Check Valve Failures or Degradation") there is increased scrutiny and oversight of check valve trending.

In June of 2001 the Nuclear Industry Check Valve Group (NIC) started to determine the trendable attributes of all the testing and test methodologies that are being used to determine check valve conditions. Because of this, several activities were started that included an update to the NIC Check Valve Analysis Guide, the start of a tracking & trending guide for check valves, and the creation of a Technical Advisory group (TAG) for the development and implementation of a program for Check Valve Performance Trending.

In November 2002, the TAG performed its first set of testing and, in 2003, published the results. The results are very encouraging and, as anticipated, the technologies evaluated have trending capabilities which are discussed in detail within the report. This effort was funded by 20 nuclear sites. However, with the incorporation of the initial test results, new milestones were developed and further testing is still being considered as well as the validation of the level of knowledge and training which is required to trend data.

In December 2005 NIC published the "Tracking and Trending Guide for Check Valves." This tracking and trending document builds on the technologies and methods commonly used by utilities for determining check valve conditions including methods described in the NIC Nonintrusive Analysis Guide. A working knowledge of this document will help the reader understand the testing activities and attributes. Training and qualification are also background prerequisites for successfully applying test methods and technologies.

What is the driving force for utilities to seek additional information as to the need for this program? A major reason for this project would be that the NRC has mentioned (in numerous places including the 1999 rulemaking, NUREG-1482, IN 2000-21, and in past meetings) that trending and evaluation of existing data need to be used to reduce or extend testing intervals on check valves. That is what this test program is designed to provide, a solid basis for trending parameters and to provide uniformity throughout the industry. The NRC staff has been very candid about their interest and is receptive to the approach we are taking. If we do not continue with our proposed activities and meet our objectives in a timely fashion, others may set their own criteria which we will then have to follow.

Basics

Before we get started with the discussion about what is currently trendable we need to discuss the basics. For trending to be effective a decision on how the information is going to be gathered and how it is going to be reviewed must be made. The most effective way is in a Check Valve Program which systematically evaluates all available data pertinent to check valve performance for the purpose of maintaining a high level of check valve reliability. It does so by identifying those check valves susceptible to degradation and implementing appropriate inspection, test, or maintenance activities.

A solid Check Valve Program utilizes an approach by which the inspection and testing schedule, developed based upon valve design, application, maintenance history, and industry data, is continually reviewed, in response to the results of these tests and inspections to ensure optimal application of program resources. The objective of this review and optimization is to prevent check valve failures by identifying deficient valve applications, determining the effects of these deficiencies and appropriately testing, inspecting, modifying, or performing periodic maintenance as required, ensuring continued reliability and performance.

Within the program there should be two types of activities and attributes, Performance and Condition. Performance refers to data collected to determine the operational and/or functional readiness of a component and Condition refers to data collected to determine the accumulative effects of aging and degradation. Performance attributes are collected using a variety of activities including but not limited to full or partial open flow with system flow, closure by differential pressure, backflow, or seat leakage.

Condition attributes refer to data collected to determine the accumulative effects of aging and degradation over time.

Technologies & Methods – Performance Vs. Condition

The technologies that we reviewed include but are not limited to acoustics, pulsed EM (EC), DC/AC magnetics (DCM/ACM), ultrasonics (UT), airborne ultrasonic (AU) leak detection, radiography (RT), infrared thermography imaging (IRI), Disassembly and Inspection, and performance based testing; forward flow, differential pressure/ temperature, and quantified leak rate.

The data collected using these various methods and techniques have parameters that are both measurable and trendable. When a measured parameter changes in relation to a known cause at repeated test conditions, it is considered a trendable parameter. The ability of a measured parameter to change in any given direction based on valve degradation is referred to as its trendability.

Check valves can have both performance and condition attributes that are collected at periodic intervals and under differing plant conditions. Whenever possible, data collected should be obtained at similar system conditions (e.g., power level, pressures, temperatures, and flows). Test lineups need to be determined that make the data obtained relevant to the valve and not the system. It is imperative for trending, that test conditions be duplicable to the extent possible, so that any contributions to the measured parameter's change from other possible variables are minimized.

Operational / Functional Activities

These activities are more commonly known as the Surveillance and Monitoring activities. Here are the activities that are used for check valves:

Open Flow (Full or Partial)

Flow is passed through the valve where measurements are directly or indirectly taken. This can be determined by position indicators, pressure drop, or non-intrusive technologies, such as acoustics, magnetics, radiography or electromagnetic technologies.

Close

Upon cessation or reversal of flow the valve obturator moves to the closed position and seats. Closure is confirmed by direct or indirect means using the backflow methods below or by other non intrusive means.

Backflow

Pressure/Flow Profiles taken upstream and downstream of valves can confirm that the valve is closed, leaking by, or flowing in reverse.

Pump Reverse Rotation Check of a stopped parallel pump can be used to confirm that the valve obturator is in contact with the seat by verifying that the pump shaft is not rotating backwards.

Monitoring of System Parameters such as changes in tank levels, system pressure alarms, flow alarms, etc.

Temperature Profiles taken upstream and downstream of a valve using a contact pyrometer or other temperature measurement device can indicate if it is closed. This can be a pass/fail test or criterion applied where temperature is limited to maximum value.

Infrared Thermo Imaging (IRI) analysis is used to detect and analyze temperature differences or gradients. IRI can detect seat leakage when warm fluid is allowed to pass back through a closed disc and produces a temperature gradient. This can be a pass/fail test or criterion applied where temperature is limited to maximum value.

Mechanical Exerciser

An external actuation lever is used to verify the travel of the valve disc, thereby verifying disc travel from valve seat to valve disc backstop.

Seat Leakage

Acoustic (audible range from 0 to 20 kHz) and airborne ultrasonic (non-audible range above 20 kHz to 1 MHz) leak detection methods can provide a means to monitor online seat leakage when a valve is closed and pressure differential is established.

Condition – Based and Predictive Activities

Inspections (Intrusive Techniques)

There are two primary vantage points for collecting inspection data: The first is external and the second internal.

External inspections are more useful for those check valves that have external operating mechanisms and shaft packing than for those with no external moving parts.

Internal inspections provide a direct and proof positive means of collecting condition data.

Disassembly and Inspection

This method is used to verify the ability of a check valve to move through its full stroke via visual observation of the valve internals. It is used when system or plant conditions cannot easily be established to verify operability, if required, at design basis accident conditions. Additionally, the valve internals are visually and mechanically inspected for wear, corrosion, erosion, and other degradation. The information gathered during disassembly and inspection can be used in conjunction with diagnostic testing signature analysis to monitor degradation during subsequent diagnostic testing. This is also the time to collect information and measurements for NIT—verification of seat angle, disc thickness, or collection/confirmation of optimum sensor placements, EC stroke delta by manual disc stroking, etc.

Boroscopic Inspection (Fiber Optics)

Fiber optic or boroscope probes provide a means to perform a visual inspection of valve internals without a complete disassembly.

Seat Leakage

Mass Make-up and Pressure Decay leak rate methods are effective at quantifying and monitoring seating capability and valve condition. Typical valves tested are Appendix J (CIVs - Containment Isolation Valves), Technical Specification High/Low pressure interface valves (PIVs – Pressure Isolation Valves), and OM Code required valves. Leakage rate tests may provide trend data that predict future leakage problems. The leakage rate of a valve may also be a good predictor of future failures associated with hinge pin wear and other valve degradation of the closed disc position changing relative to the valve seat.

Diagnostics (Non-intrusive Techniques / Technologies / Methods)

The various techniques, technologies, and methods used for collecting non-intrusive diagnostic condition data will be examined below. These techniques and methods are highly subjective and based on personnel experience performing the test and analysis of data. For this reason they are open for interpretation and evaluation.

Acoustics

Acoustic monitoring during flow conditions can identify backstop tapping, seat tapping, and relative wear/looseness of internal components. When a valve is seated, acoustic monitoring can detect leakage in some cases, providing a pressure differential across the disc exists. When flow is initiated, acoustic monitoring can confirm the full open position providing the disc or other member impacts the backstop depending on variables that may require evaluation for any specific check valve. When flow is terminated, acoustical monitoring can confirm disc closure providing the disc impacts the seat. This also depends on variables that may require evaluation for any specific check valve. The force imparted during either event has to be sufficient to generate a measurable impact exceeding the background RMS levels. A second technology should always be used to corroborate the open and/or closed positions to ensure the highest level of confidence possible.

Magnetics

Magnetic Flux Analysis (AC or DC) – Magnetic flux analysis can determine disc motion/flutter and assist in confirming open and close positions in conjunction with acoustic monitoring.

Eddy Current (pulsed electromagnetic) analysis can determine disc full open and close under stroke test conditions (after initial baseline test where acoustic impact, characterization from a similar check valve, or disassembly stroke qualified full stroke voltage delta is obtained).

Ultrasonics

Ultrasonic monitoring can determine disc position under flow or detection of disc in the closed position or stuck open under no flow conditions for fluid systems other than steam, gas or air. Ultrasonic monitoring can also detect and quantify disc flutter and indicate conditions that will cause accelerated wear or further degradation of the valve. Manual scanning methods can also be used to confirm that the internals are intact.

Radiography

Standard/Conventional Radiography – Radiographic examination is a diagnostic tool to assess disc position, to confirm that internals are intact, and to some extent to indicate their condition. RT is difficult on cast thick steels where the absorption of the energy is more likely to occur. Precise source placement is required to achieve desired resolution.

Phosphor Plate Radiography – Phosphor plate radiography examination has many advantages over conventional RT. The radiograph is fed into an electronic developer and downloaded to a computer, where, with software the exposure can be manipulated and distances can be determined. Precise source placement is required to achieve the desired resolution.

Leak Detection

Acoustic and Airborne Ultrasonic leak detection methods can provide a means to monitor seat leakage when a valve is closed and pressure differential is established. Note: Ultrasonics for leak detection is not the same as ultrasonics for disc position and disc flutter. They are two different technologies.

Mechanical Exerciser

An external actuation lever is used to verify the travel of the valve disc, thereby verifying disc travel from valve seat to valve disc backstop. Criteria are applied to breakaway and full open torque values to determine if additional frictional load is present or if the disc is attached.

Infrared Thermo Imaging (Thermography)

A technique based on measuring and comparing infrared radiation emitted from various equipment surfaces. Infrared thermography can aid in determining tank levels and internal valve leaks.

Stroke Timing

The valve stroke is measured based on a predetermined test configuration and trended over time to monitor for abnormal changes that may be indicative of valve degradation or a change in test conditions. When using stroke time, test conditions should be similar at each test to minimize timing differences caused by them (for example, measuring the time it takes from a pump trip to the discharge check valve closing, or a motor-operated valve or air-operated valve [MOV/AOV] actuation to the check valve open/close acoustic impact, etc.). Binding may be evident by a longer stroke time, or a loss of disc may reveal itself in a shorter stroke time (e.g., hinge arm in a swing check with no disc attached).

Quantitative Wear Prediction

The need for and benefits of applying quantitative wear and fatigue predictions are significant as they relate to screening and prioritizing safety-related and economically significant check valves. Qualitative data, though generally easier to produce and compile, is varied in consistency and usefulness. Quantitative data requires a greater level of effort to produce, but the end result is generally more tangible and definitive. Wear quantification enhances condition-monitoring activities for safety-related, production-critical and/or economically significant check valve applications by providing an analytical framework for trending valve performance data. For example, it allows for the proper normalization of

tracked parameters to account for variations in condition that influence them, thus improving the active feedback process and facilitating problem resolution through planned design changes.

Test Performance and Tracking (Operational Readiness)

One purpose of the Inservice Testing (IST) Program is to assess the operational readiness of pumps and valves in the program. However, caution is advised when using IST results as the sole basis for proving operability. Any other available information that has a bearing on equipment operability should also be considered.

Valve disc movement tests (open and closed) do not generally require the use of reference values. However, it is the owner's responsibility to determine acceptance criteria for the test conditions. Consequently, when using Non-Intrusive Testing (NIT) techniques to fulfill Code check valve testing provisions, a baseline inservice test demonstrating disc movement should be conducted to establish acceptance criteria. The baseline test should indicate valve response when known to be operating acceptably (good condition).

It is the owner's responsibility to verify that a valve is operating acceptably at the time the acceptance criteria is established. A disassembly and inspection, radiograph, back-leakage and flow test, or multiple technologies that provide an effective assessment of condition may be used to establish valve condition. Bi-directional testing should be used whenever possible. Information from inspections and tests from similar valves in the check valve group, industry data, operating experience, and maintenance history should also be considered.

The initial test of a check valve's open or closed safety function using NIT techniques that subsequent tests will be assessed against is considered a baseline test. The baseline test shall only be established when the check valve is known to be operating acceptably. It is also the owner's responsibility to qualify the method/technique(s) used for NIT. NIT baseline data for future comparison is best acquired when a valve is new, or has been rebuilt and restored to a "new" condition.

When applying NIT technologies to prove that a check valve is in an acceptable condition, the use of multiple technologies is recommended, provided no technology limitations exist. In addition, combining an open stroke with a close stroke test increases failure detection and provides the optimum effectiveness for failure monitoring. Test conditions should be used that are easily duplicated and provide repeatable results for trending effectiveness.

The "Generic Implications" section of IN 2000-21, states the following:

"If NIT techniques used to verify the opening or closing capability of safety related check valves are not properly qualified and a baseline established for each individual valve when the valve is known to be operating acceptably, potentially inadequate valve performance may be undetectable in the analysis of NIT results."

IN 2000-21 identifies the consequences of not qualifying NIT to safety-related check valve testing.

Diagnose Valve Health/Condition

Performance

The goal of operational/functional testing is to ensure the readiness of a check valve to perform when called upon. The activities associated with operational/functional testing are performed at a given interval to provide an acceptable level of assurance, or confidence level. The combination of testing needs to verify the valve's ability to stroke open and close for maximum failure detection capability.

Condition

The goal of condition-based activities is to ensure that the valve will perform its functions over a predetermined period of time. The activities selected are periodically performed and data collected at specified intervals that will adequately monitor the check valve's condition. The attributes associated with each activity is extracted from the data and analyzed. A monitoring plan must be determined based on many factors; using predictive or inspection condition-based activities, or a combination thereof. The desired outcome is being able to effectively monitor the aging and degradation

effects on the check valve that the system imposes on it over time. A thorough diagnosis of valve health is essential for continued reliable operation.

Conclusion

Now that you have a taste for the testing methods, technologies, and methodologies that are available for check valves, you need to know which are trendable and how to apply them. The attachments contain the determination by the Nuclear Industry Check Valve Group as to which technologies or methods are trendable. However, to apply trending to your program we suggest that you read the "Tracking and Trending Guide for Check Valves," published by NIC in 2005, the "Check Valve Analysis Guide" published in May 1999, and the NIC Phase four report "Evaluation of Non-intrusive Diagnostic Examination Technologies for Check Valve Trending" (NIC-04-Trending) published in October 2003.

Also, just because you did not see a specific technology or method that you are using for trending doesn't mean that it is not acceptable or is not trendible. The technologies or methods that were discussed in this paper are those that the Nuclear Industry Check Valve Group deemed to be the most widely used. If you are using other method(s) than those discussed here, we urge you to attend a meeting of the Nuclear Industry Check Valve Group and share your knowledge. Also, further information may be found at the Nuclear Industry Check Valve Group's Website www.checkvalve.org.

References

1. The Maintenance Engineer Fundamentals Handbook. TR106853. Palo Alto, CA: EPRI, November 1996.
2. Improving Maintenance Effectiveness Guidelines. TR-107042. Charlotte, NC: NMAC, March 1998.
3. Check Valve Maintenance Guide. TR-100857. Palo Alto, CA: EPRI, August 1995.
4. Predictive Maintenance Primer. NP-7205. Palo Alto, CA: NMAC, April 1991.
5. Predictive Maintenance Primer Revision to NP-7205. 1007350 Final Report, October 2003, EPRI, Palo Alto, CA: 2003.
6. NRC Information Notice 2000 21: Detached Check Valve Disc Not Detected By Use of Acoustic and Magnetic Nonintrusive Test Techniques, December 15, 2000.
7. Evaluation of Nonintrusive Diagnostic Examination Technologies for Check Valve Trending, (NIC-04-Trending), Published by NIC, October 2003.
8. Check Valve Nonintrusive Analysis Guide, prepared by NIC, Final Report - Revision 0, May 9, 1999.
9. Equipment Reliability Process Description, AP-913 Revision 1 from INPO, November 2001.
10. Preventive Maintenance Basis Project Overview Report, EPRI TR-106857-V40, November 1998.
11. EPRI PM Basis Database, Version 5.0, Electronic MSAccess Application (software application with built-in documentation).
12. NIC Non-intrusive Phase 1-3 Reports, Nuclear Industry Check Valve Group, NIC-01, 02, & 03.
13. INPO Significant Operating Experience Report, 86-03, Check Valve Failures or Degradations, dated October 15, 1986.
14. Appendix II, "Check Valve Condition Monitoring Program," in the ASME OM Code-1995 Edition through 1996 Addenda.
15. Guidelines for In-service Testing at Nuclear Power Plants, NUREG-1482 Rev.1, dated June 2004.

Trendable Attributes of Operational / Functional Activities

Activity	Attribute Collected	Measured Parameter	Trendable
Full/ Partial Stroke Open	Full Open	Flow rate or change in tank level per unit time	Yes
	Full Open Indication	Flow or P	Pass/ Fail
	Partial Open	Normal Flow or P	Pass/ Fail
	Position Indication	Position (degrees/inches)	Yes
Stroke Timing	Obturator Stroke	Time in seconds	Yes
	Valve Actuation to check valve opening/closing	Time in seconds	Yes
	Pump Start/ Stop to check valve	Time in seconds	Yes
Close/ Backflow	Pressure Profile	System Pressure readings (ΔP)	Yes
	Flow Profile	System Flow readings (flow met in parallel train)	Yes
	Temp Profile	Temperature Gradient (ΔT)	Yes
	Pump Reverse Rotation Check	Shaft rotation	Pass/Fail
	System Parameters	Tank Levels (Δ Level per unit time)	Yes (depends on capability of instruments to detect a problem)
	IR Imaging	Temperature Gradient (ΔT) and viewable image for comparison	Yes (application dependant)
Seat Leak Detection	Seat Leak Detection	RMS Level (with baseline threshold)	Yes
	Airborne Ultrasonics	Decibel	Yes (but not for all applications)

Trendable Attributes of Condition – Based & Predictive Activities

Activity	Attribute Collected	Measured Parameter	Trendable
Internal Inspection	Wear Measurements (valve internals disassembled)	ID or OD of piece/parts	Yes
	Seat / Disc alignment and contact	Blue Check - contact band position and width	Pass/Fail
		Light Check	Pass/Fail
		Feeler Gauge / Waxed Paper	Pass/Fail
	Internal corrosion / erosion / FAC	Wall thickness	Yes
	External corrosion / leakage	Extent / Amount	No
	Manual Stroke Checks	No binding or hanging up	Pass/Fail
	Visual indications and looseness checks (valve not disassembled and alternate measurements used)	Dial indicator used to obtain gap/clearances between moveable parts (e.g., disc post to hinge arm by measuring side to side and up and down movement to determine gap is less than design clearance). There are other alternate means and techniques used to monitor wear that the CVP engineer can use.	Yes
Boroscopic	Visual for wear/physical damage/seat contact for close General condition checks	Visual and recorded description	Pass/Fail
Seat Leakage	Pressure Decay (App J)	Leakage past seat	Note 1
	Mass M/U (App J)	Leakage past seat	Note 1
	PIV	Leakage past seat	Note 2
	Code	Leakage past seat	Note 2

Activity	**Attribute Collected**	**Measured Parameter**	**Trendable**
Acoustics	Time Waveform	Trace Overlay	Yes using comparison analysis
	Frequency (PSD/FFT/ Waterfall)	Shift in frequency content at stable flow	Yes, but valve dependant
	Impacts	Magnitude, Amplitude, and Ringdown Duration	Yes, but valve dependant
	Impact Rate	# per unit time	Yes, but valve dependant
	Audible Noise	Waveform file played back for audible analysis	No
	Event Origin	Time of Arrival	Yes for larger valves.
Magnetics	DC (used with acoustics)	Voltage Delta/Gauss strength	Used for monitoring disc flutter and stroke, but valve dependant
	AC (used with acoustics)	Voltage Delta	Used for monitoring disc flutter and stroke, but valve dependant
Eddy Current	Full stroke voltage delta	Delta Volts	Yes, once verified
	Stroke Time	Seconds	Yes
Ultrasonic (UT)	Disc Angular Velocity	Disc Angular Velocity	Yes
	Disc open angle	Degrees off the seat	Yes
	Disc Flutter	Change in distance per unit time	No, but severity can be monitored
	Confirmation of internals	Manuals scanning A scan presentation	Pass/ Fail

Activity	Attribute Collected	Measured Parameter	Trendable
Radiography (RT)	Radiograph/digital image	Visual record	No
	Dimensional data	Wear in inches or %	Yes
Leak Detection	Acoustics	RMS Level (with baseline threshold)	Yes
	Airborne Ultrasonics	Decibel (dB) level	Yes (not all applications)
Mechanical Exerciser	Breakaway Torque	Force/Friction in ft lbf	Yes
	Full Open Torque	Force/Friction in ft lbf	Yes
	Position	Degrees (°) rotation	Yes
IR Imaging	IR Imaging Temperature Gradient	Temperature (ΔT) and viewable IR image for comparison	Yes
Stroke Timing	Obturator Stroke	Time in seconds	Yes
	Valve Actuation to check valve opening/closing	Time in seconds	Yes
	Pump Start/Stop to check valve opening/closing	Time in seconds	Yes

Notes:

1. Leakage rates under Appendix J are not trendable as a linear progression, but when leakage approaches a valve's alert limit in a step wise fashion, the reason for change should be pursued. Most Appendix J tests have multiple boundary isolations being tested simultaneously, so other actions are taken to determine where the leakage is occurring. Most administrative limits use the Code guidance for determining when to take action. The typical administrative limit uses the Code specified limit of 7.5 times nominal valve size standard ft^3 per day (air).
2. Pressure Isolation Valves (PIVs) are more apt to be individually tested and leakage may be trended. However, with the allowable limit set at 1 gallon per minute (gpm)—trending may not start until the 1 gpm limit is met. A good overall parameter to track is the 24 hour primary leakage rate. Once seat leakage reaches the 0.02 gpm level, the plant Operations Department is reacting to the effects on plant systems. This action level is used to start additional monitoring activities and investigation.

Flow-Induced Vibration Effects on Nuclear Power Plant Components Due to Main Steam Line Valve Singing

S.A. Hambric
Pennsylvania State University

T.M. Mulcahy and V.N. Shah
Argonne National Laboratory

T. Scarbrough and C. Wu (1)
U.S. Nuclear Regulatory Commission

Abstract

Nuclear power plant components can be subjected to strong fluctuating loads and experience unexpected high-cycle fatigue failures while operating at extended power uprate (EPU) conditions. In particular, physical damage has occurred to steam dryers in certain boiling water reactor (BWR) plants during EPU operation, resulting in the generation of loose parts that could interfere with the functionality of safety-related valves and other components. In addition, steam line safety relief valves (SRVs) and a solenoid valve actuator have been damaged by high-cycle vibration during power uprate operation at BWR plants. The objective of this paper is to discuss the source(s) generating these fluctuating high-amplitude loads, present the methods used to estimate these loads, and discuss monitoring of nuclear power plant components to identify potential adverse flow effects. When turbulent flow of a fluid over a cavity formed by one of the SRVs installed on the main steam line (MSL) locks in to acoustic modes within the cavity, high-frequency, high-amplitude pressure fluctuations can be generated. These pressure fluctuations can be estimated by on-line measurement of strains in gages installed on the MSLs. Acoustic models can then be used to estimate the pressure loads on plant components. The potential for adverse flow-induced vibration effects reveals the importance of assessing the impact of EPU conditions on nuclear power plant components and of monitoring the performance of plant components during power ascension to uprate conditions.

Note 1: Staff members of the U.S. Nuclear Regulatory Commission contributed to the preparation of this paper. It may present information that does not currently represent an agreed-upon NRC staff position. NRC has neither approved nor disapproved the technical content.

1 Introduction

Boiling water reactors (BWRs), such as the ones shown in Figure 1 and Figure 2 (from [1]), use reactor cores to boil water. Wet steam emanates from the boiling water and travels vertically through tube banks, called steam separators, to remove moisture. Above the steam separator, a perforated hooded structure, called steam dryer (see images in Figure 3), further removes moisture from the steam. The steam exits the dryer and collects at the top of the reactor pressure vessel (RPV), then flows into one of four main steam lines (MSLs), where it flows to turbines and generates electricity.

Utilities have been using power uprates since the 1970s as a way to increase the power output of their nuclear power plants. As of July 2004, the NRC had completed 101 reviews of power uprate applications, resulting in a gain of approximately 4,183 MWe (megawatts electric) at existing plants, an equivalent of about four additional nuclear power plants. Over the next five years, the utilities plan to ask for additional power uprates, which would add another 947 MWe to the nation's generating capacity.

Power uprates can be classified in three categories:

(1) Measurement–uncertainty recapture-power uprates are power increases of less than 2% and are achieved by the use of enhanced techniques for calculating reactor power.

(2) Stretch power uprates are power increases up to 7% and usually involve changes to instrumentation settings.

(3) Extended power uprates (EPU) are usually greater than stretch power uprates and have been approved for increases as high as 20%. Extended power uprates usually require significant modifications to major pieces of plant equipment, such as the high pressure turbines, condensate pumps and motors, main generators, and/or transformers.

As of June 2004, EPU operation has been approved for 11 BWR plants, with uprates ranging from 6.3% for Monticello in 1998 to 20% for Clinton in 2002. Seven of these plants have not experienced major problems under EPU operating conditions. But the four remaining plants, Quad Cities Units 1 and 2 (QC1 and 2, respectively) and Dresden Units 2 and 3 with uprates in the range of 17 to 18%, have experienced significant increases in flow-induced vibration in the MSLs and within the RPV. The increased vibrations, along with increased fluctuating pressures within the steam, have led to damage of relief valves and steam dryers in the plants.

A summary of the steam dryer failures was issued by the Nuclear Regulatory Commission (NRC) [3]; and GE, the plant designer, has issued a Services Information Letter (SIL) to owners of GE BWR plants [4]. A schematic of the dryer failures, along with accompanying photographs, are reproduced from [4] in Figure 4. In June 2002, a large cover plate on the outside of the original QC2 steam dryer broke off, and pieces of the plate were carried by the steam through the MSLs. Before and after the failure, increases in moisture content in the MSL steam were evident, indicating that large cracks and/or holes in the dryer were allowing wet steam to flow directly into the MSLs. High cycle fatigue was identified as the cause of the dryer failure, and Exelon, the plant owner, installed thicker cover plates and used stronger welds to repair the dryer. However, in May 2003, moisture carryover in the MSL steam increased significantly again, and the plant was shut down in June 2003 so the dryer could be inspected. This time, large cracks had formed through the walls of the dryer outer bank hood. Also, several braces and tie bars on the top of the dryer had cracked.

Cracks had also formed in the steam dryer at the QC1 plant, and in October 2003 the moisture content in the MSL steam increased. In November, QC1 was shut down, and a steam dryer inspection revealed that a portion of the outer bank hood had broken loose (about 16 cm x 23 cm x 1.3 cm).

While the steam dryers in the QC plants were cracking and breaking, valves on the MSLs were also experiencing higher vibration levels at EPU conditions. An electromatic relief valve (ERV) on a QC1 MSL, along with several MSL support clamps and tie-back supports, failed in November 2003. Recently, in January 2006, several ERVs in the QC1 and QC2 plants were found to be degraded (powered relief mode was not available, but spring safety function was available) due to damage induced by strong pressure fluctuations and vibrations [5]. Although steam dryers do not perform safety-related functions, safety relief valves are responsible for relieving reactor overpressure and must remain functional.

Shortly after the first dryer failure in QC2, Exelon began monitoring MSL moisture content more frequently so that any steam dryer damage could be inferred. The GE SIL 644 [4] recommends weekly moisture content monitoring to all BWR owners, along with periodic inspections of the dryers during refueling outages. However, recent efforts by the QC1 and QC2 plant owners and their subcontractors, along with Entergy, who obtained an EPU license amendment for the Vermont Yankee (VY) nuclear power station, have led to more proactive monitoring of the fluctuating pressure levels within MSLs and RPVs, which should identify potential steam dryer fatigue failures (and potential valve failures) before they occur. In this paper, we discuss the new monitoring techniques, along with the mechanisms associated with pressure fluctuations incident on steam dryers and MSL valves in BWR plants.

To summarize the current understanding of the dryer excitation sources, we draw information from documents submitted to the NRC by Entergy and Exelon, which report measurements and simulations of the steam dryer loading in the QC1, QC2, and VY BWRs. All of the information used is from non-proprietary documents in the public domain.

For more information, see the NRC's Agencywide Documents Access and Management System (ADAMS), at www.nrc.gov.

2 Acoustic and Fluid-Dynamic Excitation of Steam Dryers

Several sources cause the pressure fluctuations acting on BWR steam dryers. The steam flowing through and around the dryer is turbulent, and turbulence induces random, oscillating pressures on the dryer surface, with the magnitude of the pressures increasing with flow speed. The turbulent flow also excites large-scale, low-frequency acoustic modes in the RPV steam volume; these modes, in turn, oscillate against the dryer surface. Finally, various acoustic disturbances in the MSLs, some of which are caused by turbulent flow, propagate through the steam in the MSLs and radiate sound into the RPV steam. The radiated sound impinges on the dryer and can be amplified by acoustic modes in the RPV.

To determine the strengths of the various sources causing pressure fluctuations on the steam dryer, Exelon Nuclear instrumented a replacement steam dryer for their QC2 plant with several pressure sensors, as shown in Figure 5 (from [2], [6] and [7]). The pressure sensors were mounted flush with the surface of small metal domes to reduce localized noise induced by small-scale turbulent flow structures passing over the sensors. Power spectral density measurements of pressure at the original licensed thermal power (OLTP) level (790 MWe) and two locations on the dryer (P12 and P24) are shown in Figure 6, reproduced from [7]. Sensor P12 is located on the lower corner of the hood on the 90 degree side of the dryer (see Figure 5), and sensor P24 is mounted about halfway down the skirt. The graphs indicate that a plateau of energy excites the hood and skirt below about 60 Hertz (Hz), which includes periodic peaks due to acoustic modes within the RPV steam and perhaps acoustic modes in the MSL steam columns. Some of the low-frequency peaks are stronger in amplitude in the skirt region.

High-amplitude pressure tones load the dryer near 150 Hz, particularly in the outer hood region. The fluctuating pressure amplitudes are high (about 0.02 psi^2/Hz [pounds per square inch squared per Hertz] at sensor P12) and increase considerably when the QC2 reactor power increases to EPU levels (930 MWe). Figure 7 shows pressure spectra for sensors P12 and P24 at EPU conditions (also reproduced from [7]), and the results indicate that the peak pressure amplitudes on hood sensor P12 increase to 0.3 psi^2/Hz. Table 1 summarizes the peak spectral levels at four hood sensors (two on each of the hoods). The highest peak pressure loads on the dryer at EPU conditions are not at sensor P24, but sensor P21, with levels of about 0.65 psi^2/Hz (~168 dB Re: 20 μPa). Figure 7 indicates that the pressures at frequencies below 60 Hz, however, increase only slightly on the hood, and change little near the skirt.

The peak pressure spectral levels near 151 Hz (on the 90 degree hood) increase in amplitude by a factor of about 15-18 between OLTP and EPU conditions. The peak spectral levels on the 270-degree hood occur at a slightly higher frequency of 157 Hz and increase by a factor of about 7 between OLTP and EPU conditions. Typical broad-band fluctuating pressures in turbulent flow increase proportionally to the square of flow velocity, while pressure spectra (pressure^2) increase with the fourth power of flow velocity. Steam flow velocities increase linearly with plant power, so pressure spectral levels are proportional to the fourth power of plant power. Given a power increase of 18% (930 MWe/790 MWe) and a corresponding flow velocity increase of 18%, the expected increase in pressure spectral level for turbulent flow is about 94%, or a factor of 1.94. The significantly higher increase in the pressure spectral levels near 151 and 157 Hz observed in the measurements (factors of 7 and 15 on the 270 and 90 degree hoods, respectively) indicates that loading mechanisms other than turbulent flow are present in the QC BWRs. We will present evidence later in the paper that attributes the 150 Hz peaks to flow tones induced in MSL valves.

2.1 Low-Frequency Acoustic Resonances of RPV Steam Volume

Reactor pressure vessels are instrumented with water level sensors, which may be used to qualitatively assess the fluctuating pressures in the steam volume. Two sensors are installed in each of the QC plants, offset by 180 degrees, about 45 degrees from the normal directions of the hoods, and located in the skirt regions of the dryers. Figure 8, reproduced from [8], presents the plots of fluctuating pressures within the QC1 RPV steam volume at the two level sensor locations for 790 MWe reactor power level. As with the instrumented QC2 steam dryer pressures, a

low-frequency plateau of energy is evident below about 60 Hz, along with a dominant tone slightly above 150 Hz. Additional peaks appear in the low-frequency range of the level sensor data, some of which are likely due to acoustic resonances within the long (about 60 meters) instrument lines between the RPV and the data acquisition system.

Acoustic resonances of the steam volume within the RPV of the VY nuclear power station have been computed by Entergy and its contractors in support of their EPU application to the NRC. Some of the resonances, extracted from a computational fluid dynamics (CFD) compressible flow model and presented in [9], are shown in Figure 9. (Note that the mode shapes only span the steam around the dryer and do not include the hemisphere of steam at the top of the RPV.) The low-order acoustic modes for the RPV steam volume are generally shaped like half- or full-acoustic waves across the RPV diameter and vertically between the water level and top of the RPV. The modes are clearly more active in the annulus between the dryer skirt and the RPV wall, explaining the increased low-frequency acoustic pressures observed in the skirt region of the QC2 dryer.

Note that the frequencies of the VY RPV acoustic resonances do not match those of the QC plants, since the inner diameter of the VY RPV (5.21 m) is smaller than that of the QC RPVs (6.38 m). The QC RPV acoustic resonance frequencies should be about 80% of those of the VY RPV.

2.2 Flow Tones, or "Singing" in MSL Valves

Several valves are connected to the BWR MSLs, including safety relief valves (SRVs) and main steam isolation valves (MSIVs). These valves perform important safety functions. SRVs reduce reactor steam pressure in the event of primary system overpressurization. MSIVs isolate the reactor system in the event of an MSL break outside the containment.

The SRVs are attached to stubbed pipes, or side branches, which extend perpendicular to the MSLs. A short column of steam in the connecting pipe is exposed to the turbulent steam flowing past the valve, and the fundamental acoustic mode of the steam column in the side branch can couple strongly to flow excitation over the stub pipe opening. The MSIVs are a "Y" configuration valve in the main steamline, with the valve disk oriented at about a 45 degree angle off the pipe axis. The flow through the MSIVs can be a strong source of turbulent excitation.

Figure 10 shows a schematic of an SRV excited by a flow tone excitation (courtesy of the Southwest Research Organization [SWRI], at www.swri.edu [10] and also described in a paper by McKee [11]). The steam flow separates at the leading edge of the stub pipe opening and a shear layer forms. At key frequencies, the effective wavelengths of the shear layer vortices match the diameter of the stub pipe opening, leading to strong coherent excitation of the steam cavity within the stub pipe.

A constant dimensionless parameter, called Strouhal number, can be defined for most shear layers as fD/U, where f is the frequency at which the shear layer oscillates, D is the side-branch opening diameter, and U is the steady flow speed of the shear layer. Ziada and Shine [12] measured the characteristic values of the Strouhal number for flow over circular side branches to be about 0.4, but also observed that Strouhal numbers vary with pipe diameter ratio (MSL diameter/branch line diameter), distance from upstream elbows, and acoustic damping. The characteristic value of the Strouhal number can be used to compute frequencies of strong shear layer loading at specific MSL flow speeds and side-branch opening diameters.

The steam columns within all closed side branches (the stubbed pipe in the SRV) have characteristic acoustic resonance frequencies at (2n - 1)c/(4L), where c is the sound speed in the fluid (about 488 m/s for MSL steam), L is the length of the branch, and n is an integer. The mode shapes of the acoustic resonances have a point of maximum pressure at the closed (valve) end of the branch and a point of minimum pressure at the open end of the branch (intersecting with the MSL). The fundamental (n=1) mode shape is a ¼ acoustic wave across the side branch length, with the next (n=2) mode being a ¾ acoustic wave across the side branch length.

[1] To provide context to these dB levels, the threshold of pain in the human ear is at sound pressure levels of about 140 dB, and most eardrums rupture when sound levels reach about 160 dB. Most window glass breaks at pressure levels of about 165 dB, and residential housing begins to fall apart at pressure levels of 170 dB (fluctuating pressures of about 1 psi).

The minimum pressure at the open end corresponds to a maximum in acoustic particle velocity (which is proportional to the pressure gradient) resulting from the velocity fluctuations within the shear layer. Should the frequency of a side-branch acoustic mode coincide (or nearly coincide) with the shear layer frequency, the acoustic oscillations in the side-branch steam can increase the strength of the vortices in the shear layer considerably, which in turn strengthens the acoustic fluctuations. The feedback and subsequent lock-in between the acoustic and shear layer mechanisms, should it occur, leads to extremely high fluctuating pressure amplitudes, commonly referred to as flow tones, or "singing".

Several of the valves in the QC plants operate at locked-in singing conditions, with tones occurring at various frequencies near 150 Hz. Figure 10 (right side) shows the measured vibration response of a valve on a QC2 MSL against increasing plant operating power (from [13]). A tone near 150 Hz first appears at about 740 MWe and increases significantly in amplitude as power increases to 930 MWe (at a far greater rate than the 94% estimated earlier for turbulent flow excitation between OLTP and EPU conditions). Other valves show similar vibration response but at frequencies between 140 and 160 Hz. The frequency differences may be due to slightly different geometries (including upstream geometries, like elbows) and flow speeds. Given a fluid flow speed of about 60 m/s and a stub pipe diameter of about 0.15 m, the characteristic Strouhal number is (157 Hz)(0.15 m)/(60 m/s) ~ 0.39, which is comparable to the values reported by Ziada and Shine [12] .

In the QC plants, the singing within the valves also excites the acoustic modes of the steam columns in the MSLs, which in turn radiate sound directly against the portion of the steam dryer outer hood near the MSL inlets on the RPV. The MSL acoustic pulsations also couple to the volumetric modes of the steam dome in the RPV to drive the steam dryer in regions away from the MSL inlets. A schematic of the loading mechanisms is shown in Figure 11.

The frequencies of the acoustic modes of the steam columns in the MSLs are integer multiples of c/LMSL, where LMSL is the length of the MSL between the RPV and the turbine. Compared to most BWRs, the MSLs in the QC plants are quite short (50-70 m), and the first acoustic modes appear at low frequencies, (488 m/s)/(50-70 m) ~ 7 – 10 Hz . The acoustic wavelength in the MSL steam at the valve singing frequencies near 150 Hz is about (488 m/s)/(150 Hz) ~ 3 m. It is highly likely that the MSL steam column acoustic modes are excited by valve singing at frequencies near 150 Hz. We will next examine this possibility by using measurements of the acoustic pulsations within the MSLs.

2.3 Measurement of Acoustic pressure fluctuations in MSLs

Early during the investigations of QC steam dryer failures, Exelon attempted to use existing plant instrumentation to quantify the fluctuating pressure loads acting on the steam dryers. Venturi line measurements showed the presence of the singing frequencies, but data measured at other frequencies were unreliable due to low signal-to-noise ratio, and corruption of the signal by acoustic modes in the long instrument lines between the venturis and the data acquisition systems.

Later, signals from strain gages mounted to the MSLs were used to infer internal acoustic pressure by relating pressure to the hoop strain on the outer surface of the pipe wall. However, the gages were mounted only at one circumferential location around the pipe and were measuring more than the hoop, or "breathing" motion of the pipe. The cut-on frequency of higher order acoustic modes in the steam is estimated from $1.84c/[\pi D]$, where D is the pipe diameter [14], and are about 620 Hz in the QC MSLs. Below the cut-on frequency, all acoustic motion is due to plane waves, which induce breathing in the pipe wall. However, the pipes are driven dynamically by many other sources, including turbulent flow impinging on elbows, and mechanical sources throughout the reactor.

---

* Ziada and Shine report measured Strouhal numbers not only for single side branches, but for pairs of side branches in tandem (on the same side of a pipe) and coaxially aligned (diametrically opposed to each other). Groups of SRVs are often aligned in tandem along the MSLs in BWRs. The load amplification induced by pairs of side branches can exceed significantly that of a single side branch.

* MSL lengths in other BWRs average 140 m, with some MSLs approaching 300 m in length.

At low frequencies, the pipe wall motion is dominated by its bending and ovaling modes, examples of which are shown in Figure 12. Single strain gages mounted to pipe walls cannot distinguish between strains induced by breathing (the signal of interest) and by bending and ovaling. However, uniformly spaced circumferential arrays of strain gages can filter bending and ovaling signals, retaining only the hoop motion. Figure 13 shows strain gage arrays mounted to one of the MSLs in the QC plants (reproduced from [15]). The time signals of four gages, separated by 90 degree circumferential increments, are summed in each array, normalized by the number of gages, and multiplied by a calibration factor converting hoop strain to internal acoustic pressure (hoop strain spectral density [$\mu\xi^2$/Hz] is multiplied by about 1.9 to compute the acoustic pressure spectral density in the QC plants).

An example of the filtered strain spectrum, along with individual strain measurements at the four circumferential locations, is also shown in Figure 13, reproduced from [16]. At most frequencies, the filtered signal is lower than the individual signals, suggesting that most of the pipe vibrations at low frequencies are caused by structural and hydrodynamic forces throughout the plant, rather than acoustic pulsations within the steam. At some frequencies, however, particularly those around the valve singing frequencies near 150 Hz, some individual strain measurements are lower than the filtered signal, indicating that the individual gage was mounted at a location of low local vibration. Therefore, it is not sufficient to measure strain at a single piping location and assume it represents an upper bound on acoustic signals within the MSL.

The strain signals clearly show the acoustic excitation of the MSL steam columns from the singing valves in the QC2 plant at frequencies at and around 150 Hz. The peaks with highest amplitude occur at about 151 and 157 Hz, which is consistent with the peaks in the pressure signals measured on the instrumented steam dryer (Figure 6 and Figure 7). Also, multiplying the peak microstrain spectral measurements (~ 0.03 $\mu\xi^2$/Hz) by the 1.9 conversion factor yields acoustic pressure spectral densities levels of about 0.06 psi^2/Hz, which are similar to the peak levels measured on the dryer (Figure 7).

For the MSL and dryer, the similarity in fluctuating pressure amplitudes near the valve singing frequencies around 150 Hz implies a strong acoustic coupling between the MSL steam and the steam within the RPV volume. Simple acoustic analysis of the sound power radiated by a flanged, or baffled, open-ended pipe [17] may be used to estimate a power transmission coefficient between the acoustic pulsations within the RPV volume and MSL steam columns. The transmission coefficient, τ, may be computed at any frequency f by combining the sound speed c in the steam and MSL pipe radius a with Equation 9.16a from [17]:

$$\tau = \frac{2(ka)^2}{\left[1+\frac{1}{2}(ka)^2\right]^2 + \left(\frac{8}{3\pi}\right)^2 (ka)^2}$$

where k is $2\pi f/c$. The power transmission coefficient is directly proportional to pressure squared and may therefore be used to estimate the ratio of pressure spectra in the RPV and MSL steam. The power transmission coefficient for the QC plants is shown in Figure 14. At low frequencies, the coupling between acoustic pressures in the RPV and MSL steam is weak (at 50 Hz the transmission coefficient is 0.05). However, near 150 Hz, the coupling is much stronger – about 0.34. It is not surprising, therefore, that strong acoustic pressure pulsation at 150 Hz in the MSL steam couples well to the RPV steam volume.

Acoustic modal analysis may be a more useful tool for predicting potential coupling of excitation sources in the MSLs with the acoustic modes in the RPV. Finite element or boundary element models of the entire steam system could be generated and analyzed to determine how specific MSL and RPV modes couple, in some cases, amplifying the source pressures.

Entergy also installed strain gage arrays in the MSLs of the VY plant. A filtered strain spectrum measured in the VY plant at current licensed thermal power (CLTP) conditions (535 MWe) is compared to spectra measured in the QC2

* Higher-order acoustic modes across the MSL cross section occur when the acoustic wavelengths (sound speed/frequency) in the steam become comparable to the pipe diameter. Since wavelengths decrease with increasing frequency, the high-order modes are said to ‘cut-on’ at specific frequencies.

plant at OLTP (790 MWe) and EPU power (930 MWe) in Figure 15 (reproduced from [18]). The VY data show no evidence of singing valves, but peaks similar in nature to those observed in the QC plants are evident at low frequencies of about 24, 35, 47, and 62 Hz (arrows in Figure 15). We will later explain how the peaks are likely associated with the low-order acoustic modes of the RPV volume, which are excited by turbulent flow within the steam dome and near the MSL inlets.

Both Exelon and Entergy have installed two strain gage arrays on each MSL in the Quad Cities and Vermont Yankee plants, so that relative amplitudes and phase delays between the filtered pressure signals in an array pair can be used to determine the strength and direction of acoustic plane wave propagation. However, the spacing between the arrays limits the frequency at which such processing may be used; the array spacing must be larger than half of an acoustic wavelength (sound speed/frequency). In the Quad Cities plants, for example, the spacing between arrays is about 9 m, establishing a lower frequency limit of (488 m/s)/(2x9 m) ~ 27 Hz. Also, at frequencies where integer multiples of half-acoustic wavelengths correspond to the array spacing, the signals may be reduced in amplitude to the point where they are too small to use (this is when node points, or points of zero amplitude in the acoustic waves coincide with the array locations). To resolve this issue, additional arrays with nonuniform spacing between arrays could be considered (logarithmic distributions are popular for measuring acoustic wave propagation in piping systems).

Along with the technical guidance above, we offer the following practical insights regarding vibro-acoustic data acquisition. While installing strain gage arrays (and other instrumentation) in laboratory environments is straightforward, doing so in a commercial nuclear power plant is quite challenging. The harsh plant environment can cause sensor and instrumentation line failures. Also, extraneous noise signals, such as those due to electrical ground loops and auxiliary machinery often appear in the sensor signals, and must be filtered. So that proper phasing between sensors is maintained, all signals must be synchronized and acquired simultaneously. So that sufficient data are acquired to assess acoustic wave amplitudes and phasing, long data records are required, and adequate storage capacity in the data acquisition system must be budgeted for. Computers with memory sufficient to process the large, multiple data records must be used, and software capable of handling large data records must be exercised.

2.4 Turbulent Flow Excitation of Steam Dryers

At low frequencies, turbulent flow emanating from the dryer vanes convects over the top of the dryer and along the hood outer surfaces on its way into the four MSL inlets. The flow speeds within the steam dome are low, on the order of 5-15 m/sec, as shown in the CFD simulation of the VY plant in Figure 16 (the flow speeds in the MSLs are much higher and range from 50 to 70 m/sec for various power plants at EPU conditions). The dominant pressure fluctuations in turbulent flow are concentrated around frequencies associated with the flow speed and characteristic dimension (a constant Strouhal number, fL/U). Slowly moving turbulence induces low-frequency excitation on neighboring structures. As flow speed increases, the frequency of excitation increases (since Strouhal number remains constant), and the amplitudes of the fluctuating pressures increase proportionally to dynamic head (which is proportional to the square of flow velocity). The total fluctuating force (pressure x effective loading area) applied to dryer surfaces by turbulent flow increases with the cube of velocity, as the loading areas over which the pressures are correlated grow proportionally with increasing velocity.

Direct measurements of the fluctuating pressures on the outer surfaces of the QC2 steam dryer (see Figure 6) show that amplitudes at low frequencies are small with respect to those caused by the valve singing near 150 Hz. The low-frequency pressures measured within the MSLs of the QC and VY reactors are also low with respect to those at valve singing frequencies. However, several low-frequency peaks in the VY MSL strain gage data are likely associated with acoustic resonances in the steam dome, where turbulent flow (either over the dryer surface, in the annulus between the dryer and MSL inlets, or at the MSL inlets) excites the steam dome modes. The steam dome modes couple with the acoustic modes in the MSL steam columns, so that they are visible in the MSL strain gage measurements.

The CFD model used to analyze turbulent flow around the VY dryer and within the steam dome [19] included time-accurate modeling of large-scale turbulence, as well as compressibility effects, so that acoustic modes of the volumes were effectively included in the simulation. Also included in the simulation was the coupling between the turbulent flow and the acoustic modes (the quantitative coupling was not modeled accurately, however, due to computational constraints on the time step used in the simulations). In spite of the modeling

inaccuracies, the simulations may be used to qualitatively analyze the coupling of flow turbulence and steam dome acoustic modes.

Figure 17 shows the pressures simulated by the compressible, time-accurate CFD analysis at various locations on the VY steam dryer. The three strong peaks at 32, 46, and 62 Hz are caused by turbulent flow excitation of low-frequency acoustic resonances in the steam dome (there are also weaker peaks at 17 and 22 Hz). Mode shapes reproduced from [9] are also shown in the figure and were computed using the CFD model. The peak frequencies agree well with those measured in the MSLs of the VY plant using the strain gage arrays (Figure 15) *. The CFD model was not employed to find the acoustic modes at the lower frequencies (17 and 22 Hz). The excellent qualitative agreement between the VY pressure measurements in the MSLs and simulated pressures on the dryer is encouraging and provides hope that strong acoustic pulsations within the steam dome can be measured in the MSLs.

* There is, however, the possibility that the low-frequency peaks in the measurements shown in Figure 17 are due not to steam dome modes, but to acoustic modes within the MSL steam columns. If this is the case, further study into how well low-frequency steam dome acoustic modes couple to MSL steam columns should be conducted.

3 Conclusions

Motivated by repeated structural fatigue failures of steam dryers in the Quad Cities BWR plants while operating at EPU conditions, Exelon Nuclear and GE designed stronger steam dryers and instrumented one of them (installed in the QC2 plant) with arrays of pressure transducers. Measurements of the pressures on the dryers, combined with measurements of pressures within the RPV and MSLs, revealed that strong acoustic tones emanating from the SRVs are propagating through the steam in the MSLs into the RPV steam, loading the dryer at several frequencies near 150 Hz. The fluctuating pressure amplitudes approach 1 psi, which is extremely high. Also, low-frequency excitation caused by steam flow turbulence around the dryer and MSL inlets, amplified slightly by acoustic modes within the RPV, is evident in the measured pressure spectra.

Based on the Exelon measurements and other studies performed by Entergy in support of its EPU application for the VY BWR, the current understanding of steam dryer fluctuating loads is summarized in Table 2, along with their propagation paths and means of detection. Most of the dominant pressure loads on the dryer can be detected with level sensors currently installed in the RPV and with circumferential strain gage arrays installed on the outer surfaces of the MSLs (at locations close to the RPV).

Low-frequency fluctuating loads induced by turbulence near the dryer surface are not generally detectable by remote sensors, unless the turbulence couples strongly with acoustic modes within the RPV. Usually, these direct loads are low in amplitude and do not induce fatigue cracking. All measurements and simulations to date have focused on frequencies below 200 Hz. Other high-frequency excitation sources may exist, such as singing of other valves within or downstream of the MSLs. Should such excitation occur, it would be visible in the measurements of the MSL strain gage array.

A frequently asked question is: why are MSL valves singing and steam dryers failing only in the QC1 and QC2 plants, and not at other BWRs already operating at EPU conditions? SRV singing is related directly to MSL steam flow speed and stub pipe diameter and length. The MSL diameters in the QC and Dresden reactors are smaller in proportion to their RPV diameters and rated power compared with most other BWR/3 plants, causing higher MSL flow speeds (see Table 3). The Dresden plants have smaller stub pipe diameters than the QC plants, such that valve singing occurs at power levels lower than EPU conditions (at about 78% of OLTP). Other BWRs with larger MSL diameters may encounter flow-tone problems if the flow velocities within the MSLs are increased to the range where the standpipes are excited.

A key conclusion from these studies is that singing assessments of valves in the MSLs are important for BWR plants considering implementation of an EPU to ensure that strong acoustic excitation does not occur. Also, monitoring of MSL acoustic pressures (such as through the use of MSL strain gages)is important for BWR plants during power ascension from OLTP to EPU conditions to detect the onset of any flow tones within the valves. If a tone occurs, its potential impact on valves (and other MSL components) and the steam dryer needs to be assessed.

Since remote monitoring approaches can only infer integrity of MSL components and the steam dryer, periodic inspection is important in identifying degradation and ensuring long-term component integrity from EPU operation. Walkdowns of MSL components and enhanced visual inspections (EVT-1) of steam dryers during refueling outages are highly beneficial in identifying degradation. Should unexpected fatigue-related damage occur, more study into excitation mechanisms would be warranted, along with more frequent and enhanced visual inspections of MSL components and the steam dryer.

4 Acknowledgements

We thank our colleagues at General Electric and Exelon for their helpful and insightful comments on an earlier version of this paper.

References

1. USNRC Technical Training Center, Reactor Concepts Manual - Boiling Water Reactor (BWR) Systems, pp. 3-1 – 3-18, 2003.
2. Exelon Nuclear letter RS-05-061, "Request for Additional Information for Review of Quad Cities Replacement Steam Dryer," Response to RAI 5(a), 12 May 2005.
3. NRC, Additional Flow-Induced Vibration Failures after a Recent Power Uprate, NRC Information Notice 2002-26, Supplement 2, 9 Jan 2004.
4. GE Nuclear Energy, BWR Steam Dryer Integrity, Services Information Letter (SIL) No. 644, Rev. 1, 9 Nov 2004.
5. NRC News, NRC Begins Special Inspection at Quad Cities Nuclear Plant, No. III-06-002, 10 Jan 2006.
6. Exelon Nuclear, Non-Proprietary Version of Exelon Presentation "Steam Dryer Design Technical Meeting," 25-27 April 2005; Enclosure 2 to GE Energy Nuclear letter GE-ENG-DRY-086, 17 May 2005.
7. Ramsden, K., Acoustic Circuit Benchmark Quad Cities Unit 2 Instrumented Steam Path 790 MWe and 930 MWe Power Levels, Document Number AM-2005-02, 15 June 2005; Enclosure 2, Attachment 2 to Exelon letter RS-05-095, "Technical Documentation Related to Analysis and Design of Quad Cities Replacement Steam Dryers," NRC Docket Nos. 50-237, 50-249, 50-254, and 50-265, 20 July 2005.
8. Ramsden, K., Engineering Evaluation of Reduced Strain Gage Data Sets on the Quad Cities Unit 1 Test Condition 15A, Document Number AM-2005-03, Rev. 0, 29 June 2005; Enclosure 2, Attachment 3 to Exelon letter RS-05-112, "Technical Documentation Related to Analysis and Design of Quad Cities Replacement Steam Dryers," NRC Docket Nos. 50-237, 50-249, 50-254, and 50-265, 24 Aug 2005.
9. Entergy, Vermont Yankee Nuclear Power Station Proposed Technical Specification Change No. 263 – Supplement No. 30, Extended Power Uprate Response to Request for Additional Information, BVY 05-072, Docket No. 50-271, Attachment 5, August 2005.
10. Southwest Research Institute, Machinery Vibration Services Flow Induced Vibration and Noise Web Page, www.swri.edu/4org/d18/mechflu/planteng/machvib/dt5.htm (used with permission).
11. Baldwin, R.M, and Simmons, H.R., "Flow-induced vibration in safety relief valves," ASME Journal of Pressure Vessel Technology, Vol. 108, pp. 267-272, Aug 1986.
12. Ziada, S. and Shine, S., "Strouhal Numbers of Flow-Excited Acoustic Resonance of Closed Side Branches," Journal of Fluids and Structures, Vol. 13, pp. 127-142, 1999.
13. Structural Integrity Associates, Quad Cities Unit 2 Main Steam Vibration Assessment, SIR-04-048 Rev. 0/KKF-04-020, 4 May 2004; Attachment 2 to Exelon letter RS-05-005, "Submittal of Information Regarding Extended Power Uprate Vulnerability Reviews," NRC Docket Nos. 50-237, 50-249, 50-254, and 50-265, 5 Jan 2005.
14. Pierce, A.D., Acoustics – An Introduction to its Physical Principles and Applications, Acoustical Society of America through the American Institute of Physics, pp. 315-317, 1991.
15. Structural Integrity Associates, Quad Cities Unit 1 Main Steam Line Strain Gage Reductions, SIR-05-036 Rev. 2/KKF-05-036, 6 July 2005; Attachment 2 of Enclosure 2 to Exelon letter RS-05-012, "Technical Documentation Related to Analysis and Design of Quad Cities Replacement Steam Dryers," NRC Docket Nos. 50-237, 50-249, 50-254, and 50-265, 24 Aug 2005.
16. Entergy, Vermont Yankee Nuclear Power Station Proposed Technical Specification Change No. 263 – Supplement No. 33, Extended Power Uprate Response to Request for Additional Information, Revised Exhibit EMEB-B-18 and Exhibit EMEB-B-18-1, (Non-proprietary version), BVY 05-084, Docket No. 50-271, Attachment 8, September 2005.
17. Kinsler, L.E., Frey, A.R., Coppens, A.B., and Sanders, J.V., Fundamentals of Acoustics, 3rd Edition, John Wiley and Sons,1982.
18. Entergy, Entergy Vermont Yankee Extended Power Uprate, presented to Advisory Committee on Reactor Safeguards, Extended Power Uprate Subcommittee, 29 Nov 2005.
19. Fluent Report: CFD Modeling of the Vermont Yankee Steam Dryer Phase –II, TM-675, Attachment 1 to BVY 05-061, "Vermont Yankee Nuclear Power Station Technical Specification Proposed Change No. 263 – Supplement No. 29, Extended Power Uprate – Steam Dryer Computational Fluid Dynamics," Docket No. 50-271, 2 June 2005.

20. Entergy, Vermont Yankee Nuclear Power Station Proposed Technical Specification Change No. 263 – Supplement No. 33, Extended Power Uprate Response to Request for Additional Information, Revised Exhibit EMEB-B-143-1 (Non-proprietary version), BVY 05-084, Docket No. 50-271, Attachment 9, September 2005.

Table 1. Peak spectral levels and frequencies at selected instrumented QC2 steam dryer locations at OLTP (790 MWe) and EPU (930) plant power levels (from [7]).

	90 degree hood		270 degree hood	
	P3	**P12**	**P20**	**P21**
Peak Frequency (Hz)	157	157	151	151
Spectral level at 790 MWe (psi^2/Hz)	0.012	0.020	0.025	0.090
Spectral level at 930 MWe (psi^2/Hz)	0.220	0.300	0.160	0.650
Ratio of spectral levels (930 MWe/790 MWe)	**18.3**	**15.0**	**6.4**	**7.2**

Table 2. Overview of fluctuating pressure sources acting on BWR steam dryers.

Frequency	**Cause**	**Source Propagation**	**Source Detection**
Very Low (below 80 Hz)	Turbulant flow over dryer	Directly incident on the dryer	Directly on the dryer (not generally available)
Low (below 80 Hz)	Turbulent flow over dryer	Into low-frequency acoustic modes of the RPV steam volume, which pulsate against the dryer and against the entrances to the MSLs	In the RPV level sensors, and in the MSLs
Mid (80 to 200 Hz)	Turbulent flow and flow instabilities (shear layers) in MSLs coupling to acoustic modes in valve standoff pipes	Into low and mid-frequency acoustic modes in the steam columns within the MSLs, which couple to RPV steam volume modes, which pulsate against the dryer	In the MSLs and in the RPV level sensors
High (above 200 Hz)	Unknown	Unknown	Unknown

Table 3. QC and VY BWR dimensions and parameters.

Quantity	Quad Cities and Dresden	VY
Pressure (MPa)	6.9 - 7.3	6.9 - 7.3
Temperature (degrees C)	282	282
Density (kg./m^3)	36	36
Dynamic Viscosity (Pa-s)	1.9E-5	1.9E-5
Sound Speed (m/s)	488	488
MSL Steam Velocity (m/s)	52 at OLTP (790 MWe) 61 at EPU (930 MWe)	42 at CLTP (535 MWe), 51 at EPU (642 MWe)
MSL Pipe Outer Diameter (m/in.)	0.51 m / 20 in.	0.46 m / 18 in.
MSL Pipe Inner Diameter (m/in.)	0.46 m / 17.9 in.	0.41 m / 16.1 in.
SRV Stub Pipe Diameter (m/in.)	0.146 m / 5.76 in. (QC) 0.117 m / 4.63 in. (Dresden)	0.132 m / 5.18 in.
RPV Inner Diameter (m/in.)	6.38 m / 251 in.	5.21 m / 205 in.

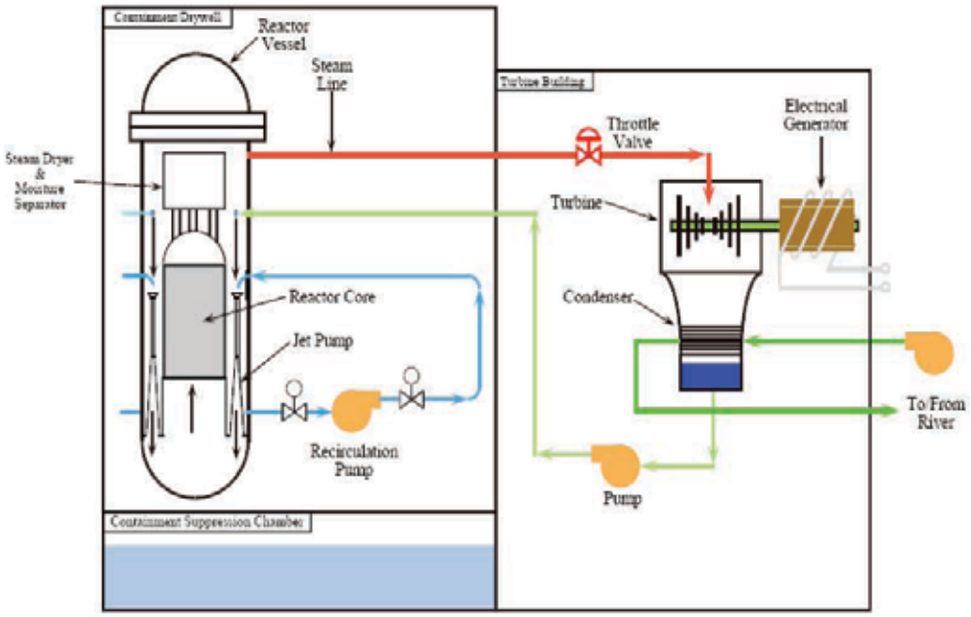

Figure 1 – Schematic of BWR components (from [1]).

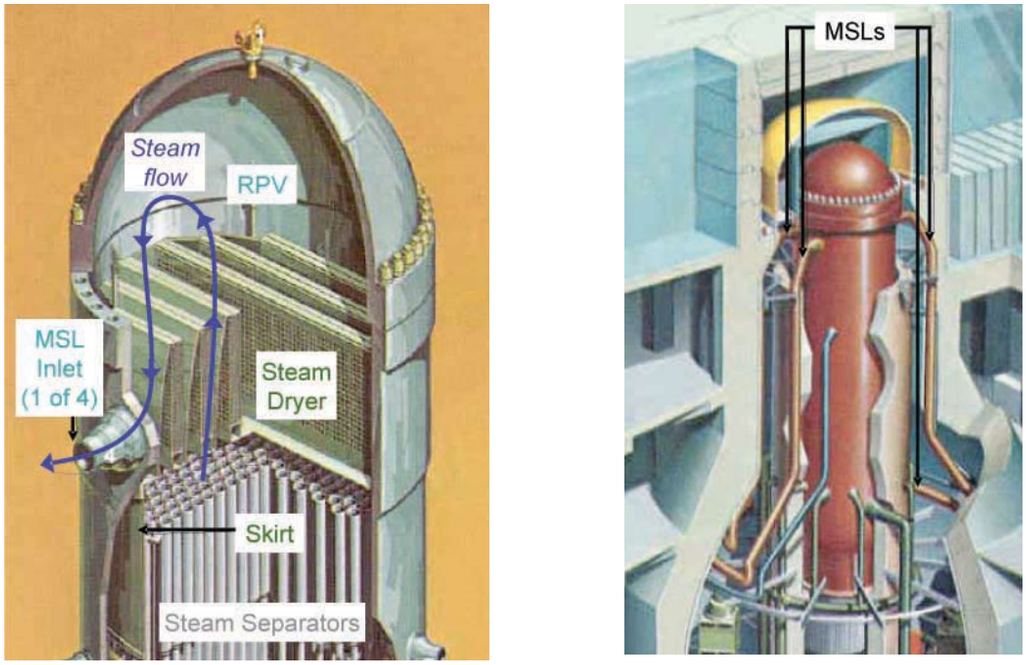

Figure 2 – Artist renderings of BWR with annotations by current authors: left - steam dryer within RPV, right - RPV and MSLs surrounded by containment structures (both images from [1]).

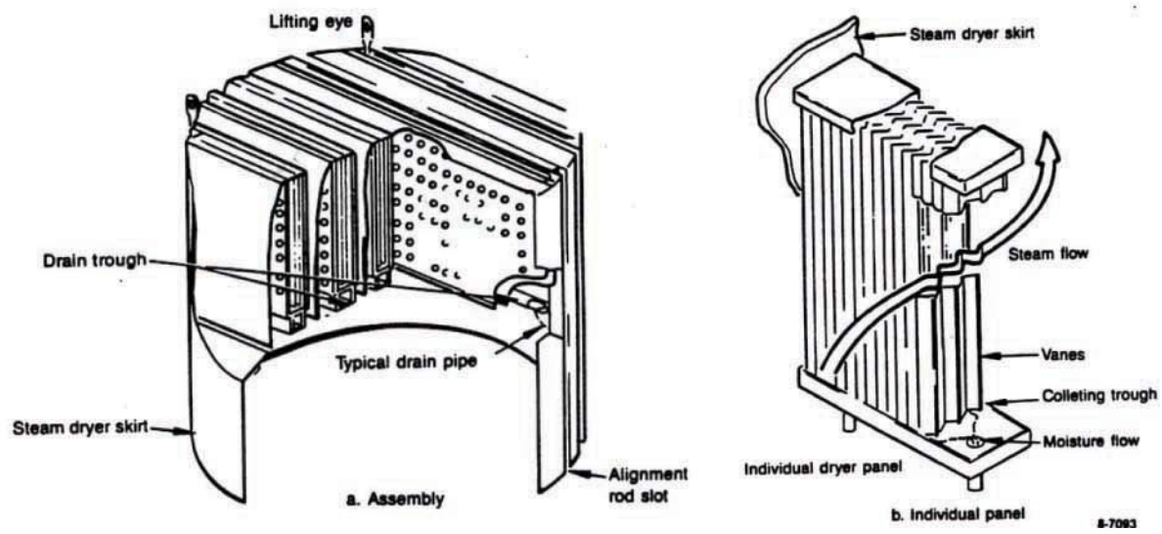

Figure 3 – Schematic of typical original BWR steam dryer: left – assembly, right – single panel.

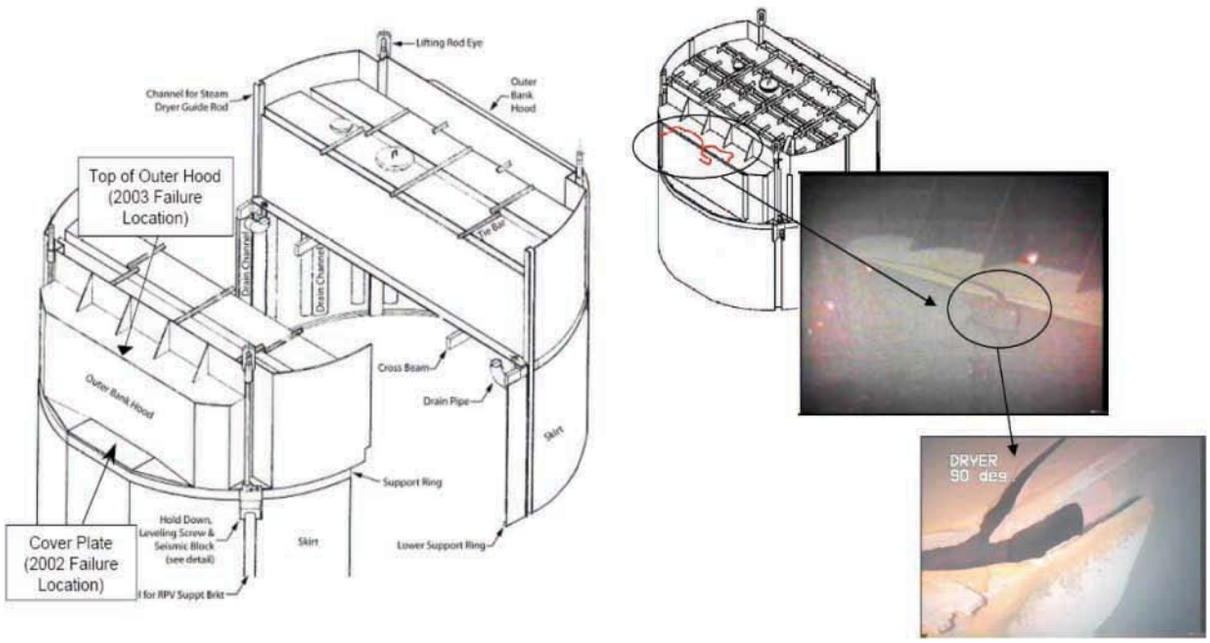

Figure 4 – Structural failures of Quad Cities 2 original steam dryer, from [4].

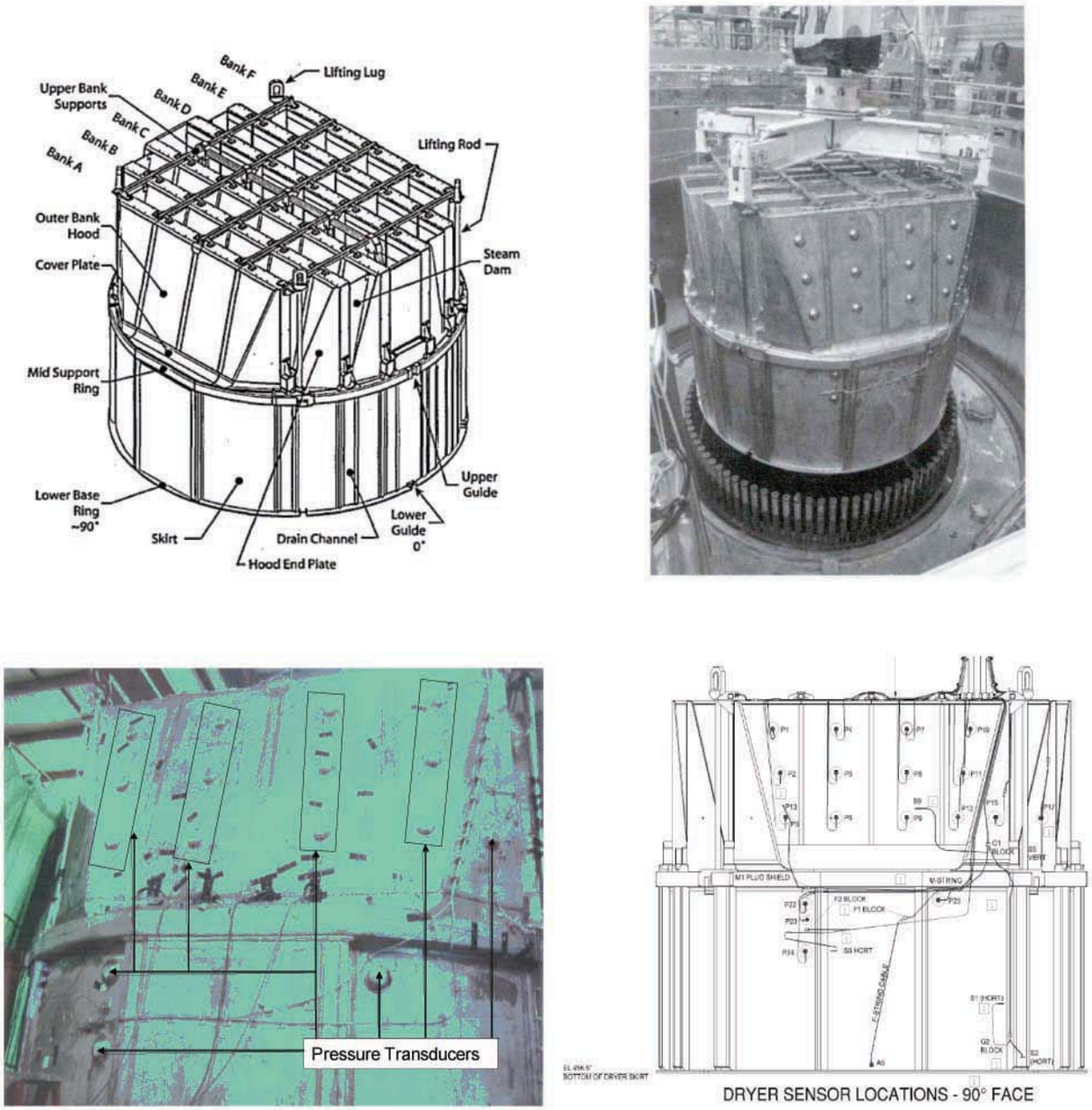

Figure 5 – Replacement steam dryer for QC1 and QC2: top left – schematic from [2]; top right – photograph taken during installation in QC2 (note that the dryer is rotated about 90 degrees between the images); bottom left – photograph of instrumented replacement steam dryer in QC2 plant - from [6]; bottom right – schematic of instrumentation - from [7].

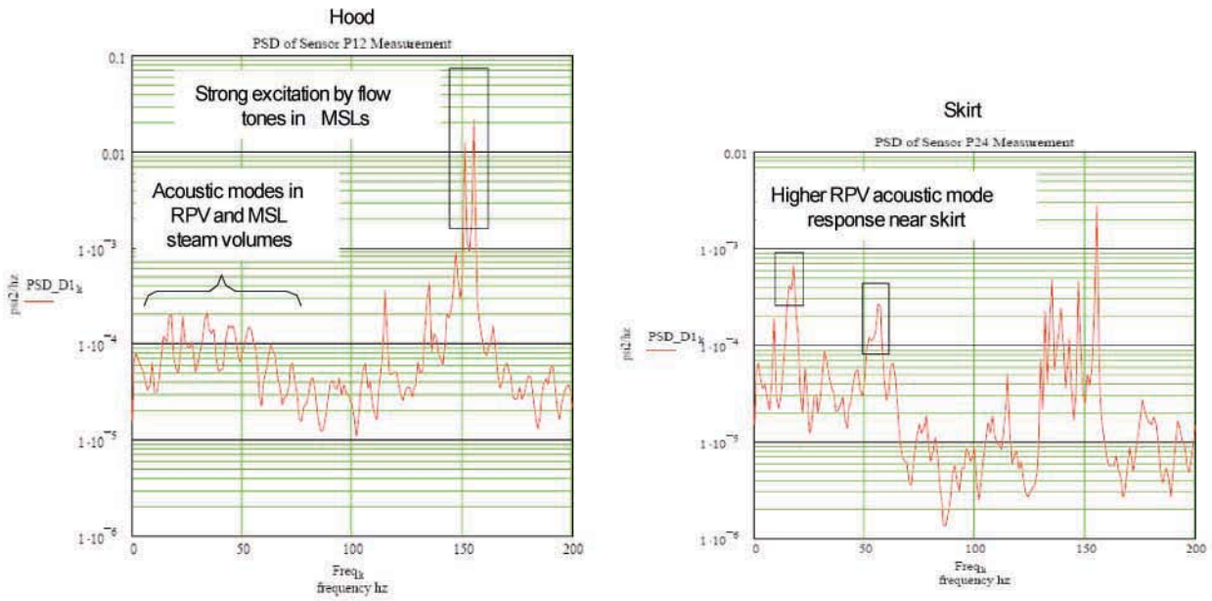

Figure 6 – Pressure spectral densities measured on hood of instrumented steam dryer in QC2 plant (from [7]) at 790 MWe. Sensor P12 is on lower corner of hood, and sensor P24 is on the skirt.

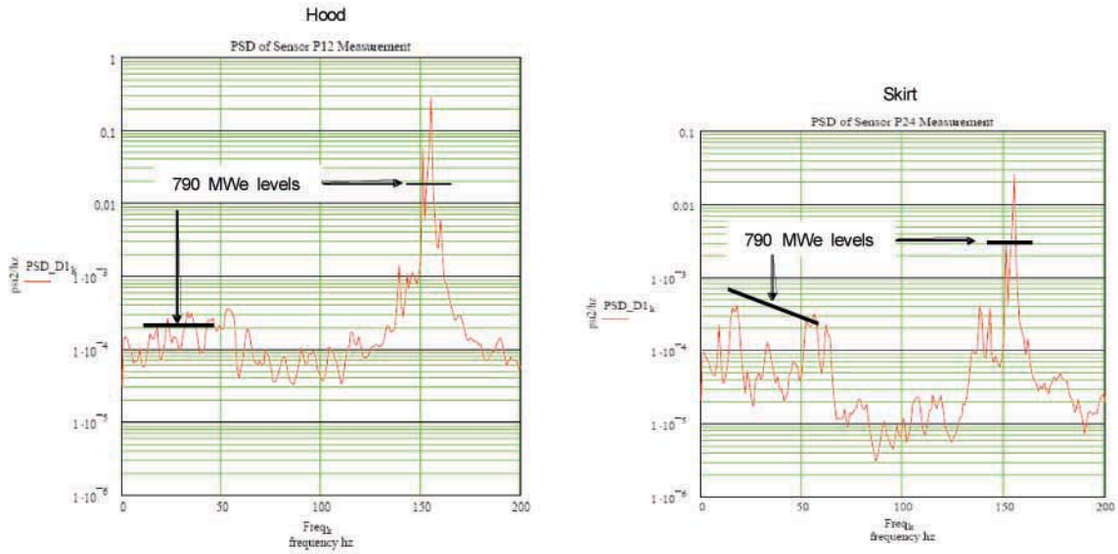

Figure 7 – Pressure spectral densities measured on hood of instrumented steam dryer in QC2 plant (from [7]) at 930 MWe, along with approximate peak levels at low (below 50 Hz) and high (near 150 Hz) frequencies at 790 MWe. Sensor P12 is on lower corner of hood, and sensor P24 is on the skirt.

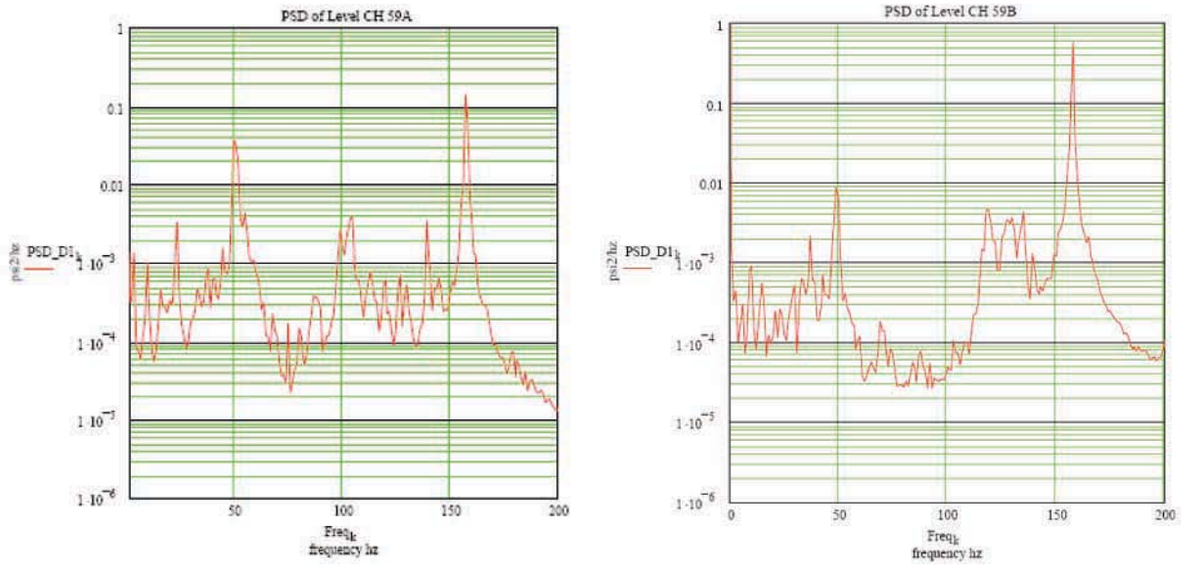

Figure 8 – Pressure spectral densities measured in RPV level instruments near skirts of steam dryers in QC1 plant (from [8]) at OLTP (790 MWe).

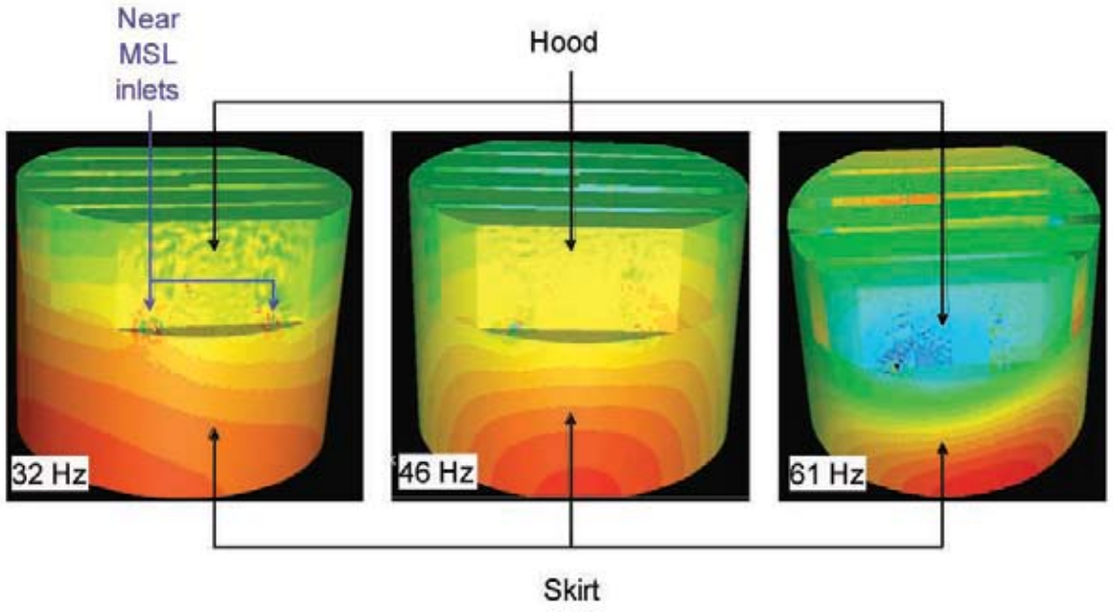

Figure 9 – Simulated RPV steam volume acoustic modes in VY BWR, computed by Entergy [9]. Top half-spherical section of RPV volume has been truncated from the mode shapes.

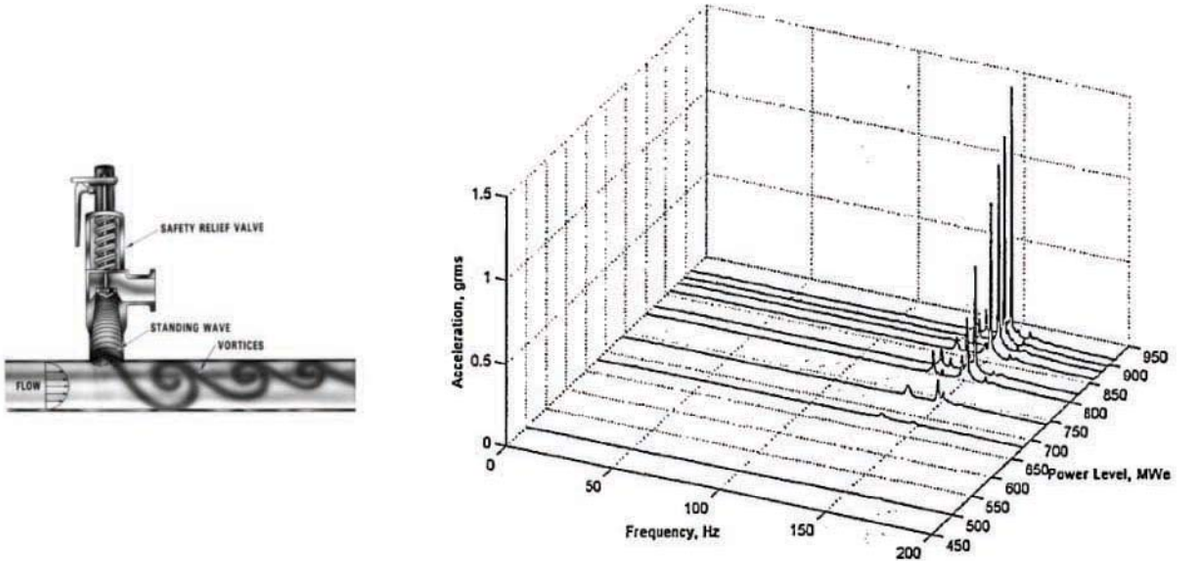

Figure 10 – Left – artist rendering of a "singing" safety relief valve (from [10] and [11]); Right – plot of acceleration measurements (perpendicular to pipe) for Quad Cities 2 electro-matic relief valve (ERV) 3D inlet flange at varying plant power levels (from [13]).

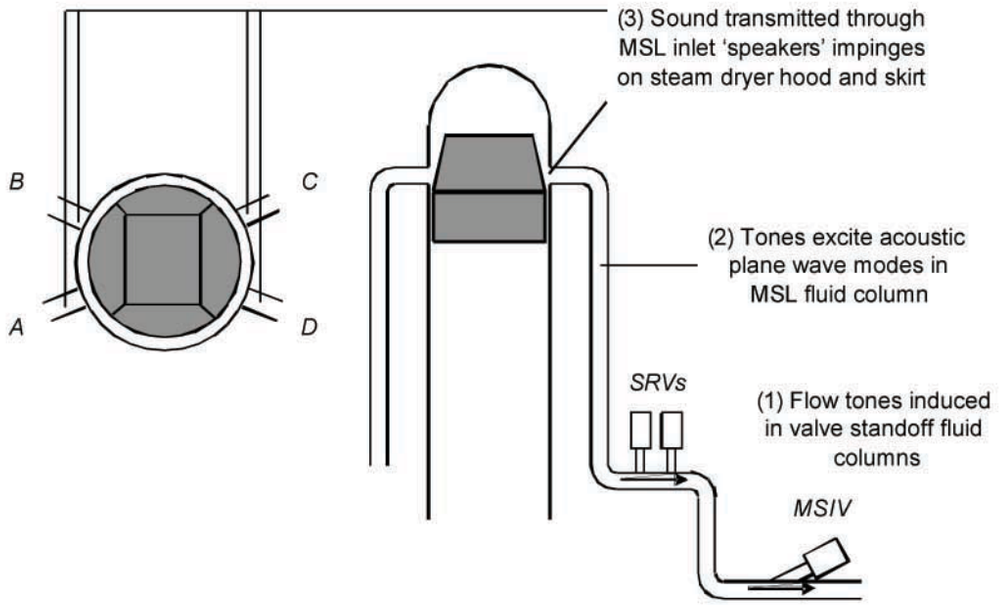

Figure 11 – Valve flow tone excitation of MSL fluid columns and of steam dryer.

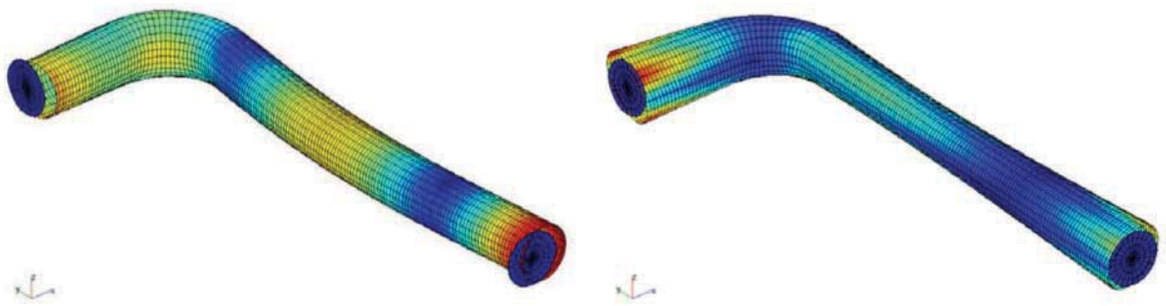

Figure 12 – Typical pipe bending (left) and ovaling (right) modes of vibration. Stationary end "plates" were added to aid in mode shape visualization.

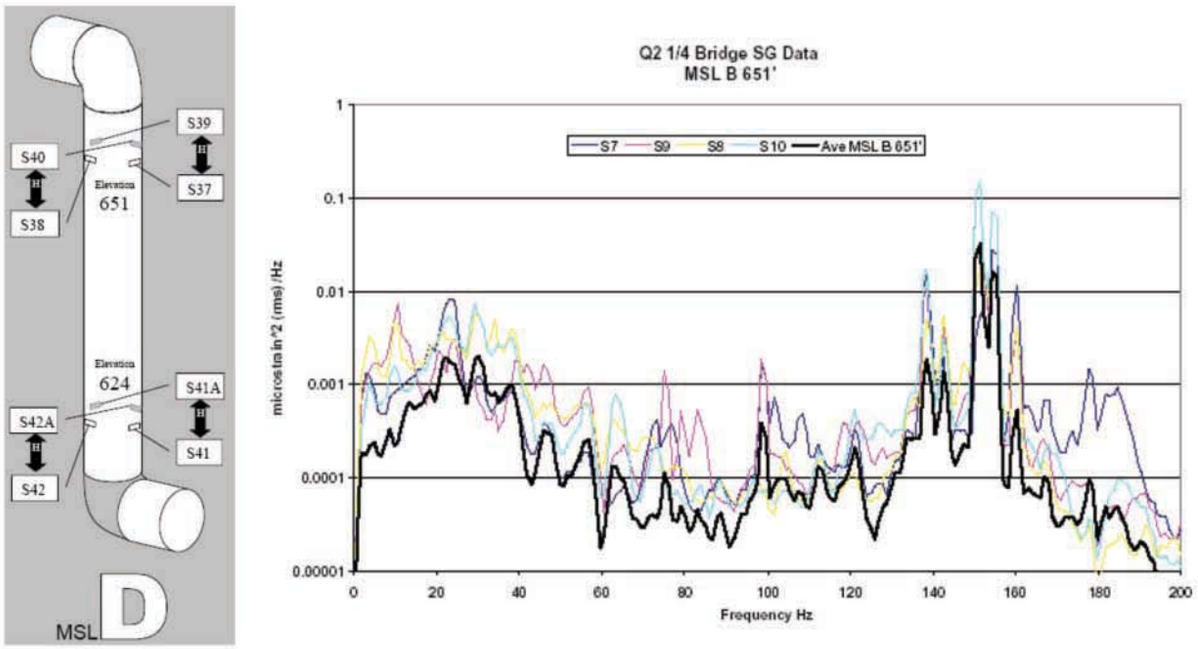

Figure 13 – Left – strain gage arrays installed on MSL in Quad Cities BWR (from [15]); Right - strains measured by strain gage array elements and averaged array on MSL B of the QC2 plant at EPU conditions, from [16]. The average (Ave) spectrum is directly related to the acoustic pressure levels in the steam within the MSL.

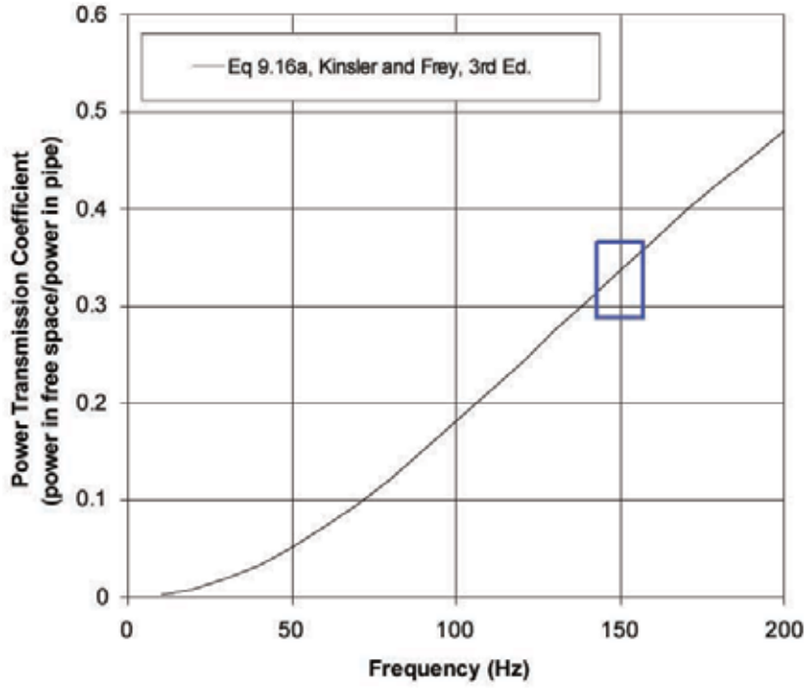

Figure 14 – Power transmission coefficient between RPV and MSL. Steam pipe radius=0.25 m, steam sound speed=488 m/s. Box indicates frequencies of valve singing.

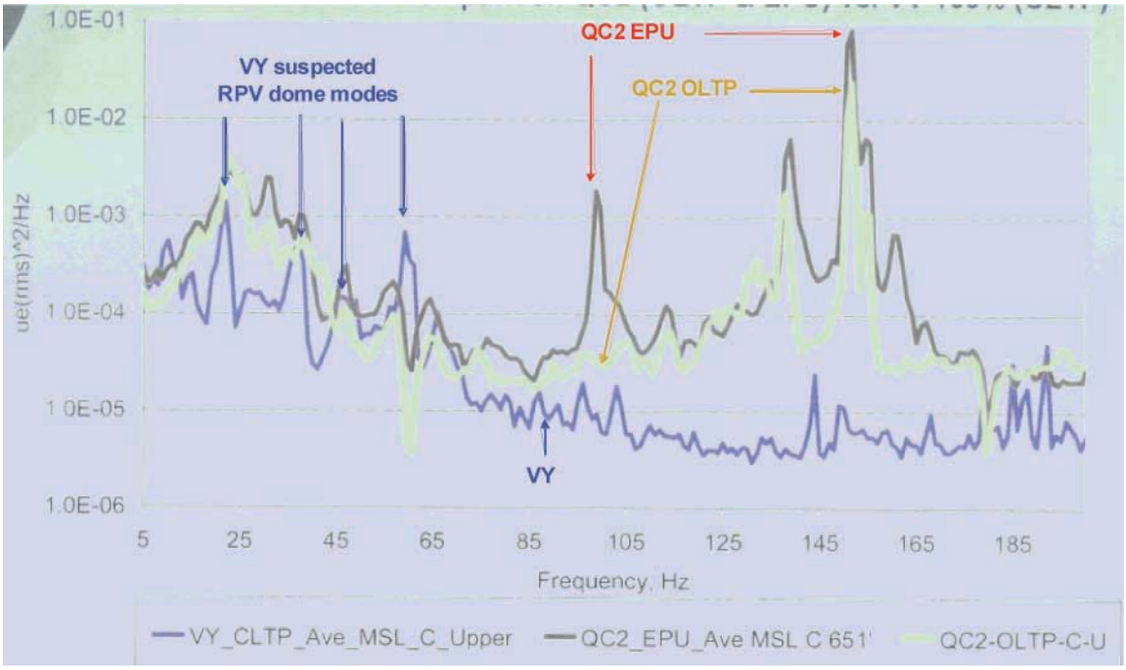

Figure 15 – Averaged strain gage measurements on MSLs at CLTP in the VY plant (lower curve) and EPU (upper curve) and OLTP (middle curve) in the QC2 power plant (from [18]).

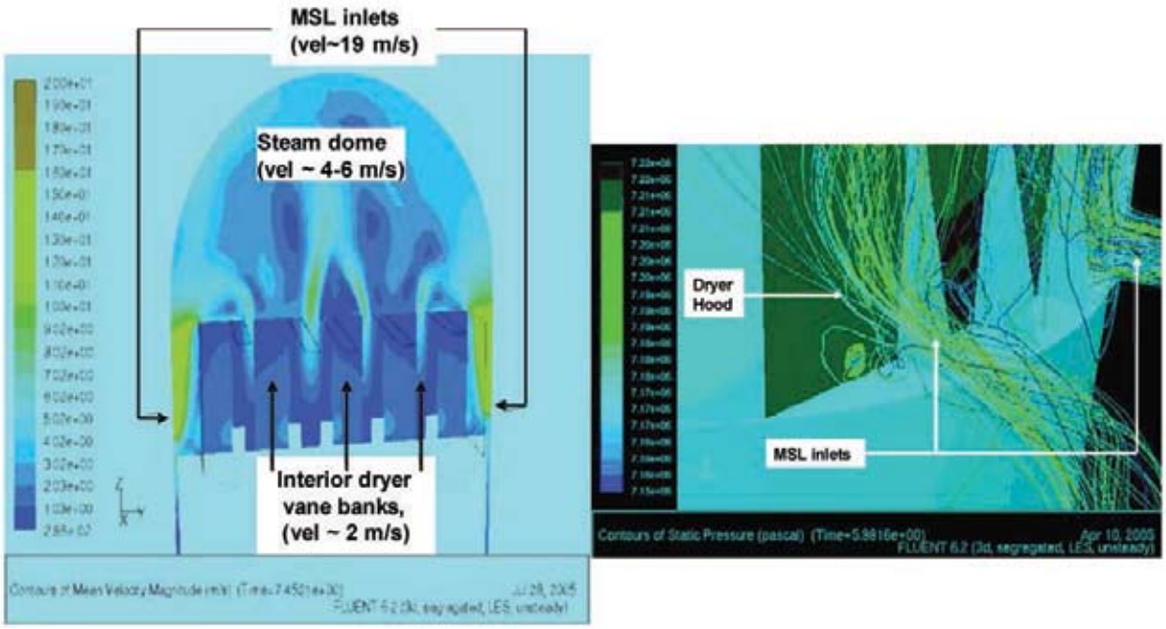

Figure 16 – Left - CFD simulation of flow speeds in VY steam dome (from [9]); Right - flow streamlines into MSL inlets colored with contours of instantaneous pressure (from [19]).

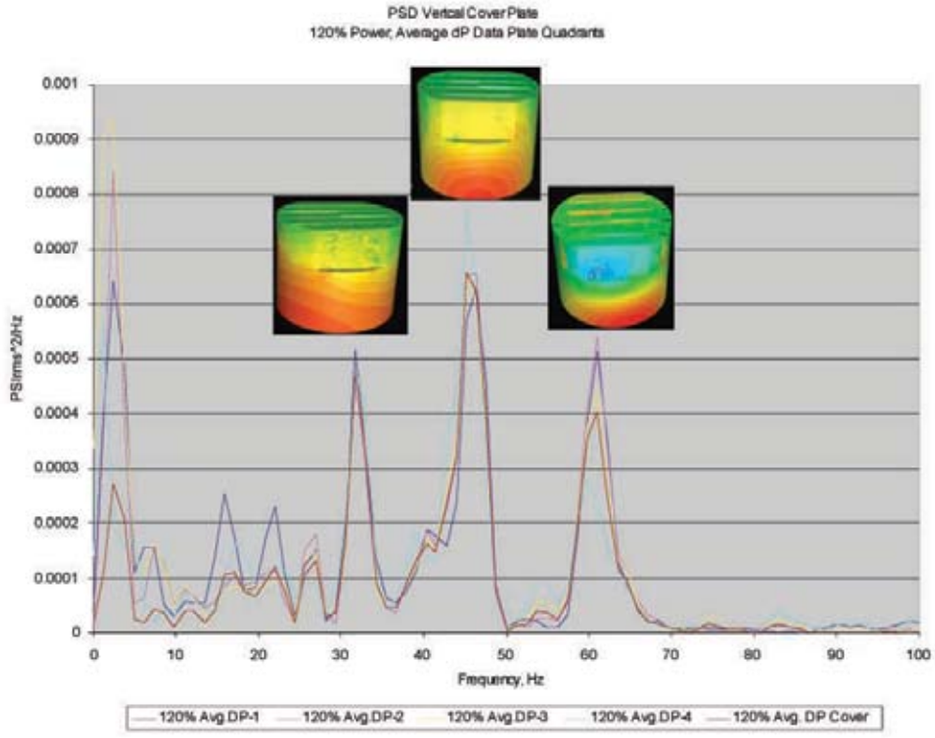

Figure 17 – Pressure loading on VY steam dryer hood estimated using CFD simulations (from [20]), supplemented with acoustic mode shapes of the steam dome volume computed from the CFD model (from [9])

Use of MCC-Based Motor Torque Measurements for Periodic Verification of Motor-Operated Valves

J. S. Gratz and P. S. Damerell, *MPR Associates*
J. F. Hosler, *Electric Power Research Institute*
D. Graf, *Crane Nuclear*

Abstract

Historically, diagnostic testing of motor-operated valves (MOVs) for periodic verification (PV) has been conducted using at-the-valve tests. Although nuclear power plants have recognized the potential benefits of PV testing conducted at the motor control center (MCC), there is a lack of validated methods for use of MCC-based measurements in PV.

This paper summarizes work funded by Electric Power Research Institute (EPRI) to develop, justify and validate a methodology for use of MCC-based measurements (most importantly, motor torque) in PV of MOVs. The MCC-based Motor Torque Periodic Verification (MTPV) method is applicable to torque-switch controlled closing strokes of rising stem MOVs with AC motors.

The MTPV method uses a baseline "parallel" test with simultaneous motor torque measurements (at the MCC) and stem thrust measurements (at the valve), to determine a relationship between motor torque and stem thrust. Upper and lower thrust limits are converted to motor torque limits using this relationship, with appropriate consideration of uncertainties. Motor torque data from subsequent tests is compared to these motor torque limits to verify adequate setup and to determine margin.

The MTPV method is validated using data from tests of 4 MOVs at a nuclear power plant. For these MOVs, a second "parallel" test provided the necessary data to evaluate how well MCC-based measurements predict stem thrust. For all 4 MOVs, the predicted thrust based on measured motor torque matched the measured stem thrust favorably. Variations were well within measurement uncertainty.

Further, the validation cases showed that the apparent margin is lower with MCC-based measurements compared to at-the-valve measurements, due to greater measurement uncertainty. Accordingly, the MTPV method will be most beneficial for MOVs that have high margin with at-the-valve measurements (> 40%).

Background

In 1989, the US Nuclear Regulatory Commission (NRC) issued Generic Letter 89-10, Safety-Related Motor-Operated Valve Testing and Surveillance, which requested that nuclear power plant licensees review and validate design basis requirements for safety-related motor-operated valves (MOVs) to ensure that these MOVs were capable of performing their required safety-related functions. To ensure continued reliability of safety-related MOVs, the NRC later issued Generic Letter 96-05, Periodic Verification of Design-Basis Capability of Safety-Related Motor-Operated Valves, which requested that facilities develop a periodic verification program to address potential valve and/or actuator degradation.

One component of a successful periodic verification program is regular diagnostic testing of MOVs. Historically, this type of testing has required access to the valve for installation of transducers and other equipment necessary to assess valve performance. This process is time-consuming and limited by accessibility to the plant's MOVs. Although technologies are available that allow diagnostic testing to be performed from a remote location at the motor control center (MCC), this type of diagnostic testing has not been implemented at many sites because widely accepted methods for use of MCC-based testing within a periodic verification program have not been defined.

This paper summarizes work funded by Electric Power Research Institute (EPRI) to develop, justify and validate an MCC-based Motor Torque Periodic Verification (MTPV) method for torque-switch controlled closing strokes of rising stem MOVs, with AC motors. The paper provides a

summary of the evaluation of motor torque data obtained from electrical measurements at the MCC and covers use of these (and other) measurements in MOV PV testing.

It is important to note that this work focused on the evaluation of measured motor torque data as it pertains to an MOV's upper and lower setpoint limits. This paper does not address how to measure motor torque from the MCC. Motor torque is assumed to be measured using a vendor-provided diagnostic system with a justified measurement uncertainty. Justification of motor torque measurement is the responsibility of the user (and the diagnostic equipment vendor), and is not included in this report.

Overview

The MTPV method is an approach for comparing measurements of motor torque that are taken at the MCC to pre-determined limits to assess the operational margin of an MOV. The general procedure is analogous to current PV methods based on direct stem thrust measurements:

1. Minimum and maximum "raw" limits are calculated. The minimum limit is based on the required thrust to actuate the valve under its design basis conditions and the maximum limit is based on the load capability of the valve, actuator, and motor.

2. Test equipment accuracy, torque switch repeatability, and other uncertainties are accounted for and used to develop "adjusted" limits.

3. Data is acquired from a test to verify that the measured values fall between the adjusted limits and to quantify the operational margin.

The MTPV method requires a baseline "parallel" test which includes MCC-based motor torque measurements and direct stem thrust measurements from sensors at the valve. Results from this test are used to determine parameters needed to interpret data from subsequent PV tests where measurements are made only at the MCC. All testing (baseline and subsequent tests) is performed with no flow, pressure or DP in the pipe (referred to as "static" testing).

In the MTPV method, motor torque upper and lower limits are determined based on information from the baseline test. These limits are adjusted to account for uncertainties such as test equipment accuracy, torque switch repeatability, etc. In subsequent tests, measured motor torque at control switch trip (CST) is compared to these limits to verify that the setup of the MOV is acceptable, and to quantify the margin for successful operation.

Figure 1 provides a graphical overview of the MTPV method. The left side of the figure shows how limits and margin are evaluated for measurements of stem thrust. The right side of the figure shows how limits are evaluated using measurements of motor torque. Details of this figure are described under "Implementation."

Applicability

The MTPV method is applicable to torque-switch controlled closing strokes of rising stem MOVs with AC motors. Use of the MTPV method beyond these conditions (e.g., limit-switch controlled strokes and opening strokes) has not been validated. Accordingly, users have the responsibility to justify and validate the method for conditions beyond those described in this paper.

Implementation

This section outlines the approach for implementation of the Motor Torque Periodic Verification method. The discussion provides a summary of the methods for (a) analysis of baseline "parallel" test data, (b) development of acceptable upper and lower motor torque limits, and (c) analysis of subsequent MCC-only test data, including determination of margin.

Figure 2 is a flow chart of the process to implement the MTPV method.

Evaluation of Baseline Parallel Test Data

As discussed above, the MTPV method requires an initial valve test (baseline test) which records data simultaneously at (a) the MCC, to determine motor torque and other data (e.g., switch actuation), and (b) the MOV, to determine stem thrust. This parallel test data is used to develop key parameters which relate motor torque to stem thrust for the tested valve. These parameters are needed to establish the minimum and maximum MTPV limits and are discussed further below.

Motor Torque Hotel Load

Motor torque hotel load is the motor torque required to engage the actuator gearing and stem nut, without any load on the stem (i.e., zero stem thrust and stem torque). This load is typically determined from diagnostic testing during the portion of the stroke when the stem nut rotates through its clearance with the stem threads (see Figure 3). As shown in Figure 1, hotel load acts as an "offset" in measurement of motor torque (i.e., hotel load is the small portion of motor torque that is not effective in generating thrust).

Inertial Thrust

Inertial thrust is the additional stem thrust developed after control switch trip due to the inertia of moving parts, primarily the motor. The inertia value from the baseline parallel test of record is used in establishing the upper mechanical limit.

MOV Factor at CST

The MOV Factor is a ratio of measured motor torque (above hotel load) to measured stem thrust, as determined from the baseline parallel test, at control switch trip. This ratio is affected by the stem factor, overall actuator ratio and actuator efficiency. The relationship between MOV factor and these parameters can be expressed as (the terms in the equation are detailed under "Nomenclature" at the end of this paper),

$$F_{MOV} = \frac{(MT_{MEAN,CST} - MT_{HOTEL})}{TH_{CST}} = \frac{(FS)}{(OAR)(EFF)} \quad (1)$$

This value is used as the conversion factor between stem thrust limits and motor torque limits, as shown in Figure 1.

It is important to note that the MOV Factor is based on the Mean Motor Torque at CST for the baseline parallel test. Parallel test data from MOVs often show oscillations in measured motor torque near control switch trip (see Figure 4). However, these data do not exhibit similar oscillations in the measured stem thrust signal indicating that stem thrust is insensitive to these variations (see Figure 5). As such, the MOV Factor, which defines the relationship between measured motor torque and stem thrust, should be determined based on the mean motor torque signal at CST ($MT_{MEAN, CST}$).

Determination of Upper and Lower Motor Torque Limits

For the MTPV method, raw minimum and maximum limits are based on existing stem thrust limits which plants have previously established as part of their MOV programs. These thrust limits are converted to raw upper and lower motor torque limits using the MOV Factor determined from the baseline parallel test, and then adjusted to address sources of uncertainty.

The Upper Motor Torque Limit is the most limiting (i.e., lowest value) of the MOV mechanical limit and the reduced voltage motor torque capability (both adjusted for uncertainties). The MOV mechanical limit is based on of the actuator's thrust and torque ratings and the valve's maximum allowable thrust, whichever is most limiting. This mechanical limit is then adjusted to remove inertia (which is not measured by the MCC-based motor torque signal) and to account for uncertainties, as shown in Figure 1. The reduced voltage motor torque capability is typically calculated using the following equation[2].

$$MT_{VRED} = (MT_{NOM})\left(\frac{V_{RED}}{V_{NOM}}\right)^2 \quad (2)$$

This value of motor torque at reduced voltage is adjusted to account for uncertainties, as shown in Figure 1.

The Lower Motor Torque Limit is based on the tested MOV's required thrust at CST, adjusted for uncertainties.

As discussed above, the raw motor torque limits need to be adjusted appropriately for uncertainties to determine the adjusted upper and lower motor torque limits. These uncertainties may include (but are not limited to)[3] :

- torque switch repeatability
- thrust measurement uncertainty
- motor torque measurement uncertainty
- stem factor uncertainty
- actuator efficiency uncertainty
- inertial thrust uncertainty
- rate of loading (ROL)

[1] Equation (1) is similar to the Limitorque sizing equation (Reference 1), except that Equation 1 accounts explicitly for hotel load and the Limitorque equation uses an Application Factor.

Most of these uncertainties are identified within existing plant MOV programs. In-plant MOV data was used to justify values for those uncertainties which are not typically quantified (i.e., actuator efficiency variation and inertial thrust variation). Plants may use the EPRI-justified values for these uncertainties or may elect to justify their own values for these terms.

As shown in Figure 1, the gap between the upper and lower motor torque limits is likely to be narrower than the gap between stem thrust limits developed for direct thrust measurements. This difference is due to the additional uncertainties associated with the MTPV method, the most significant of which is motor torque measurement uncertainty.

Evaluation of MCC-Only Test Data

Periodic verification tests subsequent to the initial baseline test need only obtain measurements at the MCC. During these tests, the MCC measured motor torque at control switch trip (CST) is compared to the upper and lower motor torque limits (see Figure 6).

Evaluation at Lower Limit and Calculation of Operational Margin

If the measured Mean Motor Torque at CST is greater than the lower limit, the valve is assured to have positive operational margin. The margin can then be quantified using the equation below and the resulting value fed back into the valve's PV program. This determination of margin is consistent with the margin definition within the Joint Owners' Group PV Program (Reference 3).

$$\text{MARGIN} = \frac{(MT_{MEAN,CST} - MT_{LL,CST})}{(MT_{LL,CST} - MT_{HOTEL,2nd\,TEST})} \quad (3)$$

If the measured Mean Motor Torque at CST is less than the lower limit, then it cannot be assured that the valve has positive margin based solely on MCC testing. Accordingly, a new parallel test is required to satisfy the valve PV requirements and quantify margin, using direct thrust measurements in addition to MCC measurements. If the new parallel test is successful in establishing positive margin, then the parallel test becomes the new baseline MTPV test.

Evaluation at Upper Limit

As discussed above, the Upper Motor Torque Limit is the most limiting (i.e., lowest value) of the MOV mechanical limit and the reduced voltage motor torque capability (both adjusted for uncertainties). The MOV mechanical limit is a thrust limit converted to a motor torque limit using the MOV Factor, which is based on the mean motor torque at CST. However, the reduced voltage motor torque capability represents the maximum motor output torque for the MOV. Since the upper limit could be defined by either the MOV mechanical limit or the reduced voltage motor torque capability, the MTPV method conservatively requires comparison of the Maximum Motor Torque at CST to the Upper Motor Torque Limit. If the Maximum Motor Torque at CST is less than the upper limit, the valve is assured to have margin related to the load capability of the MOV.

Conditions Requiring a New Baseline Parallel Test

Once a baseline test is established for an MOV, this baseline can be used indefinitely going forward, so long as the setup and general conditions of the MOV do not change significantly. The events listed below are judged to significantly alter the setup and conditions of a valve. Accordingly, if any of these events occur after the baseline test of record, the original baseline test is invalidated and a new baseline "parallel" test needs to be performed.

- Change to torque switch setting
- Motor replacement
- Actuator refurbishment, gear ratio change, or replacement
- Valve replacement
- Change in stem lubricant (from one lubricant to another)

[2] Per Reference 2, for certain motors the exponent in Equation (2) may be 2.5 rather than 2.0. See Reference 2 for additional information.

[3] It is important to note that not all of these uncertainties are applicable to each limit.

Validation

Validation of the MTPV method required measured stem thrust and motor torque data from multiple "parallel" tests of the same MOV. From MOVs with available test data, four similar gate valves (3 inch valves with SMB 00 actuators) met the MTPV applicability requirements and had test data with stem thrust and motor torque measurements from two separate tests. All four of these valves were used in the validation. The validation method included the following comparisons:

- Measured Thrust at CST vs. Predicted Thrust at CST based on measured Motor Torque
- Upper/Lower Limits and Margin calculated based on measured Stem Thrust vs. Upper/Lower Limits and Margin calculated based on measured Motor Torque

Measured Thrust at CST vs. Predicted Thrust at CST

The predicted mean thrust at CST ($TH_{MEAN,CST}$), based on measured motor torque, matched the measured stem thrust at CST (TH_{CST}) relatively well. As shown in Table 1, the maximum deviation from measured stem thrust was 13.3%. This variation is well within the uncertainty associated with determination of stem thrust from measurement of motor torque rather than direct measurement of stem thrust. This is illustrated in Figure 7, which plots Predicted and Measured Stem Thrust, including measurement uncertainties.

Upper Limit Comparison (Limit Based on Stem Thrust Measurement vs. Motor Torque Measurement)

With regard to the MOV Mechanical Upper Limit, the limit calculated in the MTPV method was lower (i.e., more restrictive) than the limit determined using methods which directly measure stem thrust (see Table 2). This reduction in setup "window" is due to the higher measurement uncertainty for motor torque compared to thrust.

However, the Reduced Voltage Upper Limit in the MTPV method was typically higher (i.e., less restrictive) than the limit determined using methods which directly measure stem thrust (see Table 2). This limit is based on motor output torque capability under conditions of reduced voltage. Because the MTPV method directly measures motor output torque, there are fewer parameter uncertainties to apply to the limit than if measured stem thrust is used.

Lower Limit Comparison (Limit Based on Stem Thrust Measurement vs. Motor Torque Measurement)

The Lower Limit calculated in the MTPV method was higher (i.e., more restrictive) than the limit determined using methods which directly measure stem thrust (see Table 3). This reduction in setup "window" is due to the higher measured uncertainty for motor torque compared to that for direct thrust measurement.

Operational Margin Comparison (Margin Based on Stem Thrust Measurement vs. Motor Torque Measurement)

The Operational Margin, or JOG PV Margin, is based on a comparison of the measured thrust or motor torque to the required thrust or motor torque. As expected, this margin is lower for analyses performed with the MTPV method, compared to analyses performed based on measured stem thrust (see Table 4). As discussed above for the Lower Limit, this reduced margin is due to higher uncertainty for measured motor torque than for thrust.

Conclusions

Based on the observations from the validation, the MTPV method satisfactorily determines Operational Margin as well as Motor Torque Upper and Lower Limits. Users should expect a reduction in apparent margin, a reduction in upper mechanical limit, and most likely an improvement (increase) in upper motor capability limit, when using this method in place of direct stem thrust measurement.
Accordingly, the MTPV method would be most beneficial for MOVs that have an operational margin (margin to lower limit) of at least 40% and a margin against structural damage (margin to upper mechanical limit) of at least 20%. There is no constraint with regard to margin against motor torque capability and, in fact, the MTPV method may

be a particularly good PV methodology for evaluation of MOVs whose setup is limited by motor torque capability at degraded voltage.

References

1. Limitorque SEL-3.
2. Limitorque Technical Update 05-01, "Actuator Output Torque Calculation SMB/SB/SBD Actuators/3 Phase Motors," January 2005.
3. "The Joint Owners' Group Program for Motor-Operated Valve Periodic Verification," Proceedings of the Fifth NRC/ASME Symposium on Valve and Pump Testing, July 1998, NUREG/CP-0152, Vol. 2.

Nomenclature

The nomenclature used in this paper is summarized below.

EFF	=	actuator efficiency
F_{MOV}	=	MOV factor
FS	=	stem factor
MARGIN	=	margin above required thrust at CST
MT_{HOTEL}	=	measured motor torque hotel load
$MT_{LL, CST}$	=	lower limit of motor torque at CST
$MT_{MEAN, CST}$	=	measured mean motor torque at CST
MT_{NOM}	=	nominal motor torque capability (motor start torque)
MT_{VRED}	=	motor torque capability at reduced voltage
OAR	=	overall actuator ratio
TH_{CST}	=	measured stem thrust at CST
V_{NOM}	=	nominal voltage
V_{RED}	=	reduced voltage

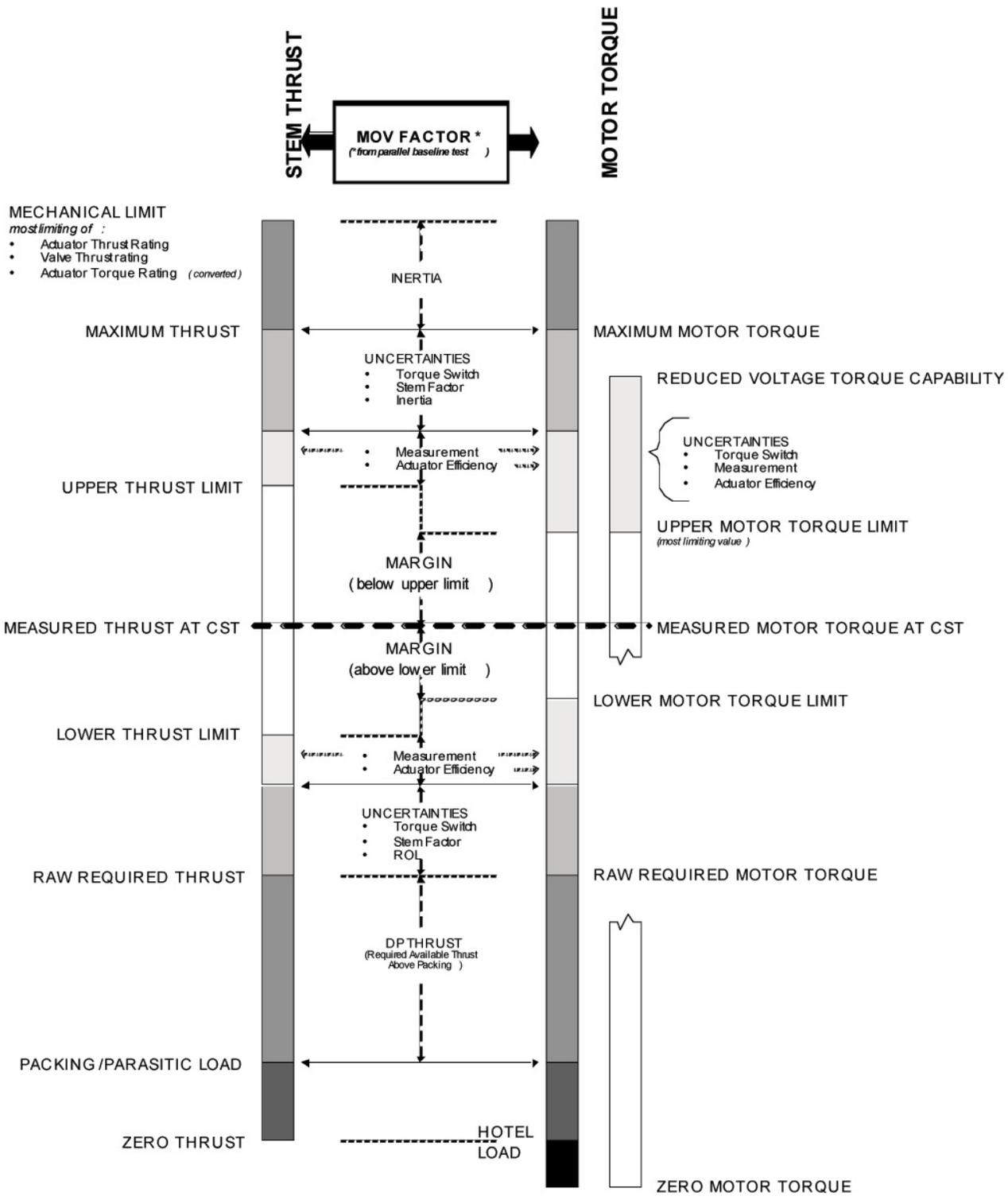

Figure 1 – Motor Torque Periodic Verification Method Limits and Margin

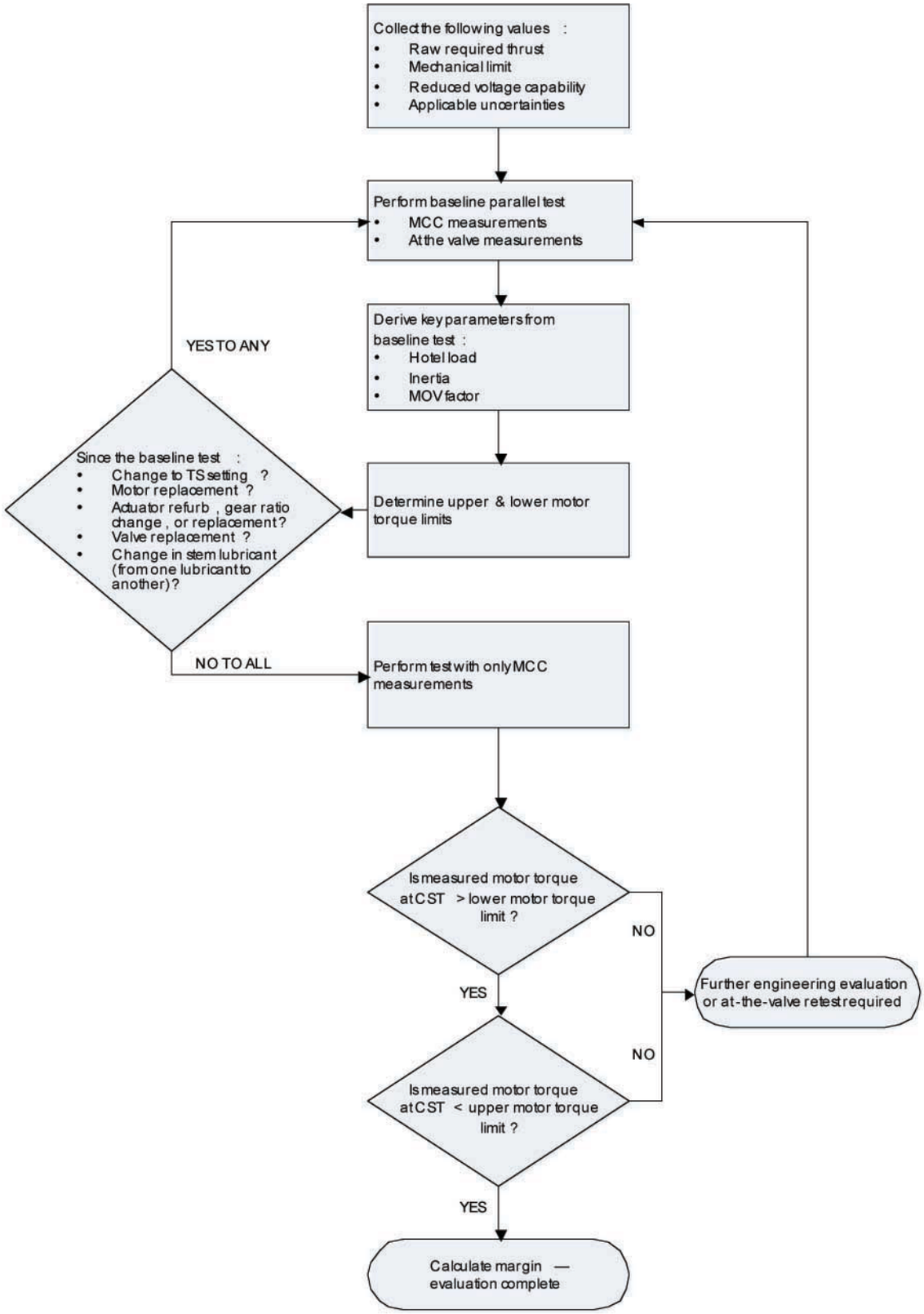

Figure 2 – Motor Torque Periodic Verification Method Flowchart

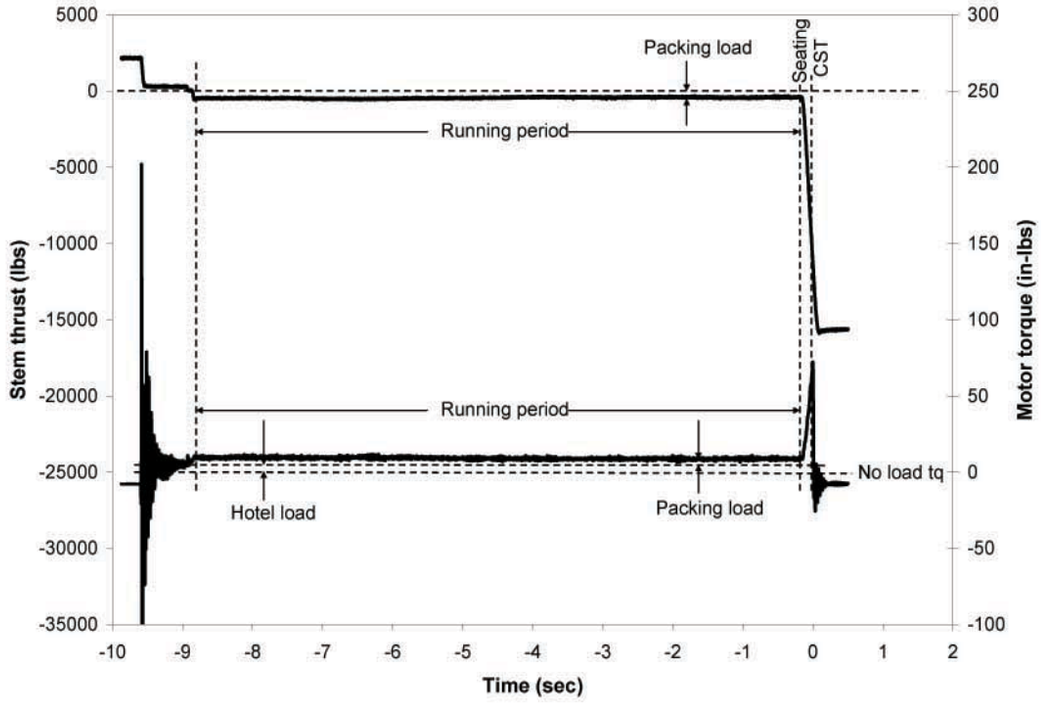

Figure 3 – Overlay of Measured Motor Torque (bottom trace) and Stem Thrust (top trace)

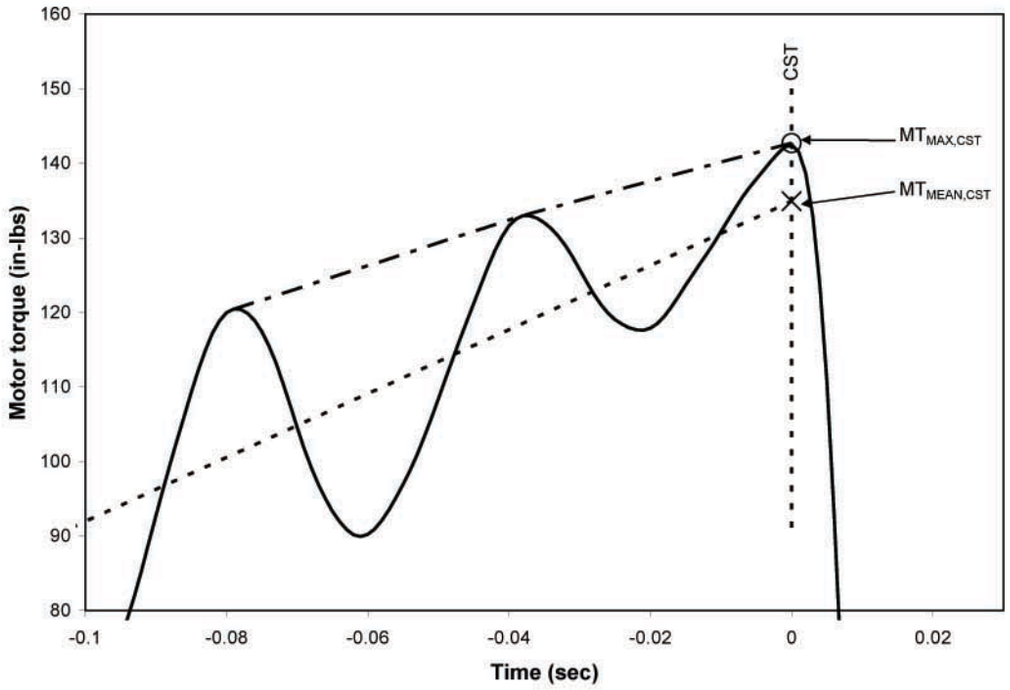

Figure 4 – Measured Motor Torque Near CST – Example with Significant Oscillations

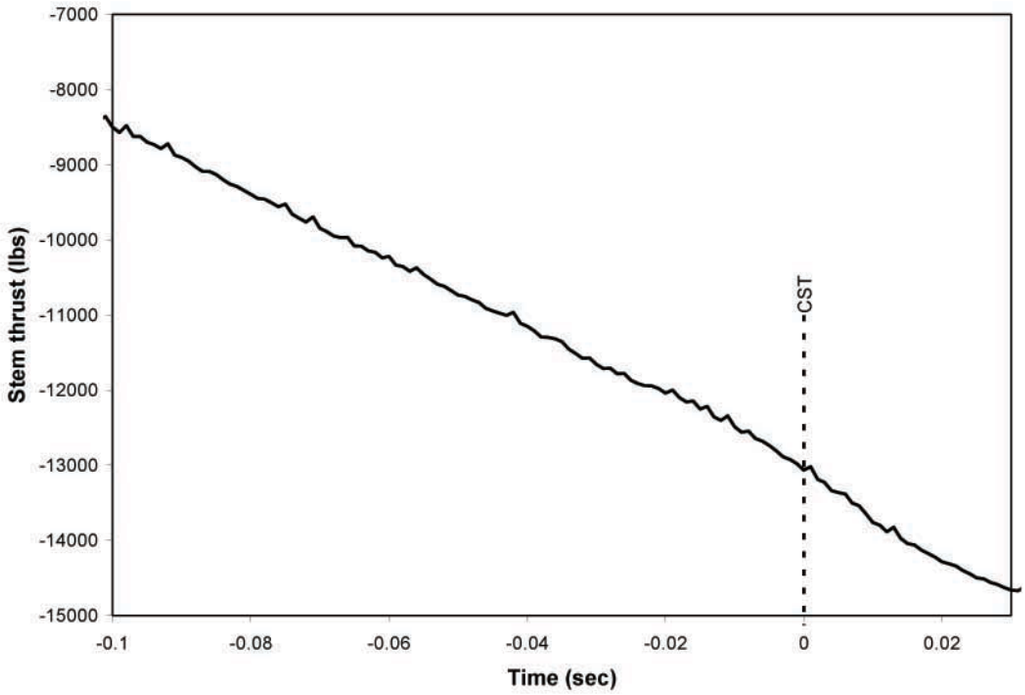

Figure 5 – Measured Stem Thrust Near CST for Example Corresponding to Figure 4

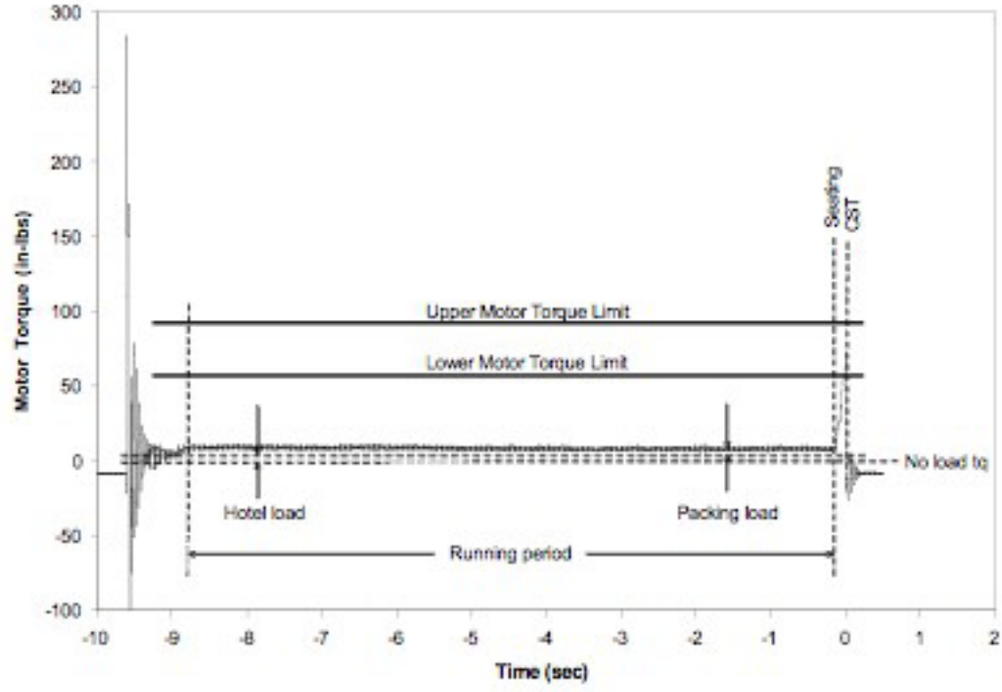

Figure 6 – Measured Motor Torque from MCC-Only Test

Table 1
Measured Thrust vs. Predicted Thrust Based on Measured Motor Torque

Valve	Measured Stem Thrust at CST (TH_{CST}), lbs	Predicted Mean Thrust at CST ($TH_{MEAN, CST}$), lbs	% Difference
MOV 1	12,501	12,202	-2.4%
MOV 2	13,474	13,017	-3.4%
MOV 3	13,224	11,466	-13.3%
MOV 4	12,608	14,174	12.4%

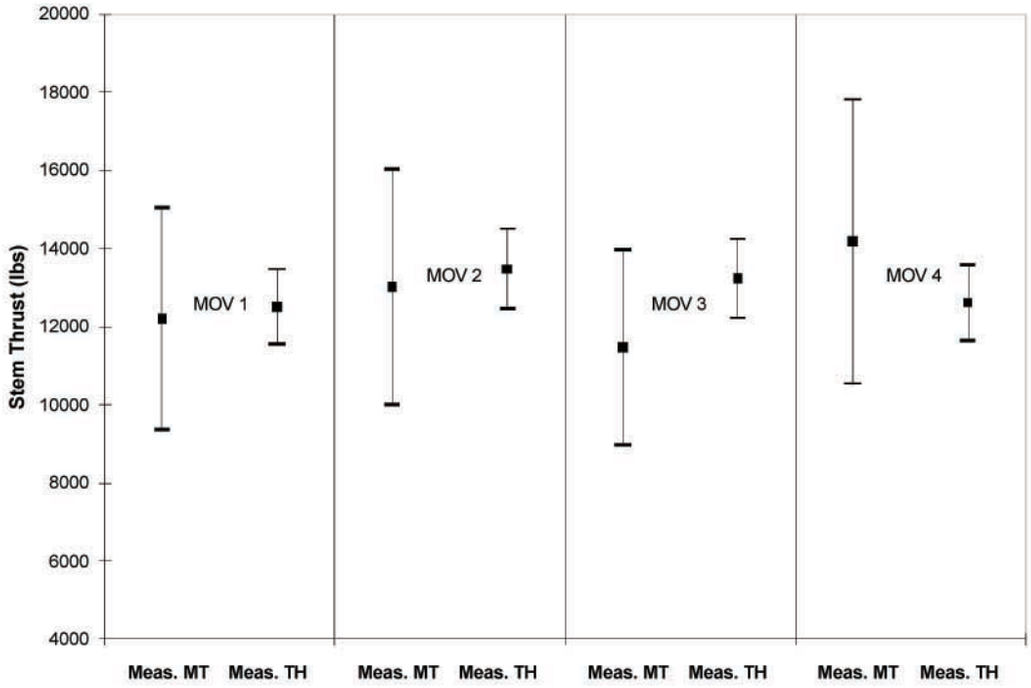

Figure 7 – Comparison of Predicted Mean Thrust at CST (based on measured motor torque) to Measured Stem Thrust at CST, Including Measurement Uncertainty

Table 2
Upper Limit Comparison

Valve	Thrust Upper Limit Based on Measuring Stem Thrust, lbs		Thrust Upper Limit Based on Measuring Motor Torque, lbs	
	Mechanical Limit	**Red Voltage Limit**	**Mechanical Limit**	**Red Voltage Limit**
MOV 1	14,052	19,444	12,040	19,892
MOV 2	14,457	18,241	12,407	20,502
MOV 3	13,151	16,417	11,434	16,028
MOV 4	14,062	23,878	11,477	28,462

Table 3
Lower Limit Comparison

Valve	Thrust Lower Limit Based on Measuring Stem Thrust, lbs	Thrust Lower Limit Based on Measuring Motor Torque, lbs 4
MOV 1	10,527	12,404
MOV 2	7,801	9,573
MOV 3	7,801	9,265
MOV 4	10,527	13,045

Table 4
Operational Margin Comparison

Valve	Operational Margin Based on Measuring Stem Thrust	Operational Margin Based on Measuring Motor Torque
MOV 1	18.8%	-1.6%
MOV 2	72.7%	36.0%
MOV 3	69.5%	23.8%
MOV 4	19.8%	8,7%

[4] Motor Torque Limit converted to Thrust Limit using MOV Factor; $TH = (MT - MT_{HOTEL})/(F_{MOV,CST})$

Elimination of RHR Piping Vibration

Mike Davis and Sekhar Samy

CCI

This paper discusses the vibration and pipe failure problems experienced in the Residual Heat Removal (RHR) system at the Grand Gulf Nuclear Power Plant. The root cause analysis of the problem showed that excessive fluid velocity across the plug and seat ring as it flows through the E21- F003 valve was the prime reason.

Grand Gulf was able to retrofit (replacement of the original valve internals with internals supplied by another company) a new and innovative trim design in this Motor Operated isolation type globe valve with minimal changes to the existing valve. The result is the complete elimination of vibration and control problems.

System:

RHR system in a Boiling Water Reactor (BWR) has several modes including:

- Low pressure coolant injection (LPCI)
- Suppression pool cooling
- Fuel pool cooling assist
- Shutdown (S/D) Cooling

Shutdown cooling RHR throttle valves E12F003A & B are 18", 300# ANSI Powell Globe type with the need to control low flows for extended periods of time to remove decay heat and accommodate in vessel activities. It must have high flow capability at lower pressure drops for the postulated LPCI mode of operation.

At the Grand Gulf NPP, both E12F003A and E12F003B exhibited poor throttle control capability over the years, eventually developing seat and guide damage to both valves from throttle use. E12F003A throttle use in Refueling Outage (RF) 12 resulted in a small bore piping failure and water spill in the RHR room. In addition, there was internal erosion damage found in the valve body and seat. This led to the development of an engineering request to look at various repair options and long term solutions. Solutions considered were:

1. Purchase a new valve body
2. Send the old 3A body to a hot shop and have valve vendor personnel repair it.
3. Repair the valve body at Grand Gulf using their extremely qualified welders.

Option one was outside the time limit. Option two would work but would be extremely expensive and could be time limiting. Option three was the best choice. Grand Gulf has the technicians in house with a hot shop and necessary boring bar for performing the post welding machine work.

The initial choice and determination for RF12 was to repair the body as it was determined to be a repair that could be handled.

Grand Gulf contacted the Original Equipment Manufacturer (OEM) and other valve companies for a long term solution to this problem. Step one was to look at the service conditions and see if this sheds light on the probable causes for valve damage.

In the above service conditions the trim exit velocities for the "Shutdown Cooling" cases are in excess of 200 ft/sec! The Cavitation Index is also around 1.25 for two of the cases and 1.67 for a third. This is an accurate prediction that the process conditions are resulting in cavitation damage. Note: the Cavitation Index is not scaled for pressure or size. So, the conclusion was excessive trim exit velocity is the root cause of vibration and cavitation.

TABLE 1 – SERVICE CONDITIONS

Fluid	Water/Steam					
Critical Pressure	psig	3194				
Critical Temperature	deg F	705.5				
Condition		**S/D Cooling 1**	**S/D Cooling 2**	**S/D Cooling 3**	**LPCI 1**	**LPCI 2**
Fluid State		Water	Water	Water	Water	Water
Liquid Vol. Flow Rate	gpm	2500.0	2500.0	3000.0	7589.0	8635.0
Inlet Pressure	psig	450.0	450.0	425.4	105.5	92.86
Outlet Pressure	psig	173.0	173.0	173.0	101.549	88.0
Pressure Differential	psi	277.0	277.0	252.4	3.951	4.86
Inlet Temperature	deg F	344.0	70.0	344.0	185.0	185.0
Density	lbm/ft^3	55.91	62.39	55.9	60.49	60.49
Vapor Pressure	psig	109.7	-14.33	109.7	-6.303	-6.303
Cavitation Index	σ_1	1.23	1.67	1.25	28.6	20.4
Required Flow Capacity	Cv	142.2	150.2	178.7	3759.1	3856.4
Ported Valve Trim Exit Velocity	ft/sec	214	203	205	24.6	27.3
8 Turn Disk Stack Velocity	ft/sec	44.5	42.1	42.4	No Disk	No Disk

psig = pounds force per square inch gage

gpm = gallons per minute

deg F = degrees Fahrenheit

lbm/ft^3 = pounds mass per cubic feet

ft/sec = feet per second

Solution

Any solution must meet the following criteria:

- No cutting or welding to be performed during implementation
- Provide trim to reduce the S/D cooling velocity to a level below valve industry recommended guidelines
- Do not impact LPCI accident performance & maximum Cv
- Package the trim inside the existing valve body
- Minimal impact on weight and Cg
- No change in stroke length or stroke time
- Solution must be robust & reliable
- Must be capable of implementation with unit on-line

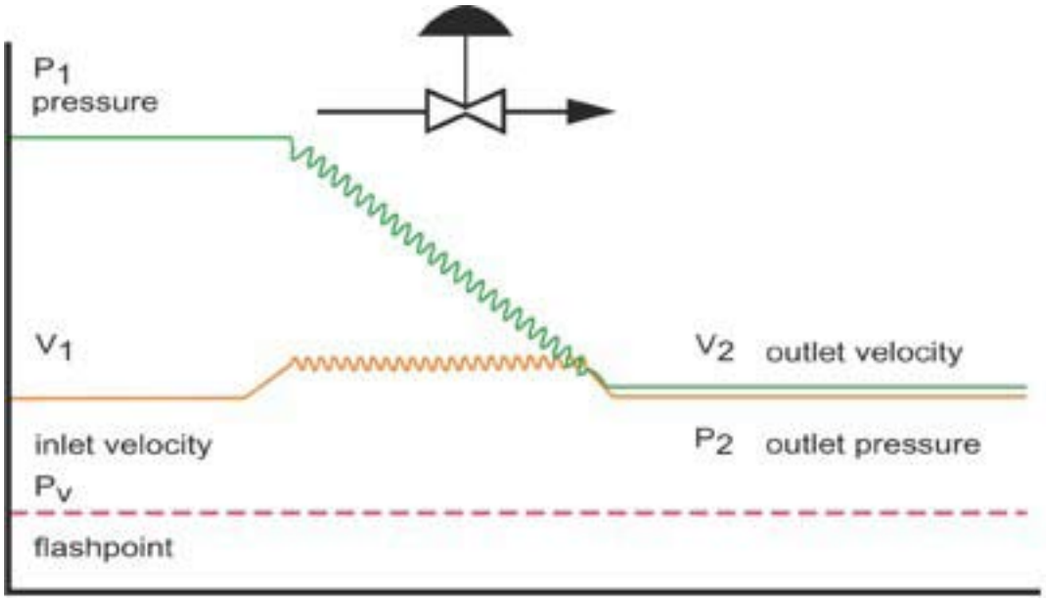

Figure 1 – Flow path in a multi-path multi-stage trim

For long term the selected solution was to replace the existing valve stem and plug with a custom throttle plug assembly inserted in the existing valve body. The throttle plug must be designed to reduce pressure in stages and as a result limit the velocity of the fluid in the trim (Figure 1) so that the pressure never falls below the fluid's vapor pressure.

By using multiple right angle tortuous flow paths as shown in Figure 2, it is possible to reduce the trim velocity to acceptable levels. The selected velocity limit to reduce the potential for vibration and cavitation was 40 ft/sec per ISA recommendations in Reference (1).

Each individual flow path has a series of turns that breaks up the pressure drop across the valve into multiple stages, and has expanding passages to reduce fluid exit velocity.

This approach uses a series of flat metal disks to form a trim assembly. Each disk has a flow pattern of successive right angle turns cut into its flat surface. When stacked, these pathways can be matched or mismatched between individual disks to create a labyrinth flow pattern that enables trim to be infinitely tuned to control flow in a manner that maintains positive operating characteristics throughout the valve's operating range (Figure 2). The flow path for each disk is opened as the plug moves within the center opening of the seat ring

This flow method controls the damaging effects of velocity in two ways: by dividing the flow into many small streams of low mass flow rate, and by forcing fluid through a series of sharp right angle turns to affect the pressure drop steps.

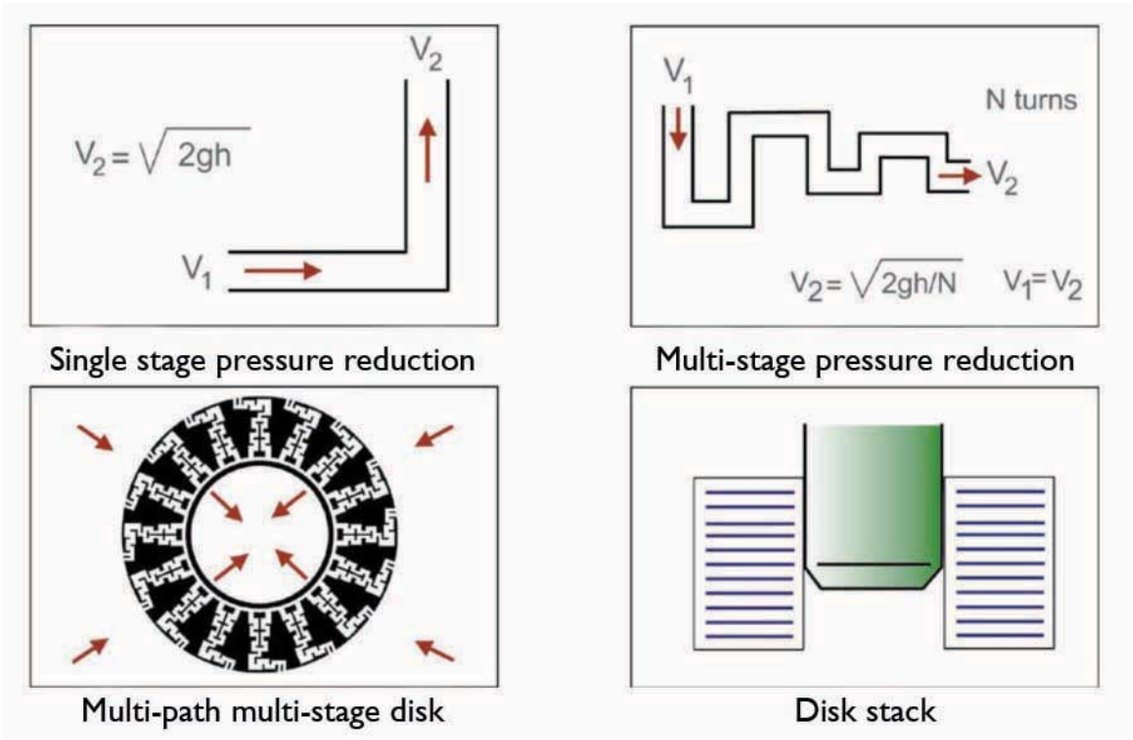

Figure 2 – Multi-Stage Multi-Path Flow Geometry

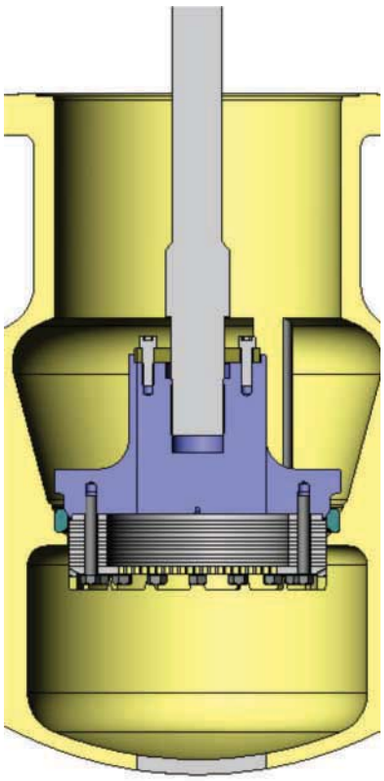

Figure 3 – Plug with Disk Stack

Retrofit

The valve is an isolation type valve with a welded seat ring in the body. Further there is no appreciable place in the valve body to install a disk stack or cage. Therefore the only available solution is to replace the existing William Powell stem and plug with a custom throttle plug inserted in the existing William Powell valve body.

The new solution is to provide a disk stack that is bolted to the plug. For 40% of the stroke the flow passes through the disk stack, this is the range of conditions in the S/D cooling mode. For the remaining 60% of the stroke, the disk stack is retracted from the flow and the flow is through the seat ring, and valve maximum Cv is not affected.

At these stroke positions, the energy in the fluid flow will be sufficiently controlled so that cavitation and vibration are eliminated.

Implementation/Installation

Because 1E12F003A had recently been replaced, thus insuring good internal condition, the decision was made to modify it first while the unit was on-line to provide Operations a Shutdown Cooling loop that could be throttled as needed, prior to and during RF 13. The steps in the retrofit process are as follows:

1. Pre-stage all required tools and test equipment prior to entering the Limiting Condition for Operation (LCO)
2. Prepare work area to accommodate the work scope. De-con-shield, scaffold, rigging.
3. Hang the required tag outs, isolate, and commence LCO and drain down (6 hours)
4. Determine the main and control power from the Limitorque (2 hours)
5. De-tension the bonnet using a multi head hi-torque (2 hours)

6. Unpack the valve once drained (1 hour)
7. Remove the stem nut from the Limitorque and rig for removal from stem (2 hours)
8. Remove mounting bolts and rig the Limitorque from the yoke (2 hours)
9. Remove yoke and bonnet (2 hours)
10. Rig out old valve plug and stem (1 hour)
11. Set up mill and perform valve seat skim cut for preparation to install new trim (4-6 hours)
12. VT visual examination of valve body internal and rail areas (2 hours)
13. Install new plug and stem (3 hours)
14. Blue check seat area (2 hours)
15. Install seal ring and bonnet/yoke assembly (4 hours)
16. Re-pack the valve (2 hours)
17. Fill, vent, restore RHR system to standby line up (4 hours)
18. Install Limitorque, then stem nut, and torque fasteners (3 hours)
19. Re-terminate and rough set the limits on the Limitorque (2 hours)
20. Clear tags and perform proper line up for static and dynamic VOTES diagnostic test (2 hours)
21. Perform Static and In-situ dynamic VOTES test and vibration testing with flow at 0, 20, 40, 60, 80, 100% with E12F048 closed then open (4 hours)
22. Engineering review of test data (4 hours)
23. Return to service (2 hours)

E12-F003A was modified and tested successfully during the second week of December 2003. Testing proved the new plug design was successful in restoring full throttle capability to E12-F003A and that the existing capacity was not affected. Similar retrofit and testing as outlined was successfully completed on the E12-F003B valve in March 2004 during RF 13.

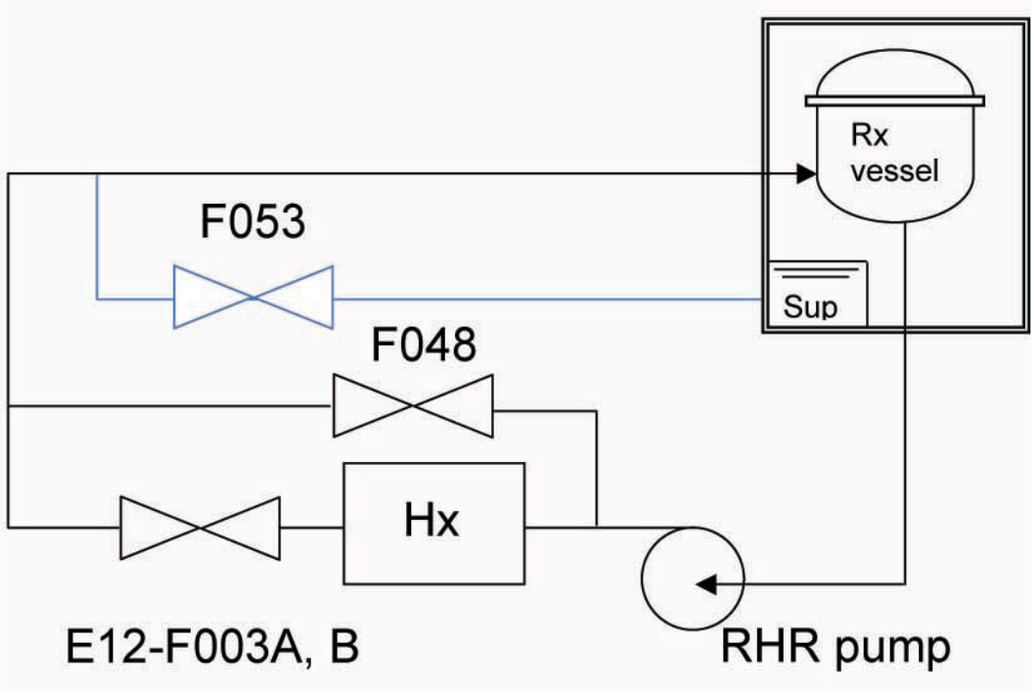

Figure 4 – RHR System Layout

As a post maintenance requirement, the 1E12F003A Limitorque actuator was set up to achieve design requirements for torque and thrust.

Flow

Initial conditions for the flow or dynamic testing had RHR "A" lined up to provide 100% of the pump flow through the 1E12F003A valve. At pump start, the lE12F003A valve was 100% open. Operations closed the valve in a continuous mode with the valve achieving full flow shutoff against RHR A pump shutoff head. Additionally, full flow capability through lE12F003A was satisfied with a recorded value of 7950 gpm (gallons per minute). The next portion of the test performed a step down from full open to significant throttle then back to full open valve position. This established minimum throttle conditions and also established a vibration data baseline. All flow was passed through the lE12F003A valve during this portion of the test. This particular section of the test determined the throttle range to recommend to Operations for long-term use. Beginning at 100% flow, the valve was throttled in steps with the following results

Phase two of the dynamic flow test was performed with 1E12F048A full open as 1E12F003A was throttled closed in -20% increments from 100% open to full close. This

TABLE 2 FLOW THROUGH VALVES

Actual flow	% 1E12F003A OPEN
7950 gpm	100%
7100 gpm	50%
6000 gpm	40%
5000 gpm	32%
4000 gpm	19%
3000 gpm	7%
2500 gpm	2%

TABLE 3 E12F003A VIBRATION DATA

Actual Flow, gpm	Percent 1E12F003A open	Vibration Recorded at Highest Plane, g's
7950	100%	0.041
7100	50%	0.152
6000	40%	0.1
5000	32%	0.1
4000	19%	0.035
3000	7%	0.031
2500	2%	0.1

documented that full flow capability through 1El2F048A of 8200 gpm could be achieved and maintained while 1E12F003A was throttled from 100% to zero.

Additionally, vibration baseline determined no unexpected resonance developed in these various throttle modes.

Vibration recorded at Highest Plane actual flow 7950 gpm was 0.041 g.

Vibration

Pre-retrofit, the vibration of the system was "similar to a train derailing." It was a frightening sound so special instruction were written to only allow low flow throttle for a short duration in order to slow down the harmonic damage. Obviously that did not work in the long term.

As part of the post retrofit test, vibration measurements were taken on the valve body in three planes during the throttling steps with full flow going through lE12F003A, and also with flow shared with lE12F048A full open as lE12F003A was throttled. Preliminary percent lE12F003A OPEN results of the vibration data indicate minimal vibration in all three planes of measurement. Acceleration peaks were less than 0.2 g at all frequencies less than or equal to 100 Hertz. Acceleration peaks remained less than 0.1 g at all frequencies less than or equal 30 Hertz. These conditions satisfied the acceptance criteria of less than 0.3 g at 30 Hertz equivalent.

It should be noted that, during the throttling evolution, the noise level was very acceptable with no impacts noted when greater than or equal to 3000 gpm. At 2500 gpm, there was some low level impact-type sounds which were attributed to the valve being <2% open. Given the total stroke length of the valve (9.1") at 2%, the disc seat and the in-body

TABLE 4 E12F003B VIBRATION DATA

Actual Flow, gpm	Percent 1E12F003B open	Vibration Recorded at Highest Plane, g's
7900	100%	0.081
5000	40%	0.143
4000	29%	0.026
3000	20%	0.036
2500	16%	0.042

valve seat were only approximately 1/16” apart; potentially allowing minor seat contact to create the impact noise. Vibration was still within acceptable limits at this point.

During the last refueling outage in 2005, the valves performed without vibration and fuel pool clarity was maintained.

References

1. “Control Valves – Practical Guides for Measurement and Control,” edited by Guy Borden, Jr., and Paul G. Friedman, 1998 edition, published by ISA.

Session 4(a):
Regulatory Issues

Session Chair

Thomas G. Scarbrough

U.S. NRC

POWER-OPERATED VALVE ACTIVITIES AND ISSUES

Thomas G. Scarbrough
Division of Component Integrity
Office of Nuclear Reactor Regulation
U.S. Nuclear Regulatory Commission
Ninth NRC/ASME Symposium on Valve and Pump Testing
July 2006

I. Introduction

The safe operation of a nuclear power plant depends on motor-operated valves (MOVs) in fluid systems successfully performing their safety functions. MOVs must be capable of operating under design-basis conditions, which may include high differential pressure and flow, high ambient temperature, and degraded motor voltage. The design of the MOV must apply valid engineering equations and parameters to ensure that the MOV will operate as intended during normal plant operations and design-basis events. Manufacturing, installation, preoperational testing, operation, inservice testing (IST), maintenance, and replacement must be conducted by trained personnel using proper procedures. Surveillance must be performed and testing criteria must be applied on a soundly based frequency in a manner that suitably detects questionable operability or degradation. Moreover, these activities must be monitored by a strong quality assurance program.

The regulations of the U.S. Nuclear Regulatory Commission (NRC) require that components that are important to the safe operation of a U.S. nuclear power plant be treated in a manner that ensures their performance. Appendix A, "General Design Criteria for Nuclear Power Plants," and Appendix B, "Quality Assurance Criteria for Nuclear Power Plants and Fuel Reprocessing Plants," to Part 50 of Title 10 of the Code of Federal Regulations (10 CFR Part 50) contain broadly based requirements in this regard. In 10 CFR 50.55a, the NRC initially required U.S. nuclear power plant licensees to implement provisions of the American Society of Mechanical Engineers (ASME) Boiler & Pressure Vessel Code (B&PV Code) for testing of MOVs as part of their IST programs. In 1999, the NRC revised 10 CFR 50.55a to incorporate by reference the ASME Code for Operation and Maintenance of Nuclear Power Plants (OM Code) for inservice testing of MOVs. The NRC also supplemented the quarterly MOV stroke-time testing specified in the ASME Code by requiring that licensees verify MOV design-basis capability on a periodic basis. In 2004, the NRC issued 10 CFR 50.69 that allows for an alternative approach in establishing requirements for treatment of SSCs at nuclear power plants using a risk-informed method of categorizing SSCs according to their safety significance.

II. MOV Design-Basis Capability

Operating experience at nuclear power plants in the 1980s and 1990s revealed weaknesses in many activities associated with MOV performance. For example, some engineering analyses used in the original sizing and setting of MOVs did not adequately predict the thrust and torque required to open and close valves under design-basis conditions. Both regulatory and industry research programs later confirmed the weaknesses in the initial design and qualification of MOVs. For example, the NRC Office of Nuclear Regulatory Research sponsored an extensive program at the Idaho National Laboratory (INL) to study the performance of MOVs under various flow, temperature, and voltage conditions. In addition, the nuclear industry sponsored a program by the Electric Power Research Institute (EPRI) to develop a computer methodology to predict the performance of MOVs under a wide range of operating conditions. Poor MOV performance also resulted from shortcomings in maintenance programs, such as inadequate procedures and training. Further, testing of MOVs to measure valve stroke times under zero differential-pressure and flow conditions was shown not to detect deficiencies that could prevent MOVs from performing their safety functions under design-basis conditions.

This paper was prepared by staff of the U.S. Nuclear Regulatory Commission. It may present information that does not currently represent an agreed-upon NRC staff position. NRC has neither approved nor disapproved the technical content.

In response to weaknesses in MOV performance, the NRC staff issued Generic Letter (GL) 89-10 (June 28, 1989), "Safety-Related Motor-Operated Valve Testing and Surveillance." In GL 89-10, the NRC staff requested that licensees ensure the capability of MOVs in safety-related systems to perform their intended functions by reviewing MOV design bases, verifying MOV switch settings initially and periodically, testing MOVs under design-basis conditions where practicable, improving evaluations of MOV failures and necessary corrective action, and trending MOV problems. The NRC staff requested that licensees complete their GL 89-10 programs within approximately three refueling outages or 5 years of the issuance of the generic letter.

In support of the regulatory activities to ensure MOV design-basis capability, the NRC Office of Nuclear Regulatory Research identified areas in which research and analysis were needed to assist in evaluating MOV programs at nuclear power plants. For example, the NRC performed research to evaluate (1) performance of MOVs under pump flow and blowdown conditions; (2) output of ac-powered and dc-powered MOV motor actuators; (3) the increase in friction of aged samples of valve materials; (4) methods to determine appropriate values for stem friction coefficient; (5) pressure locking and thermal binding of gate valves; and (6) the effect of ambient temperature on stem lubricant performance. The NRC sponsored flow testing of several MOVs by INL under normal flow and blowdown conditions. The testing revealed that (1) more thrust was required to operate gate valves than predicted by standard industry methods; (2) some valves were internally damaged under blowdown conditions and their operating requirements were unpredictable; (3) static and low flow testing might not predict valve performance under design-basis flow conditions; (4) during valve opening strokes, the highest thrust requirements might occur at unseating or in the flow stream; (5) partial valve stroking did not reveal the total thrust required to operate the valve; (6) torque, thrust, and motor operating parameters were needed to fully characterize MOV performance; and (7) reliable use of MOV diagnostic data requires accurate equipment and trained personnel. The NRC summarizes some of the results of the MOV research program in NRC Information Notice (IN) 90-40 (June 5, 1990), "Results of NRC-Sponsored Testing of Motor-Operated Valves."

To assist nuclear power plant licensees in responding to GL 89-10, EPRI developed the MOV Performance Prediction Methodology (PPM) to determine dynamic thrust and torque requirements for gate, globe, and butterfly valves based on first-principles of MOV design and operation. EPRI described the methodology in Topical Report TR-103237 (Revision 2, April 1997), "EPRI MOV Performance Prediction Program." The EPRI MOV PPM program included the development of improved methods for prediction and evaluation of system flow parameters; gate, globe, and butterfly valve performance; and motor-actuator rate-of-loading effects (load sensitive behavior). EPRI also performed separate effects testing to provide information for refining the gate valve model and rate-of-loading methods; and conducted numerous MOV tests to provide data for development and validation of the models and methods, including flow loop testing, parametric flow loop testing of butterfly valve disk designs, and in-situ MOV testing. EPRI integrated the individual models and methods into an overall methodology including a computer model and implementation guide. On March 15, 1996, the NRC staff issued a safety evaluation (SE) accepting the EPRI MOV PPM with certain conditions and limitations. On February 20, 1997, the staff issued a supplement to the SE on general issues and two unique gate valve designs. On April 20, 2001, the staff issued Supplement 2 to the SE on Addendum 1 to EPRI Topical Report TR-103237 addressing an update of the computer model. The staff alerted licensees to lessons learned from the EPRI MOV program in IN 96-48 (August 21, 1996), "Motor-Operated Valve Performance Issues."

On September 8, 1999, the Nuclear Energy Institute (NEI) submitted Addendum 2 to EPRI Topical Report TR-103237-R2, which described the development of the Thrust Uncertainty Method that takes into account conservatism in the EPRI MOV PPM to provide a more realistic (less bounding) estimate of the thrust required to operate gate valves than predicted by the PPM. In Supplement 3 (dated September 30, 2002) to the SE on the EPRI PPM, the NRC staff concluded that the Thrust Uncertainty Method developed by EPRI is acceptable for the prediction of minimum allowable thrust at control switch trip (or flow isolation) for applicable motor-operated gate valves under cold water applications within the scope of the Thrust Uncertainty Method, based on the NRC staff's review of Addendum 2 to the EPRI Topical Report as supplemented by NEI submittals dated January 5 and December 6, 2001, and June 10, 2002. The NRC staff stated that the Thrust Uncertainty Method may be applied consistent with the criteria specified for the EPRI MOV PPM in EPRI TR-103237-R2 and Addenda 1 and 2 to TR-103237-R2, as supplemented by NEI submittals dated January 5 and December 6, 2001, and June 10, 2002. More recently, NEI has submitted additional addenda to the EPRI MOV PPM that are under review by the NRC staff.

Nuclear power plant licensees implemented the recommendations of GL 89-10 through a combination of design-basis reviews, revision of MOV calculations and procedures, static and dynamic diagnostic testing, industry-sponsored research programs, and trending of test results. The industry expended significant resources to resolve the deficiencies in the design, qualification, and application of safety-related MOVs that led to the issuance of GL 89-10. The results of the GL 89-10 programs and their implementation include (1) MOV sizing calculations and switch settings have been revised to reflect actual valve performance; (2) improved valve performance prediction methods have been developed; (3) valve internal dimensions are being addressed to provide assurance of predictable gate valve performance under blowdown conditions; (4) friction coefficients in new or refurbished gate valves have been found to increase with service until a plateau is reached; (5) MOV output prediction methods have been updated; and (6) personnel training and maintenance practices have been improved. The NRC staff evaluated the MOV programs at nuclear power plants through onsite inspections of the design-basis capability of safety-related MOVs. The NRC staff closed its review of GL 89-10 for each active U.S. nuclear power plant. The NRC staff will be reviewing the GL 89-10 program at Browns Ferry Unit 1 prior to its restart.

On August 17, 1995, the NRC issued GL 95-07, "Pressure Locking and Thermal Binding of Safety-Related Power-Operated Gate Valves," to request that licensees perform, or confirm that they had previously performed, (1) evaluations of the operational configurations of safety-related, power-operated gate valves for susceptibility to pressure locking and thermal binding; and (2) further analyses, and any needed corrective actions, to ensure that safety-related power-operated gate valves that are susceptible to pressure locking or thermal binding are capable of performing their safety functions within the current licensing basis of the facility. The NRC staff completed its review of licensee responses to GL 95-07 through issuance of an SE addressing each active U.S. nuclear power plant.

On September 18, 1996, the NRC staff issued GL 96-05, "Periodic Verification of Design-Basis Capability of Safety-Related Motor-Operated Valves," to provide recommendations for assuring the capability of safety-related MOVs to perform their design-basis functions over the long term. In GL 96-05, the NRC staff requested that licensees establish a program, or ensure the effectiveness of their current program, to verify on a periodic basis that safety-related MOVs continue to be capable of performing their safety functions within the current licensing basis of the facility.

In response to GL 96-05, nuclear power plant owners' groups developed an industry-wide Joint Owners Group (JOG) Program on MOV Periodic Verification to obtain benefits from sharing information between licensees on MOV performance. The JOG described its program in Topical Report MPR-1807 (Revision 2, July 1997), "Joint BWR, Westinghouse and Combustion Engineering Owners' Group Program on Motor-Operated Valve (MOV) Periodic Verification." Elements of the JOG program included (1) an "interim" MOV periodic verification program of static diagnostic testing based on MOV safety significance and capability margin for licensees to use in response to GL 96-05; (2) a 5-year dynamic testing program to identify potential age-related increases in required thrust and torque to operate gate, globe, and butterfly valves under dynamic conditions; and (3) a long-term MOV diagnostic program based on information from the dynamic testing program. On October 30, 1997, the NRC staff issued an SE accepting the JOG Program on MOV Periodic Verification with certain conditions and limitations. Licensees of 98 reactor units have participated in the JOG program. The JOG 5-year dynamic testing program included about 200 valves that received repetitive dynamic tests with at least a 1-year time interval between the tests. On February 27, 2004, the JOG submitted Topical Report MPR-2524 (Revision 0, February 2004), "Joint Owners' Group Motor Operated Valve Periodic Verification Program Summary," providing the long-term recommendations for MOV periodic verification to be implemented by licensees as part of their commitments to GL 96-05. The long-term JOG program includes static diagnostic testing of GL 96-05 MOVs based on their safety significance and capability margin with dynamic testing as determined by the results of the JOG testing program and plant-specific evaluations. The NRC staff is completing an SE on its evaluation of the JOG topical report.

In that the JOG program focused on potential increases in valve operating requirements, licensees address potential degradation in the output of MOV motor actuators by their plant-specific programs. In the late 1990s, the NRC sponsored research at INL to study the performance of ac-powered MOV motor actuators manufactured by Limitorque Corporation, under various temperature and voltage conditions. For the Limitorque ac-powered motor-actuator combinations tested, the research indicated that (1) actuator efficiency might not be maintained at "run" efficiency

published by the manufacturer; (2) degraded voltage effects can be more severe than predicted by the square of the ratio of actual to rated motor voltage; (3) some motors produce more torque output than predicted by their nameplate rating; and (4) temperature effects on motor performance appeared consistent with the Limitorque guidance. The NRC study of ac-powered MOV output is described in NUREG/CR-6478 (July 1997), "Motor-Operated Valve (MOV) Actuator Motor and Gearbox Testing." The nuclear industry also evaluated the output capability of ac-powered MOVs at several plants. In response to the new information on ac-powered MOV performance, Limitorque provided updated guidance in its Technical Update 98-01 (May 15, 1998) and Supplement 1 (July 17, 1998) for the prediction of ac-powered MOV motor actuator output. The NRC alerted licensees to the new information on ac-powered MOV output in Supplement 1 (July 24, 1998) to IN 96-48.

Following the NRC review of ac-powered MOV performance, the NRC sponsored research at INL to study the performance of Limitorque dc-powered MOV motor actuators under various temperature and voltage conditions. For the Limitorque dc-powered motor-actuator combinations tested, the research indicated that (1) ambient temperature effects were more significant than predicted; (2) use of a linear voltage factor needs to consider reduced speed, increased motor temperature, and reduced motor output; (3) stroke-time increase is significant for some dc-powered MOVs under loaded conditions; and (4) actuator efficiency may fall below the published "pullout" efficiency at low speed and high load conditions. The research results are provided in NUREG/CR-6620 (May 1999), "Testing of dc-Powered Actuators for Motor-Operated Valves." On June 23, 2000, the Boiling Water Reactor Owners' Group (BWROG) forwarded Topical Report NEDC-32958 (March 2000), "BWR Owners' Group dc Motor Performance Methodology - Predicting Capability and Stroke Time in dc Motor-Operated Valves," to the NRC staff for information. On August 1, 2001, the NRC issued Regulatory Issue Summary (RIS) 2001-15, "Performance of dc-Powered Motor-Operated Valve Actuators," that informs licensees of the availability of improved industry guidance for predicting dc-powered MOV actuator performance. In RIS 2001-15, the NRC staff stated that, based on a sample review, the BWROG methodology represents a reasonable approach to improvement of past industry guidance for predicting dc-powered MOV stroke time and output. The staff considers the BWROG methodology to be applicable to Boiling Water Reactor and Pressurized Water Reactor plants because of the similarity in the design and application of dc-powered MOVs.

Each U.S. nuclear power plant licensee submitted a description of plans for periodic verification of the design-basis capability of safety-related MOVs in response to GL 96-05. The NRC staff reviewed the licensee submittals and conducted sample inspections of GL 96-05 programs. The staff prepared an SE to document its review of the response to GL 96-05 by each licensee. Where a licensee committed to implement the JOG program, the NRC staff relied to a significant extent on that commitment in preparing the SE without the need for plant-specific inspection activity. The NRC staff reviewed GL 96-05 programs of licensees that did not commit to the JOG program by a separate process of submittals and inspections, as appropriate. As licensees implement their long-term MOV programs including incorporation of the JOG program results, the NRC will monitor those programs using Inspection Procedure 62708, "Motor-Operated Valve Capability," as part of the NRC reactor oversight program.

III. Design-Basis Capability For POVs (Other Than MOVs)

The NRC established Generic Safety Issue (GSI) 158, "Performance of Safety-Related Power-Operated Valves Under Design-Basis Conditions," to evaluate whether additional regulatory actions were necessary to address performance issues for POVs (other than MOVs) after MOV operating experience and research results indicated that testing under static conditions was insufficient to demonstrate consistent performance of these valves under design-basis conditions. Operating events involving observed or potential common-cause failures were documented in NUREG-1275, "Operating Experience Feedback Report," Volumes 2 and 6 for air systems and AOVs, respectively. These issues are also discussed in NUREG/CR-6644, "Generic Issue 158: Performance of Safety-Related Power-Operated Valves Under Operating Conditions." Two related documents, NUREG-1275, Volume 13, "Evaluation of Air-Operated Valves at U.S. Light-Water Reactors," and NUREG/CR-6654, "A Study of Air-Operated Valves in U.S. Nuclear Power Plants," are focused specifically on AOVs.

The NRC staff previously requested that the industry verify the capability of AOVs with respect to issues involving the plant instrument air supply system. In GL 88-14, "Instrument Air Supply System Problems Affecting Safety-Related Equipment," addressees were requested to verify by test that air-operated safety-related components will perform as expected in accordance with all design-basis events. All addressees were required to respond to the generic letter with

confirmation that this verification had been performed. All responses were received by 1993 and the generic letter was subsequently closed.

In IN 96-48, the NRC staff noted that some of the lessons learned from MOV operating experience and testing are applicable to other POVs. For example, the thrust requirements to operate some gate valves under pump flow and blowdown conditions were higher than predicted by the valve manufacturers. The potential exists for gate valves to be damaged when operating under blowdown conditions such that the thrust requirements can be unpredictable. The effective flow area in some globe valves can be larger than expected and can cause thrust requirements to be higher than predicted. The friction coefficients for sliding surfaces in gate valves can increase with service before reaching a plateau.

In RIS 2000-03, "Resolution of Generic Safety Issue 158, 'Performance of Safety Related Power-Operated Valves Under Design-Basis Conditions," dated March 15, 2000, the NRC closed GSI-158 on the basis that current regulations provide adequate requirements to ensure verification of the design-basis capability of POVs, and no new regulatory requirements are needed. In RIS 2000-03, the staff stated that it would continue to work with industry groups on an industry-wide approach to the POV issue to provide timely, effective, and efficient resolution of the concerns regarding POV performance. If the actions of the industry did not adequately address the functionality of POVs under design basis dynamic conditions, the NRC staff noted that it would take additional regulatory action as appropriate.

The Joint Owners Group on Air Operated Valves (JOG AOV), which is facilitated by NEI, presented a voluntary program to address AOV issues to the NRC staff in a public meeting on June 3, 1999. The JOG AOV program provides guidance to verify valve performance at design conditions and long-term periodic verification of safety-related AOVs categorized as high-risk-significant. For safety-related, low-risk-significant AOVs and AOVs that are not safety-related but are determined to be high-risk-significant, the JOG AOV program also provides guidance for a less-rigorous verification of valve functionality. The methodology to determine valve safety significance, as specified in the industry program, may include such risk insight methods as described in Regulatory Guide 1.174, "An Approach for Using Probabilistic Risk Assessment in Risk-Informed Decisions on Plant-Specific Changes to the Licensing Basis," or programs established to meet the requirements of 10 CFR 50.65, "Requirements for monitoring the effectiveness of maintenance at nuclear power plants," in combination with individual plant examinations and the review performed by a separate expert panel. NRC comments on the JOG AOV program and its implementation were sent to NEI in a letter dated October 8, 1999. Although the program was noted to have limitations, the NRC staff recognized that industry-wide implementation of this program would achieve a uniform level of consistency that would provide increased confidence in the design-basis capabilities of high-risk-significant AOVs in nuclear power plants.

In RIS 2000-03, the NRC staff provided the following list of attributes of a successful power-operated valve design capability and long-term periodic verification program:

1. Include all maintenance rule scope POVs in the program.

2. Verify POVs in their non-safety position are capable of returning to their safety position if the train is assumed operable with the valves in their non-safety position.

3. For air-operated valves, verify guidance in GL 88-14, "Instrument Air Supply System Problems Affecting Safety-Related Equipment," has been successfully implemented, including periodic monitoring of air quality.

4. Evaluate MOV risk-ranking methodologies developed by the Boiling Water Reactor Owners Group and the Westinghouse Owners Group for applicability to risk ranking of POVs at the specific plant, as applicable.

5. Focus initial efforts on safety-related, active, high-risk POVs. Information obtained from these valves and lessons learned may be used to verify and maintain design-basis capability of similar safety-related POVs.

6. Verify methods for predicting POV operating requirements using MOV lessons learned or specific POV dynamic diagnostic testing. Use of the EPRI

MOV PPM must include all guideline aspects of that methodology and not only individual EPRI valve test results.

7. Justify the method for predicting POV actuator output capability by a test-based program established by the vendor, licensee, or industry.

8. Address all applicable weak links, including the actuator, valve, and stem.

9. Ensure quality assurance program coverage.

10. Provide sufficient diagnostics when baseline testing to verify capability. Diagnostics might not be needed if normal plant operation frequently demonstrates design-basis capability.

11. Specify when dynamic or static diagnostic periodic testing is needed.

12. Ensure post-maintenance testing is adequate to verify the capability of all safety-related POVs and risk-significant functions of non-safety-related POVs.

13. Ensure POV maintenance procedures are reviewed to incorporate lessons learned from other valve programs.

14. Upgrade training to incorporate lessons learned from other valve programs.

15. Apply feedback from plant-specific and industry information, including test data, to all applicable safety-related POVs.

16. Establish quantitative (test data) and qualitative (maintenance and condition reports) trending of POV performance with detailed review following each refueling outage.

As noted above, the NRC will continue to work with industry groups to ensure that safety-related POVs are capable of performing their specified functions under design-basis conditions.

IV. ASME Activities On POV Qualification And Inservice Testing Programs

With respect to the qualification of POVs to perform their safety functions, the ASME Committee on Qualification of Mechanical Equipment used in Nuclear Facilities has prepared a proposed revision to Section QV, "Functional Qualification Requirements for Active Valve Assemblies for Nuclear Power Plants," of the ASME Standard QME-1, "Qualification of Active Mechanical Equipment used in Nuclear Power Plants." The recent proposed revision to QME-1 reflects valve performance information obtained from nuclear industry programs and NRC-sponsored research since development of the QME-1 standard in the 1980s. The NRC staff is reviewing the latest revision of QME-1 for acceptance and possible endorsement in an NRC regulatory guide.

The ASME BPV Code and the more recent OM Code specifies that stroke-time testing of POVs be conducted as part of the IST programs of nuclear power plants on a quarterly frequency where practical. The NRC and the industry have long recognized the limitations of stroke-time testing as a means of assessing the operational readiness of MOVs to perform their design-basis safety functions. The NRC requires U.S. nuclear power plant licensees implementing the ASME OM Code to supplement the quarterly MOV stroke-time testing specified in the Code with a program to verify MOV design-basis capability on a periodic basis.

In response to concerns regarding the adequacy of MOV stroke-time testing, ASME developed performance-based ASME Code Case OMN-1, "Alternative Rules for Preservice and Inservice Testing of Certain Electric Motor Operated Valve Assemblies in LWR Power Plants," as an alternative to quarterly stroke-time testing. In Code Case OMN-1, ASME allows periodic exercising of all safety-related MOVs once per refueling cycle and periodic diagnostic testing under static or dynamic conditions, as appropriate, on a frequency determined by MOV performance in terms of margin and degradation rate. In GL 96-05, the NRC staff noted that the method in ASME Code Case OMN-1 could be used as part of a licensee's response to the generic letter.

ASME subsequently developed Code Case OMN-11, "Risk-Informed Testing for Motor-Operated Valves," to provide guidance for applying risk insights in the implementation of Code Case OMN-1. With respect to AOVs and HOVs, the ASME prepared ASME Code Case OMN-12, "Alternate Requirements for Inservice Testing Using Risk Insights for Pneumatically and Hydraulically Operated Valve Assemblies in Light-Water Reactor Power Plants." Code Case OMN-12 provides guidance for risk-informed inservice testing of AOVs and HOVs as an alternative the ASME Code provisions for these POVs. In Regulatory Guide (RG) 1.192 (June 2003), "Operation and Maintenance Code Case Acceptability, ASME OM Code," the NRC staff accepts the use of ASME Code Cases OMN-1, OMN-11, and OMN-12 with certain exceptions.

Currently, ASME is preparing a revision to Code Case OMN-1 to improve its application by clarifying several aspects of the code case while retaining the safety improvement that is achieved through increased knowledge of the design-basis capability of MOVs obtained from diagnostic testing. In addition, ASME is preparing a revision to the OM Code to revise the IST provisions for AOVs to incorporate lessons learned from industry experience. ASME is also considering revising the IST provisions in the OM Code for MOVs to incorporate the performance-based provisions of Code Case OMN-1.

V. POV Issues

Nuclear power plant licensees need to have effective programs for maintaining the capability of POVs to perform their intended functions. The nuclear industry and NRC staff share POV operating experience at user group meetings, and other public forums. NRC and ASME work to ensure that operating experience is reflected in NRC regulatory communications and Code provisions. Current issues related to proper performance of POVs at nuclear power plants include:

1. Potential preconditioning can mask degradation in POV performance prior to testing.

2. Flow-induced vibration from power uprate operation can cause unexpected and initially undetected degradation of POVs.

3. Maintenance activities can be hazardous to plant personnel because of potential energy stored in mechanical components and fluid systems.

4. Licensees implementing 10 CFR 50.69 will apply less rigorous treatment practices for safety-related POVs with low risk significance that will need to continue to provide confidence in their design-basis capability.

VI. Conclusions

The safe operation of a nuclear power plant depends on POVs in fluid systems successfully performing their safety functions. Based on lessons learned from MOV operational experience and testing programs, the NRC, ASME, and the nuclear industry have taken actions to improve the performance of POVs in nuclear power plants. Performance issues with POVs indicate the need for their continued long-term care and maintenance. The NRC staff will monitor licensee activities related to the performance of safety-related POVs through the reactor oversight program.

VII. References

ASME, Boiler & Pressure Vessel Code.

ASME, Code for Operation and Maintenance of Nuclear Power Plants.

ASME, Code Case OMN-1, "Alternative Rules for Preservice and Inservice Testing of Certain Electric Motor Operated Valve Assemblies in LWR Power Plants."

ASME, Code Case OMN-11, "Risk-Informed Testing of Motor-Operated Valves."

ASME, Code Case OMN-12, "Alternate Requirements for Inservice Testing Using Risk Insights for Pneumatically and Hydraulically Operated Valve Assemblies in Light-Water Reactor Power Plants."

BWROG, Letter dated October 2, 2000, on BWR Owners' Group dc Motor Performance Methodology (ADAMS Accession # ML003758535).

BWROG, Topical Report NEDC-32958 (March 2000), "BWR Owners' Group dc Motor Performance Methodology - Predicting Capability and Stroke Time in dc Motor-Operated Valves."

Electric Power Research Institute, Topical Report TR-103237 (Revision 2, April 1997), "EPRI MOV Performance Prediction Program," and addenda.

JOG, Topical Report MPR-1807 (Revision 2, July 1997), "Joint BWR, Westinghouse and Combustion Engineering Owners' Group Program on Motor-Operated Valve (MOV) Periodic Verification."

JOG, Topical Report MPR-2524 (Revision 0, February 2004), "Joint Owners' Group (JOG) Motor Operated Valve Periodic Verification Program Summary."

Limitorque Corporation, Technical Update 98-01 and Supplement 1 (July 17, 1998), "Actuator Output Torque Calculation."

NRC, Code of Federal Regulations, Title 10, Part 50.

NRC, Generic Letter 88-14 (August 8, 1988), "Instrument Air Supply System Problems Affecting Safety-Related Equipment."

NRC, Generic Letter 89-10 (June 28, 1989), "Safety-Related Motor-Operated Valve Testing and Surveillance," and its supplements.

NRC, Generic Letter 95-07 (August 17, 1995), "Pressure Locking and Thermal Binding of Safety-Related Power-Operated Gate Valves."

NRC, Generic Letter 96-05 (September 18, 1996), "Periodic Verification of Design-Basis Capability of Safety-Related Motor-Operated Valves."

NRC, Information Notice 90-40 (June 5, 1990), "Results of NRC-Sponsored Testing of Motor-Operated Valves."

NRC, Information Notice 96-48 (August 21, 1996) and Supplement 1 (July 24, 1998), "Motor-Operated Valve Performance Issues."

NRC, Inspection Procedure 62708, "Motor-Operated Valve Capability."

NRC, NUREG-1275, "Operating Experience Feedback Report," Volumes 2, 6, and 13 (February 2000).

NRC, NUREG/CR-6478 (July 1997), "Motor-Operated Valve (MOV) Actuator Motor and Gearbox Testing."

NRC, NUREG/CR-6620 (May 1999), "Testing of dc-Powered Actuators for Motor-Operated Valves."

NRC, NUREG/CR-6644, "Generic Issue 158: Performance of Safety-Related Power-Operated Valves Under Operating Conditions."

NRC, NUREG/CR-6654, "A Study of Air-Operated Valves in U.S. Nuclear Power Plants."

NRC, Regulatory Guide 1.174, Revision 1 (November 2002), "An Approach for Using Probabilistic Risk Assessment in Risk-Informed Decisions on Plant-Specific Changes to the Licensing Basis."

NRC, Regulatory Guide 1.192 (June 2003), "Operation and Maintenance Code Case Acceptability, ASME OM Code."

NRC, Regulatory Issue Summary 2000-03 (March 15, 2000), "Resolution of Generic Safety Issue 158, Performance of Safety Related Power-Operated Valves Under Design-Basis Conditions."

NRC, Regulatory Issue Summary 2001-15 (August 1, 2001), "Performance of dc-Powered Motor-Operated Valve Actuators."

NRC, Safety Evaluation dated March 15, 1996, on EPRI MOV Performance Prediction Methodology (NUDOCS Accession # 9608070280).

NRC, Safety Evaluation Supplement dated February 20, 1997, on EPRI MOV Performance Prediction Methodology (NUDOCS Accession # 9704300106).

NRC, Safety Evaluation Supplement 2 dated April 20, 2001, on EPRI MOV Performance Prediction Methodology (ADAMS Accession # ML011100121).

NRC, Safety Evaluation Supplement 3 dated September 30, 2002, on EPRI MOV Performance Prediction Methodology (ADAMS Accession # ML022410364).

NRC, Safety Evaluation dated October 30, 1997, on JOG Program on MOV Periodic Verification (NUDOCS Accession # 9801160151).

DEVELOPMENT AND IMPLEMENTATION OF OPERATIONAL PROGRAMS IN COMBINED LICENSES

Joseph Colaccino
Division of New Reactor Licensing
Office of Nuclear Reactor Regulation
U.S. Nuclear Regulatory Commission

Abstract

The United States Nuclear Regulatory Commission (NRC) may be receiving several combined license applications in the next few years to license new nuclear power plants. These facilities are expected to be licensed under Title 10 of the Code of Federal Regulations (10 CFR), Part 52, "Early Site Permits, Standard Design Certifications, and Combined Licenses for Nuclear Power Plants." Unlike the current fleet of operating reactors, which was licensed under 10 CFR Part 50, "Domestic Licensing of Production and Utilization Facilities," a combined license would be issued before the plant is built. Verification of the design of the facility would be made by ensuring that the specified inspections, tests, analyses, and acceptance criteria (ITAAC) were completed by the licensee. For operational programs, such as preservice testing, inservice testing and motor-operated valve programs, NRC inspectors would perform a verification of the implementation of each operational program. This issue is discussed in an NRC policy paper, SECY-05-0197, "Review of Operational Programs in a Combined License Application and Generic Emergency Planning Inspections, Tests, Analyses, and Acceptance Criteria," which was issued by the Commission on October 28, 2005. The purpose of this paper is to describe the implications of the Part 52 regulations and commission policy on (1) the development of the preservice testing, inservice testing and motor-operated valve operational programs when the combined license application is submitted, and (2) the implementation of each program after the license is issued.

Introduction

The interest in building new nuclear power plants has grown significantly in the last couple of years. At the time this paper is being published, more than 10 combined license (COL) applications are being planned by utilities in the 2007 through the 2009 time frame, which have currently operating reactors. These applications will be submitted under the new licensing process under the requirements of 10 CFR Part 52. This process allows all the design and siting issues to be addressed before the plant is constructed. Part 52 also allows the COL applicant to reference a certified design incorporated to the appendices of Part 52 and an early site permit (ESP). It should be noted that no COL applicant at this time intends to reference both a certified design and an ESP.

Future construction is being planned at sites with both nuclear plants currently licensed by the NRC and sites where there is no plant currently licensed. Potential COL applications currently indicate that their applications will reference one of three designs:

1) Westinghouse AP1000 (certified by the Commission in January of 2006)

2) General Electric Economic Simplified Boiling Water Reactor [ESBWR] (currently under design certification review by the NRC)

This paper was prepared by staff of the U.S. Nuclear Regulatory Commission. It may present information that does not currently represent an agreed-upon NRC staff position. NRC has neither approved nor disapproved the technical content.

3) Framatome EPR (currently in the early stages of design certification pre-application review, and the applicant plans to submit its design certification application in Fall 2007).

The European version of the EPR is currently being constructed in Finland.

When a COL is issued, the holder will have a license to construct and operate a nuclear plant. This license will include a set of conditions that are referred to as inspections, tests, analyses, and acceptance criteria (ITAAC). ITAAC are a set of inspections, tests, and analyses that, if successfully completed, will verify that the plant has been constructed and will operate in accordance with the Atomic Energy Act, the regulations, and the COL. All ITAAC included in the COL must be successfully completed and verified by the NRC before the licensee can load fuel into the reactor. Although further discussion of ITAAC is beyond the scope of this paper, it is a fundamental part of the Part 52 licensing process and no discussion of Part 52 is complete without the mention of ITAAC.

The NRC staff has proposed in SECY-05-0197 that certain operational programs not have ITAAC. The remainder of this paper will discuss the scope, review, and license conditions associated with operational programs in COL applications.

What is an Operational Program?

The operations of a nuclear power plant contain numerous programs administered by the licensee. A subset of these programs are required by the regulations. SECY-05-0197 focuses on programs that meet three criteria:

1. the program is required by regulation;
2. the program will be reviewed by the NRC staff for its acceptability and the results of this review documented in the staff's final safety evaluation report (FSER); and
3. the program's implementation will be verified by NRC inspectors.

The phrase "operational program" refers to programs that meet these three criteria. Table 1 lists the operational programs that meet these criteria.

Table 1: Operational Programs that Must be Addressed in a COL Application

- Containment Leakage Rate Testing
- Fire Protection
- Operator Training
- Plant Staff Training
- Access Authorization
- Radiation Protection
- Process and Effluent Monitoring/Sampling
- Preservice Inspection
- Preservice Testing
- Equipment Qualification
- Motor-Operated Valve Testing
- Weapons Training
- Emergency Preparedness
- Maintenance Rule
- Operator Requalification
- Physical Security
- Vehicle Control
- Fitness-for-Duty
- Reactor Vessel Material Surveillance
- Quality Assurance - Operations
- Inservice Inspection
- Inservice Testing
- Safeguards Contingency Plan
- Weapons Qualification/Requalification

Fully Describing an Operational Program in a COL Application

In a September 11, 2002, staff requirements memorandum (SRM) for SECY-02-0067, "Inspections, Tests, Analyses, and Acceptance Criteria for Operational Programs (Programmatic ITAAC)," the Commission provided direction to the staff that a COL applicant is not necessarily required to have ITAAC for an operational program with the exception of emergency planning (EP). The SRM stated the following:

[An] ITAAC for a program should not be necessary if the program and its implementation are fully described in a COL application and found to be acceptable by the NRC at the COL stage. The burden is on the applicant to provide the necessary and sufficient programmatic information for approval of the COL without ITAAC.

The Commission defined the phrase "fully described" in a May 14, 2004, SRM for SECY-04-0032, "Programmatic Information Needed for Approval of a Combined License Without Inspections, Tests, Analyses, and Acceptance Criteria," that reads:

In this context, "fully described" should be understood to mean that the program is clearly and sufficiently described in terms of scope and level of detail to allow a reasonable assurance finding of acceptability. Required operational programs should always be described at a functional level and an increasing level of detail where implementation choices could materially and negatively affect the program effectiveness and acceptability.

The staff concluded in SECY-05-0197 that all the programs in Table 1 could be fully described in a COL application. This description would contain the information necessary

Table 2: Operational Programs Related to Inservice Testing

Program	Regulation	Implementation Requirements
Preservice Testing	10 CFR 50.55a (f)	None for commencing program; ASME OM Code. ITSA-2000 defines perservice test period as period of time following completion of construction activities related to the component and before first electrical generation by nuclear heat.
Inservice Testing	10 CFR 50.55a(f)	ASME Operation and Maintenance Code, ISTA-2000: after first electrical generation by nuclear heat.
Motor-Operated Valve Testing	10 CFR 50.55a(b)(3)(ii)	None specified.

for the staff to make a reasonable assurance finding on the acceptability of the operational program in the review of a COL application (i.e., before the plant is built).

Implementation of an Operational Program

SRM-SECY-05-0197 specified that the COL applicant must fully describe the implementation of the operational program in the COL application. The staff must make a reasonable assurance finding on the implementation of the operational program in the review of a COL application.

Most of the operational programs listed above do not have specific implementation requirements listed in the regulations. Therefore, it is essential that the implementation of these programs be reviewed by the staff.

The staff proposed in SECY-05-0197 an implementation condition be included in each COL. It would specify that Section 13.4 of the final safety analysis report (FSAR) contain specific implementation milestones, and the implementation of these operational programs should be fully described in the same section of the FSAR in which the program is fully described. The Commission approved the staff's recommendation.

The staff also proposed a schedule license condition for each operational program. It would require a license holder to submit an implementation schedule for each operational program semiannually starting 1 year after the issuance of a COL. The frequency of submission would increase to monthly when the licensee was within 1 year of scheduled fuel load until the last operational program has been fully implemented or the plant has been placed into commercial service. The Commission also approved the staff's proposal.

Operational Programs Related to Pump and Valve Inservice Testing

Three operational programs are related to inservice testing (IST) of pumps and valves. Table 2 provides the reference to the specific regulation that requires the program and the implementation requirements, if any, specified in the regulations.:

At the time this paper was being drafted, guidance for the information needed for the NRC to review these three operational programs was being developed by the staff in a new regulatory guide for COL applications. The draft of this regulatory guide is scheduled to be issued in summer 2006.

Alternate Treatment for Operational Programs

SECY-05-0197 states that a COL applicant may, at its option, choose to submit a complete program description for any particular program, but omit implementation information and instead include ITAAC. The staff also notes that unique circumstances involving a particular application may raise an implementation issue on an operational program that is best resolved by an ITAAC. The staff expects such circumstances to be rare.

Conclusion

Combined license applications are being prepared for nuclear plants. The first of these applications are scheduled to be submitted in Fall 2007. These applications will be submitted under 10 CFR Part 52 which allows the staff to issue a provisional license to construct and operate a commercial nuclear plant. Operational programs will be reviewed in those COL applications and the staff will make a reasonable assurance finding on the acceptability of the program and its implementation to support the issuance of the COL. The NRC will inspect the implementation of the operational program to ensure that it is being implemented as described in the application. Guidance for including an adequate description of the preservice testing, inservice testing, and motor-operated valve testing programs will be contained in the COL application regulatory guide currently being developed. A draft of the guide will be available this summer.

PUMP OPERATIONAL EXPERIENCE AT U.S. NUCLEAR POWER PLANTS

Steven M. Unikewicz
Division of Component Integrity
Office of Nuclear Reactor Regulation
U.S. Nuclear Regulatory Commission

Ninth NRC/ASME Symposium on Valves, Pumps, and Inservice Testing
July 2006

This presentation will discuss recent operational experience with the performance of pumps at U.S. nuclear power plants. The presentation will discuss the cause of pump performance issues and the corrective action in response to those issues. The discussion will provide information that could have generic applicability in maintaining the proper performance of pumps at all nuclear power plants.

This presentation will be made by staff of the U.S. Nuclear Regulatory Commission. It may present information that does not currently represent an agreed-upon NRC staff position. NRC has neither approved nor disapproved the technical content.

Pump Air Entrainment - How Lack of Analysis Can Translate Into A Potential Safety Issue and Costly Plant Shutdown

Julio Lara, P.E.
Chief, Engineering Branch 3
Division of Reactor Safety
NRC Region III

Abstract

Pump air entrainment - a well-recognized pump performance phenomenon that is occasionally not addressed during pump and process system design. The lack of such analysis can result in significant questions regarding the ability of the pump to perform during required system conditions and accident scenarios. This paper discusses the importance of establishing pump design analysis and the potential safety consequences of not having such analysis.

Protection of Safe Shutdown Equipment During Design Bases Events

One of the basic tenets of nuclear power safety is that facilities are designed, constructed, operated, and maintained as described in the facility's Updated Final Safety Analysis Report (UFSAR). The UFSAR describes the design bases events which plants must be designed to withstand and achieve safe shutdown. We all know about the "big ones": large break loss of coolant accident, loss of offsite power, steam generator tube rupture, etc... Occasionally, however, licensees and the NRC find that other events have not been thoroughly evaluated to ensure that plants can safely shut down upon occurrence. Such was the case at the Kewaunee Nuclear Power Plant (KNPP), located near Green Bay, Wisconsin.

The KNPP facility is located within the NRC Region III geographic location and, in 2005, was selected for a pilot engineering inspection. The pilot inspection approach was based on high risk, low margin components to evaluate component acceptability, as opposed to the traditional system-focused engineering inspection. The KNPP plant design is a typical early-vintage, Westinghouse 2-loop Pressurized Water Reactor, with an auxiliary feedwater (AFW) system designed to supply water to the steam generators (SGs) to remove decay heat from the reactor coolant system following postulated design bases events. The AFW system consists of two motor-driven pumps and one steam turbine-driven pump for providing the source of heat removal. The AFW pumps are normally aligned to two non-safety-related 75,000-gallon Condensate Storage Tanks (CSTs). The plant's service water (SW) system provides the Class 1 backup source of water.

In the aftermath of the Three Mile Island accident, the NRC required that licensees evaluate the design of AFW systems to determine if automatic protection of the AFW pumps was necessary following a seismic event or tornado. The primary concern was that an unprotected pump suction source (from the CST, in Kewaunee's case) could result in pump damage prior to the suction supply being shifted to the safety-related water supply.

To address the NRC requirement, Kewaunee installed a low discharge pressure pump trip signal to protect the AFW pumps against loss of suction head. The primary

This paper was prepared by staff of the U.S. Nuclear Regulatory Commission. It may present information that does not currently represent an agreed-upon NRC staff position. NRC has neither approved nor disapproved the technical content.

reason for installing the trip signal on the discharge piping, rather than on the suction piping, was to address concerns regarding the pump operating at sub-atmospheric pressures due to the long suction piping run from the CST to the AFW pumps (approximately 300 feet). Therefore, the low pump discharge pressure trip would be indicative of a loss of suction pressure and hence the pumps would be protected.

Questions Regarding Adequacy of Design and Plant Shutdown

In preparation for the NRC engineering inspection, the licensee documented the lack of a definitive basis for the AFW pump discharge pressure trip setpoints (350 psig for the two motor driven pumps and 100 psig for the turbine driven pump). Notwithstanding the lack of engineering analysis to support the trip setpoints, the licensee initially concluded that the AFW pumps remained operable (primarily based on Net Positive Suction Head [NPSH] considerations) pending further analytical reviews. The NRC questioned the licensee if the potential for air ingestion and pump damage had been evaluated for the pump discharge pressure trip design. This question was crucially important in determining pump and system operability. The primary NRC concern was that the CST supply to the AFW pumps was a common line, and a failure of the non-Class I portion of the line due to a seismic event or tornado could cause a common mode failure affecting all three AFW pumps. This, in turn, would result in air ingestion into the pumps, leading to air binding and failure of the AFW pumps. After extensive re-analysis and evaluations, the licensee ultimately concluded that the low discharge pressure trips would not perform the intended function of protecting the AFW pumps from a loss of suction supply. Accordingly, the plant commenced an extended plant shutdown to address the system operability concerns. Additionally, using hydraulic models developed following the inspection, the licensee also determined that the AFW pumps were not adequately protected from a pump runout condition.

The Solution: Protected Volume and Operator Manual Actions

As the licensee proceeded with developing an AFW hydraulic analysis, conceptual design work began on achieving an acceptable resolution to the air pump entrainment and pump runout issues. The pump air entrainment issue was resolved by establishing a protected volume of water supply to the AFW pumps along with corresponding pump low suction pressure switches. The pump runout problem was resolved by changing the design and licensing basis of the existing pump discharge trip setpoints.

Protection Against Air Entrainment

The protection of the AFW pumps against a loss of normal water supply from the non-safety CSTs required the modification of existing suction piping to add a protected volume. The existing suction piping was re-sized and re-routed to withstand a seismic event and be protected from tornado effects and high-energy line break interactions. In essence, the Class I boundary break was re-established further upstream of the existing Class I break near the pump. Additionally, three suction pressure switches were added on the new protected AFW suction piping to sense a loss of suction pressure and initiate a trip signal to the respective AFW pump. A primary consideration for establishing the low suction pressure pump trip was a postulated catastrophic failure of the non-Class I suction piping. Following such an event, the low suction pressure switches would trip the respective AFW pumps before pump damage occurred. The additional water volume in the suction piping provided a margin for the AFW pump to coast to a stop before the water in the piping was lost.

The pressure switch setpoint development required consideration of the piping pressure drop between the suction pressure switches and the pumps. The setpoint also took into consideration sub-atmospheric conditions that could exist at the AFW pump suction. Pump operation at sub-atmospheric conditions has the potential to damage the AFW pumps due to a loss of seal leak-off which lubricates and cools the pump's packing. Therefore, the licensee's setpoint needed to ensure that the AFW pump suction pressure would be equal to or greater than atmospheric pressure.

Protection Against Pump Runout

The licensee's AFW system hydraulic analysis determined that, with steam generator (SG) pressures above 650 psia, the AFW pumps would not reach run out conditions and actuate the existing low discharge pressure switches. With the exception of a main steam line break (MSLB), all design basis events resulted in SG pressures greater than 750 psia.

The licensee proposed to maintain the existing low discharge pressure switches, but revise the design and licensing basis of the components. The discharge pressure switches would continue to be used for NPSH pump protection. The inadequate available NPSH condition existed due to the AFW pumps being flow limited because of suction line losses. The discharge pressure switch set points were adjusted to trip the pumps before runout condition resulted.

For the MSLB event, the licensee proposed to prescribe local, manual operator actions to isolate the faulted SG and throttle the AFW pump flow. Several considerations were required to ensure that these actions were acceptable. This included operator training, accessability, timeline validations to accomplish the actions, design of discharge valves, and the need for a test demonstrating the capability of the turbine-driven AFW pump at low SG pressures as the plant commenced heat up.

To provide assurance of the acceptability of the AFW system hydraulic analysis and plant modifications, the licensee performed additional actions including a simultaneous start of all three AFW pumps at hot shutdown conditions. Also, each individual AFW pump was subjected to a timed coastdown test at bounding flow rates.

The NRC approved the licensee's resolution of the AFW issues in the form of an Amendment to the facility's Technical Specifications (TS). This regulatory action allowed the plant to recover from the extended shutdown.

The Lessons: Engineering Rigor, Regulatory Impact, Extended Shutdown

Questions by the licensee, regarding the adequacy of the AFW system design, first surfaced in preparation for the NRC's re-vamped pilot engineering inspection. Following extensive discussions and concerns expressed by the NRC, and after several weeks of engineering review of the basis for the discharge pressure trip setpoints, the licensee ultimately concluded that a lack of confidence in the setpoint basis could not support system operability as required by plant TS. Accordingly, the plant commenced a shutdown on February 19, 2005. The engineering challenge of re-design of the AFW system to address the potential loss of suction supply, along with resolving a plant internal flooding deficiency, resulted in an extended shutdown which ended when full power operations resumed on July 4, 2005. Needless to say, while plant and public safety dictated such a plant shutdown, the economic costs of a shutdown in the heart of the Wisconsin winter are both measurable and significant.

The NRC evaluated the risk-significance of the engineering design deficiency and ultimately concluded that the issue was of low to moderate safety, or a White finding, in NRC risk terminology. Accordingly, the NRC will factor the risk significance of the issue, along with any other findings and performance indicators, in determining what column of the agency action matrix the licensee's performance resides. Appropriate additional regulatory inspections will ensue.

As discussed in SECY 04-0071, in 2004, the NRC staff performed an analysis of the previous 3 years of inspection data from the NRC's Reactor Oversight Process (ROP). The analysis was performed to better understand the degree to which NRC inspections and licensee self assessment efforts have been effective in identifying design issues. Of the 17 greater than green design/engineering issues that fell within the scope of the review, 11 were NRC-identified, 2 were licensee-identified, and 4 were self-revealing. Of the 11 NRC-identified issues, 7 involved issues that had been previously recognized by the licensee but had not taken adequate corrective actions.

The staff also performed a review of the results of recent NRC design inspections conducted at Point Beach and Davis Besse; facilities where the licensee had identified significant design issues. The results highlighted the need for aggressive licensee self-assessments in the design area and effective corrective action programs that can evaluate and resolve the identified issues in a timely manner. The results also revealed that in some instances, the NRC had indications of programmatic design/engineering weaknesses, but did not engage further, as the programmatic weaknesses had not yet resulted in issues that could be classified as risk-significant. While this regulatory approach is in accordance with the fundamental element of the NRC's ROP, it re-emphasizes the importance of licensee's corrective action programs and self-assessments efforts.

It is often said that the plant's engineering organization serves as the plant's design and licensing basis conscience. The engineering staff own and maintain the operational margin which is often consumed by poor maintenance practices, operator errors, procedure weaknesses, and degraded components. As stated earlier in this paper,

the NRC's pilot engineering inspection focused on such components: high risk, low margin. The erosion of that margin is in many instances a hidden unknown. Some margin is easily discernible; pump flow capacity exceeds requirements by x gallons per minute. Others are not so easily discerned; as is the case with calculational errors or unverified assumptions. There is nothing new in the issues discussed in this paper; but rather it should serve as a reminder that adherence to the well-documented engineering principles of design must be maintained to ensure that design and licensing basis commitments are not victims to other competing priorities.

References

Cameron Hydraulic Data, Ingersoll-Rand, Seventeenth Edition, 1988.

American National Standard for Pump Intake Design, ANSI 9.8-1998, November 17, 1998.

SECY 04-0071, Proposed Program to Improve the Effectiveness of the Nuclear Regulatory Commission Inspections of Design Issues, April 29, 2004.

Pederson, Cynthia D., USNRC, to Lambert, Craig W., Nuclear Management Company, LLC., Re Kewaunee Nuclear Power Plant NRC Inspection Report No. 05000305/2005002(DRP), dated April 4, 2005.

Lambert, Craig W., Nuclear Management Company, LLC, to USNRC Re License Amendment Request 213 To The Kewaunee Nuclear Power Plant Technical Specifications: Auxiliary Feedwater Pump Protection, dated May 5, 2005.

Lyon, Carl F., USNRC, to Gaffney, Michael G., Nuclear Management Company, LLC, Re Kewaunee Nuclear Power Plant - Request for Additional Information Regarding Amendment Request (TAC No. MC6916), dated May 24, 2005.

Gaffney, Michael G., Nuclear Management Company, LLC., to USNRC, Re Reportable Occurrence 2005-006-00, dated May 25, 2005.

Gaffney, Michael G., Nuclear Management Company, LLC, Re Response to NRC Request for Additional information re: License Amendment Request 213 To The Kewaunee Nuclear Power Plant Technical Specifications, Auxiliary Feedwater Pump Protection, June 9, 2005.

Lyon, Carl F., USNRC, to Gaffney, Michael G., Nuclear Management Company, LLC, Re Kewaunee Nuclear Power Plant - Issuance of Amendment, dated June 20, 2005.

Gaffney, Michael G., Nuclear Management Company, LLC., to USNRC, Re Reportable Occurrence 2005-008-00, dated June 20, 2005.

Satorius, Mark A., USNRC, to Christian, David A., Dominion Energy Kewaunee, Inc., Re Kewaunee Power Station NRC Inspection Report No. 05000305/2005010(DRP) Preliminary White Finding, dated August 16, 2005.

Gaffney, Michael G., Dominion Energy Kewaunee, Inc., to USNRC, Re Licensee Event Report 2005-008-01, dated November 9, 2005.

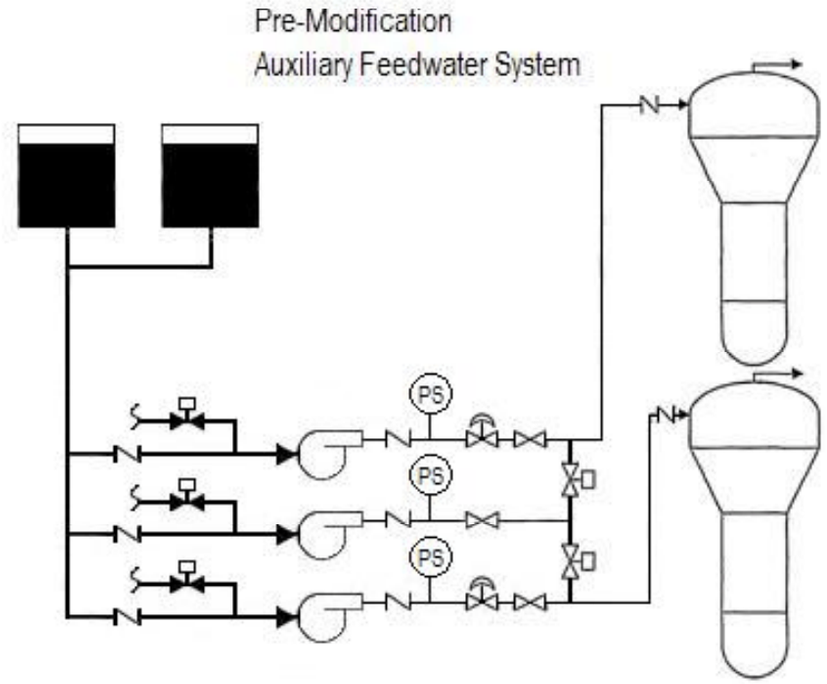
Pre-Modification
Auxiliary Feedwater System
PS
PS
PS

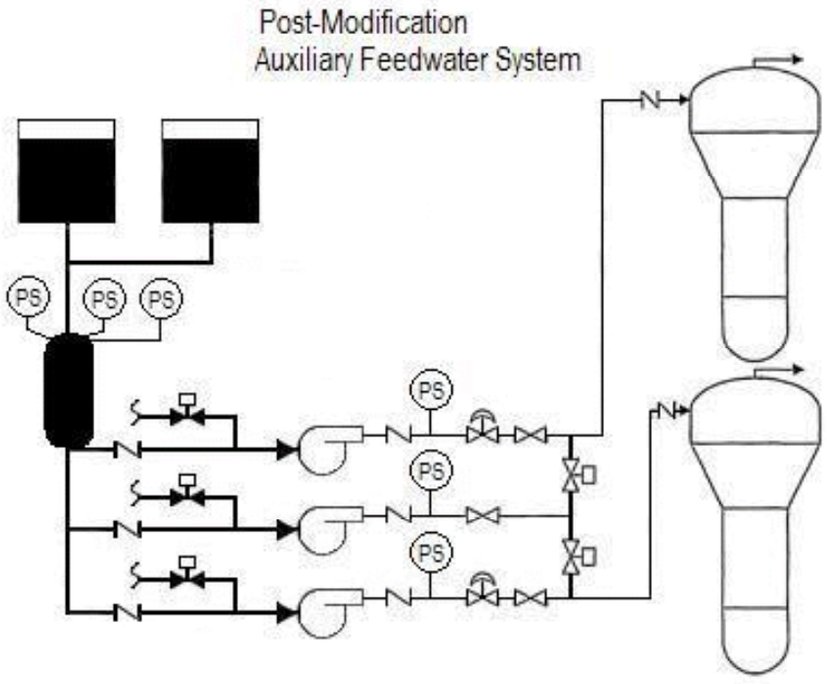
Post-Modification
Auxiliary Feedwater System
PS
PS
PS
PS
PS
PS

Nuclear Power Plant Pump and Valve Inservice Testing Issues

Gurjendra S. Bedi
Component Performance and Testing Branch
Division of Component Integrity
Office of Nuclear Reactor Regulation
U.S. Nuclear Regulatory Commission
Ninth NRC/ASME Symposium on Valves, Pumps, and Inservice Testing
July 2006

Abstract

This paper discusses recent issues related to inservice testing (IST) of pumps and valves at U.S. nuclear power plants. These issues were identified during the review by U.S. Nuclear Regulatory Commission (NRC) staff of IST programs and relief requests, and applicable operating experience. This discussion includes information that could have generic applicability in the implementation of effective IST programs at U.S. nuclear power plants.

Introduction

The NRC staff has encountered a number of pump and valve inservice testing (IST) issues since the Eighth NRC/ASME Symposium on Valve and Pump Testing in 2004. This paper discusses issues involving pump vibration, the frequency range of vibration-measuring transducers, and valve grouping for online testing of check valves. The paper discusses the relief requests received related to these issues and the NRC safety evaluations of the requests. Some current staff positions and actions in these areas are discussed. This discussion includes information that could have generic applicability in the implementation of effective IST programs at U.S. nuclear power plants.

This paper was prepared by staff of the U.S. Nuclear Regulatory Commission. It may present information that does not currently represent an agreed-upon NRC staff position. NRC has neither approved nor disapproved the technical content.

Check Valve Sample Disasembly And Inspection Online

Subsection ISTC of the American Society of Mechanical Engineers (ASME) Code for Operation and Maintenance of Nuclear Power Plants (OM Code) - 2001 with 2003 Addenda, paragraph ISTC-5221(c) allows disassembly of check valves every refueling outage as an alternative means to verify their operability. Instead of disassembly every refueling outage, ISTC-5221(c) provides the option of using a sample disassembly and inspection program for groups of identical valves in similar application. Paragraph ISTC-5221(c)(1) states that grouping of check valves for a sample disassembly examination program shall be technically justified and shall consider, as a minimum, valve manufacturer, design, service, size, materials of construction, and orientation. Further, ISTC-5221(c)(3) states that at least one valve from each group shall be disassembled and examined at each refueling outage, and all valves in each group shall be disassembled and examined at least once every 8 years. The Code requirements are based on Generic Letter (GL) 89-04, “Guidance on Developing Acceptable Inservice Testing Program.”

This paper was prepared by staff of the U.S. Nuclear Regulatory Commission. It may present information that does not currently represent an agreed-upon NRC staff position. NRC has neither approved nor disapproved the technical content.

Paragraph ISTC-3510 states that check valves shall be exercised nominally every 3 months. Paragraph ISTC-3522(c) states that if exercising is not practicable during operation at power and cold shutdown, it shall be performed during refueling outages.

More and more licensees are requesting to disassemble and inspect check valves online to reduce refueling outage time and required manpower during outages. A number of licensees have proposed, as an alternative, to perform the IST disassembly and inspection activities during normal plant operation (online), in conjunction with appropriate system outages, instead of during refueling outages. It is evident that selected refueling outage inservice testing activities could be performed during system outages online without sacrificing quality or safety. In any case, check valves disassembly, inspection, and manual exercising will be performed at least once each operating cycle on a refueling outage frequency. NRC staff has authorized online testing of check valves on a case by case basis.

Recently, the NRC has received relief requests where licensees propose, as an alternative, to perform online sample disassembly and inspection IST activities of check valves in a group.

ISTC-5224 requires that check valves in a sample disassembly program that are not capable of being full-stroke exercised or have failed or have unacceptably degraded valve internals, shall have the cause of failure analyzed and the condition corrected. ISTC-5224 also states that other check valves in the sample group that may also be affected by this failure mechanism need to be examined or tested during the same refueling outage to determine the condition of internal components and their ability to function.

Therefore, when submitting relief requests for check valve group sample disassembly and inspection online, licensees must consider the provisions as specified in paragraph ISTC-5224. Licensees can not defer disassembly and inspection of other check valves in the group. Therefore, online sample disassembly and inspection IST activities for check valves in a group is not recommended unless the allowed outage time (AOT) provides sufficient time to permit the inspection of all valves in the group. The staff has found online disassembly and inspection of valve groups containing one valve acceptable.

Pump Vibration Measuring Instruments (Transucers) Issue

The NRC has received requests from various licensees for relief from the provisions of ISTB-3510(e) of the ASME OM Code for pumps with low pump shaft rotational speeds. Paragraph ISTB-3510(e), “Frequency Response Range,” requires that the frequency response range of the vibration-measuring transducers and their readout system shall be from one-third minimum pump shaft rotational speed to at least 1000 Hz.

Most of the licensees stated that procurement and calibration of instruments to cover the lower end of the Code-specified range was impractical due to the limited number of vendors supplying such equipment, the level of equipment sophistication required, and the equipment cost. Therefore, past relief requests were typically authorized pursuant to 10 CFR 50.55a(a)(3)(ii) on the basis that compliance with the specified Code provision would result in hardship without a compensating increase in the level of quality and safety. The NRC staff prepared safety evaluations authorizing these relief requests.

Since then, the NRC has learned that, due to technology advancement and research work performed in the field of instrumentation, vibration-measuring transducers meeting the Code provisions can be easily procured from various suppliers at a reasonably low cost.

Recently, similar relief requests were received from various licensees. After review, requests for additional information, and followup discussion by the NRC, the licensees withdrew the relief request and decided to install a new transducer that met the Code provisions. Therefore, licensees are requested to carefully examine the availability, procurement, and related cost of the Code-required instruments (vibration-measuring transducers) before submitting a relief request in this area to the NRC.

High Pressure Coolant Injection (HPCI) Pump Vibration Issues

The NRC has received a number of relief requests related to HPCI pump vibration measurement criteria shown in the alert and required action ranges of Table ISTB-5100-1. The NRC staff has authorized HPCI pump vibration relief on a case by case basis, after reviewing licensees' additional monitoring and data and other justification. Recently, the NRC has received similar relief requests along with requests for relief from the provision of paragraphs ISTB-5121(d) or ISTB-5123(d), and ISTB-5121(e) or ISTB-5123(e). Paragraph ISTB-5121(d) and ISTB-5123(d) state that "Vibration (displacement or velocity) shall be determined and compared with corresponding reference values. Vibration measurements are to be broad band (unfiltered). If velocity measurements are used, they shall be peak. If displacement amplitudes are used, they shall be peak-to-peak."

Paragraph ISTB-5121(e) and ISTB-5123(e) specify that all deviations from the reference values shall be compared with the range of Table ISTB-5100-1, and corrective action taken as specified in paragraph ISTB-6200. The vibration measurements shall be compared to the relative and absolute criteria shown in the Alert and Required Action Range of Table ISTB-5100-1. For example, if vibration exceeds either 6 V_r or 0.7 inch/second, the pump is in the Required Action Range.

In one relief request, the licensee stated that the peak vibration amplitude was not related to the physical condition or rotating dynamics of the main pump rotor or bearing system. Therefore, the licensee proposed to filter the measured vibration values of the pump, such that filtered vibration values met the Code provisions of Table ISTB-5100-1. As mentioned above, Subsection ISTB of the OM Code specifies that vibration measurements be broad band (unfiltered). A typical spectrum analysis is a means to gather information as to the source of a potential vibration problem. The licensee-proposed alternative to filter the peak vibration values would only hide the vibration peak and would not correct the elevated pump vibration levels. The filtered vibration measurement would only remove the vibration signal from the calculation, not at the pump. The licensee's proposal masked elevated vibration levels by removing them from consideration. Therefore, the staff did not find the licensee's proposed filtering of the peak values acceptable.

The staff found the proposed alternative did not provide an acceptable level of quality or safety because the alternative did not provide reasonable assurance of the long-term operational readiness of the pump. For long-term assessment of the operational readiness of the pump, it is necessary that pump vibration meet the OM Code provisions as specified in Table ISTB 5.2.1-1 without filtration of vibration signal.

In addition, the licensee did not demonstrate that compliance with Code provisions would result in hardship or unusual difficulty without a compensating increase in the level of quality and safety. The NRC staff is aware that the HPCI pump supplier (Byron Jackson) performed inspections and collected vibration data from HPCI pumps at various nuclear power plants and provided various recommendations to reduce vibration levels. The NRC staff has found that some of the licensees who performed the design modification per Byron Jackson recommendations, were able to reduce HPCI pump vibration levels. Although the need to implement the Byron Jackson recommended modifications requires resources, the modification would likely lower the actual vibration levels of the HPCI pump.

Conclusion

The purpose of this paper was to make licensees aware of a number of pump and valve issues that the staff has encountered since the Eighth NRC/ASME Symposium on Valve and Pump Testing in 2004. Licensees who believe that some of the items discussed are applicable to their facilities may wish to review their current IST program and modify their program as appropriate.

References

10 CFR 50.55a, "Codes and standards."

ASME/ANSI, Code for Operation and Maintenance of Nuclear Power Plants, 2001 Edition and 2003 Addenda:

Subsection ISTB, "Inservice Testing of Pumps in Light-Water Reactor Power Plants."

Subsection ISTC, "Inservice Testing of Valves in Light-Water Reactor Power Plants."

Byron Jackson Product -Technical Service Bulletin-
Technical Note No. 9112-80-018, related to HPCI
Pump Vibration.

Generic Letter 89-04, "Guidance on Developing Acceptable
Inservice Testing Programs."

NUREG-1482, "Guidelines for Inservice Testing at Nuclear
Power Plants."

NUREG/CP-0152, Vol. 4, "Proceedings of the Eight NRC/
ASME Symposium on Valve and Pump Testing," July 2004.

NUREG/CR-6396, "Examples, Clarifications, and Guidance
on Preparing Requests for Relief From Pump and Valve
Inservice Testing Requirements."

Regulatory Guide 1.192, "Operation and Maintenance Code
Case Acceptability, ASME OM Code."

NRC FORM 335 (9-2004) NRCMD 3.7

U.S. NUCLEAR REGULATORY COMMISSION

BIBLIOGRAPHIC DATA SHEET

(See instructions on the reverse)

1. REPORT NUMBER
(Assigned by NRC, Add Vol., Supp., Rev., and Addendum Numbers, if any.)

NUREG/CP-0152, Vol. 6

2. TITLE AND SUBTITLE

Proceedings of the Ninth NRC/ASME Symposium on Valves, Pumps, and Inservice Testing

3. DATE REPORT PUBLISHED

MONTH	YEAR
August	2007

4. FIN OR GRANT NUMBER

5. AUTHOR(S)

Editor: T. G. Scarbrough

6. TYPE OF REPORT

Conference Proceedings

7. PERIOD COVERED *(Inclusive Dates)*

8. PERFORMING ORGANIZATION - NAME AND ADDRESS *(If NRC, provide Division, Office or Region, U.S. Nuclear Regulatory Commission, and mailing address; if contractor, provide name and mailing address.)*

U.S. Nuclear Regulatory Commission
and
Board on Nuclear Codes and Standards of the American Society of Mechanical Engineers

9. SPONSORING ORGANIZATION - NAME AND ADDRESS *(If NRC, type "Same as above"; if contractor, provide NRC Division, Office or Region, U.S. Nuclear Regulatory Commission, and mailing address.)*

U.S. Nuclear Regulatory Commission, Office of Nuclear Reactor Regulation, Division of Engineering, Washington, DC 20555-0001

ASME Board on Nuclear Codes and Standards, Three Park Avenue, New York, NY 10016-5990

10. SUPPLEMENTARY NOTES

11. ABSTRACT *(200 words or less)*

The 2006 Symposium on Valves, Pumps, and Inservice Testing, jointly sponsored by the Board on Nuclear Codes and Standards of the American Society of Mechanical Engineers and by the U.S. Nuclear Regulatory Commission, provides a forum for exchanging information on technical, programmatic, and regulatory issues associated with inservice testing programs at nuclear power plants, including design, operation, and testing of valve and pumps. The symposium provides an opportunity to discuss improvements in design, operation, and testing of valves and pumps that help ensure their reliable performance. The participation of industry representatives, regulatory personnel, and consultants ensures the presentation of a broad spectrum of ideas and perspectives regarding the improvement of inservice testing programs and methods for valves and pumps at nuclear power plants.

12. KEY WORDS/DESCRIPTORS *(List words or phrases that will assist researchers in locating the report.)*

Inservice Testing
Valves
Pumps
Motor-Operated Valves
Risk-Informed Inservice Testing
Air-Operated Valves
ASME Boiler & Pressure Vessel Code
ASME Code for Operation and Maintenance of Nuclear Power Plants

13. AVAILABILITY STATEMENT

unlimited

14. SECURITY CLASSIFICATION

(This Page)
unclassified

(This Report)
unclassified

15. NUMBER OF PAGES

16. PRICE

Federal Recycling Program